REPORT NO.
UCB/EERC-77/22
AUGUST 1977

EARTHQUAKE ENGINEERING RESEARCH CENTER

PRELIMINARY EXPERIMENTAL STUDY OF SEISMIC UPLIFT OF A STEEL FRAME

by

R.W. CLOUGH
A.A. HUCKELBRIDGE

Report to National Science Foundation,
American Iron and Steel Institute

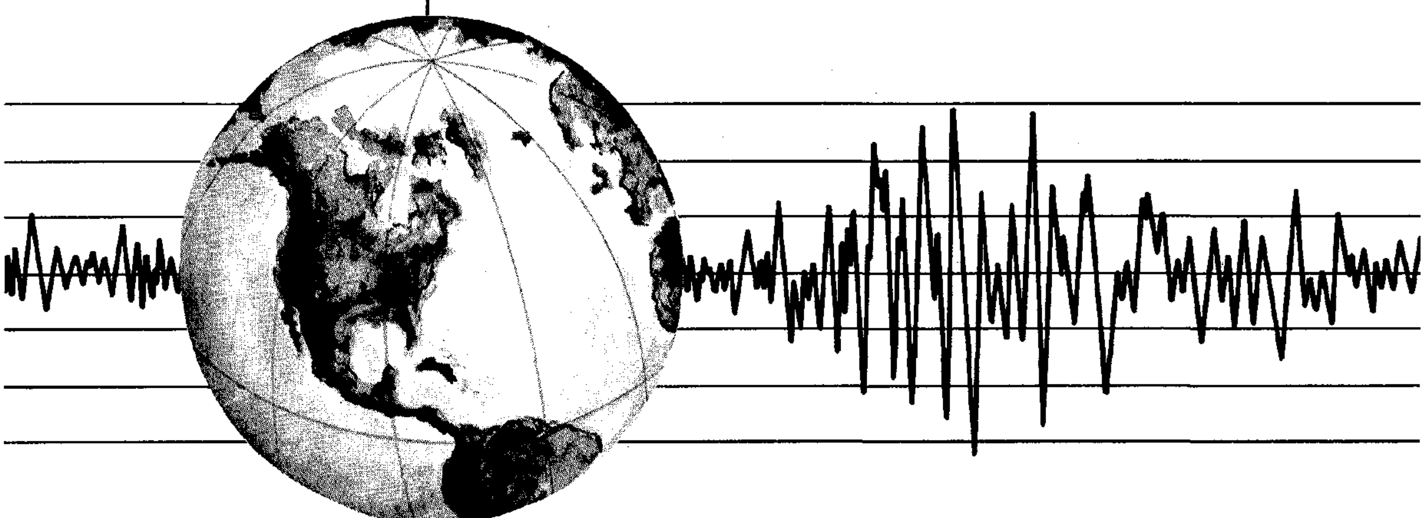

COLLEGE OF ENGINEERING

UNIVERSITY OF CALIFORNIA · Berkeley, California

BIBLIOGRAPHIC DATA SHEET	1. Report No. UCB/EERC-77/22	2.	3. Recipient's Accession No. PB278769
4. Title and Subtitle Preliminary Experimental Study of Seismic Uplift of a Steel Frame			5. Report Date August 1977
			6.
7. Author(s) R. W. Clough and A. A. Huckelbridge			8. Performing Organization Rept. No. 77-22
9. Performing Organization Name and Address Earthquake Engineering Research Center University of California, Berkeley 47th Street and Hoffman Boulevard Richmond, California 94804			10. Project/Task/Work Unit No. AISI Project #177
			11. Contract/Grant No. NSF Grant ENV76-04262
12. Sponsoring Organization Name and Address National Science Foundation 1800 G Street, N. W. Washington, D. D. 20550	American Iron & Steel Institute 1000 16th Street, N. W. Washington, D.C. 20036		13. Type of Report & Period Covered
			14.
15. Supplementary Notes			

16. Abstracts

This study represents the preliminary portion of a research program into the effects of allowing column uplift in steel building frames responding to severe seismic loading. Included in this report are experimental and analytical results for a 3-story steel frame both with and without column uplift allowed. Uplift response results are presented for tests using 2 sets of impact elements with stiffnesses differing by approximately an order of magnitude.

Allowing column uplift is shown for this frame to significantly reduce both the seismic loading and ductility demand, when compared to the fixed base response for a similar input motion. An analytical technique employing bilinear elastic foundation support elements, with no tensile capacity or stiffness in the upward direction, is shown to accurately predict the uplift response of this frame, even in the presence of large rigid body rotations. An analytical technique using concentrated bilinear plastic hinges is shown to accurately predict the nonlinear fixed base response, for moderately nonlinear response.

17b. Identifiers/Open-Ended Terms

17c. COSATI Field/Group

18. Availability Statement Release Unlimited	19. Security Class (This Report) UNCLASSIFIED	21.
	20. Security Class (This Page UNCLASSIFIED	22. Price

PRELIMINARY EXPERIMENTAL STUDY
OF SEISMIC UPLIFT OF A STEEL FRAME

by

Ray W. Clough

and

Arthur A. Huckelbridge Jr.

Report to
National Science Foundation

American Iron and Steel Institute

Report No. UCB/EERC-77/22
Earthquake Engineering Research Center
College of Engineering
University of California
Berkeley, California

August 1977

i(a)

EARTHQUAKE SIMULATION TESTS OF A THREE STORY STEEL FRAME WITH COLUMNS ALLOWED TO UPLIFT

by

Ray W. Clough
and
Arthur A. Huckelbridge Jr.

ABSTRACT

This study represents the preliminary portion of a research program into the effects of allowing column uplift in steel building frames responding to severe seismic loading. Included in this report are experimental and analtyical results for a 3-story steel frame both with and without column uplift allowed. Uplift response results are presented for tests using 2 sets of impact elements with stiffnesses differing by approximately an order of magnitude.

Allowing column uplift is shown for this frame to significantly reduce both the seismic loading and ductility demand, when compared to the fixed base response for a similar input motion. An analytical technique employing bilinear elastic foundation support elements, with no tensile capacity or stiffness in the upward direction, is shown to accurately predict the uplift response of this frame, even in the presence of large rigid body rotations. An analytical technique using concentrated bilinear plastic hinges is shown to accurately predict the nonlinear fixed base response, for moderately nonlinear response.

ACKNOWLEDGEMENTS

The research described in this report was supported by the American Iron and Steel Institute Project 177, and a National Science Foundation Grant, ENV76-04262. Both sources of support are gratefully acknowledged.

The experimental portion of this investigation was carried out in the Earthquake Simulator Latoratory of the U.C. Berkeley Earthquake Engineering Research Center. The analytical work was performed in the Computer Center of the Berkeley Campus.

The manuscript of the report was typed by Ms. Robin Cranford and Ms. Shirley Edwards. Many of the figures were prepared by Mr. Larry Bell. Mr. Yuset Ghanaat provided assistance with the data reduction.

TABLE OF CONTENTS

1. INTRODUCTION

1.1 The Overturning Effect in Seismic Response

The overturning moment at the base of a structure resulting from the lateral inertial forces which occur during a major earthquake can easily exceed the overturning resistance provided by the dead weight of the system alone. Assuming that no supplementary anchorage is provided, this condition implies a transient separation of portions of the structure from its foundation, resulting in a highly nonlinear response.

The usual linear dynamic or equivalent static analysis techniques are not capable of treating this type of nonlinear behavior. The stiffness changes associated with separation or impacting of structure and foundation are very drastic and instantaneous in nature, requiring a more sophisticated nonlinear analysis.

The traditional building code solution to this problem has been to avoid it by specifying lateral loading conditions low enough so that overturning complications are not encountered in most designs. The lower design loading conditions have been reasonably justified by requiring adequate detailing for local ductile behavior in overload situations.

No rational provision has been incorporated, however, to consider an overturning overload. Building codes generally require full overturning resisting capacity for whatever overturning moment is computed, even if this requires supplementary anchorage.

Primarily as a result of the structural failures during the 1971 San Fernando earthquake there has been a trend toward more conservative seismic design loading conditions, particularly for hospitals and other essential facilities. This trend now is leading to the necessity for a rational consideration of the overturning effect; to require full overturning constraint for a strong earthquake would seem to be both uneconomical and unnecessary. A rational consideration of overturning response to severe ground shaking, however, requires a full understanding of that response, including the nonlinear uplift phenomenon.

Analytical studies by Beck and Skinner (1) and by Meek (4) indicate the potential economies of allowing transient uplift of structures in response to strong ground shaking. Indications are that the uplift phenomenon provides a type of structural fuse, limiting the applied overturning forces to those which first produce uplift. This limiting effect can thus lead to reduced internal forces and/or ductility demand on the system, making possible a more rational and more economical design for a realistic seismic loading condition.

Before a general incorporation of uplift capability as a design feature is undertaken, however, the basic uplift response mechanism must be thoroughly investigated, including experimental verification of analytical studies. Once verified, adequate analytical consideration should then lead to a more effective design application, with greater confidence in the intended performance.

1.2 Scope and Objectives of this Study

The primary objective of this study was to investigate the seismically induced overturning effect in a simple structural system, both with and without indicated supplementary anchorage provided. The investigation was to be both experimental and analytical in nature, with the experimental data providing a basis for evaluating currently available nonlinear analytical techniques. It was felt that a simple, well-understood superstructure system would facilitate the study of the basic uplift phenomenon, the response feature of greatest interest in this study.

In scope the study has included the conduct of a series of shaking table tests of an experimental structure in the U.C. Berkeley Earthquake Simulator Laboratory. These test results, both with and without uplift allowed, were then compared directly to response predictions by a nonlinear dynamic analysis program, utilizing the experimentally measured excitation as input. The degree of correlation between analytical and experimental results for the same excitation then provided the means of evaluating the analyses.

2. EXPERIMENTAL PROGRAM

2.1 The Test Facility

The U.C. Berkeley Earthquake Simulator, shown in Fig. 2.1.1, is described fully by Rea and Penzien (6). Briefly, the facility consists of a 20' x 20' post-tensioned concrete slab shaking table with its associated control and data acquisition equipment. The shaking table can move independently in the vertical and one horizontal direction. The command displacement signals for the two degrees of freedom are supplied and test data are recorded through a Nova mini-computer system. Up to 128 channels of data can be sampled discretely, usually at a rate around 50 samples/sec/channel. The data, converted immediately to digital form, are transferred to magnetic tape for detailed reduction on the Berkeley CDC 6400 computer system.

The range of possible input signals to the shaking table is completely general within the limiting ranges of displacement, velocity and acceleration shown in Fig. 2.1.2. In addition to these limits, the maximum design payload is about 100^k and the design overturning moment capacity is about 1700 kip-ft.

2.2 The Test Model

As mentioned in the introduction, it was decided to utilize a relatively simple superstructure system for the initial investigation of the uplift phenomenon. An existing three-story, single-bay steel moment frame, described fully by Clough and Tang (2), was available for this purpose. This frame had been utilized in the initial experimental and analytical test program conducted on the then newly constructed shaking table, reported by Tang (7).

The existing structure had been fabricated from rolled A36 wide flange sections; the columns were W5 x 16 and the girders were W6 x 12. Concrete weights totaling 24^k were distributed equally on the 3 floors; each floor had sufficient in-plane bracing to provide a rigid diaphram behavior. The bay width was 12'-0"; the floor heights were 6'-8", 5'-4", and 5'-4".

It was decided for reasons of economy to adapt this existing structure to the uplift test program. As it was considered desirable to achieve a relatively high amplitude of uplift response, the column bases were pinned to allow rigid body rotation immediately upon separation of the column base and foundation. Braces to the 1st floor were introduced to restore stiffness lost through this modification; these also provided a local critical section for study at each column midheight, as shown in Fig. 2.2.1.

The uplift mechanism designed to accommodate the anticipated high amplitude uplift response is shown in Fig. 2.2.2. The vertical roller bearings provided a "shear key" for each column, essential to prevent the structure from "walking" off the foundation, yet with only negligible resistance to uplift motion.

Neoprene impact pads of two different stiffnesses were provided beneath the column bases during uplift testing. For phase I testing, relatively soft pads with an effective stiffness of approximately 44 ki/in were employed. For phase II testing, pads of approximately an order of magnitude greater stiffness were fabricated. As mentioned previously. provision was made to restrain the uplift motion for comparative purposes. This was accomplished by removing the impact pads and bolting the pin mechanism securely to the foundation. The pinned nature of the column base was thus retained while the relative vertical motion was prevented.

2.3. Instrumentation

For the phase I uplift tests a total of 124 data channels were monitored, 36 of which were devoted to various table functions. For phase II uplift tests an additional 4 channels were monitored. These additional channels were devoted to extra strain readings near the critical section of a first floor column. The instrumentation served to define the table and individual horizontal story accelerations and displacements, the member force distributions, the local member inelastic deformations and the column base relative vertical displacements during each test. Complete channel listings and descriptions are given for all tests in Appendix A.

Data sign conventions are shown in Figs. 2.3.1 and 2.3.2. All data channels were sampled at a rate of approximately 50 points per second during these tests.

Transducer types utilized for these tests consisted of accelerometers, linear potentiometers, linear DC displacement transducers, strain gages and on-off contact switches between the column bases and their respective impact elements. Descriptions of these transducers are given briefly in the following paragraphs.

The accelerometer type used was the Kistler model 305T non-pendulous, force balance servo accelerometer, with a Kistler model 515T servo amplifier attached. The amplifiers were set to give a data range of $\pm$ 5 g's.

Two different models of linear potentiometers were used in testing. To measure the absolute horizontal story displacements, Houston Scientific Inc. model 1800-30A potentiometers were used. This model has a travel range of $\pm$ 15 in. Houston Scientific model 1800-15A potentiometers were used to measure the relative column base vertical displacements. This model has a travel range of $\pm$ 7.5 in.

Sanborn model 7DCDT-500 displacement transducers with a stroke of $\pm$.5 in. were used in opposing pairs to measure local member average curvatures. For this purpose the transducers were mounted in aluminum frames set at distances of 4 and 6 in. from corresponding target frames.

Typical setups of these devices are shown in Fig. 2.3.3.

Two types of resistance strain gages were utilized in the tests. For strains in elastic regions, foil gages were utilized to derive resultant force quantities. These were manufactured by Micro-Measurements, model EA-06-250BG-120, options L and W. For strains in the plastic regions, post yield gages of types YL-10 and YL-20 by Tokyo Sokki Kenkyujo Co. were utilized to estimate ductility demands. The latter gages employ a nickel-copper alloy wire, reportedly accurate to strains of 20%.

In addition to the above mentioned instruments, mechanical strain gages manufactured by Prewitt Associates were colocated with standard resistance strain gages at several critical sections. These "scratch strain gages" are self-driven and produce a trace on a polished brass target, which is interpreted with a 100X microscope. One of these gages is shown in Fig. 2.3.4.

2.4 Input Signals

As previously mentioned, the family of possible input signals to the shaking table is practically limitless, making necessary a decision as to appropriate signals. For this test series, it was decided to use signals derived from actual strong-motion accelerograms. The two basic signals chosen were the 1940 El Centro N-S and the 1971 Pacoima Dam S74W records. Each signal was run at a wide range of intensities, and the El Centro record was used both with and without the corresponding vertical component of motion. Because the table is displacement controlled, the table motion acclerograms are not exact duplicates of the field-recorded accelerograms, but they do represent well the intensity and frequency content of typical ground motions. The acceleration time histories in the horizontal direction, along with the displacement records and response spectra of all the different test intensitites and motions discussed in this report,are presented in Figs. 2.4.2 through 2.4.11. The El Centro earthquake motions are designated EC and the Pacoima earthquake inputs are labeled PAC. The number following these designations is the "span" setting for the test: a control system setting indicating the "intensity" of the test, and linearly proportional to the table displacement. Roman numerals I and II identify the two different stiffnesses of rubber impact cushions used in test phases I and II. Where no Roman numeral is shown, the structure was fully constrained against uplift.

The response spectra for each test were obtained using a program developed by Nigam and Jennings (5). The spectral ordinates were computed at the following period intervals:

.10 sec. to .30 sec. @ intervals of .025 sec.
.30 sec. to 1.0 sec. @ intervals of .050 sec.
1.0 sec. to 3.0 sec. @ intervals of .250 sec.
3.0 sec. to 5.0 sec. @ intervals of .500 sec.

The response ordinates were computed using the accelerations as digitized during each test.

Because this test series was not intended as a model test of any prototype structure, no time scaling of the input was performed. Use of normal time scale would tend to exaggerate the amplitude of the uplift response, presuming a larger prototype. Therefore, it was felt that very useful data for analytical comparison could be obtained in this manner.

2.5 Experimental Results

A total of 52 dynamic tests was conducted on the test model, and the data were stored permanently on 9 track magnetic tape. A complete list of these tests in the sequence conducted is given in Appendix B. From this total of 52 tests, however, only 11 representative cases were selected for detailed data reduction. Table 2.5.1 shows in summary a number of the more interesting features of these 11 tests. From this table, it is apparent that a wide range of excitations and response levels is represented in the data to be discussed in this report.

Global response parameters only were examined for 6 of the selected tests; however, both global and certain local response parameters were examined for the 5 tests exhibiting the greatest extent of nonlinear behavior. The results of each individual test are presented in the following sequence:

1. Table motions.
2. Global response.
3. Local response (if applicable).

The general method of data presentation is in the form of time-history plots of the pertinent parameters. Moment-curvature plots demonstrating nonlinear hysteretic behavior are presented where they are deemed most illustrative.

2.5a <u>EC 200 I</u>

This test, with the input signal scaled to produce a maximum acceleration about 1/3 that of the actual El Centro signal, produced a response entirely within what can be considered the linear behavior range. No vertical component of excitation was applied.

Only global response quantities were examined in detail, for this case. Fig. 2.5a.1 shows the table motion and response spectra. Fig. 2.5a.2 shows the floor accelerations along with the table acceleration. The response is seen to be dominated by the first mode, although considerable 2nd mode response is evident in the 1st floor acceleration. The vibration periods of the three modes while the structure was supported on the soft pads for phase I were experimentally observed to be .463, .130 and .067 seconds respectively, as determined by a Fast Fourier Transform analysis of the 3rd floor acceleration during free vibration. The displacements shown in Fig. 2.5a.3 again point out the predominant 1st mode contribution, and the story forces shown in Fig. 2.5a.4 verify the overturning moment did not exceed the limiting value of 180 kip-ft required to initiate uplift.

2.5b EC 100 II

In this test the input signal was scaled to produce a maximum acceleration about 2/3 that of the actual El Centro record. The table motions, shown in Fig. 2.5b.1 thus are all nearly twice the amplitudes of Fig. 2.5a.1. The floor accelerations, shown in Fig. 2.5b.2 again show a 1st mode predominance, with the 2nd mode still visible, particularly in the 1st floor acceleration. With the stiffer rubber pads for this phase II test, the observed modal periods were .379, .133 and .068 seconds, determined in the same manner as previously described. It is interesting to note, that only the first mode period was reduced by the stiffer support system.

Fig. 2.5b.3 shows the relative story displacements and Fig. 2.5b.4 shows the momentary column base separations that occurred during this test. Fig. 2.5b.5 verifies that the base overturning moment did reach the uplift limit of 180 kip-ft. The momentary base separations observed in this test, however, had very little effect on the response; it was still essentially a linear behavior.

2.5c EC 200

This test very nearly duplicated the excitation of EC 200 I. This test, however, was conducted with the column base fixtures attached securely to the foundation, preventing any relative vertical motion. This resulted in a lowering of the modal periods to observed values of .339, .130 and .068 seconds respectively.

The response observed during this test was also well within what can be considered the linear range. Any nonlinearity in the base constrained case, of course, would have to be due to material yielding and not to any uplift response.

Fig. 2.5c.1 shows the table motions, nearly identical to Fig. 2.5a.1. Fig. 2.5c.2 shows the floor accelerations. The differing base conditions did not alter greatly the mode shapes, thus the 2nd mode still shows up most significantly in the first floor. The relative floor displacements, shown in Fig. 2.5c.3 were again predominantly 1st mode, as were the story forces shown in Fig. 2.5c.4. These story forces did not differ greatly in amplitude from the phase I test, even though the relative displacements of Fig. 2.5c.3 were considerably lower in amplitude than those observed in phase I. The reason for this was the rigid body rotation possible in the case where the column bases were not restrained vertically, but were supported on the relatively soft, neoprene pads.

2.5d EC 1000 I

For this test the input was scaled so as to produce a maximum acceleration more than twice that of the actual El Centro record; this excitation produced a significant nonlinear uplift response.

Fig. 2.5d.1 illustrates the greater intensity of the excitation for this test and Fig. 2.5d.2 displays the nonlinear nature of the response as evidenced by the changing response period. In particular the intervals of response between 3 and 6 seconds and around 11 seconds of the time history were obviously of a complex nonlinear nature. These were, in fact, the intervals in which the uplifting phenomenon was observed to occur. Higher order flexural response may be seen to be superposed on the rigid body rotations that are associated with the column uplift for this structure. Again the elastic 2nd mode contribution is evident in the 1st floor acceleration.

Fig. 2.5d.3 shows the large displacements possible with a rigid body response mode. Fig. 2.5d.4 shows the relative column base separations, indicative of the large rotations which occurred. In Fig. 2.5d.5 the performance of the uplift phenomenon as a structural "fuse" is exhibited; the overturning moment only momentarily exceeded the limit corresponding to initiation of uplift response.

Fig. 2.5d.6 shows the character of the local response quantities in the 1st floor columns. Because the recorded force quantities represent only dynamic forces, the column axial forces in tension were clipped off at a level representing the magnitude of the dead weight or static compression.

Fig. 2.5d.7 shows some additional local response quantities, namely the 1st floor column moments and average curvatures. These curvatures were measured over a 6" gage length near the column midheights, the most critical section of these columns due to the brace connection at that point. The hysteresis plot of these quantities, shown in Fig. 2.5d.8, demonstrates that the member distortions were still generally within what can be called a linear range, despite the high intensity of the excitation. This again is demonstrative of the fuse effect of the uplift phenomenon.

2.5e <u>EC 1000/850 I</u>

This test had essentially the same horizontal excitation as the EC 1000 I test, with the addition of the appropriately scaled vertical component of table motion. Comparison of Fig. 2.5e.1 with Fig. 2.5d.1 indicates the close resemblance of the two horizontal table motions. The acceleration response shown in Fig. 2.5e.2 similarly is nearly a duplicate of Fig. 2.5d.2.

Fig. 2.5e.3 shows that the relative story displacements were only slightly greater than in the previous test, indicating a slightly larger amplitude of rigid body rotation. This same observation can be made for the vertical displacements of Fig. 2.5e.4, and the overturning moment plots of Fig. 2.5e.5 are again nearly duplicates of Fig. 2.5d.5.

These observations demonstrate that the vertical component of excitation had little effect on the response. This effect, or lack thereof, was consistently noted with regard to any vertical excitations introduced throughout the test program.

2.5f EC 300 II

The input signal for this test was again scaled to produce a maximum acceleration more than twice that of the actual El Centro record. As shown in Fig. 2.5f.1 the table motion was very similar to the previous El Centro tests. Actually a few variances are apparent in the response spectra; these were probably due largely to the time interval of several months which elapsed between phase I and phase II testing. The analog integrator used to generate the system command signals demonstrated some inconsistency over the relatively long time period involved. The signals did not vary significantly, however, and it is believed that valid comparisons still can be made.

As seen from Fig. 2.5f.2, the response observed during this test was very similar to that seen in the previous tests. There were essentially the same number of uplift "cycles" at around the same relative times. The response during uplift perhaps showed slightly more impact effect with the stiffer foundation pads, and the response outside the uplifting intervals seemed to be more dominated by the fundamental mode.

The relative displacements, shown in Fig. 2.5f.3, were again very similar to those seen in previous tests, as were the column base vertical displacements of Fig. 2.5f.4. As shown in this figure also, the stiffer foundation pads allowed very little relative vertical motion outside the uplifting intervals. The story forces of Fig. 2.5f.5 differed little from previous observations, as did the local member forces of Fig. 2.5f.6. The column axial forces again were clipped at the level of static compression. The column moments and average curvatures, shown in Figs. 2.5f.7 and 2.5f.8, were again within the linear range despite the high intensity of the input.

By comparison of these test results with those of EC 1000 I, it may be seen that the stiffness of the rubber support pads had little effect on the response behavior even when rather large uplift displacements were induced.

2.5g EC 300/675 II

This test was identical to EC 300 II except for the addition of the appropriately scaled vertical component of input. As shown in Fig. 2.5g.1, the horizontal table motions had no significant differences from the previous test. Fig. 2.5g.2, showing response accelerations, indicates very little difference in the response, when compared to the preceding test result shown in Fig. 2.5f.2. The same similarity of response was evident in the displacements shown in Figs. 2.5g.3 and 2.5g.4 when compared to Figs. 2.5f.3 and 2.5f.4. As might be expected, the story forces shown in Fig. 2.5g.5 were also very similar in nature to those shown in Fig. 2.5f.5

From these observations it is apparent that the vertical excitation had little effect in either phase I or phase II testing. Although not shown, tests also were run including vertical excitation for the base constrained case, with a similar lack of any observable effect. It should be noted here, however, that the gravity load stresses in this model were very low. Hence this evidence should not be construed to indicate that vertical excitation should never be a design consideration in prototype structures.

2.5h EC 1000

This test, for which the input was again scaled to produce a maximum acceleration more than twice that of the original El Centro record, was the first instance in which some material yielding was observed. The input motions, shown in Fig. 2.5h.1, were very similar to the preceding high intensity El Centro tests, shown in Figs. 2.5d.1, 2.5e.1, 2.5f.1 and 2.5g.1.

However, the response accelerations, shown in Fig. 2.5h.2, demonstrated a marked difference from the previous tests where column uplift was allowed. The floor accelerations did not show the obvious nonlinearity associated with uplift in the previous tests; local material yielding produces more gradual global stiffness changes which are not so immediately apparent in the response.

The relative floor displacements, shown in Fig. 2.5h.3, were considerably less than in the uplifting case due to the elimination of rigid body motion. It should be noted, however, that even though the relative displacements are less, the accelerations and consequent forces are considerably greater than those of the uplift tests. This increase can be attributed to the lack of a fuse effect associated with the uplift mechanism. The differing response is shown clearly by comparing the story forces of Fig. 2.5h.4 with those of Fig. 2.5d.5.

Local member forces, shown in Fig. 2.5h.5, were also correspondingly higher than those observed in the uplift tests. As can be seen in the north column average curvature plot, shown in Fig. 2.5h.6, some nonlinearity was present, evidenced by the permanent set remaining at this location following the test. This yield phenomenon also is evident in the hysteresis plots of Fig. 2.5h.7. The south column did not display a significant set due to the differing sense of the static load.

Fig. 2.5h.8 shows strain data comparisons for the co-located mechanical and resistance strain gages. The correlation seems very good, considering the uncertainties inherent in the optical digitization of the mechanical gage data.

2.5i PAC 400 I

This test used the input signal shown in Fig. 2.5i.1, which was based upon the Pacoima Dam record. This motion had a relatively short duration but was very intense and produced some interesting results.

From the floor accelerations shown in Fig. 2.5i.2, it can be seen that the response was similar in most respects to that observed in the previous El Centro tests. There were more "cycles" of uplifting response; the rigid body rocking was essentially continuous over the time interval between 3 and 9 seconds of the response. Again a lot of 2nd mode response showed up in the 1st floor acceleration.

Although more uplift cycles were observed for this test, Fig. 2.5i.3 shows that the magnitude of rigid body rotation was not as large as that seen in the El Centro tests. Once uplift begins for this structure, the subsequent ground displacement determines the extent of rigid body rotation which takes place. The uplift plots of Fig. 2.5i.4 confirm the continuous uplifting response over the previously mentioned time interval. Fig. 2.5i.5 again demonstrates the action of uplift as a structural fuse in limiting the applied loads.

2.5j PAC 700 II

The input for this test was scaled slightly higher than that of the phase I Pacoima test. As mentioned previously, a long term lack of stability observed in the analog integrator used to generate command displacement signals may have led to slight variances between the phase I and phase II signals. The phase II table motions shown in Fig. 2.5j.1 are very similar in nature, however, to the phase I input with the possible exception of the lowest frequency range.

The floor acceleration responses of Fig. 2.5j.2 again were similar to the phase I results. The uplift motion, however, lasted a few seconds longer for the phase II test. The relative displacements, shown in Figs. 2.5j.3 and 2.5j.4, indicate that the envelope displacement values were comparable to the phase I test, but occurred later in the response history. The story forces plotted in Fig. 2.5j.5 indicate the same general phenomena mentioned previously.

The local member forces, shown in Figs. 2.5j.6 and 2.5j.7 bear out the previously described advantage of allowing column uplift. The column axial forces were not observed to be appreciably greater in the phase II tests as compared to the phase I tests. It should be pointed out that the small apparent permanent deformations shown in the average column curvatures of Figure 2.5j.7 are somewhat misleading. The first floor columns already had been subjected to relatively large inelastic strain during previous "base constrained" tests, and were exhibiting considerable Bauschinger effect. The hysteresis plots of Figs. 2.5j.8 and 2.5j.9 indicate that the local response was very nearly linear.

Fig. 2.5j.10 shows further strain data comparisons of the mechanical and resistance strain gages. It can be seen that the impact induced transients caused some difficulty in the optical digitization of the gage trace. The correlation was still relatively good, however.

2.5k PAC 700

The input signal for this fixed base test was scaled to approximately reproduce the phase II Pacoima Dam test. The table motion shown in Fig. 2.5k.1, indicates that the two excitations were indeed very similar. The low frequency variance in the phase II response spectra from that of the phase I test and of this test may perhaps be attributable to some instrument zero drift.

The floor accelerations, shown in Fig. 2.5k.2, indicate the high intensity of the loads imposed on the structure during this test. These forces were well beyond those required to initiate yielding of critical sections of the structure. The relative floor displacements of Fig. 2.5k.3 show a permanent set, indicative of the nonlinearity of the response. The story forces of Fig. 2.5k.4 show convincingly the increased loading resulting from anchoring the columns to the foundation; these forces were approximately 1 1/2 times greater than those of the uplift tests. A similar difference is apparent in the local member forces, shown in Figs. 2.5k.5 and 2.5k.6 when compared to those of Figs. 2.5j.6 and 2.5j.7.

As a consequence of increasing the loads acting on the structure, anchoring the columns also can increase considerably the ductility demand on critical sections of the structure. This can be seen quite readily by comparing the plots of Figs. 2.5k.7 and 2.5k.8 to those of the corresponding uplift test shown in Figs. 2.5j.8 and 2.5j.9.

Fig. 2.5k.9 shows additional comparisons of mechanical and colocated electrical strain gage data. Fig. 2.5k.10 indicates a potential problem in interpreting the mechanical gage data. Their gage length, in order to produce a readable trace, must by necessity be rather long (6" in this case). By comparing the mechanical gage data to that of resistance gages of 10 mm gage length distributed along this 6" distance, one can see the problem which occurs when the mechanical gage spans a region of varying strain gradient. The very high strains in the upper portion of the 6" gage length, associated with the plastic hinge formation at the column midheight, are averaged in with the lower elastic strains below the hinge region. As a consequence of this averaging process, the local strain ductility demand is considerably underestimated by the mechanical gage; one should therefore use some judgment in locating these gages on a structure and in the interpretation of data if obtained in regions of varying strain gradients.

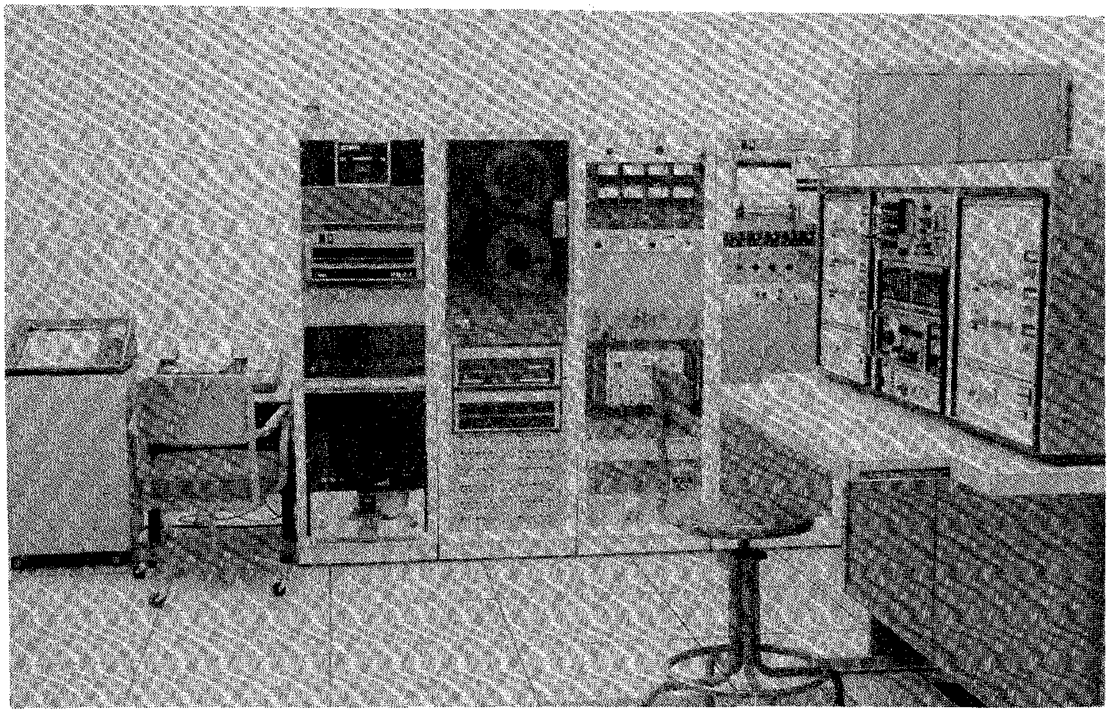

(a) Control Room

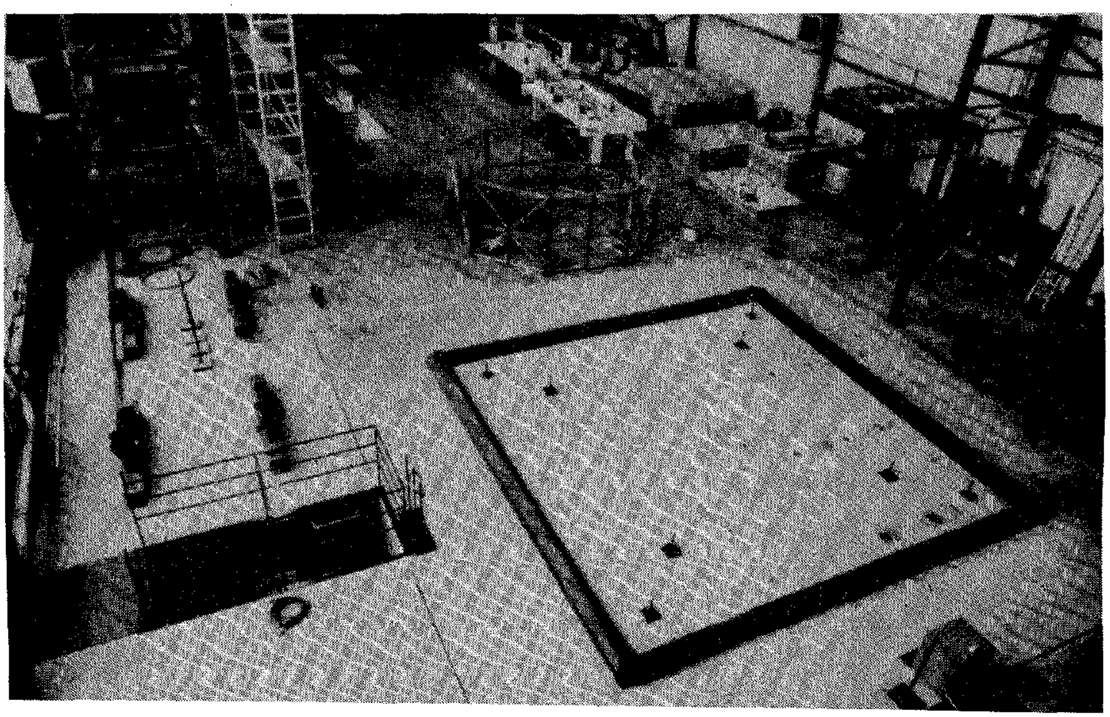

(b) Shaking Table

Fig. 2.1.1 Earthquake Simulator

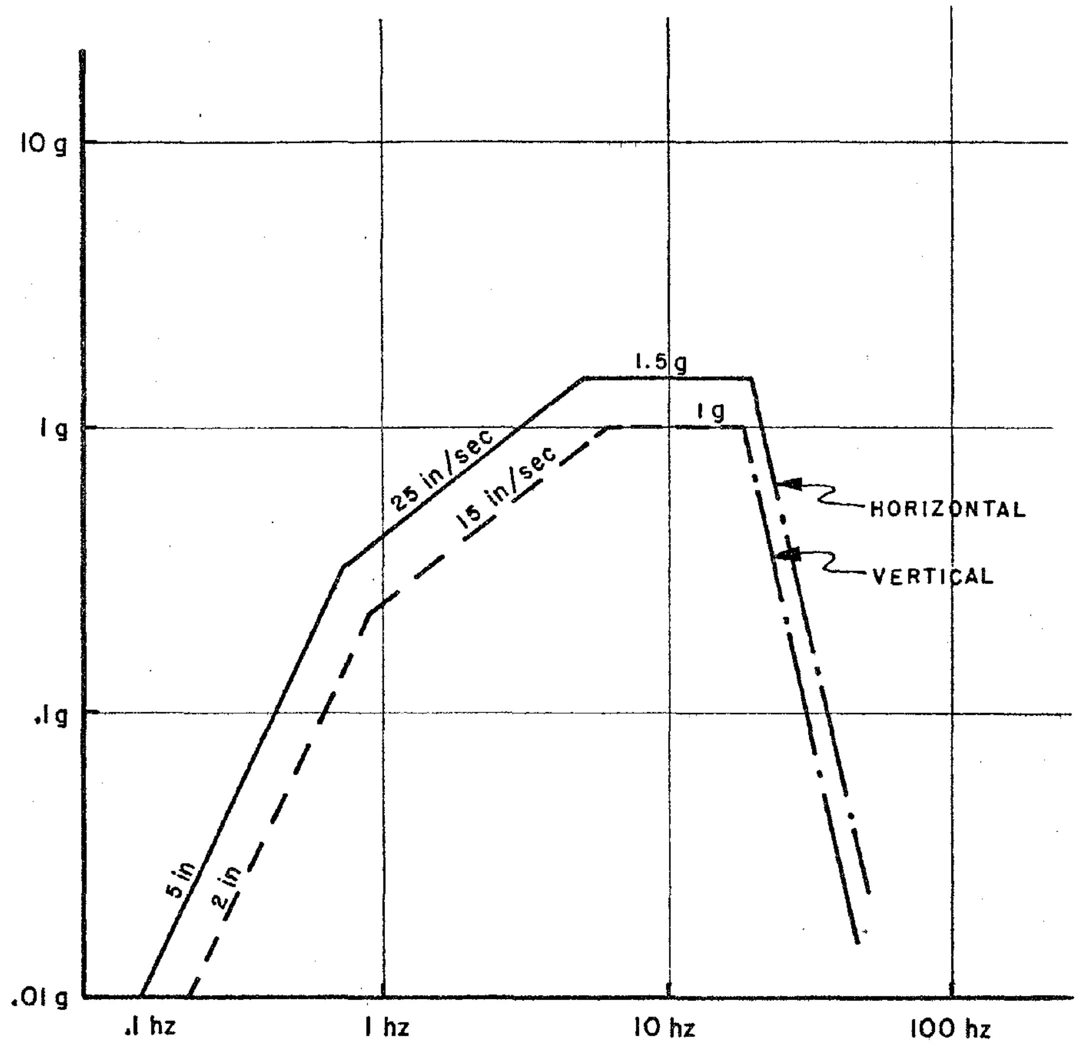

Fig. 2.1.2 Shaking Table Motion Limits

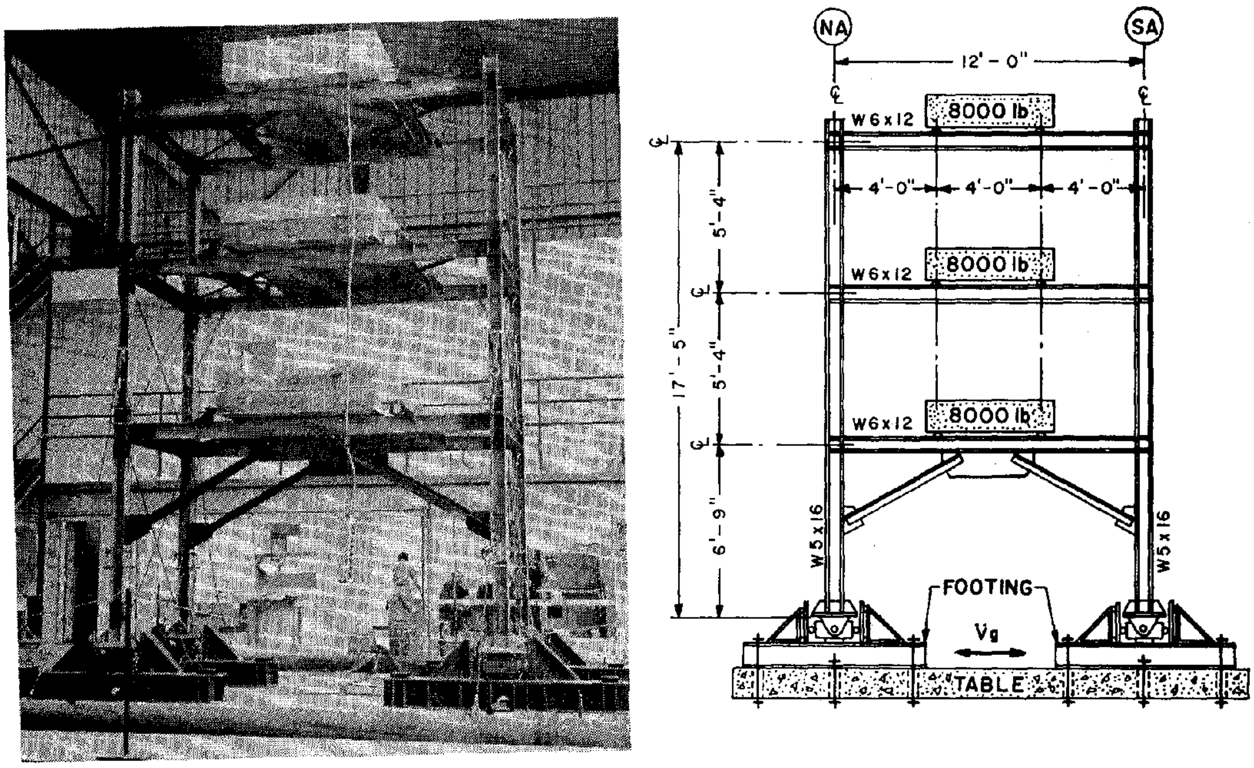

Fig. 2.2.1 Test Model

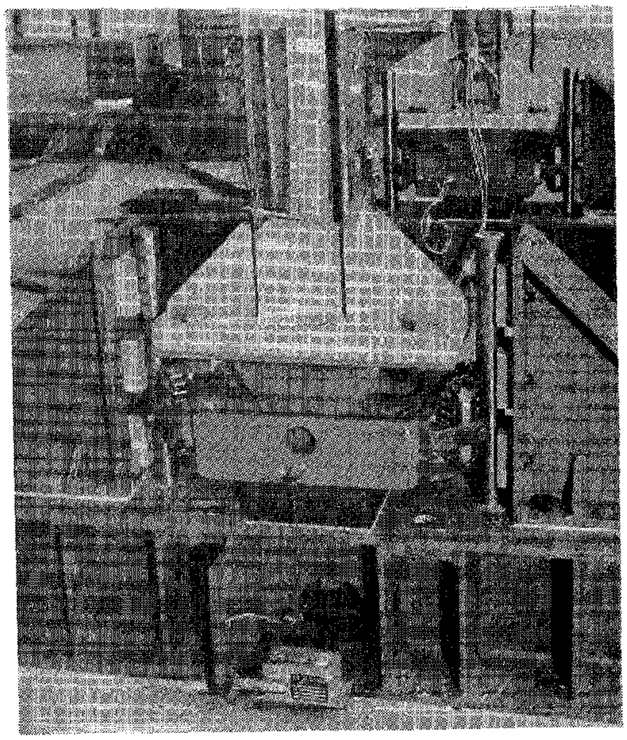

Fig. 2.2.2 Uplift Mechanism Detail

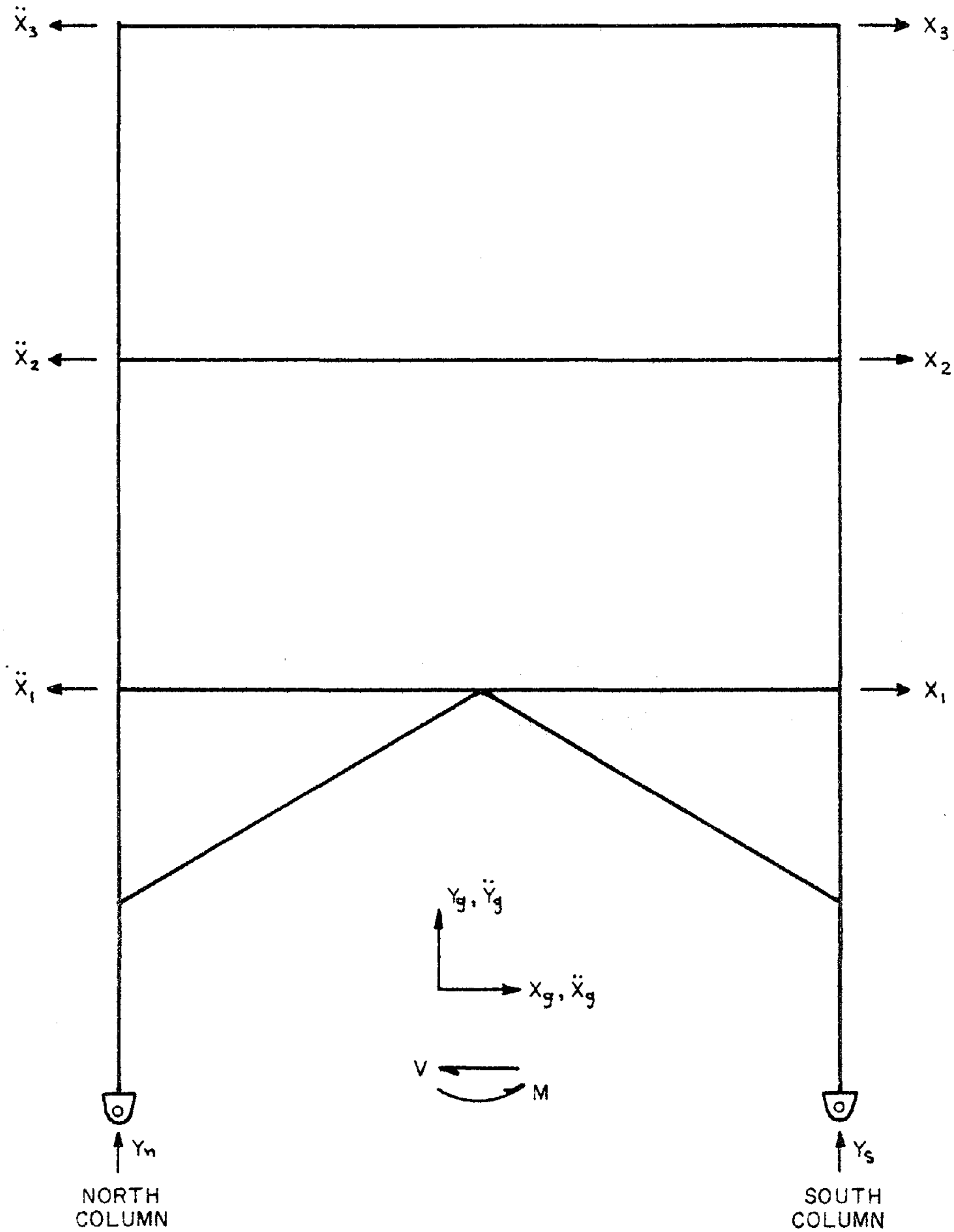

Fig. 2.3.1 Global Response Sign Convention

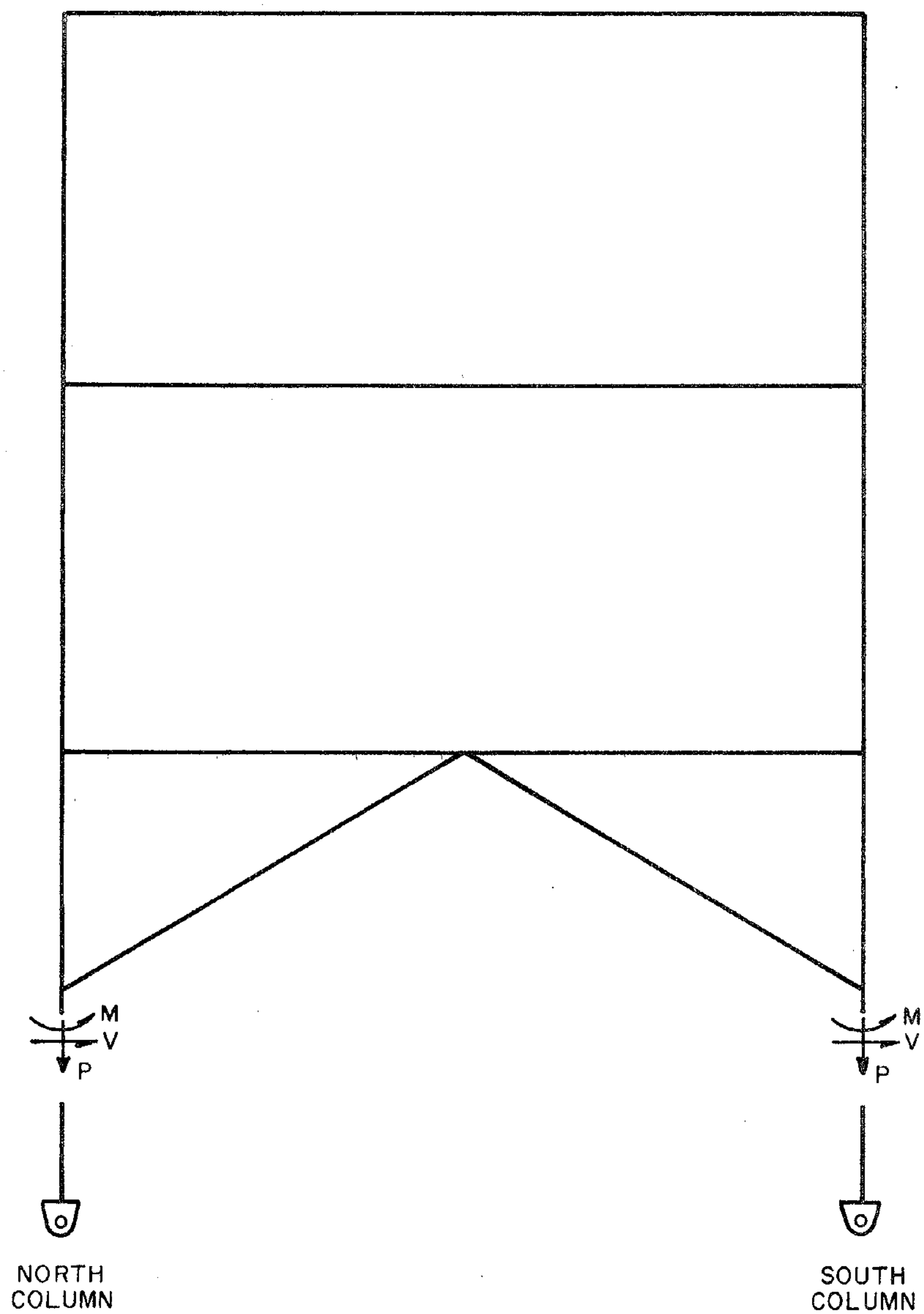

Fig. 2.3.2 Local Response Sign Convention

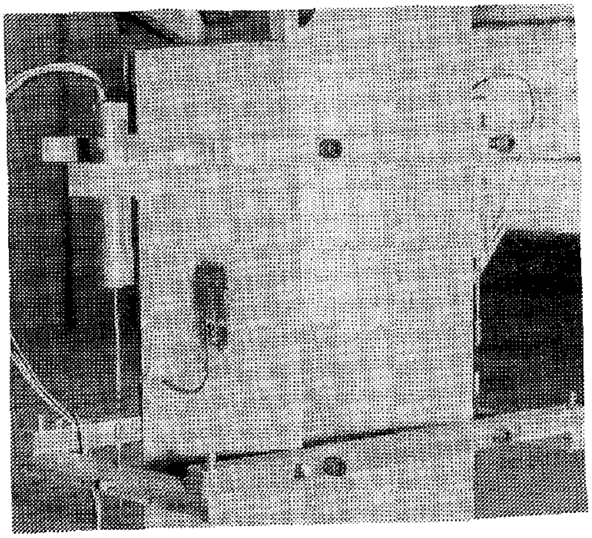

a. Column

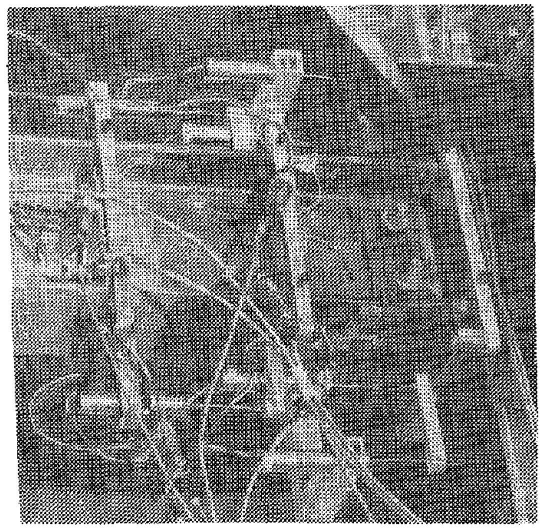

b. Girder

Fig. 2.3.3 Average Curvature Measurement

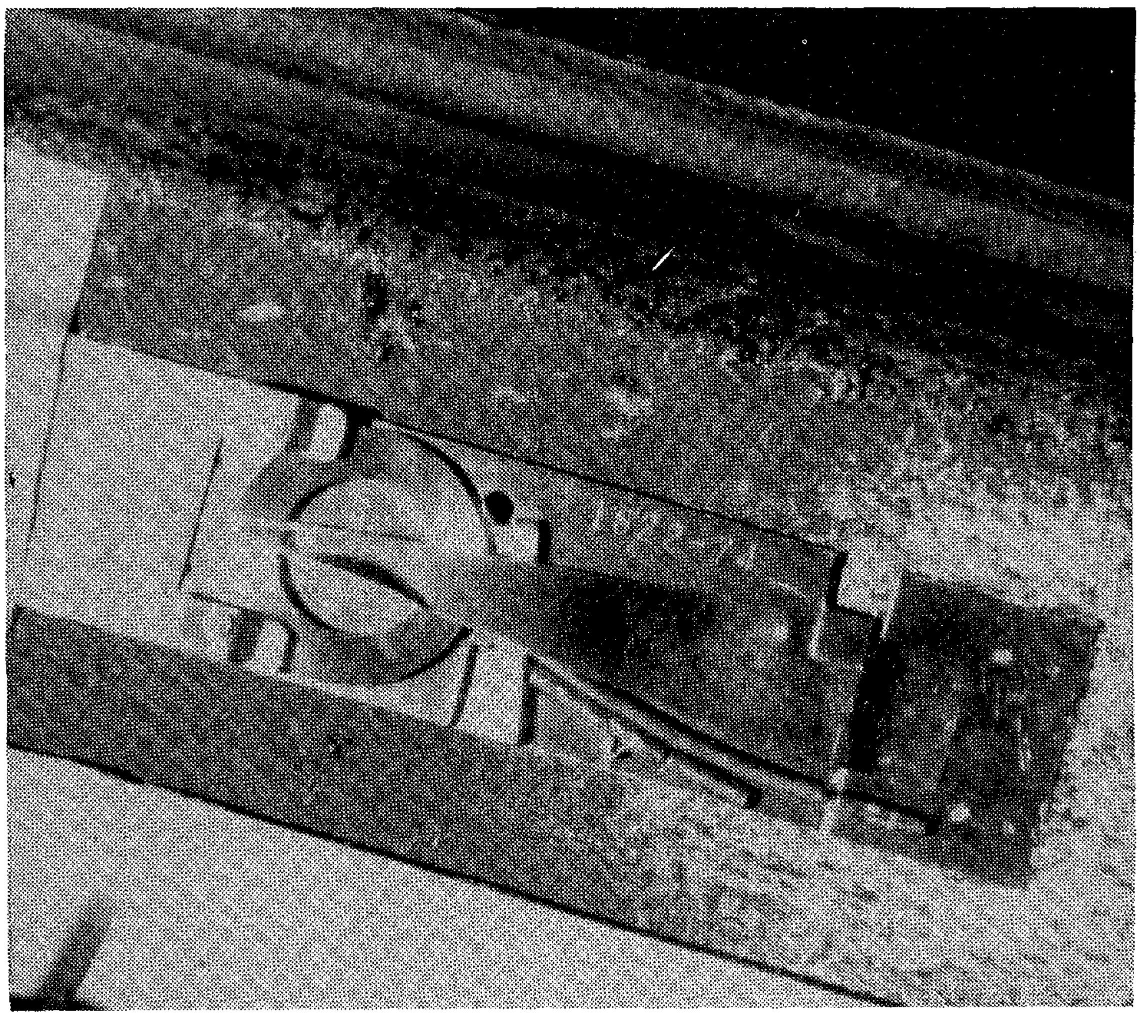

Fig. 2.3.4 Mechanical Strain Gage

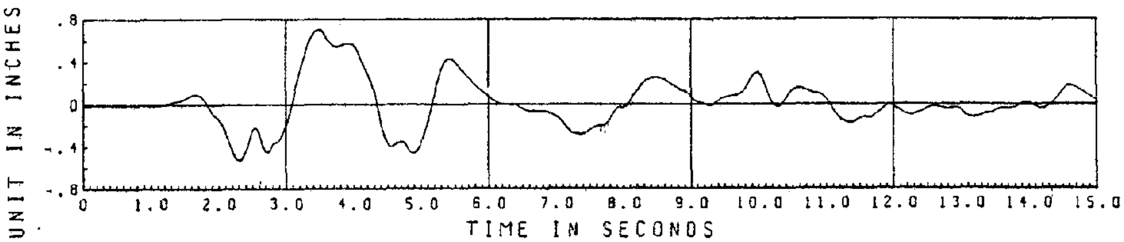

Table Displacement

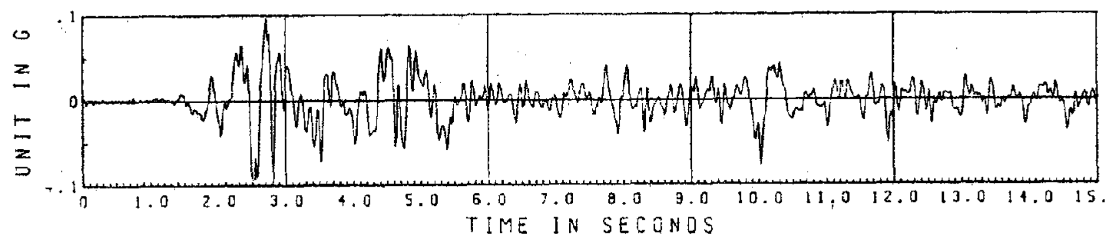

Table Acceleration

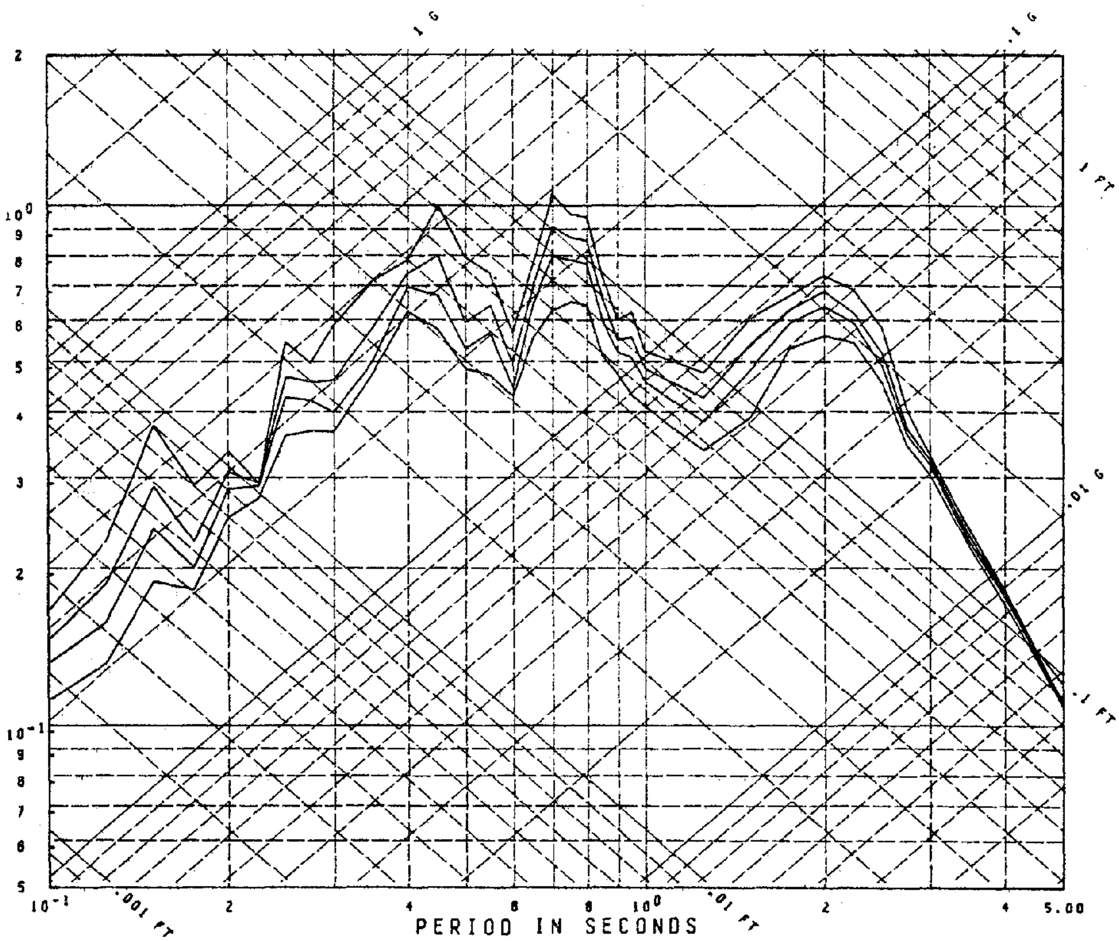

EC 200 I

Fig. 2.4.1 Response Spectra; Damping Ratios = .01, .02, .03, .05

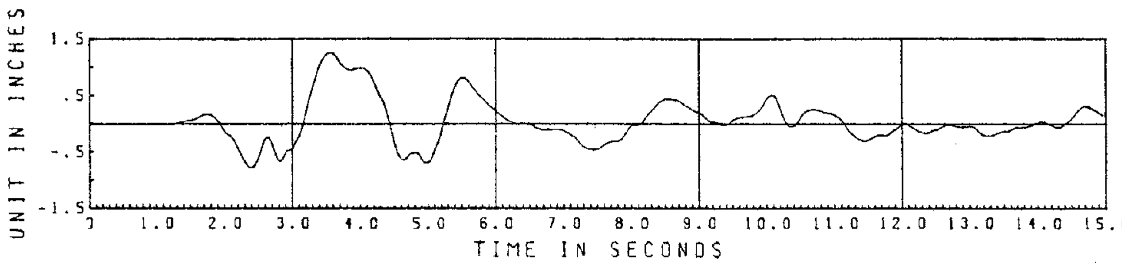

Table Displacement

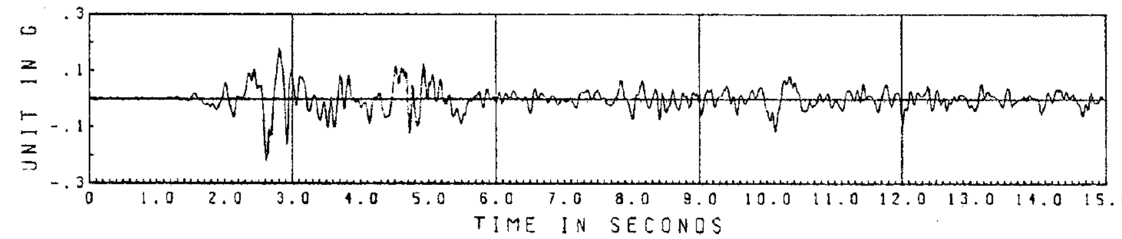

Table Acceleration

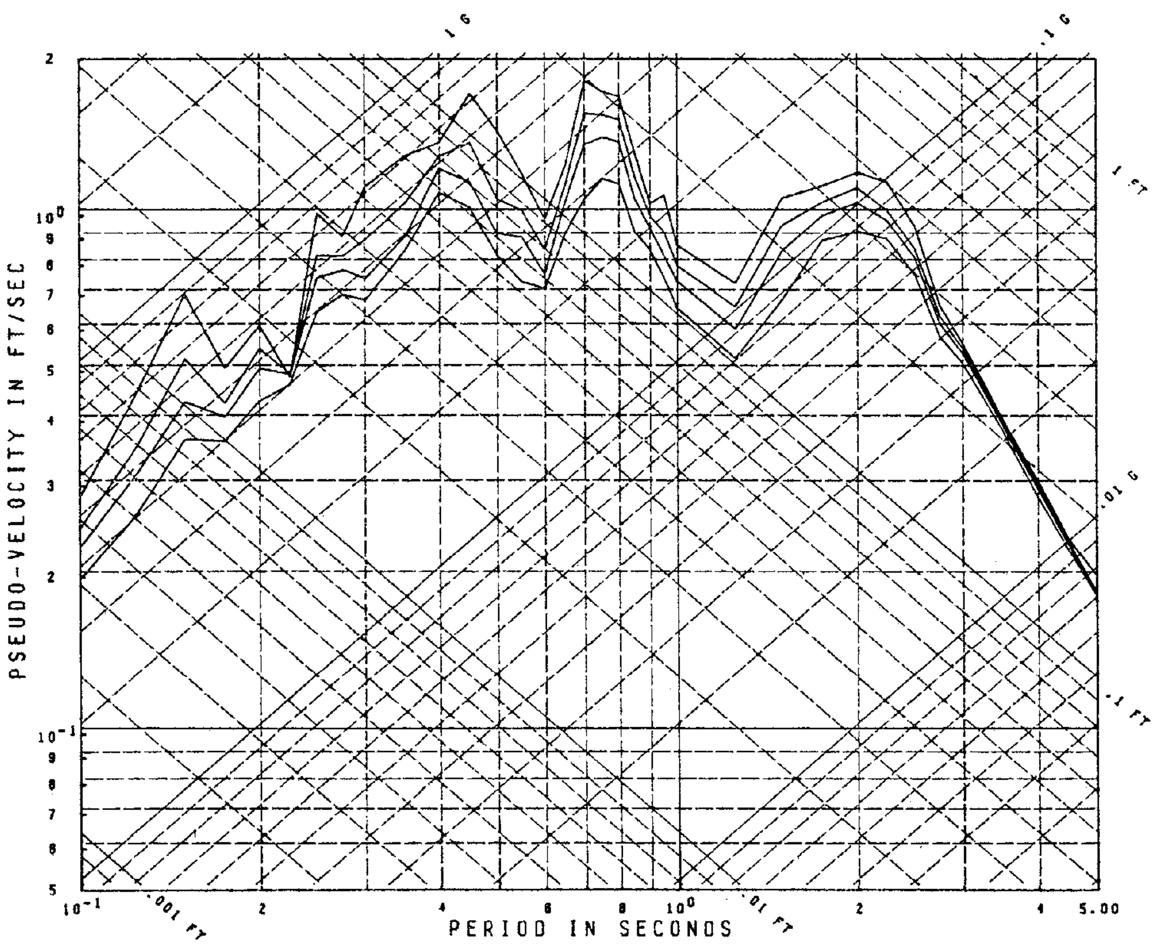

EC 100 II

Fig. 2.4.2 Response Spectra; Damping Ratios = .01, .02, .03, .05

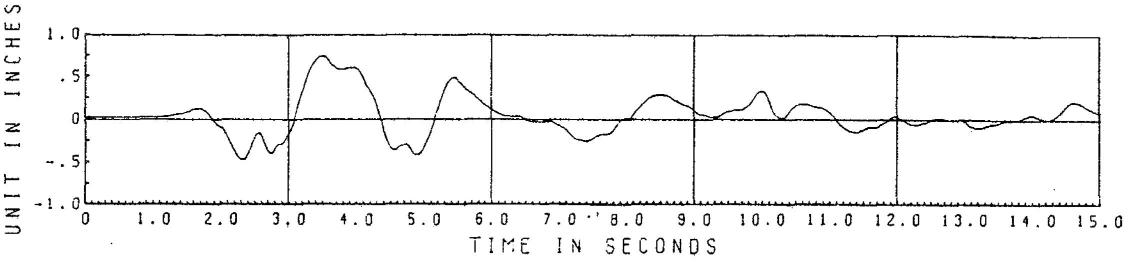

Table Displacement

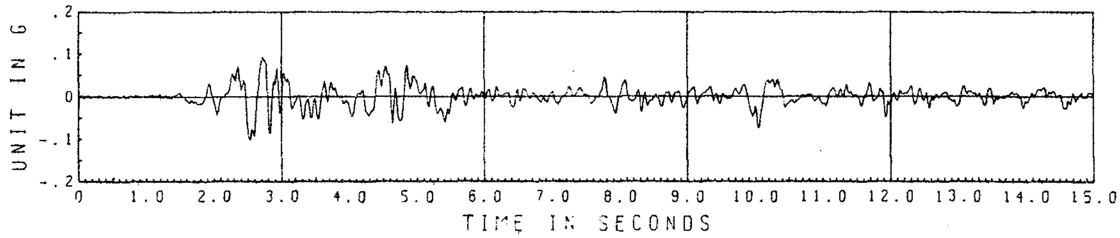

Table Acceleration

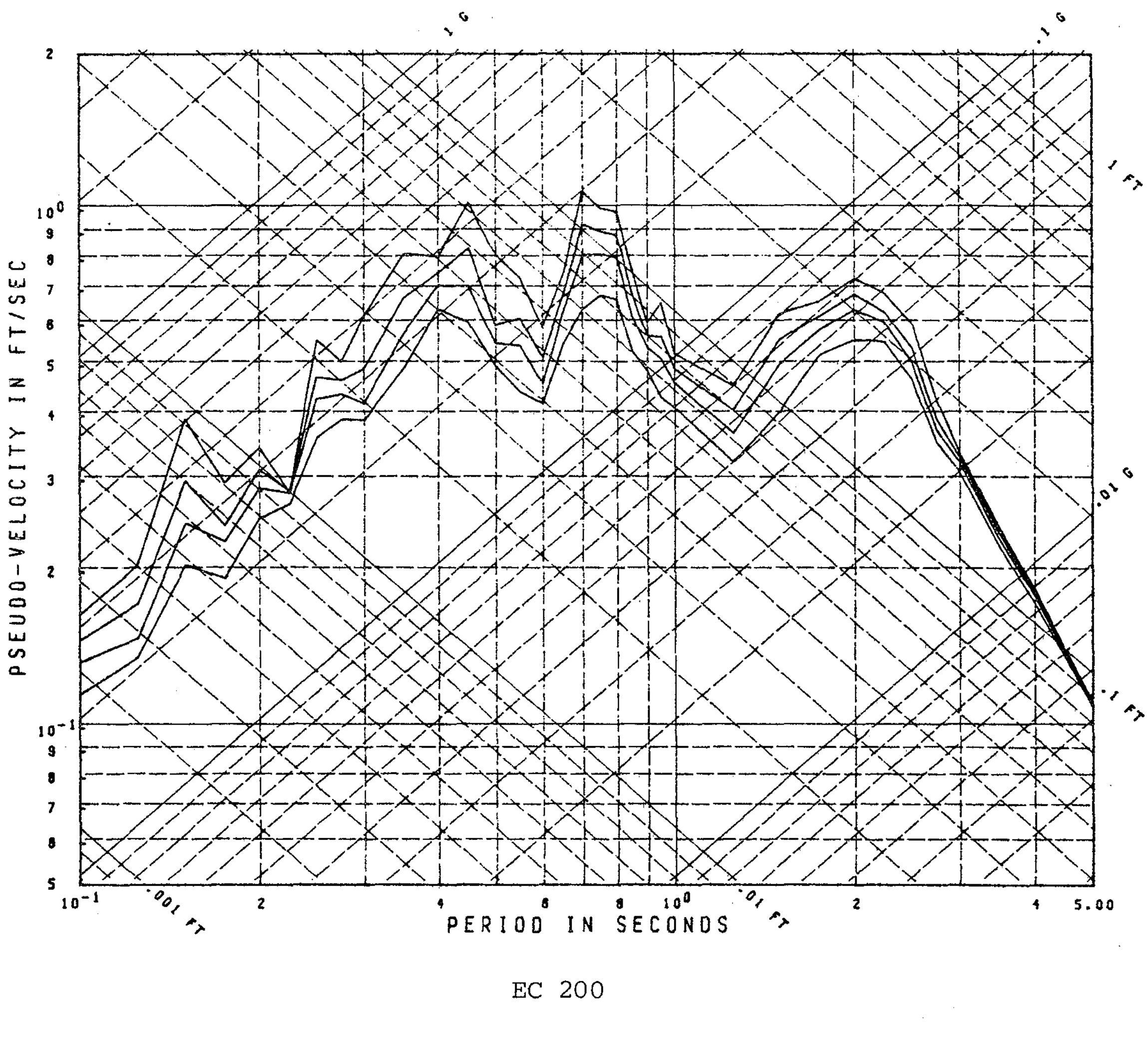

EC 200

Fig. 2.4.3 Response Spectra; Damping Ratios = .01, .02, .03, .05

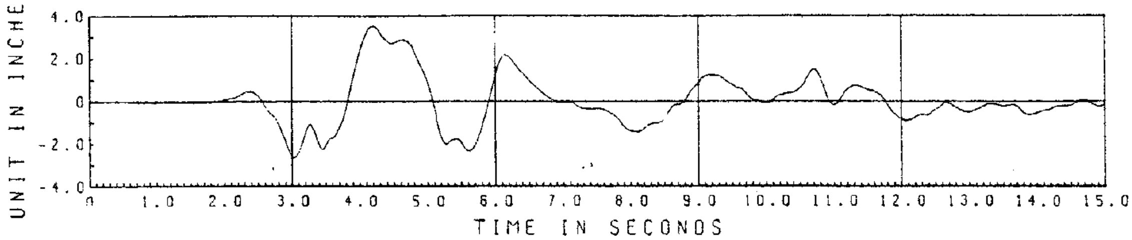

Table Displacement

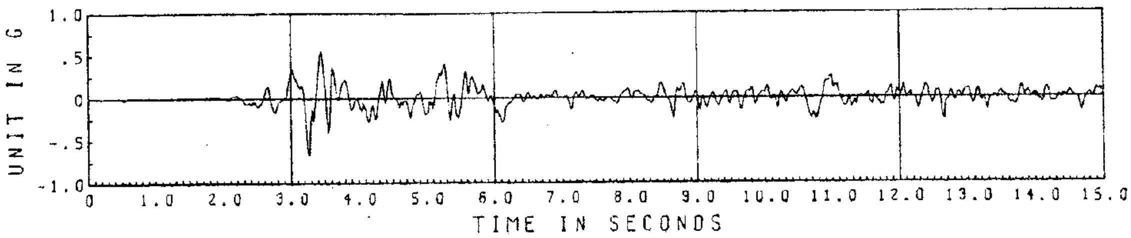

Table Acceleration

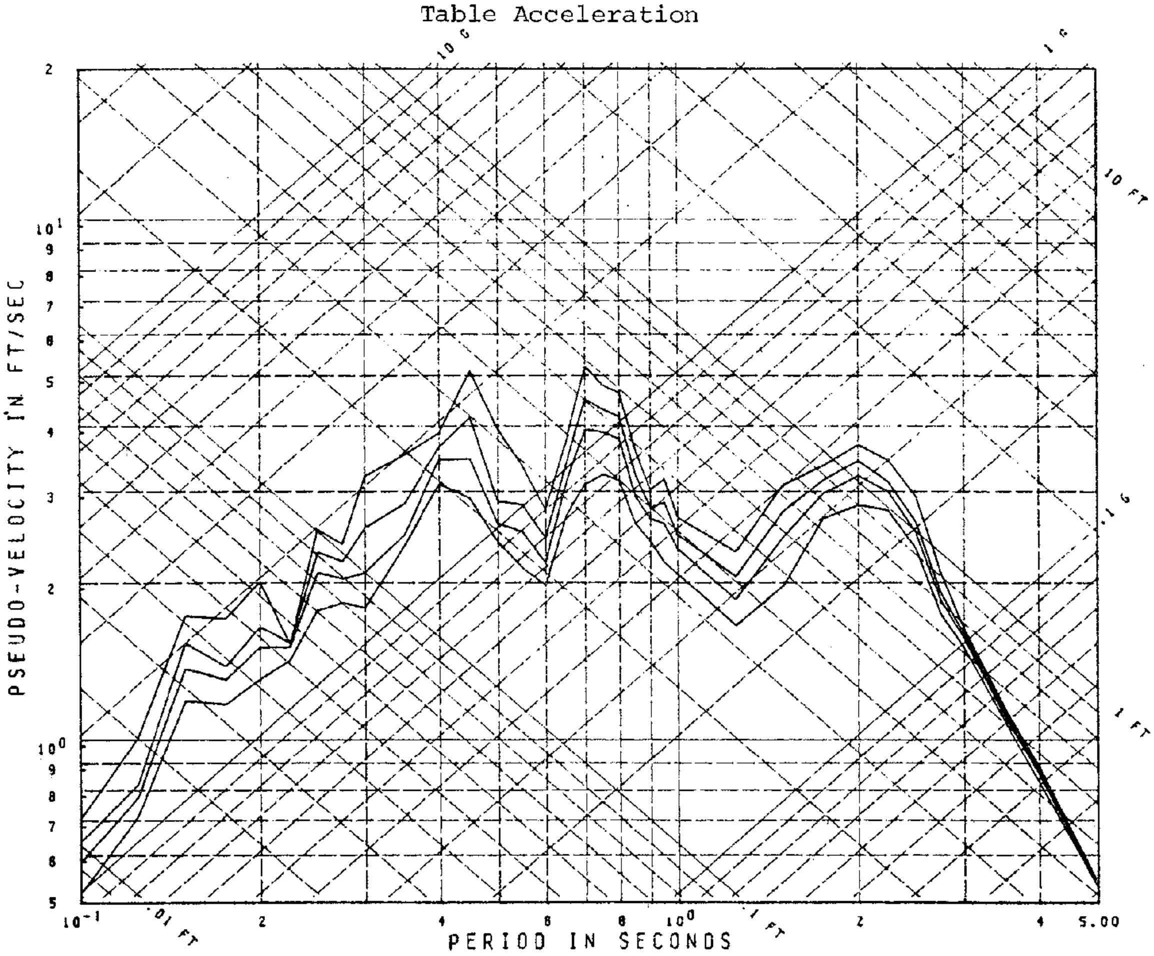

EC 1000 I

Fig. 2.4.4 Response Spectra; Damping Ratios = .01, .02, .03, .05

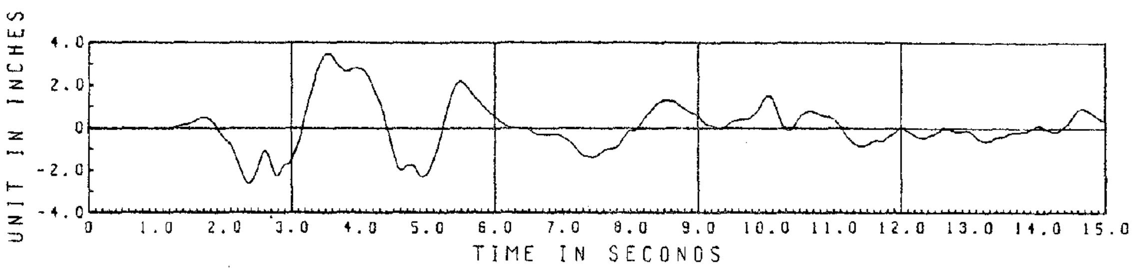

Table Displacement

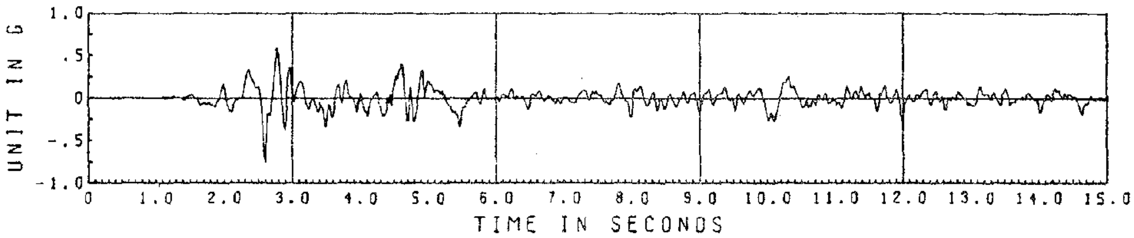

Table Acceleration

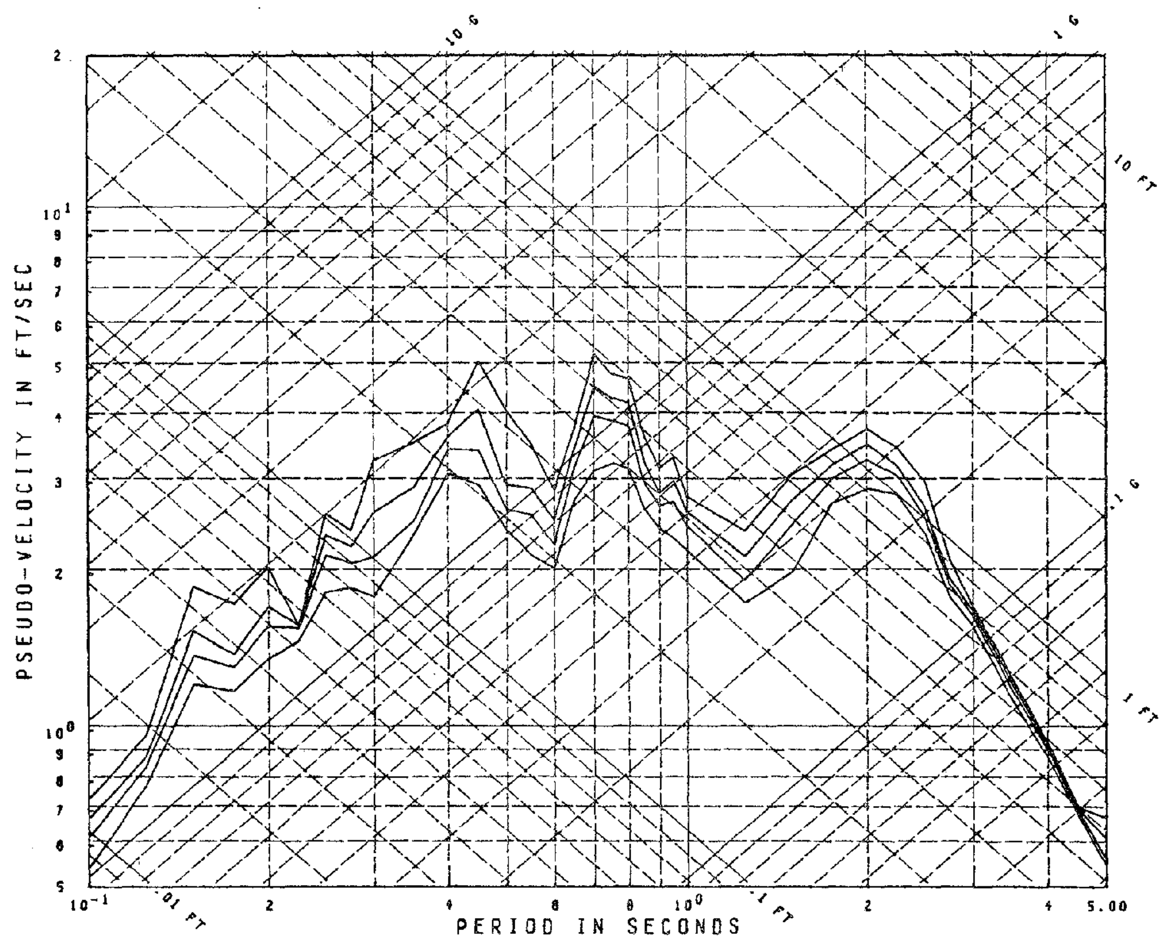

EC 1000/850 I

Fig. 2.4.5 Response Spectra; Damping Ratios = .01, .02, .03, .05

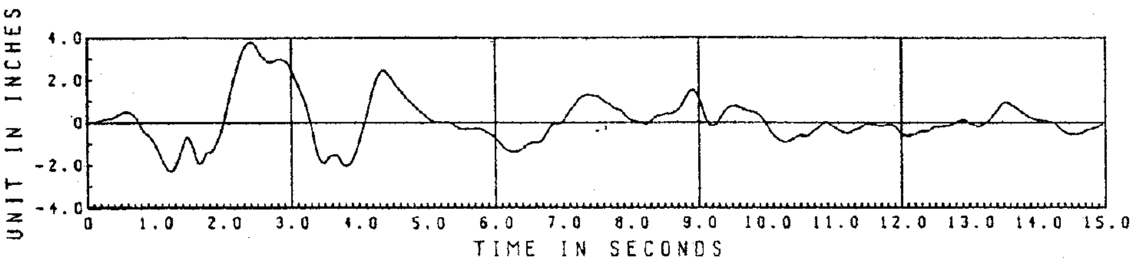

Table Displacement

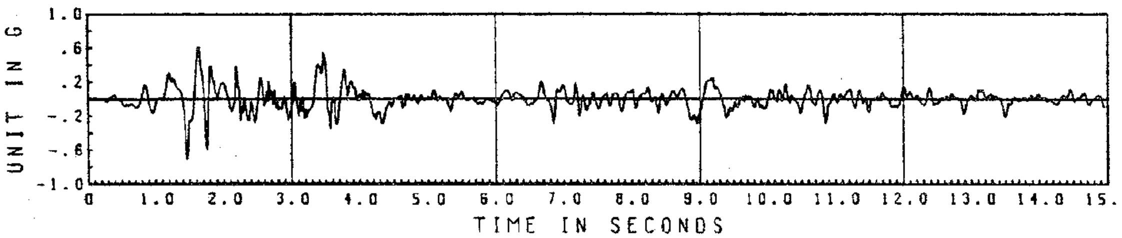

Table Acceleration

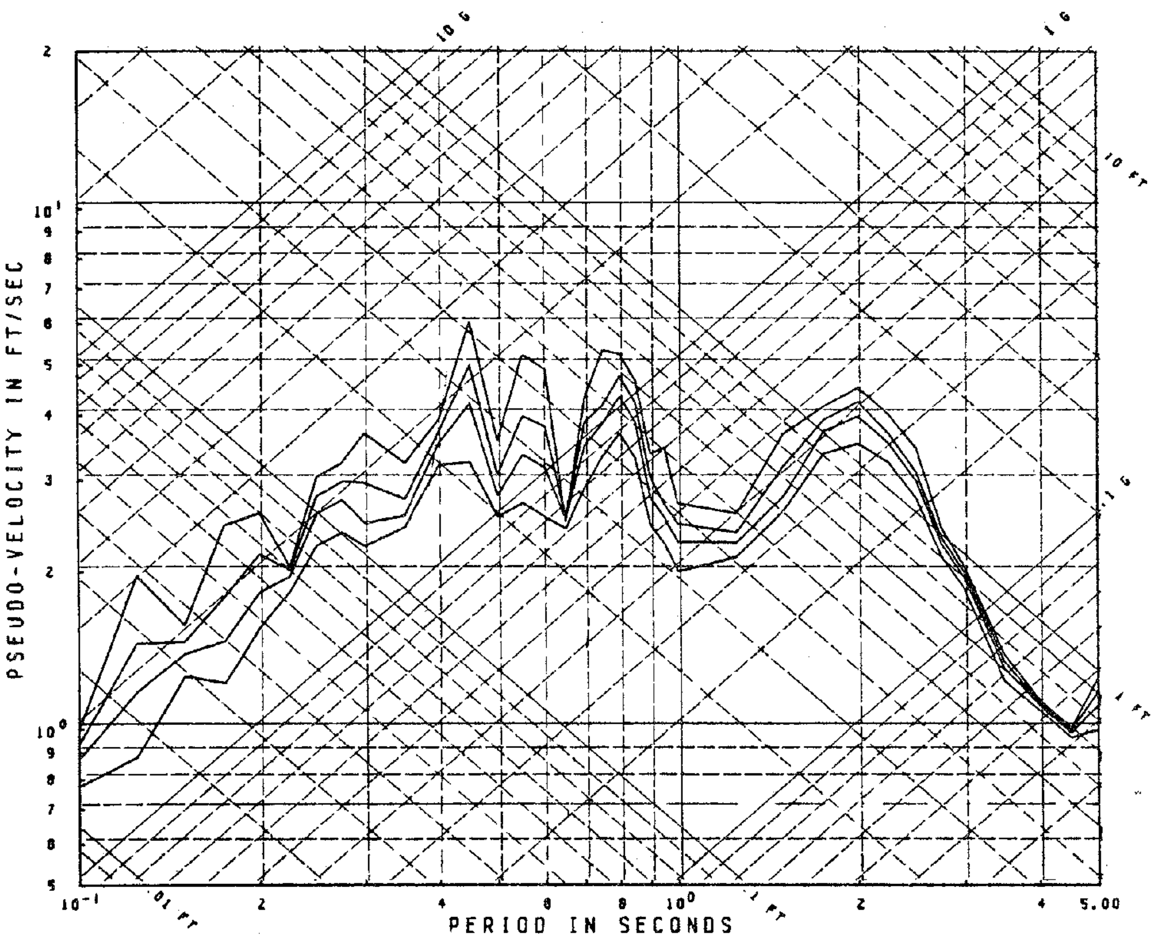

EC 300 II

Fig. 2.4.6 Response Spectra; Damping Ratios = .01, .02, .03, .05

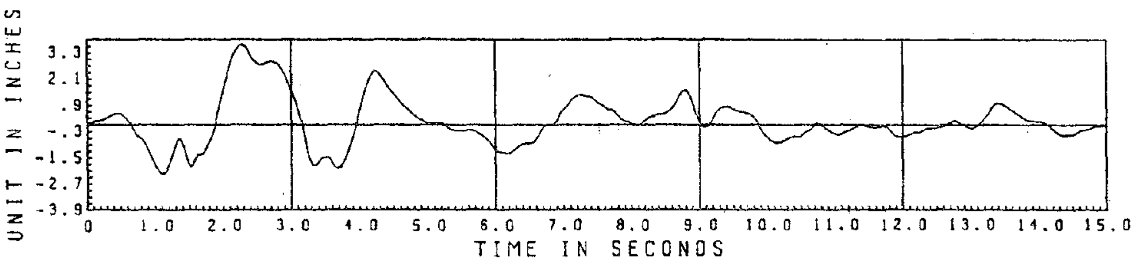

Table Displacement

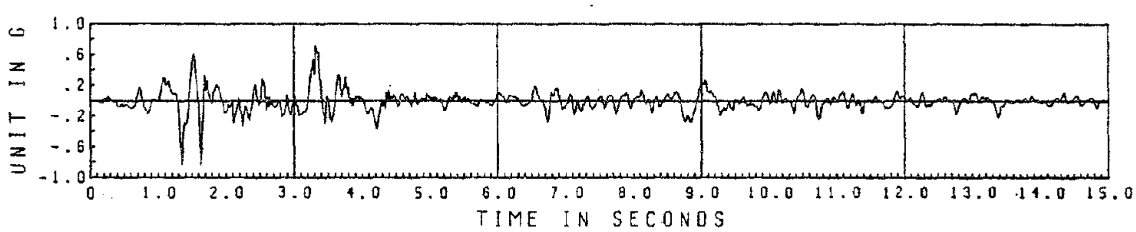

Table Acceleration

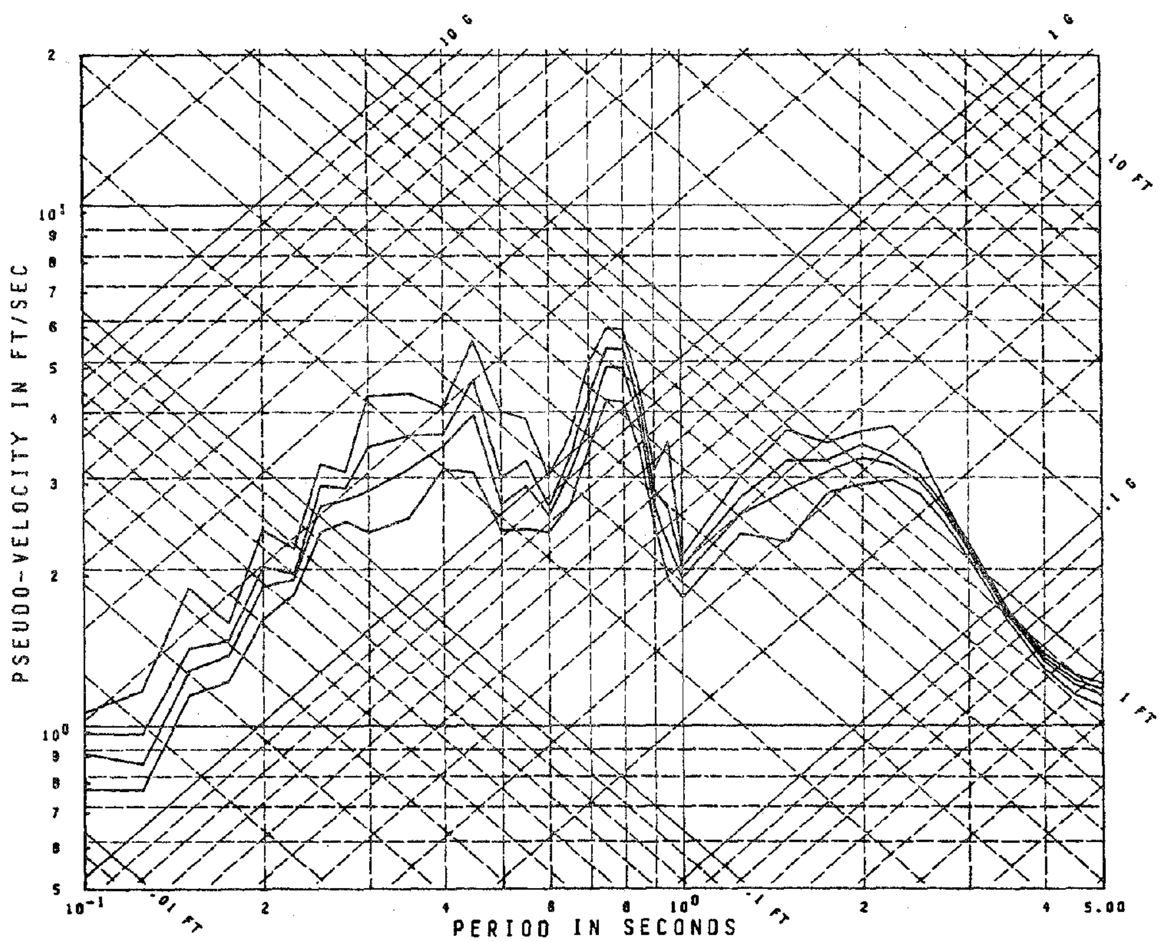

EC 300/675 II

Fig. 2.4.7 Response Spectra; Damping Ratios = .01, .02, .03, .05

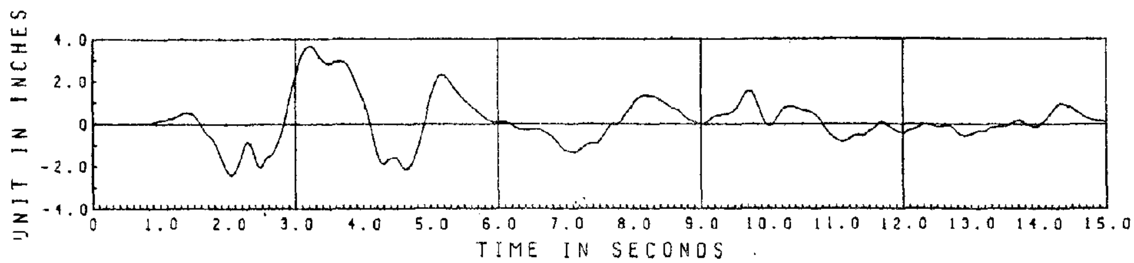

Table Displacement

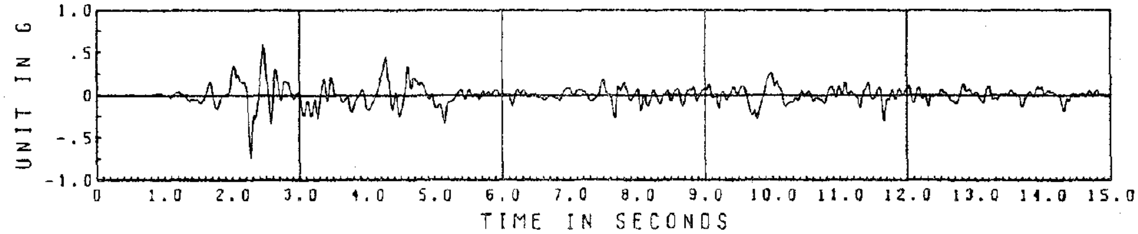

Table Acceleration

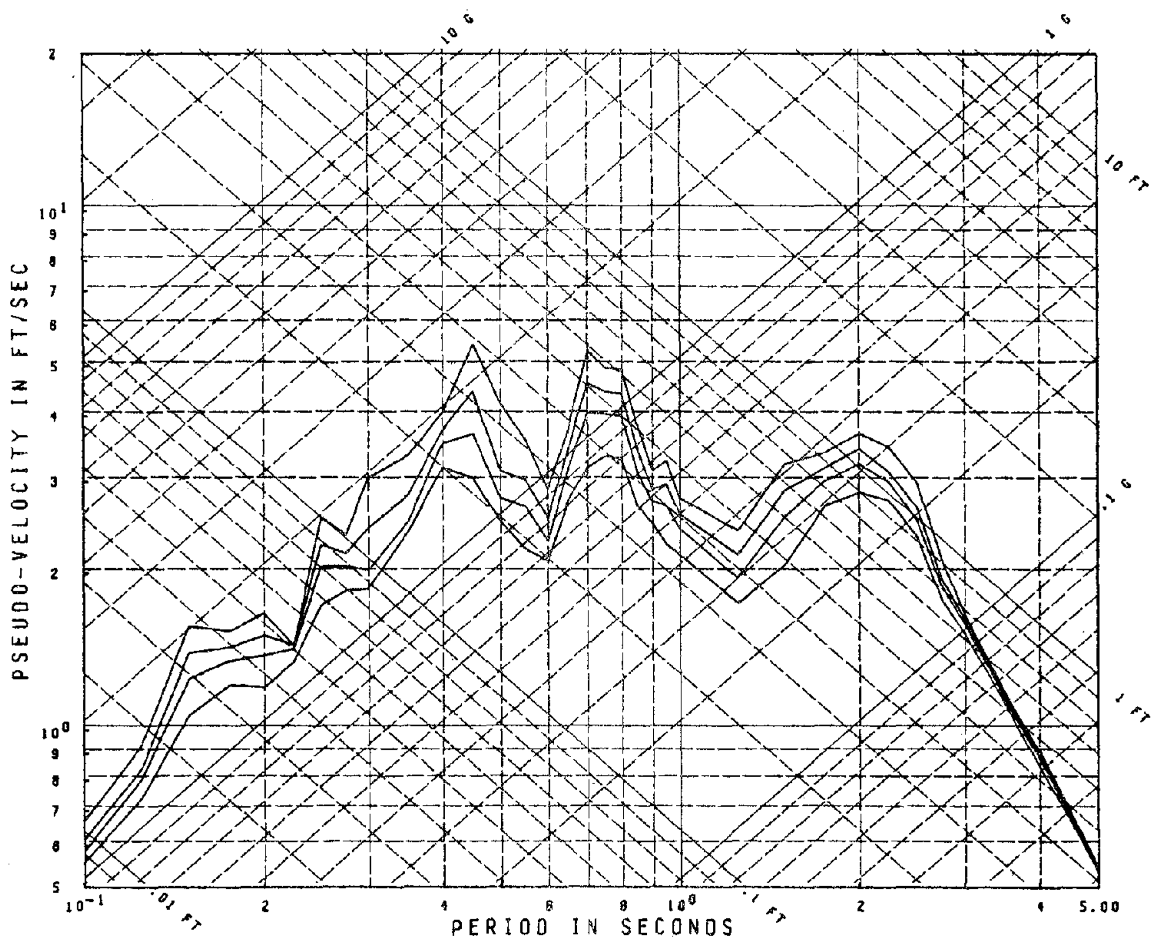

FC 1000

Fig. 2.4.8 Response Spectra; Damping Ratios = .01, .02, .03, .05

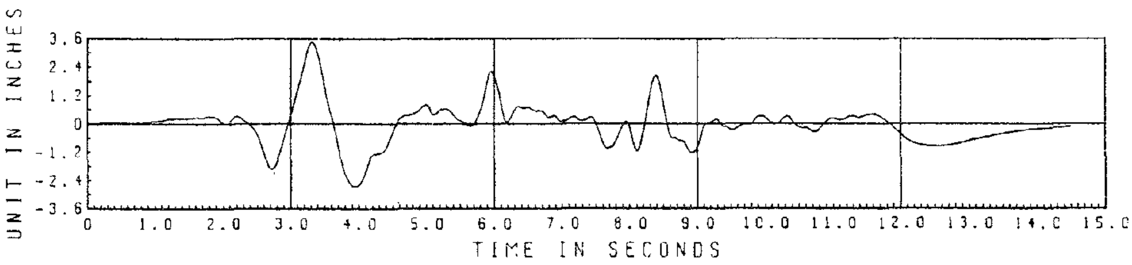

Table Displacement

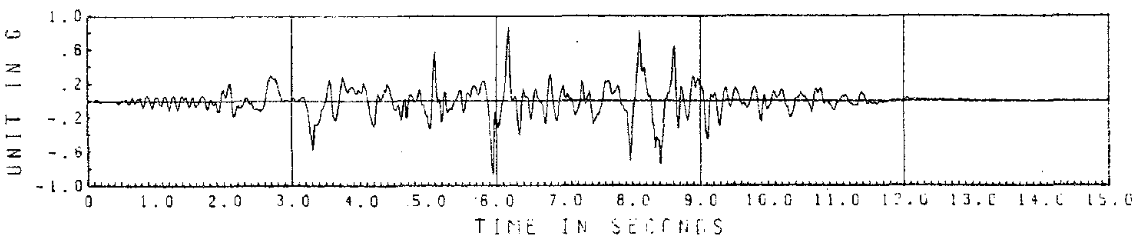

Table Acceleration

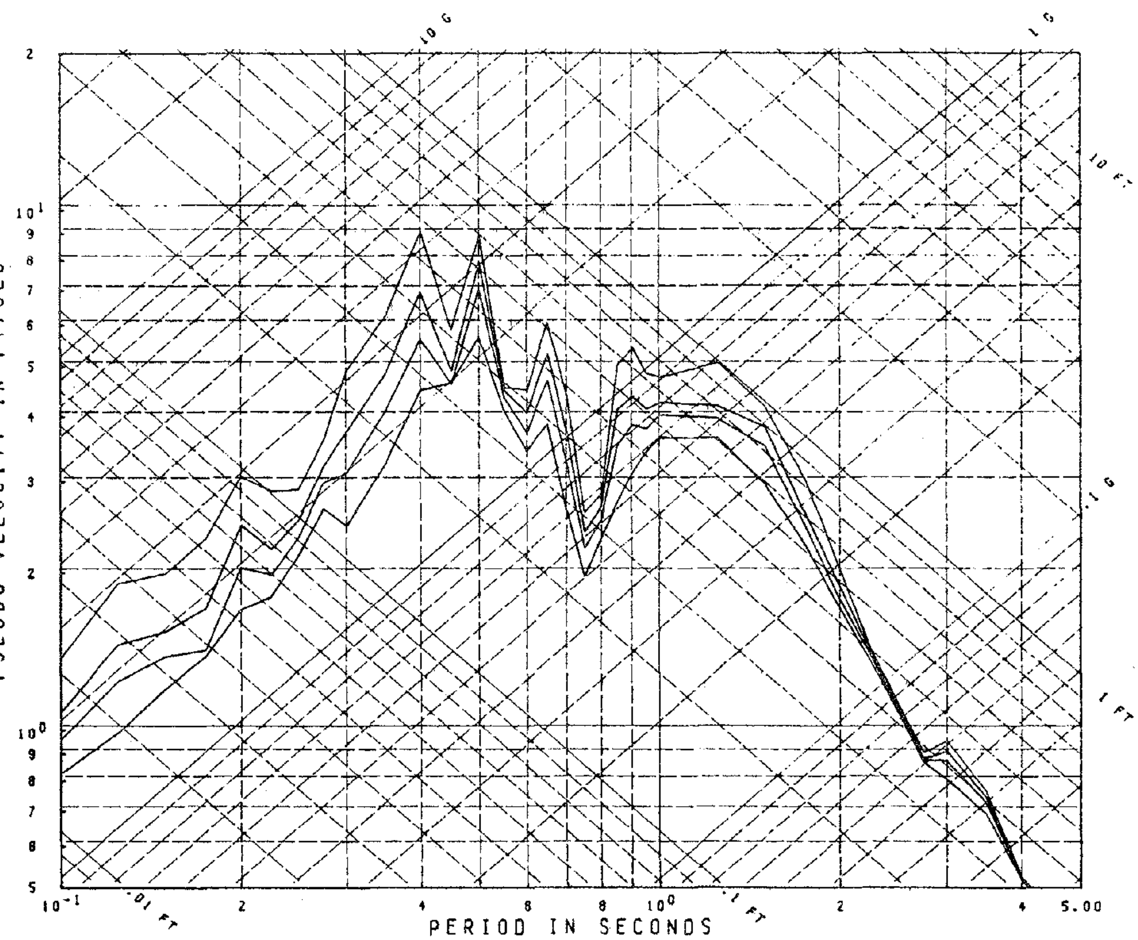

PAC 400 I

Fig. 2.4.9 Response Spectra; Damping Ratio = .01, .02, .03, .05

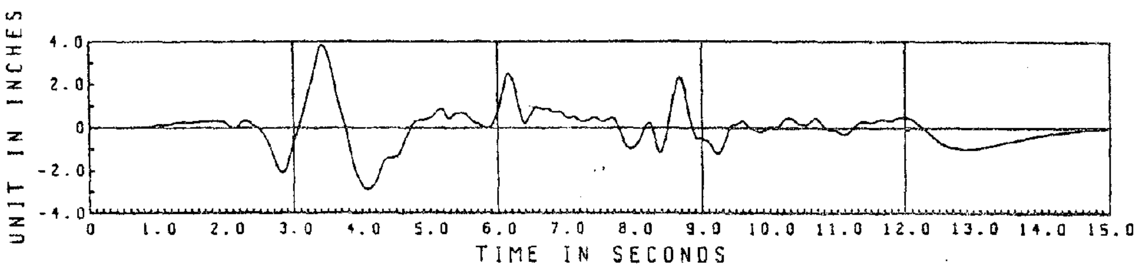

Table Displacement

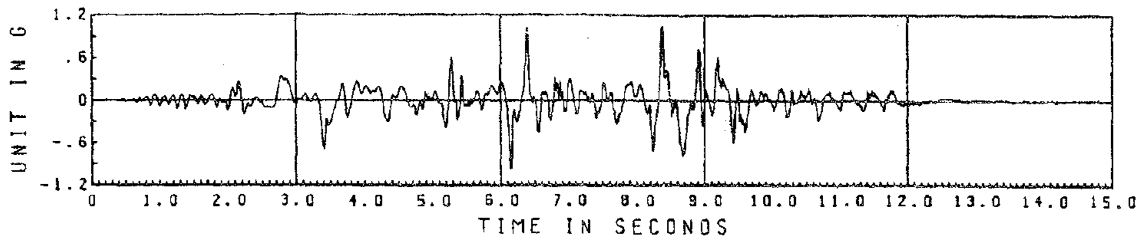

Table Acceleration

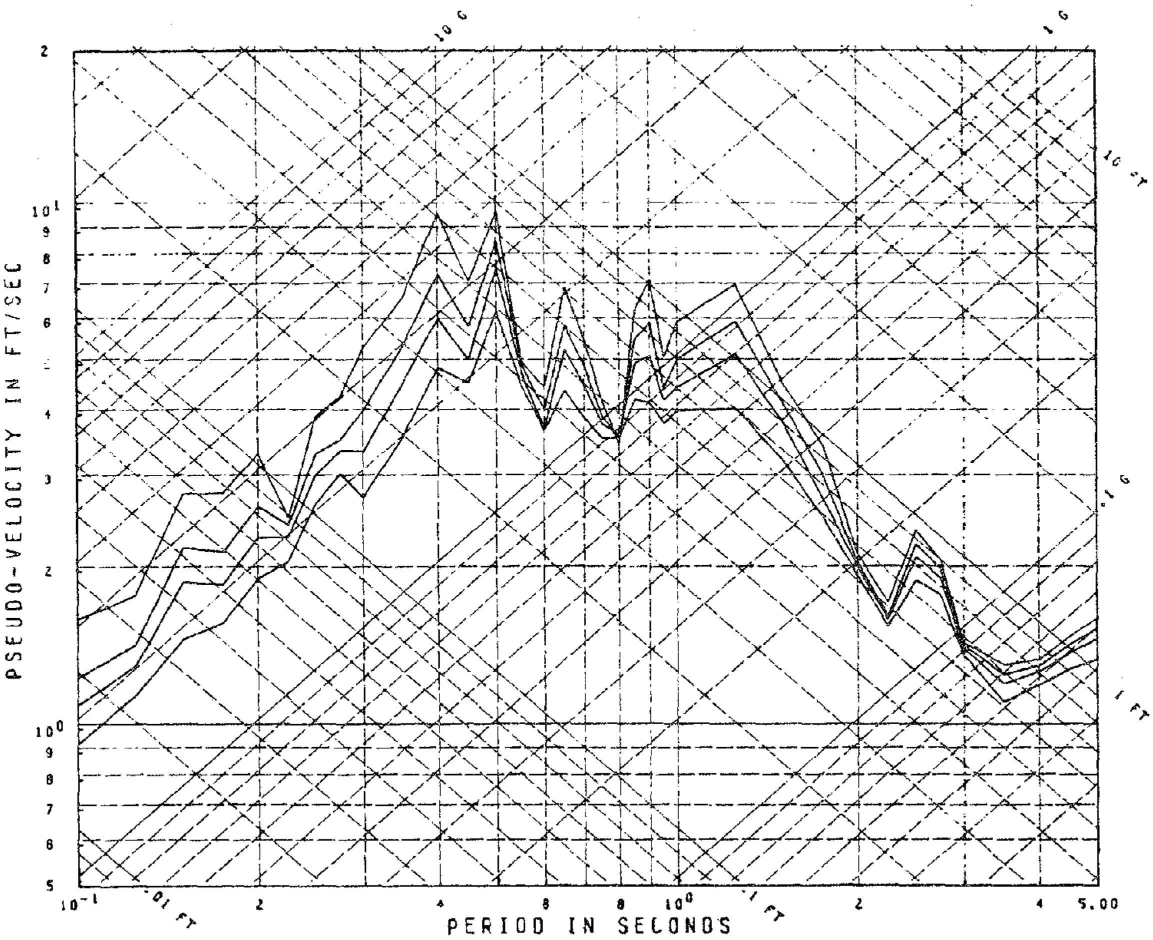

PAC 700 II

Fig. 2.4.10 Response Spectra; Damping Ratios = .01, .02, .03, .05

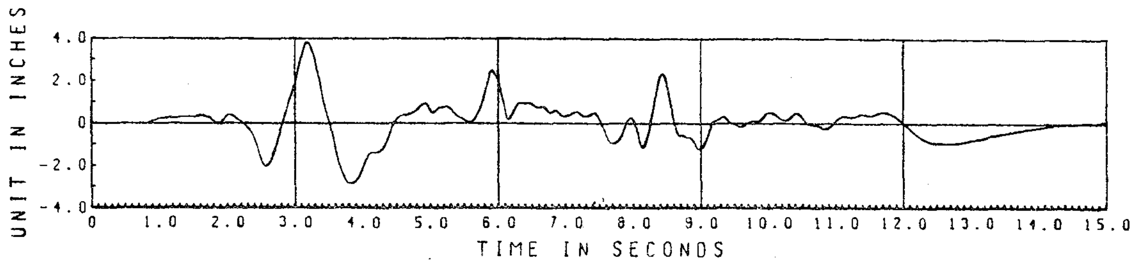

Table Displacement

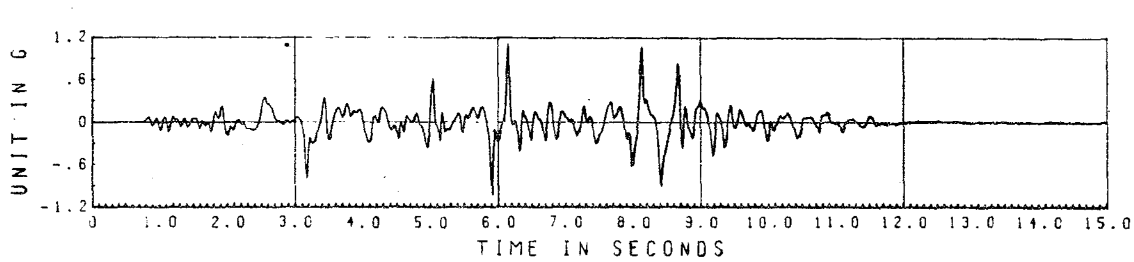

Table Acceleration

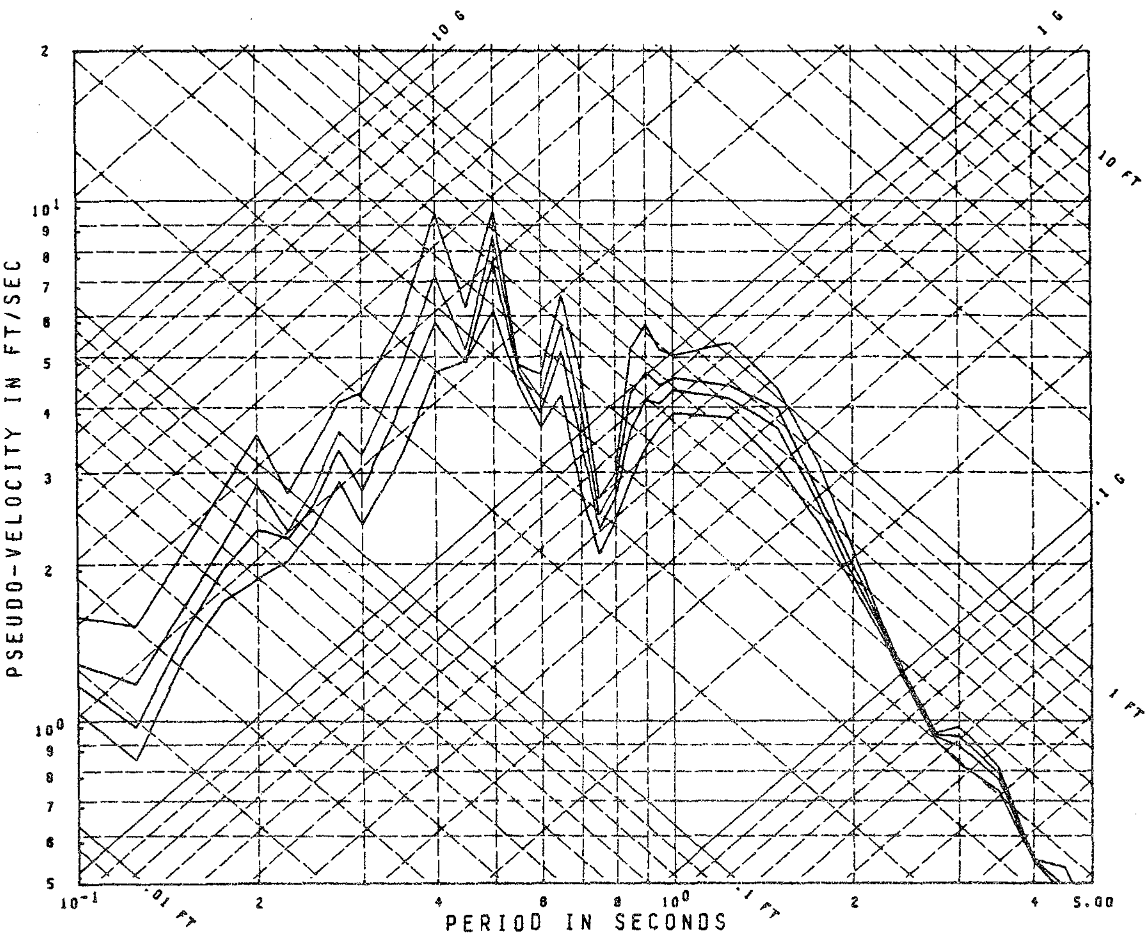

PAC 700

Fig. 2.4.11 Response Spectra; Damping Ratios = .01, .02, .03, .05

Table 2.5.1 Selected Envelope Data Quantities

No.	Test	Max. Table Acc. (g)	Max. Table Displ. (in)	Max. 3rd Flr. Rel. Displ. (in)	Max. Base Shear (%W)	Estimated Max. Strain Ductility
1	EC 200 I	.10	.70	.85	30	.25
2	EC 100 II	.22	1.25	1.1	50	.4
3	EC 200	.10	.75	.50	30	.25
4	EC 1000 I	.67	3.50	6.0	80	.6
5	EC 1000/850 I	.76	3.47	6.4	80	.6
6	EC 300 II	.72	3.80	5.3	90	.8
7	EC 300/675 II	.84	3.65	5.3	90	.8
8	EC 1000	.74	3.67	2.4	120	3.
9	PAC 400 I	.88	3.45	3.3	80	.8
10	PAC 700 II	1.04	3.86	3.5	90	.8
11	PAC 700	1.11	3.84	3.3	130	5.

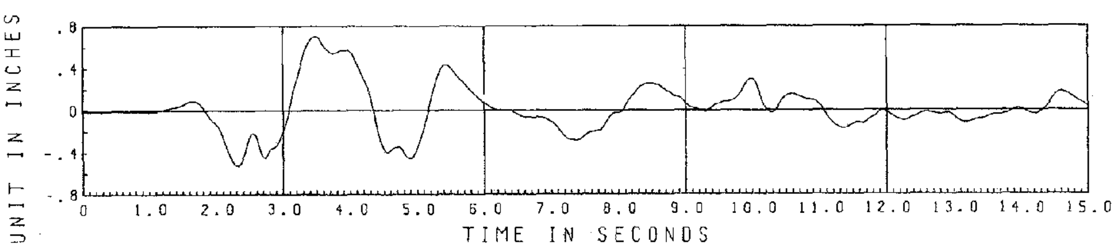

Table Displacement

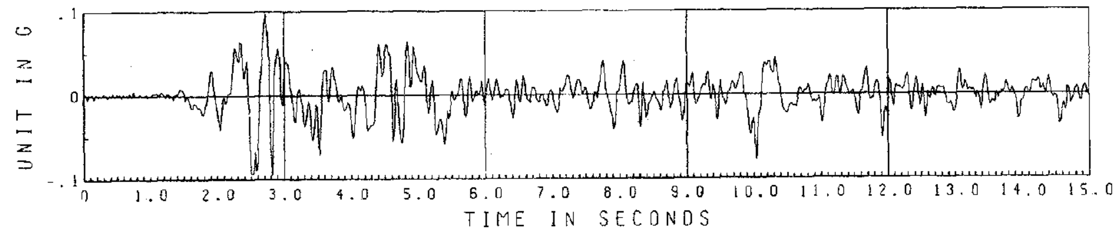

Table Acceleration

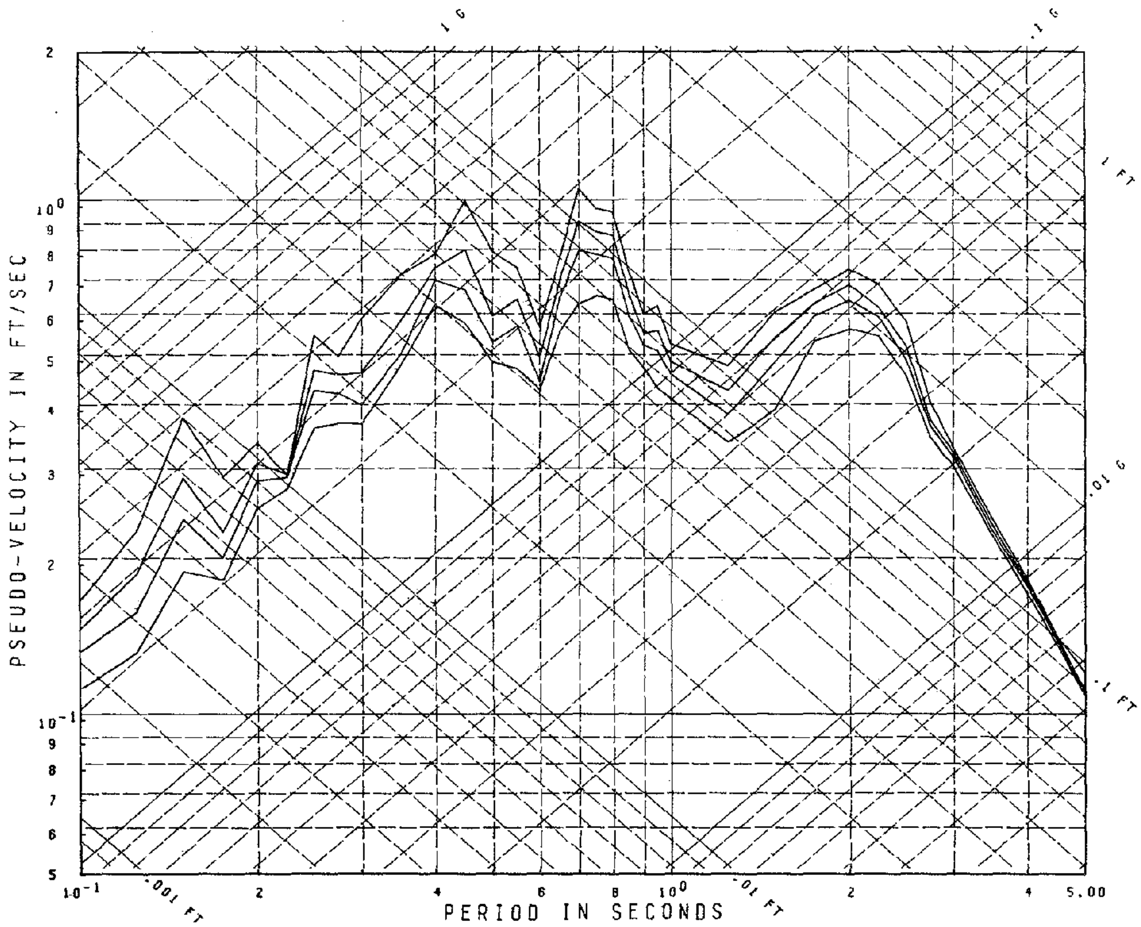

EC 200 I

Fig. 2.5a.1 Response Spectra, Damping Ratios = .01, .02, .03, .05

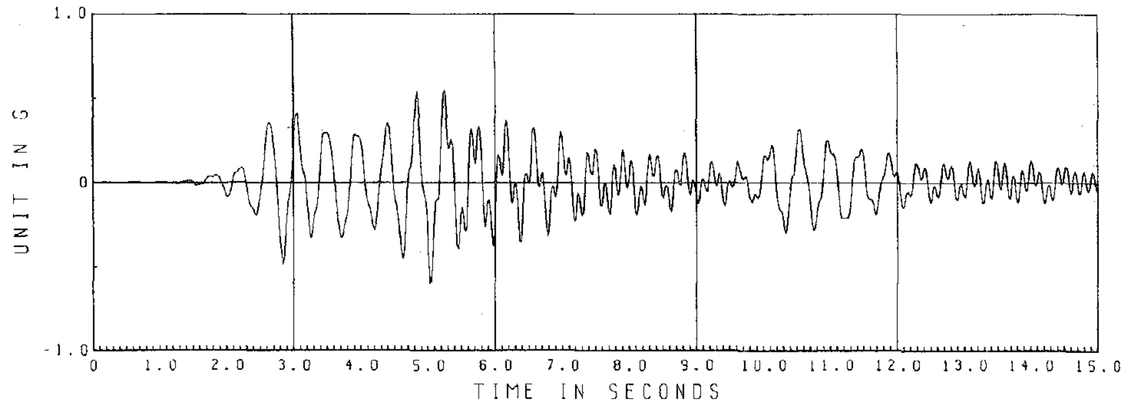

3rd Floor Acceleration

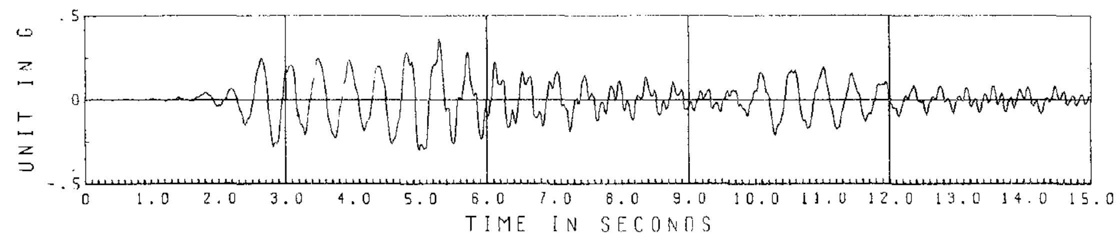

2nd Floor Acceleration

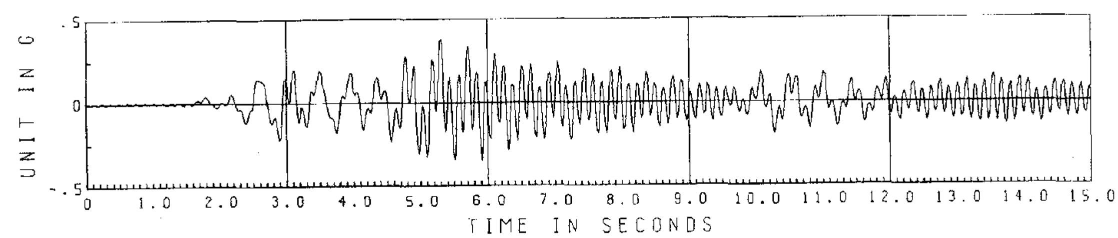

1st Floor Acceleration

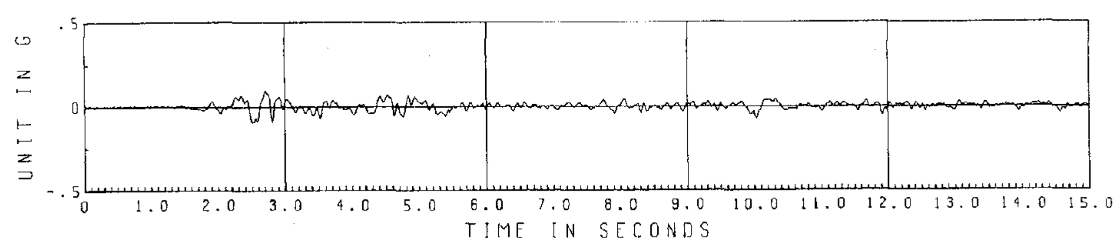

Table Acceleration

Fig. 2.5a.2 EC 200 I Accelerations

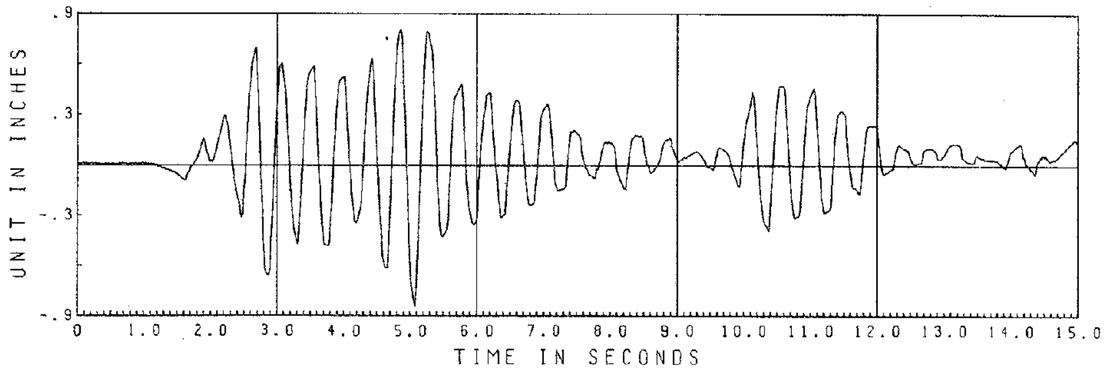

3rd Floor Relative Displacement

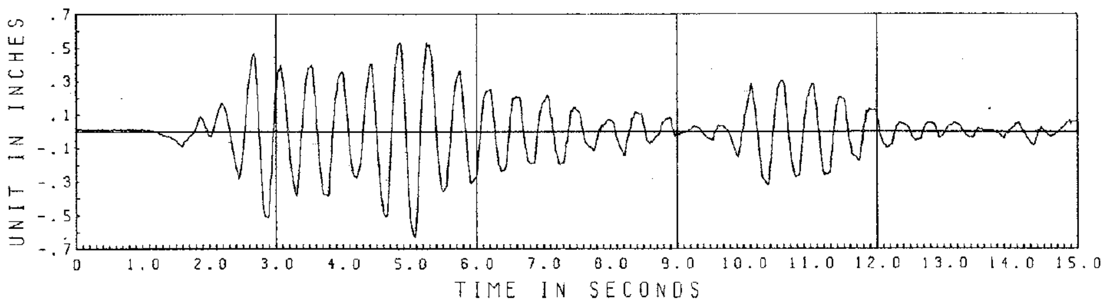

2nd Floor Relative Displacement

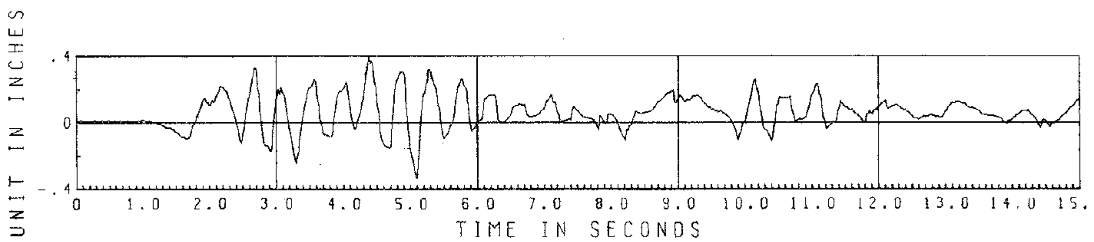

1st Floor Relative Displacement

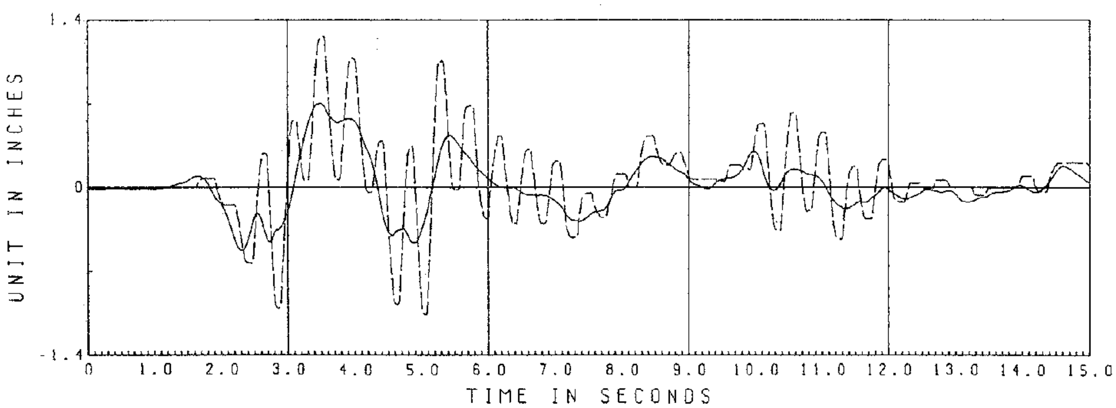

- Table Displacement -- 3rd Floor Absolute Displacement

Fig. 2.5a.3 EC 200 I Displacements

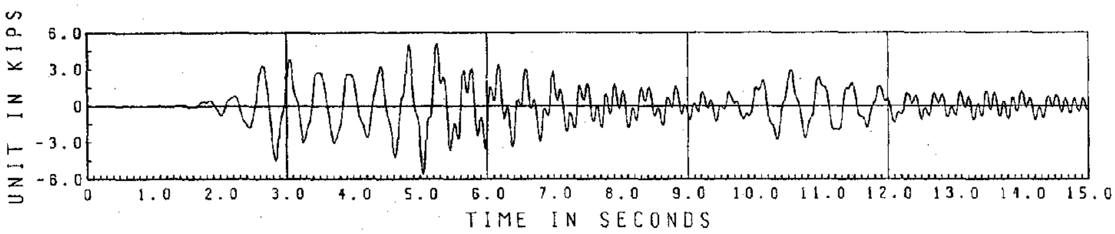

3rd Floor Shear

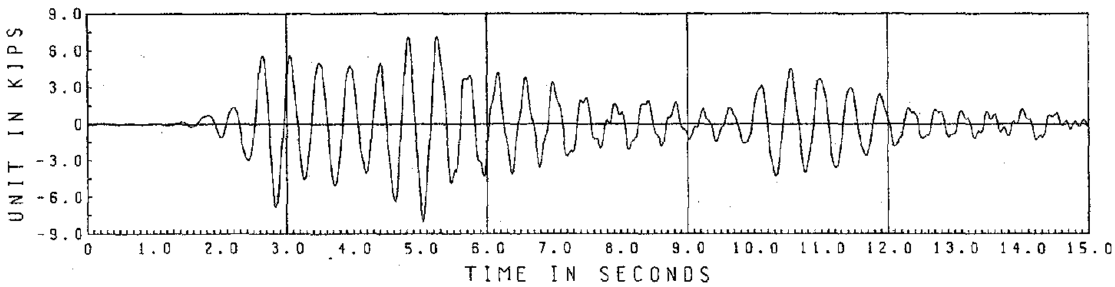

2nd Floor Shear

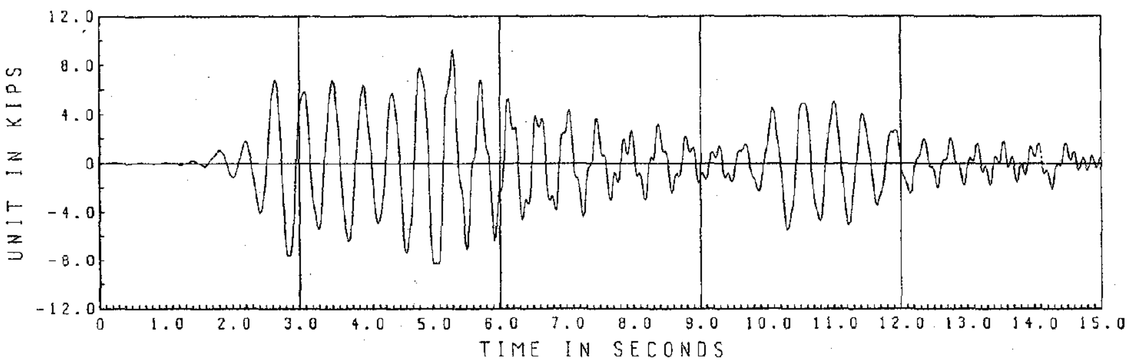

Base Shear

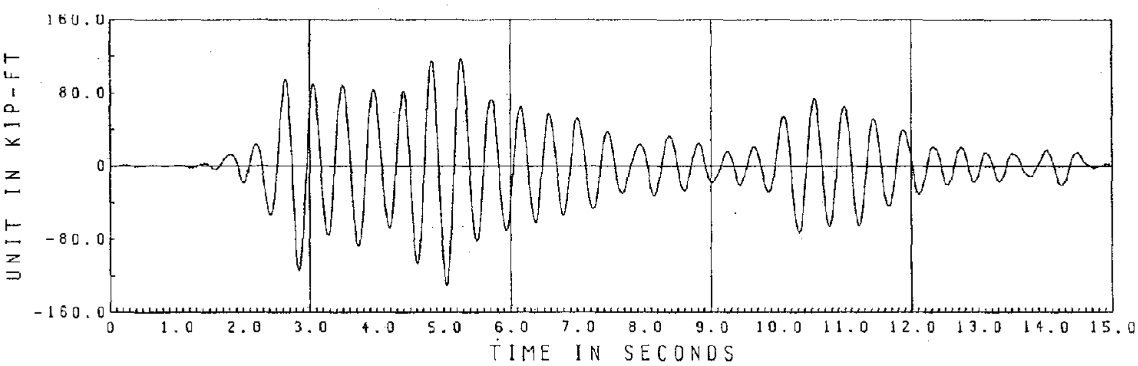

Base Overturning Moment

Fig. 2.5a.4 EC 200 I Story Forces

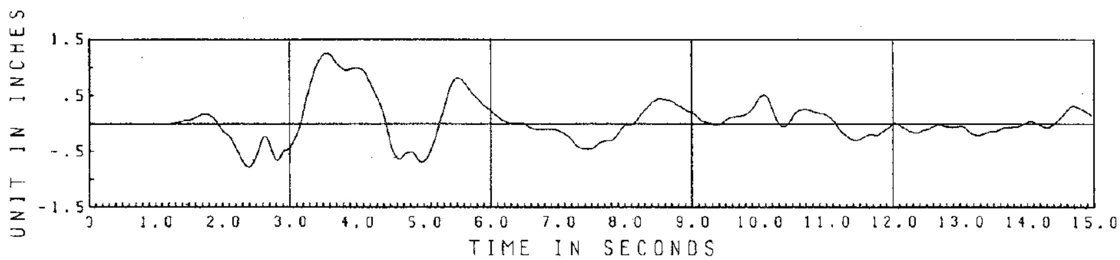

Table Displacement

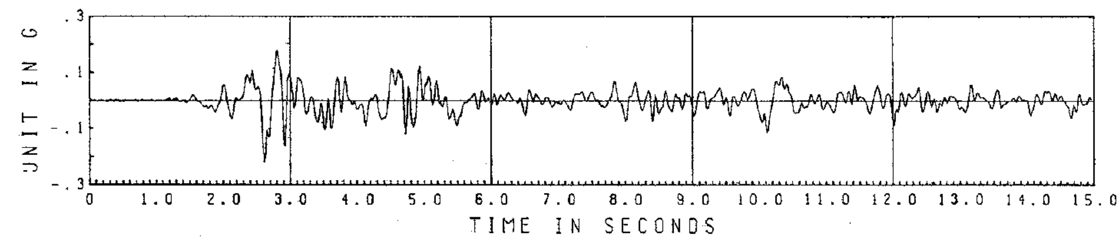

Table Acceleration

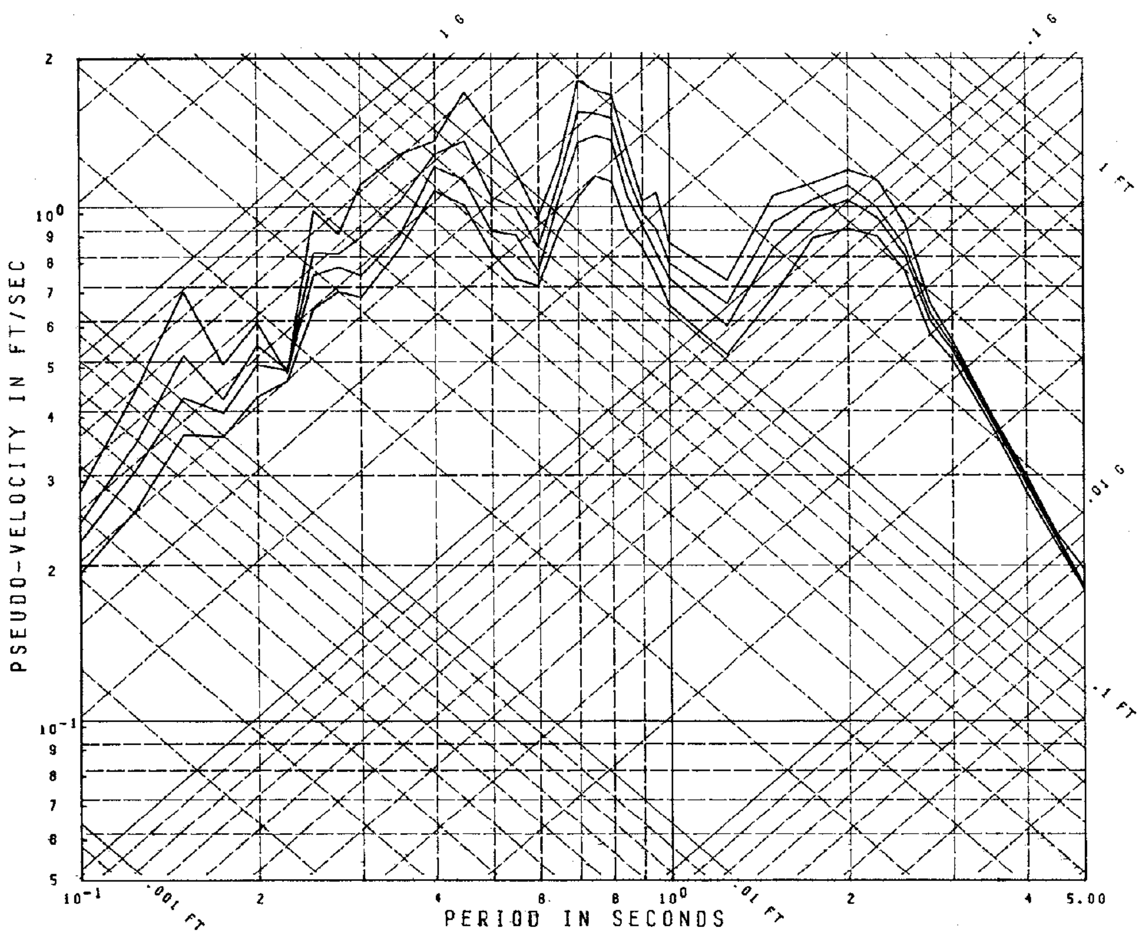

EC 100 II

Fig. 2.5b.1 Response Spectra; Damping Ratios = .01, .02, .03, .05

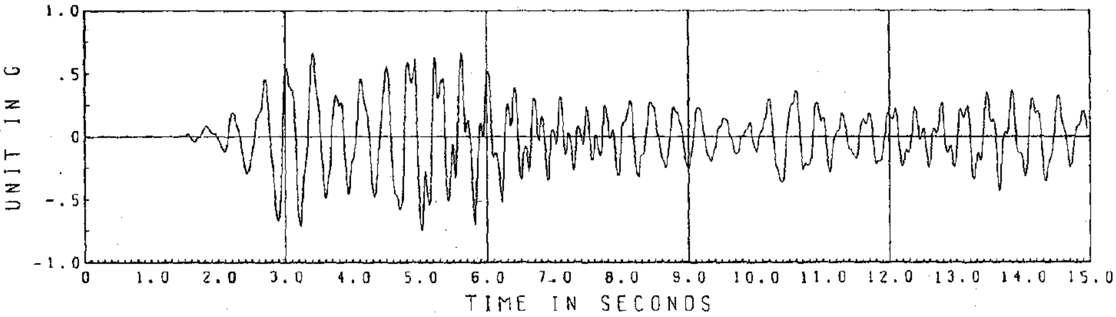

3rd Floor Acceleration

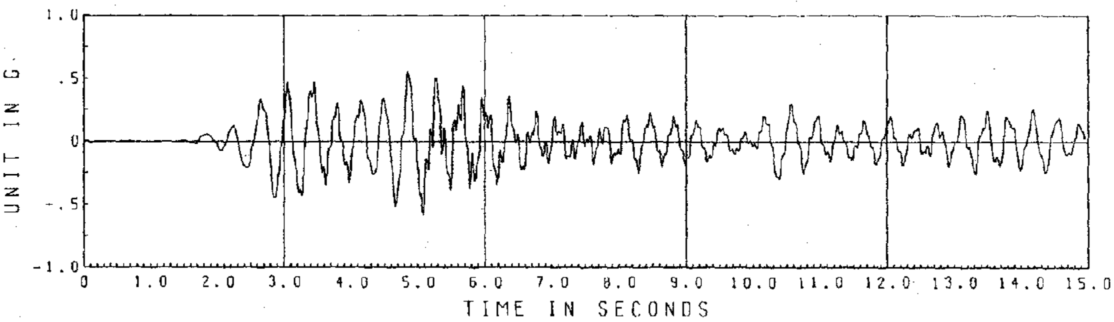

2nd Floor Acceleration

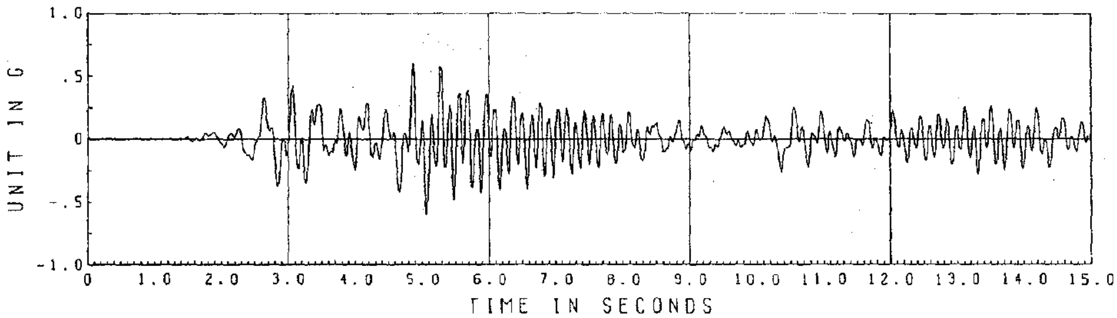

1st Floor Acceleration

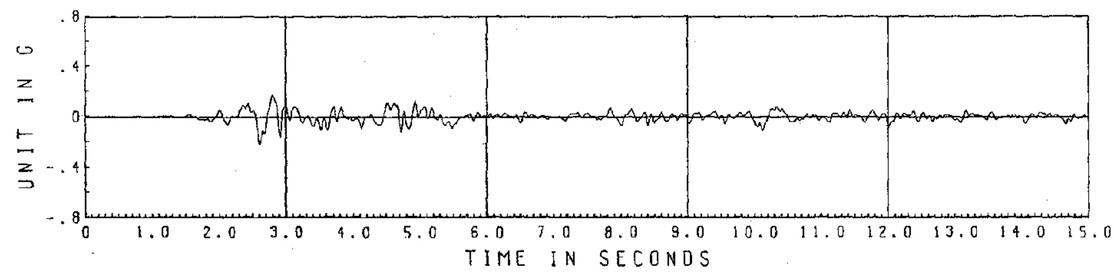

Table Acceleration

Fig. 2.5b.2 EC 100 II Accelerations

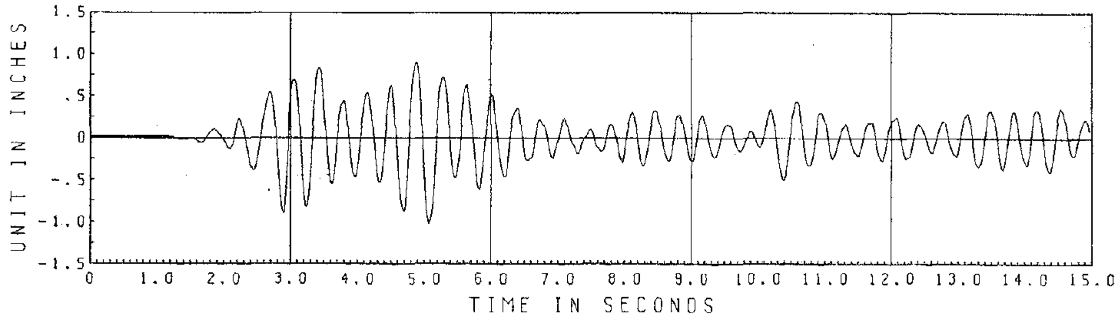

3rd Floor Relative Displacement

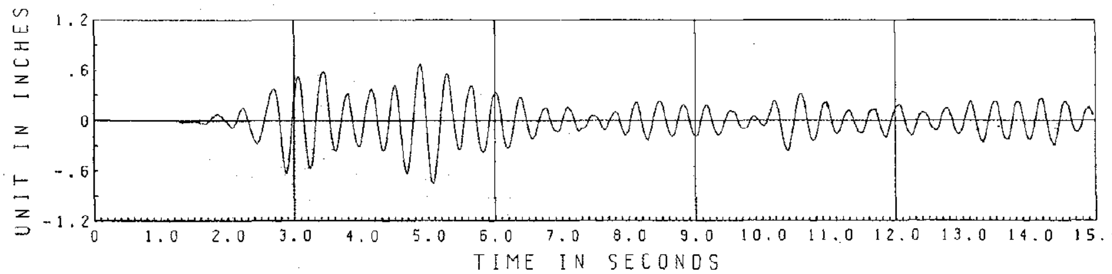

2nd Floor Relative Displacement

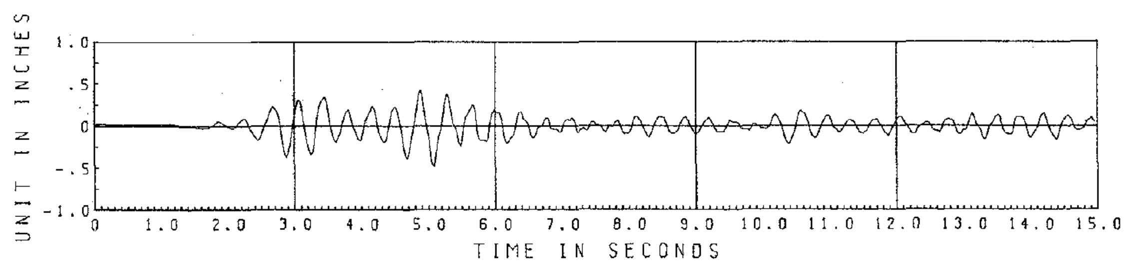

1st Floor Relative Displacement

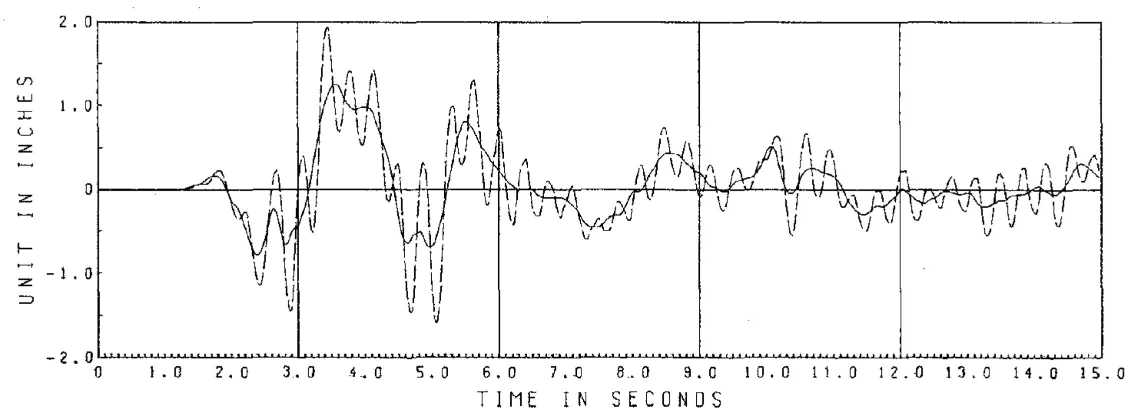

- Table Displacement -- 3rd Floor Absolute Displacement

Fig. 2.5b.3 EC 100 II Displacements

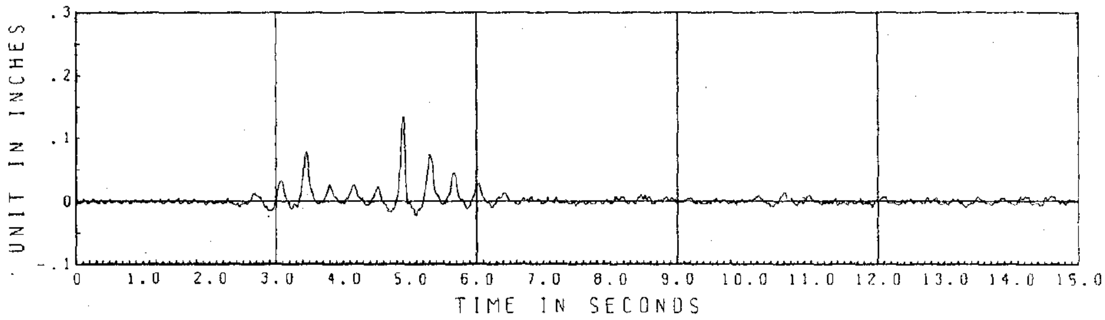

North Column West Frame

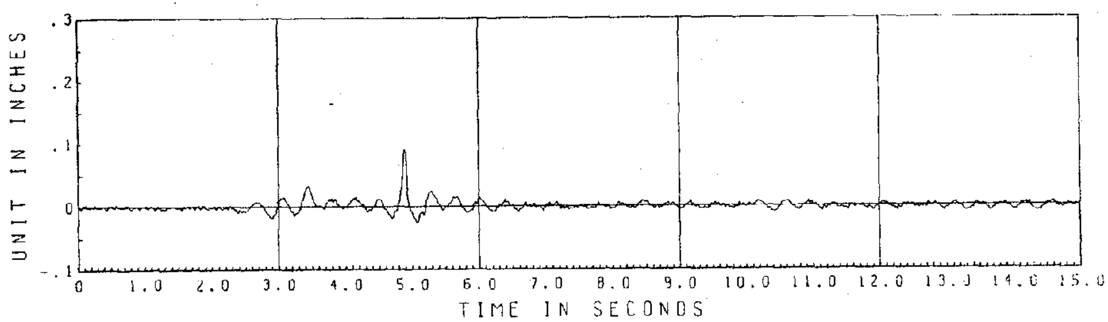

North Column East Frame

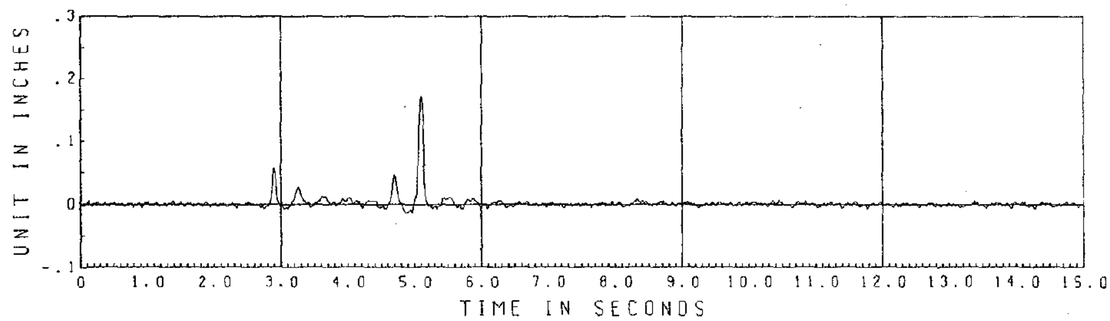

South Column West Frame

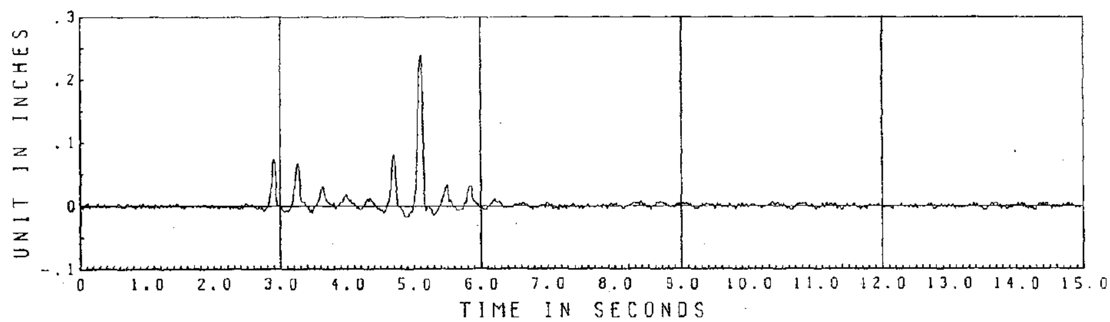

South Column East Frame

Fig. 2.5b.4 EC 100 II Relative Column Vertical Displacements

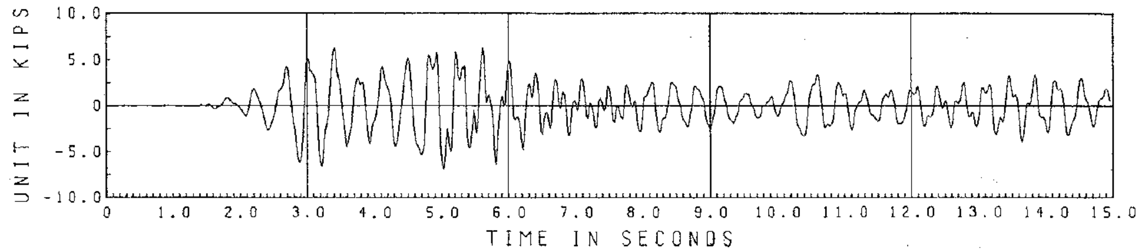

1st Floor Shear

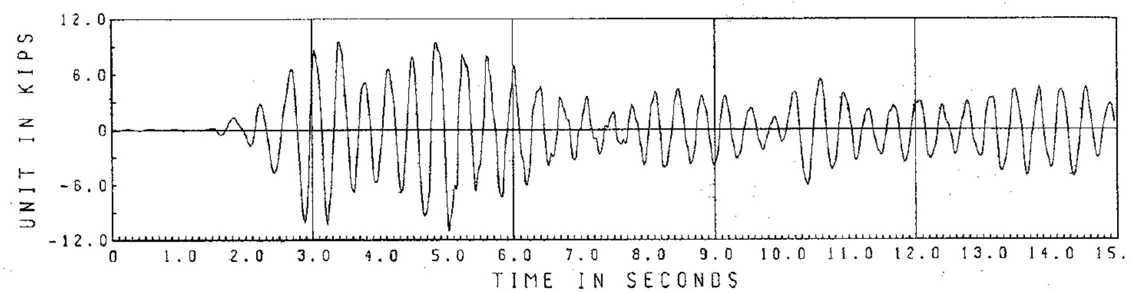

2nd Floor Shear

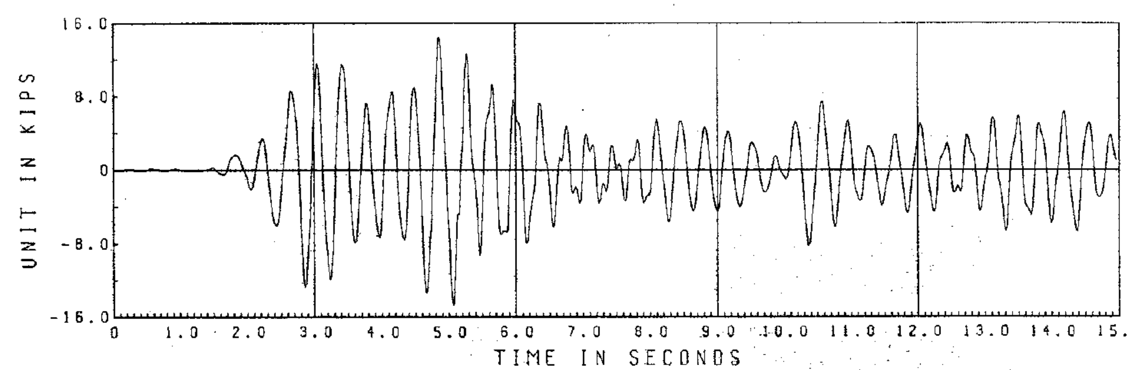

Base Shear

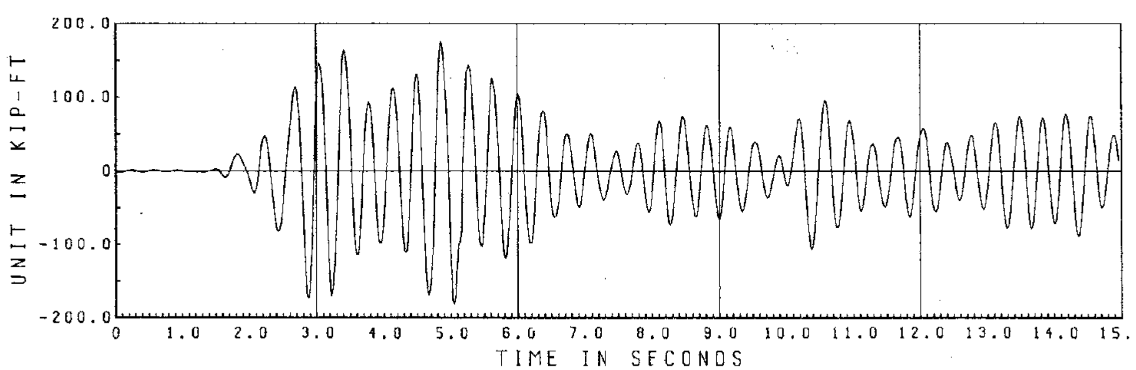

Base Overturning Moment

Fig. 2.5b.5 EC 100 II Story Forces

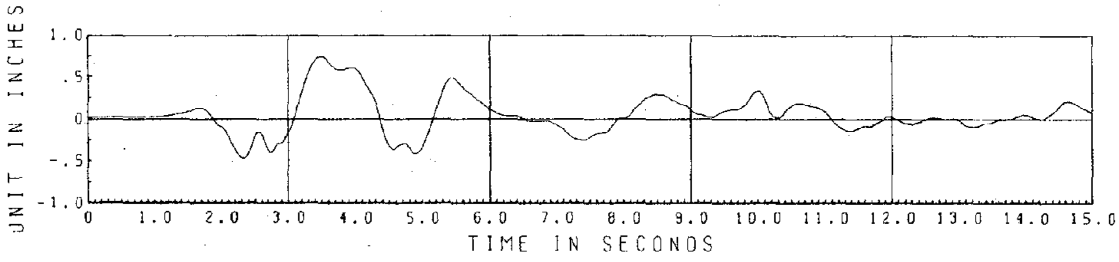

Table Displacement

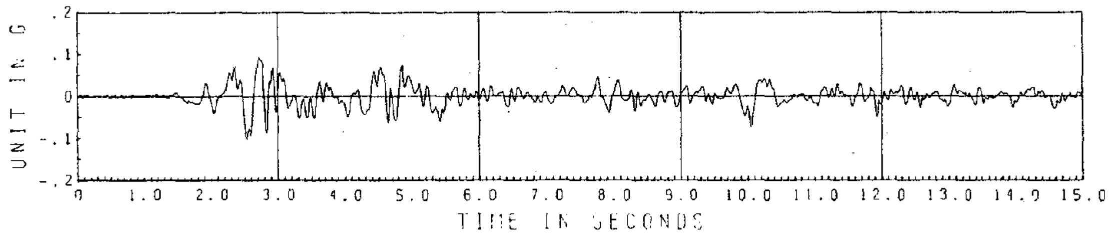

Table Acceleration

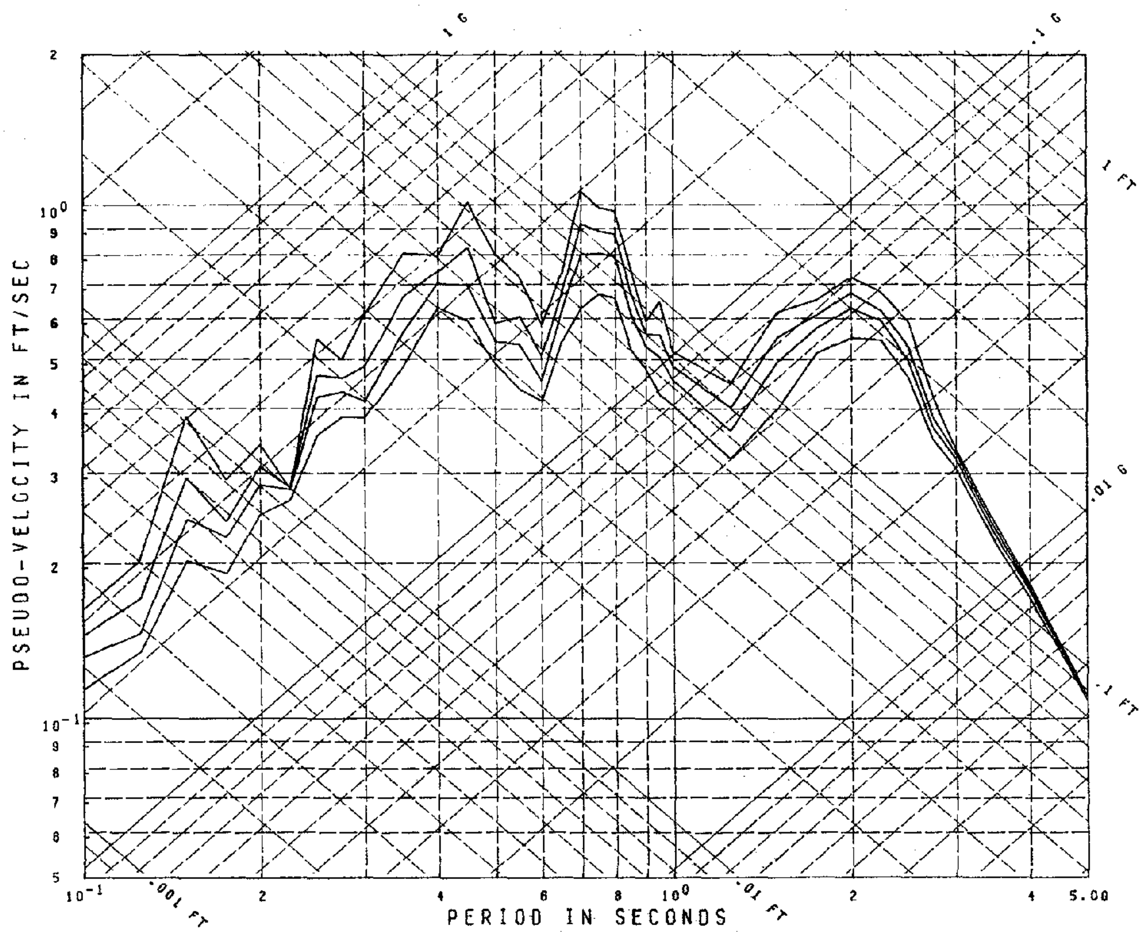

EC 200

Fig. 2.5c.1 Response Spectra; Damping Ratios = .01, .02, .03, .05

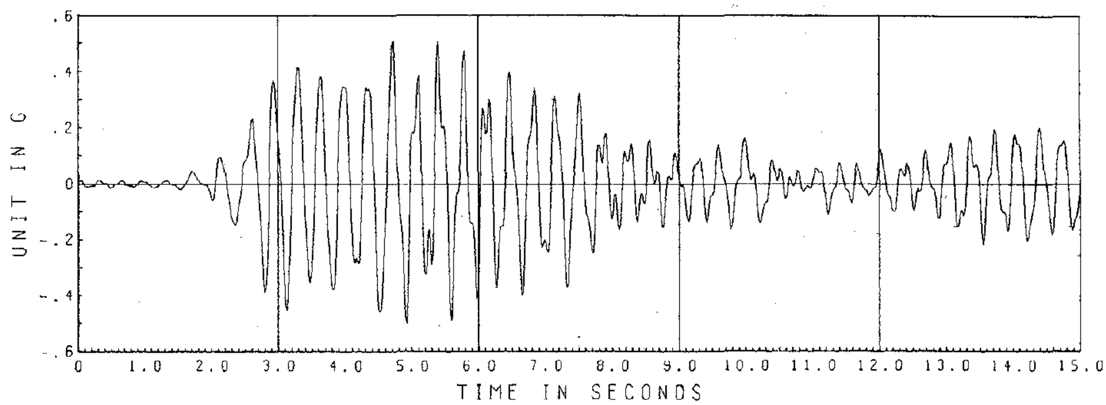

3rd Floor Acceleration

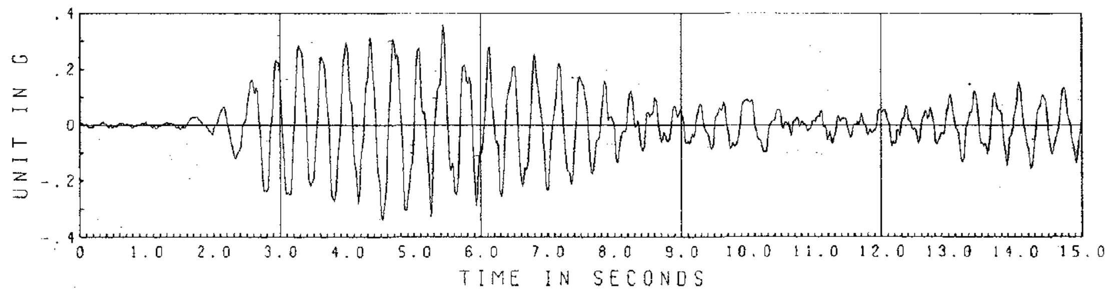

2nd Floor Acceleration

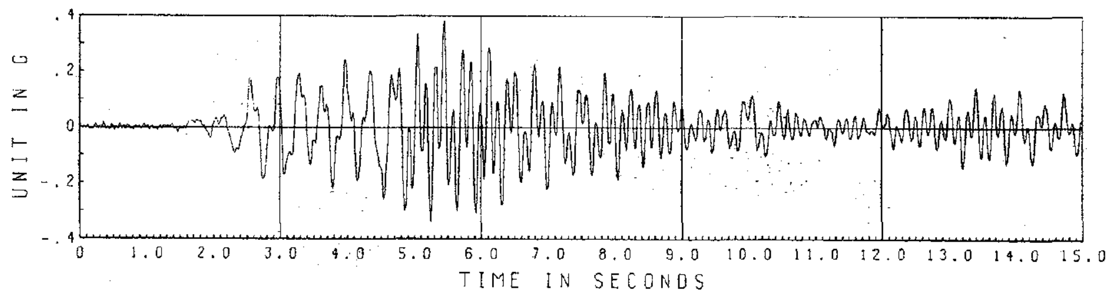

1st Floor Acceleration

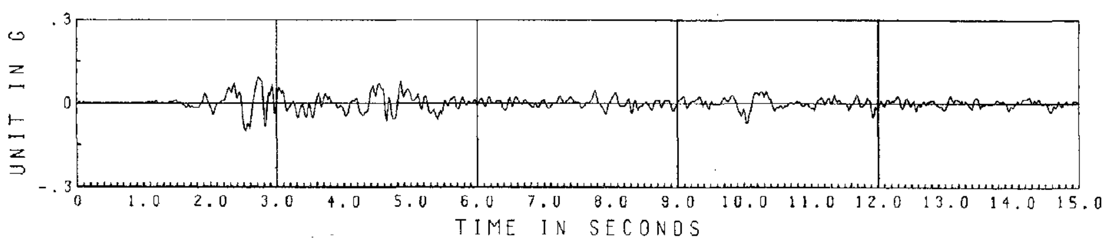

Table Acceleration

Fig. 2.5c.2 EC 200 Accelerations

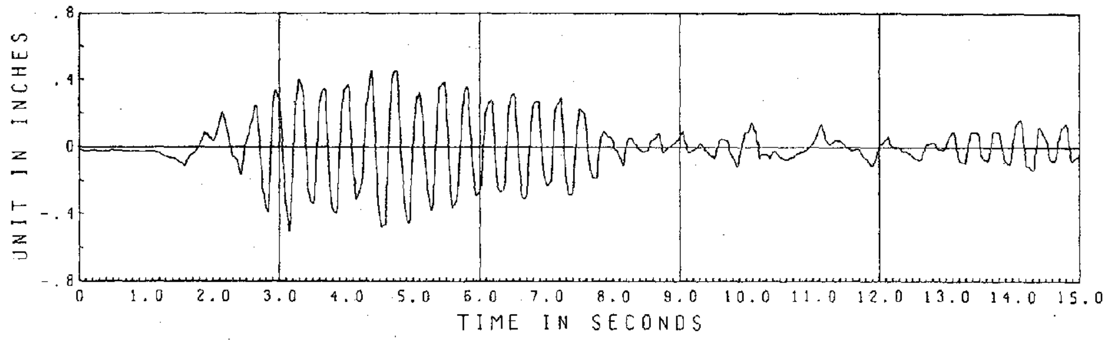

3rd Floor Relative Displacement

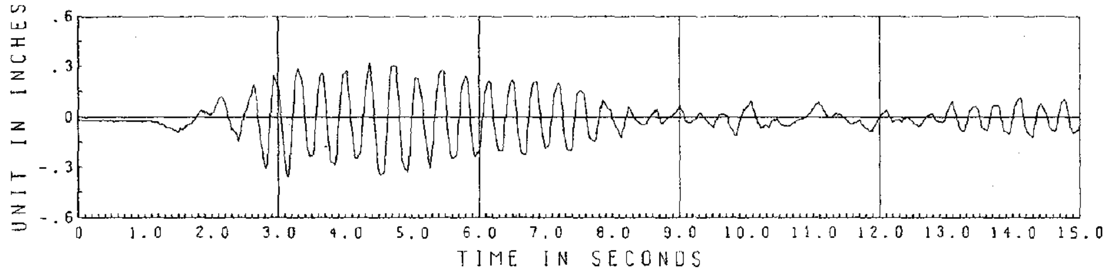

2nd Floor Relative Displacement

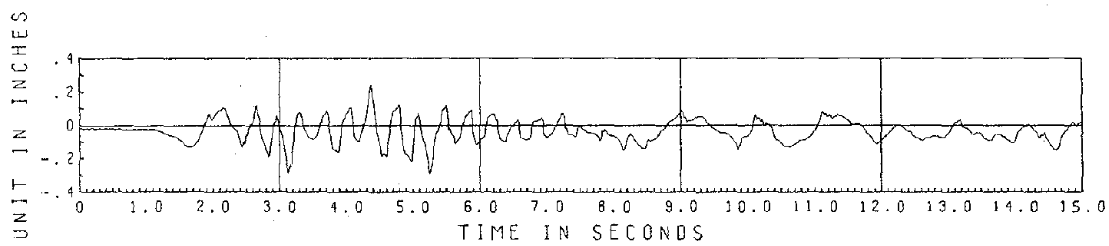

1st Floor Relative Displacement

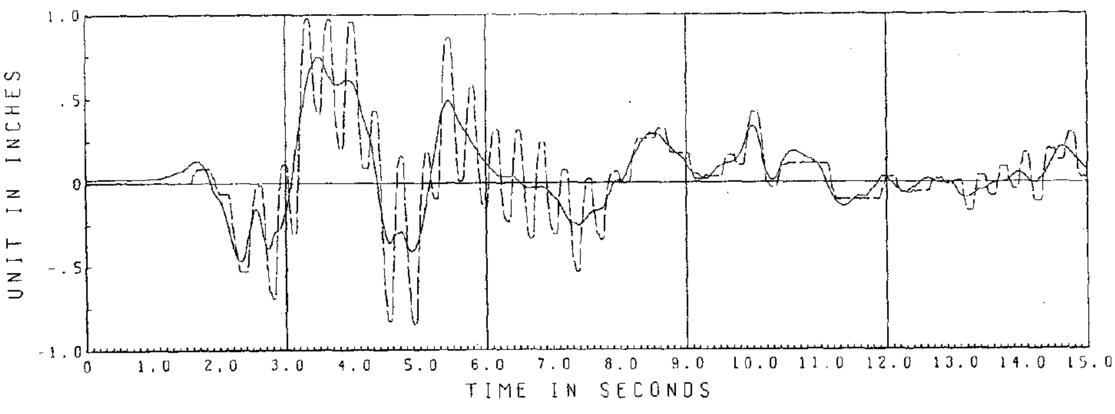

- Table Displacement -- 3rd Floor Absolute Displacement

Fig. 2.5c.3 EC 200 Displacements

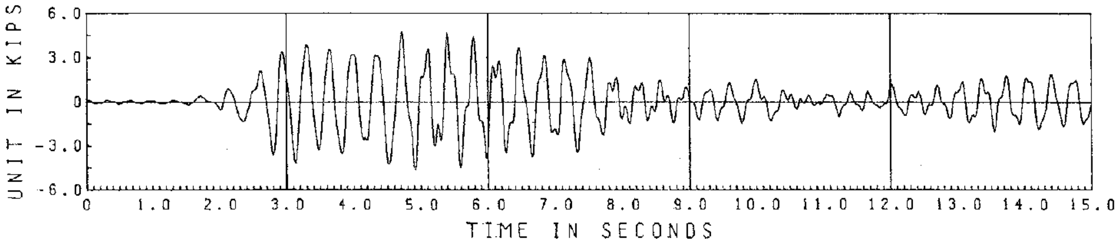

3rd Floor Shear

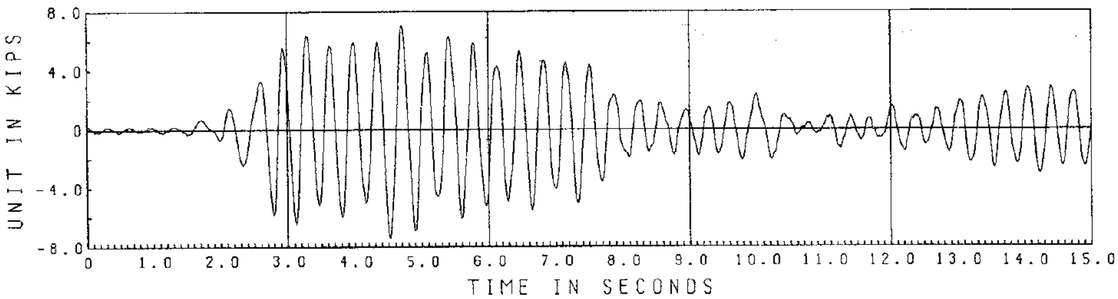

2nd Floor Shear

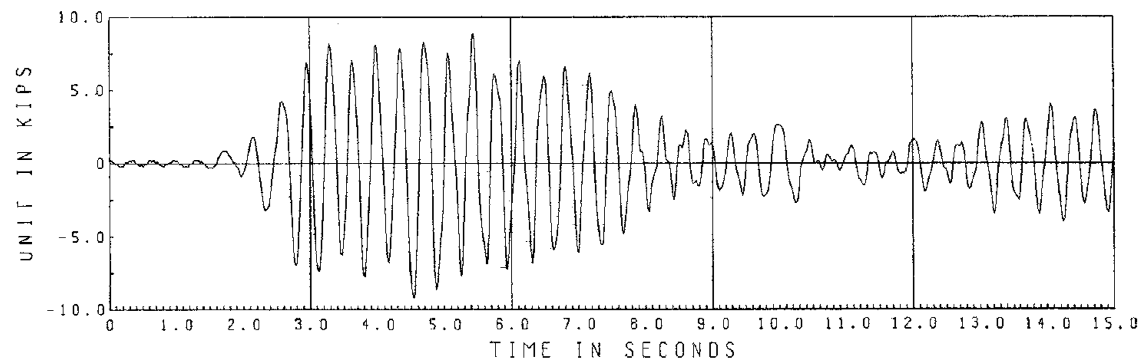

Base Shear

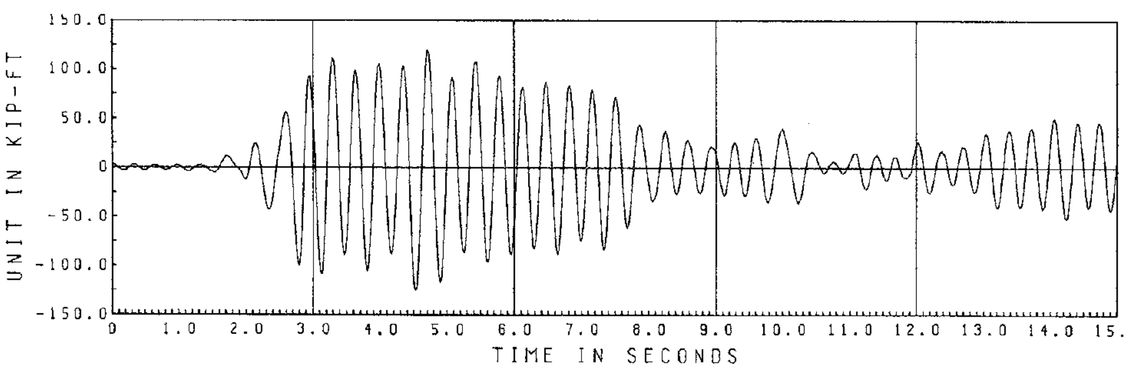

Base Overturning Moment

Fig. 2.5c.4 EC 200 Story Forces

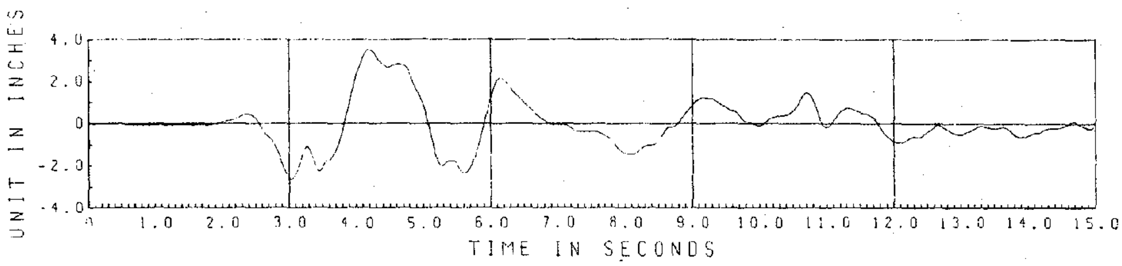

Table Displacement

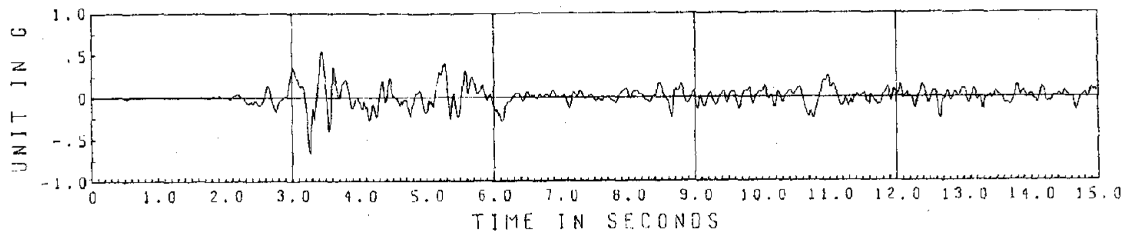

Table Acceleration

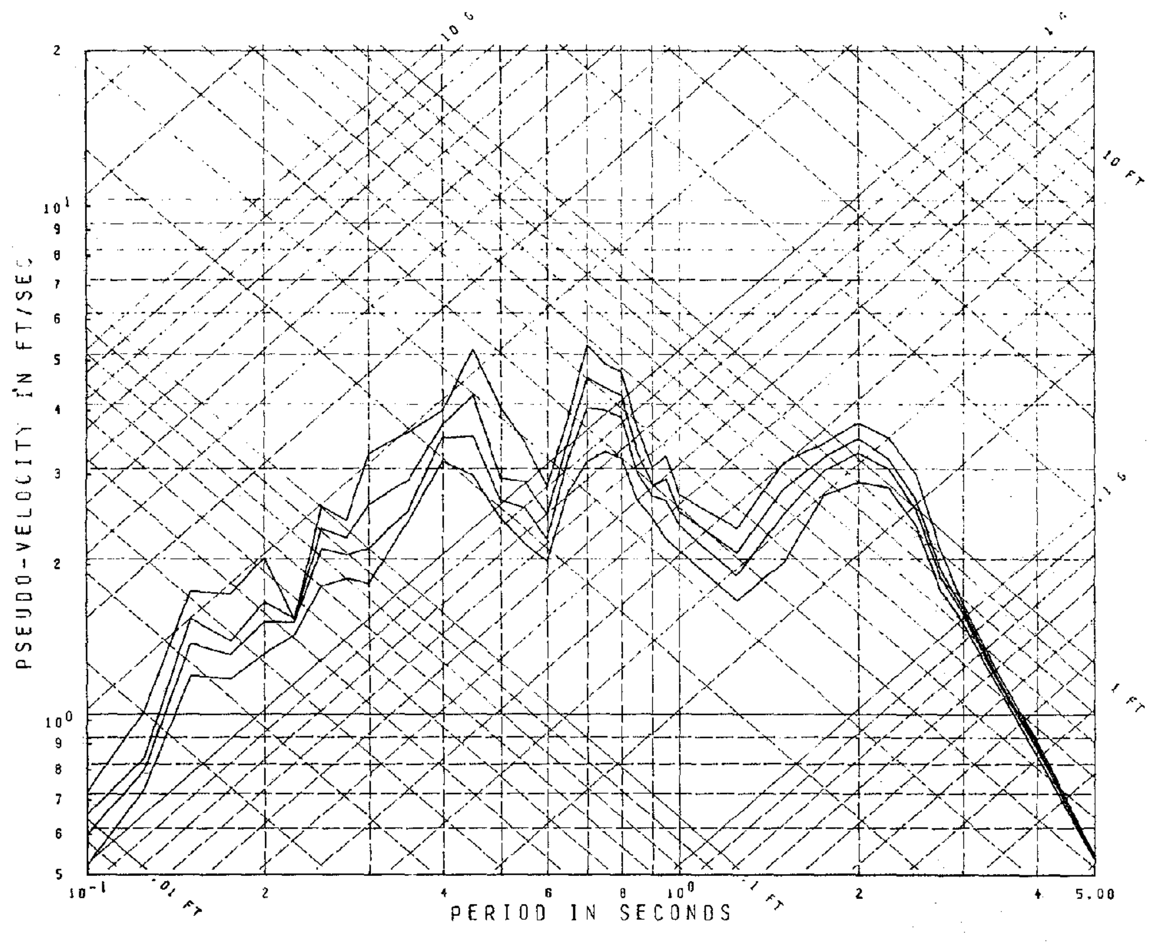

EC 1000 I

Fig. 2.5d.1 Response Spectra; Damping Ratios = .01, .02, .03, .05

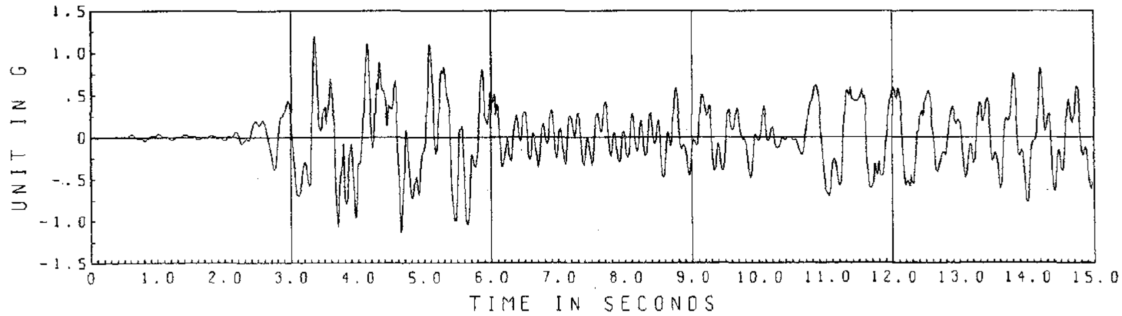

3rd Floor Acceleration

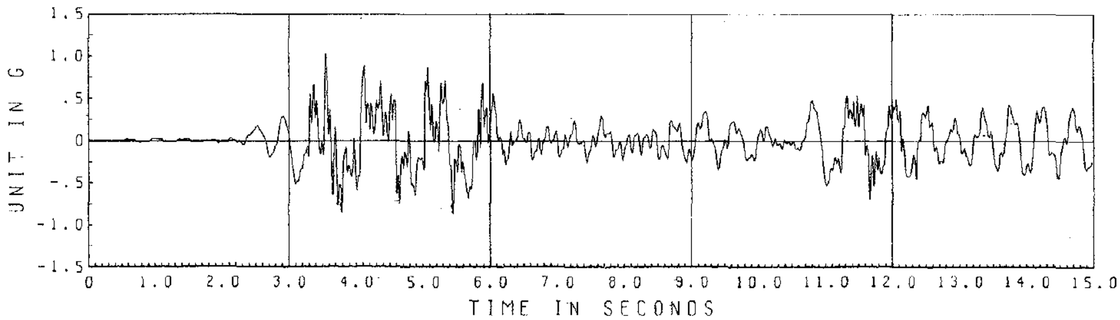

2nd Floor Acceleration

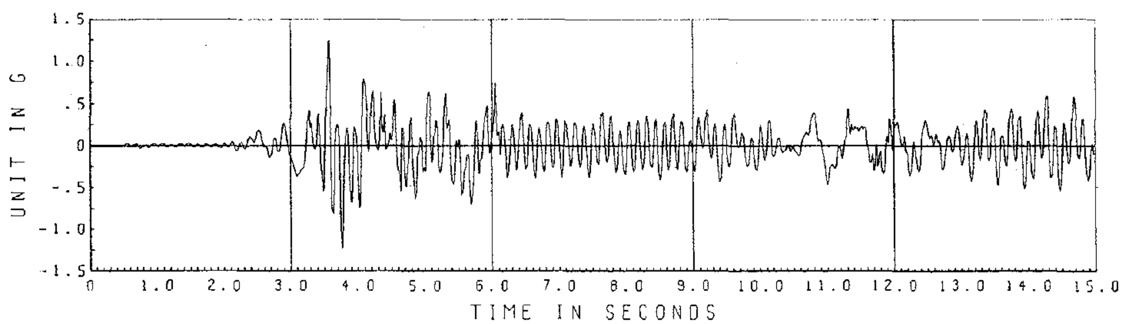

1st Floor Acceleration

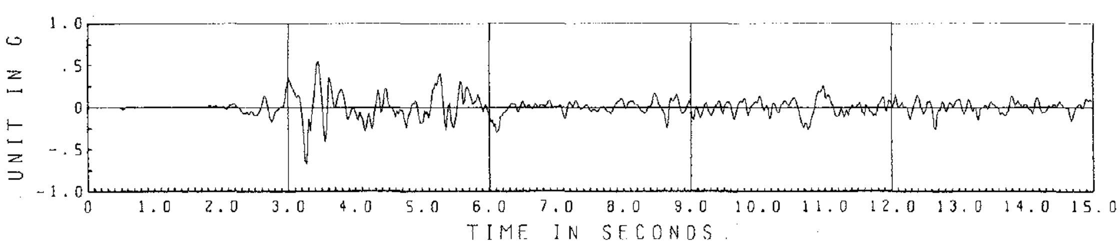

Table Acceleration

Fig. 2.5d.2 EC 1000 I Accelerations

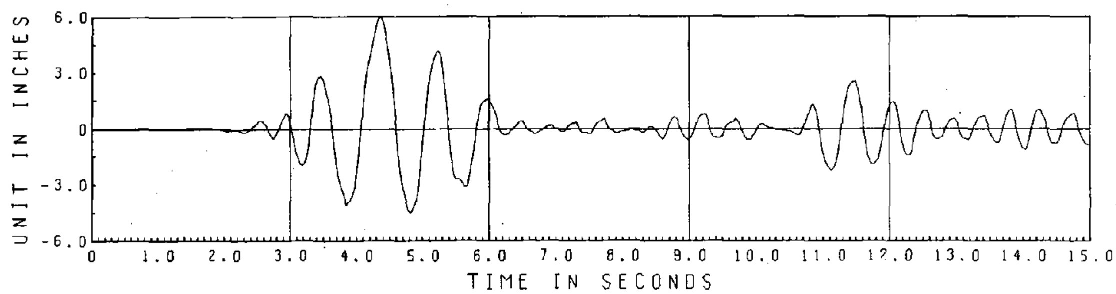

3rd Floor Relative Displacement

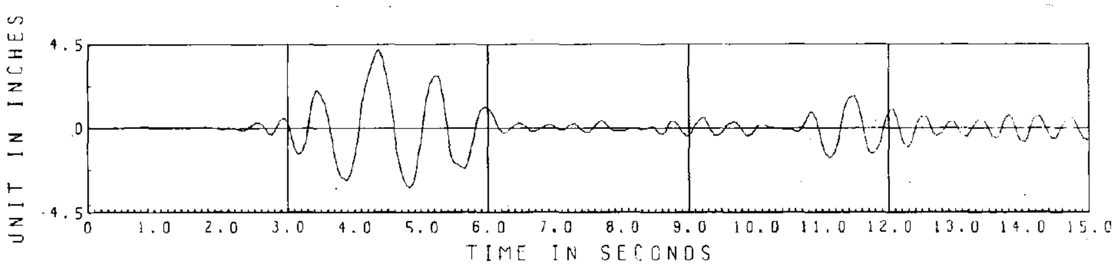

2nd Floor Relative Displacement

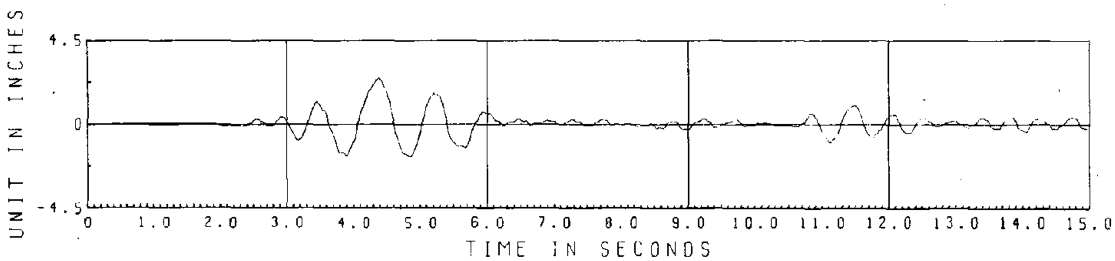

1st Floor Relative Displacement

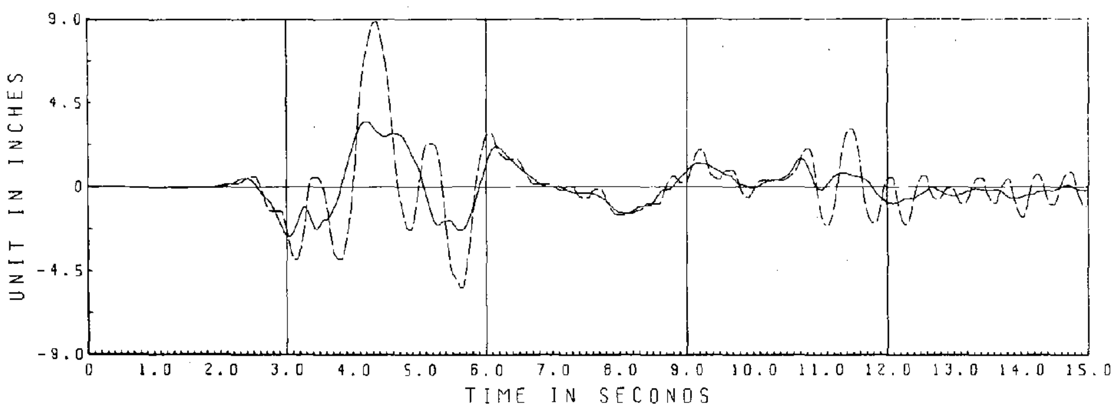

- Table Displacement **-- 3rd Floor Absolute Displacement**

Fig. 2.5d.3 EC 1000 I Displacements

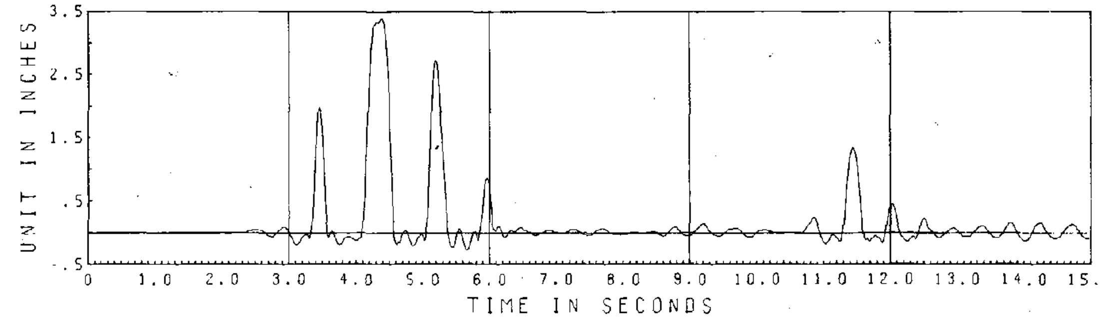

North Column West Frame

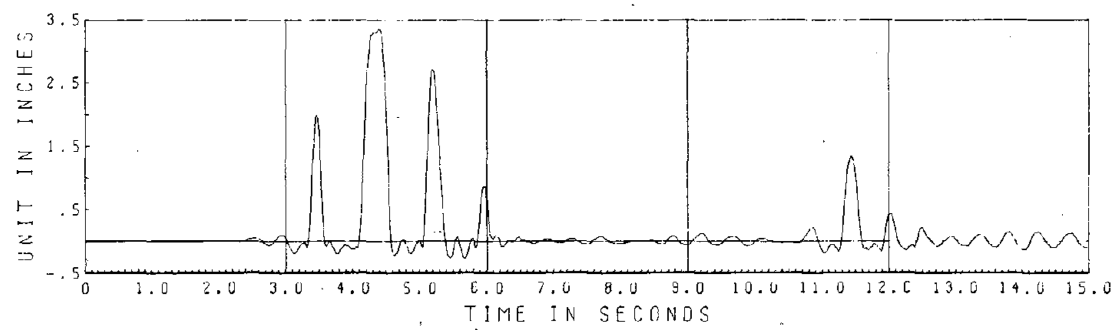

North Column East Frame

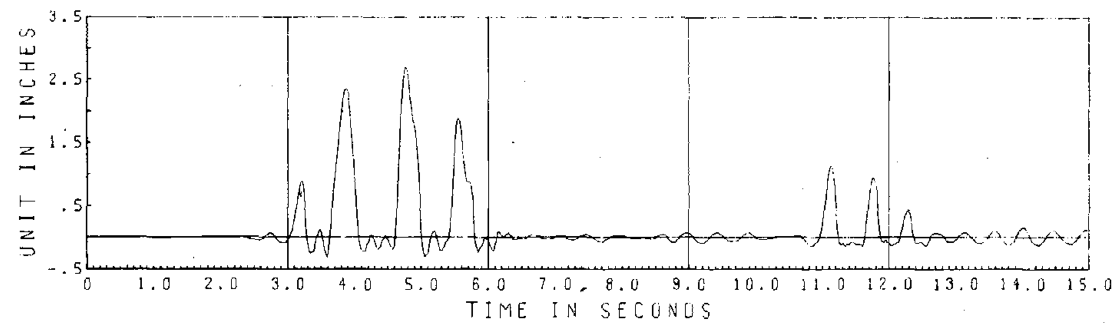

South Column West Frame

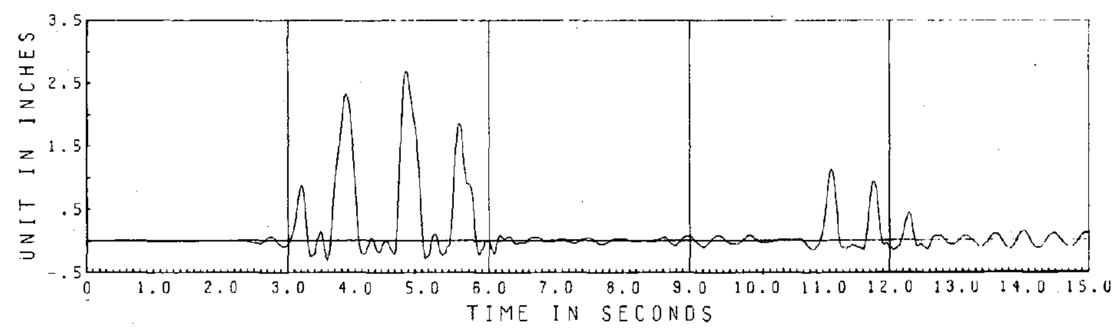

South Column East Frame

Fig. 2.5d.4 EC 1000 I Relative Column Vertical Displacements

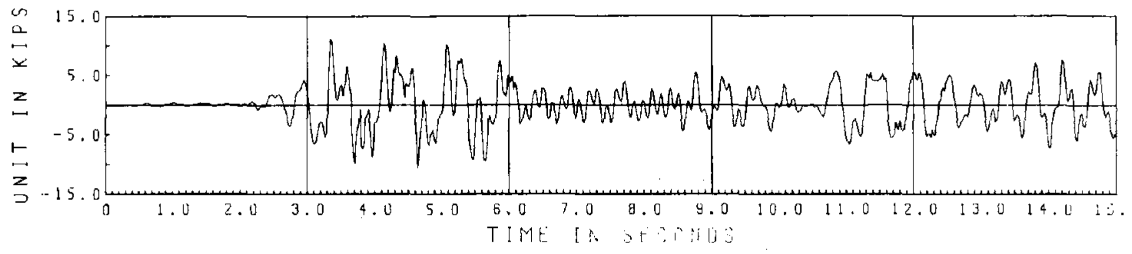

3rd Floor Shear

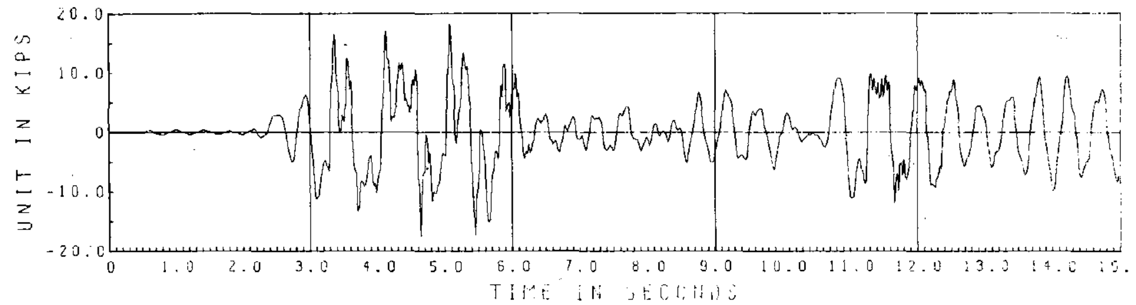

2nd Floor Shear

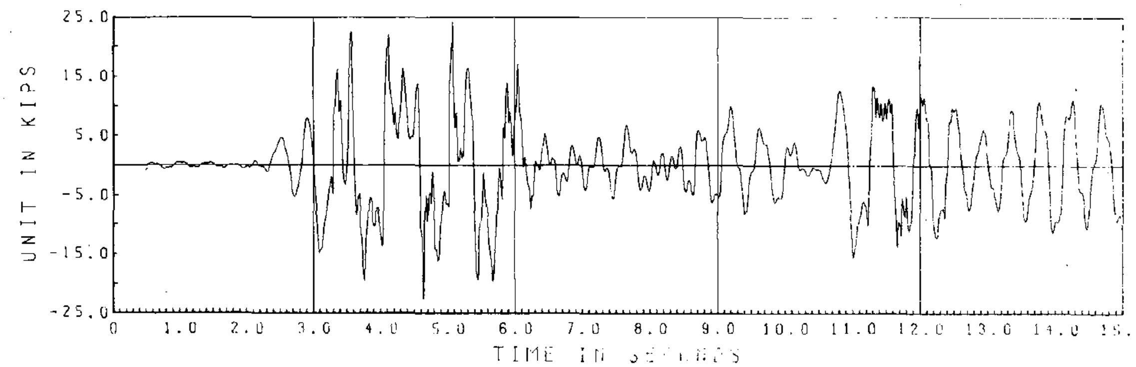

Base Shear

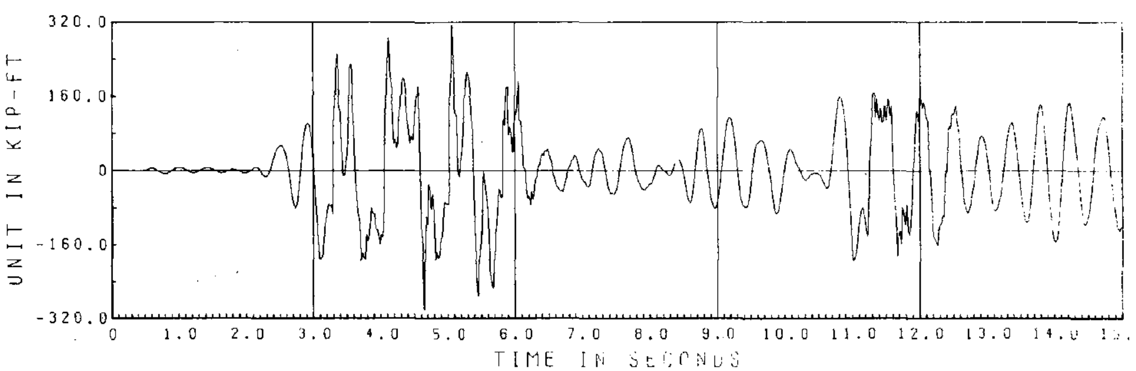

Base Overturning Moment

Fig. 2.5d.5 EC 1000 I Story Forces

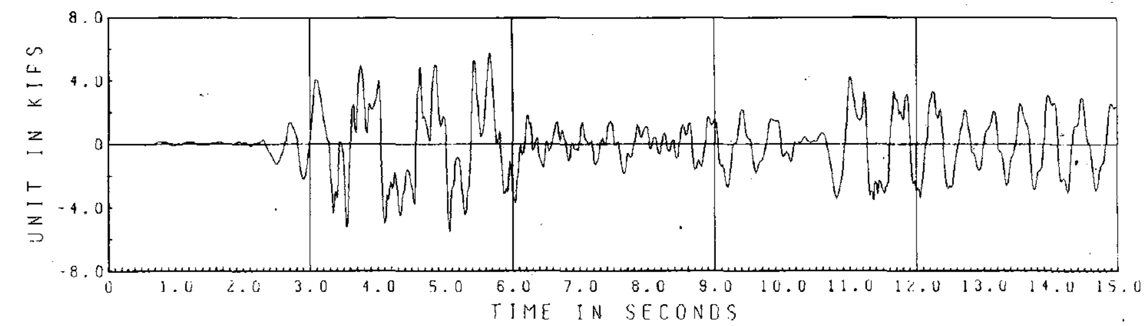

North Column Shear

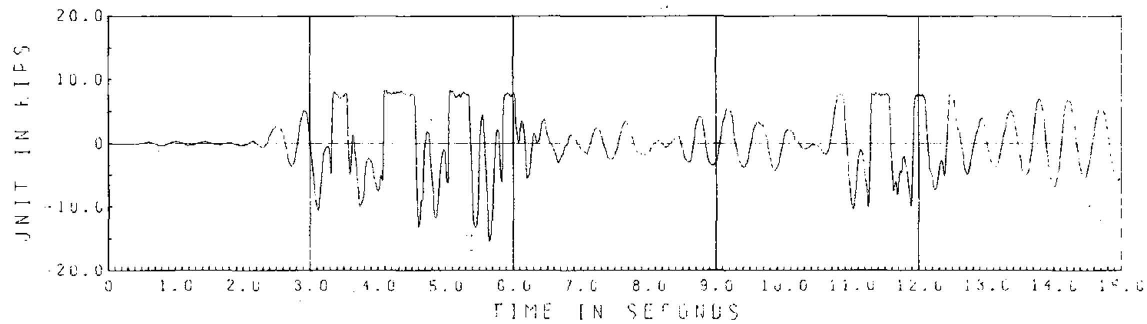

North Column Axial Force

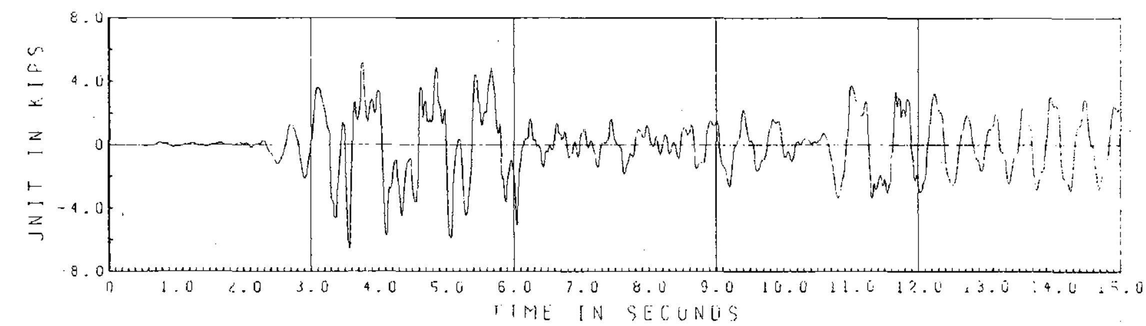

South Column Shear

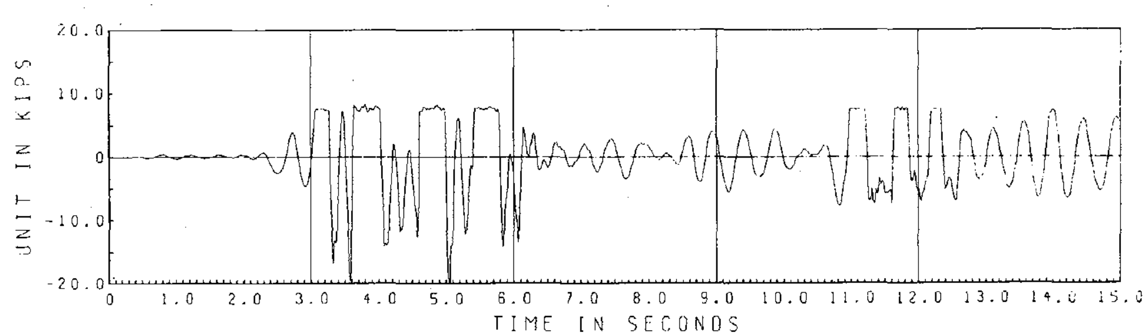

South Column Axial Force

Fig. 2.5d.6 EC 1000 I Member Forces

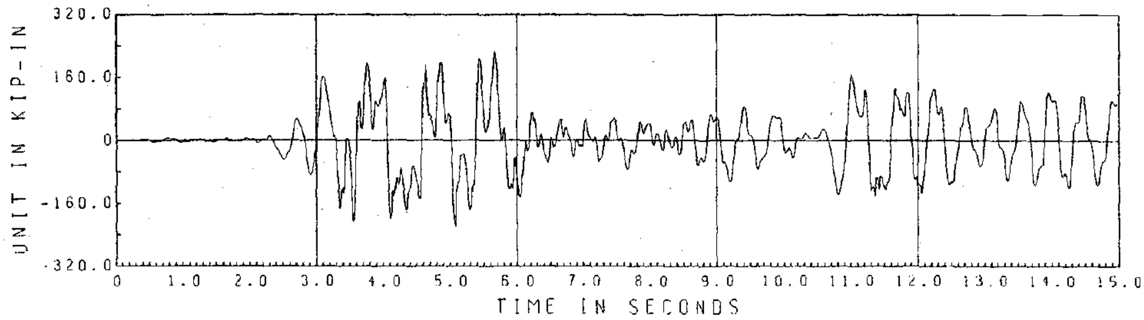

North Column Moment

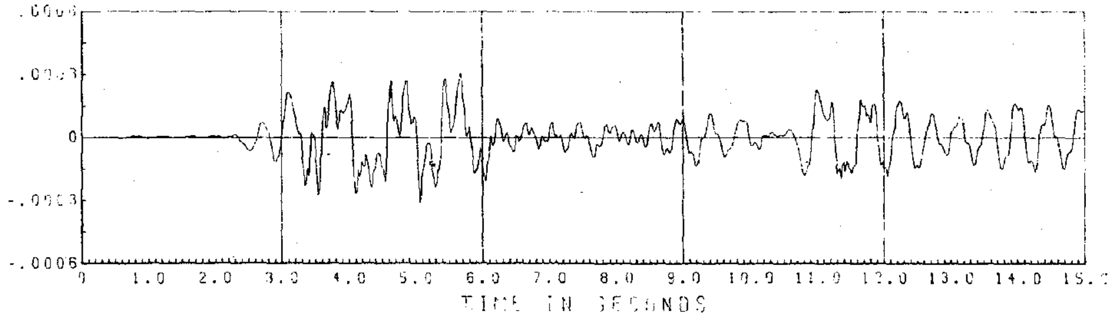

North Column Average Curvature (6" gage)

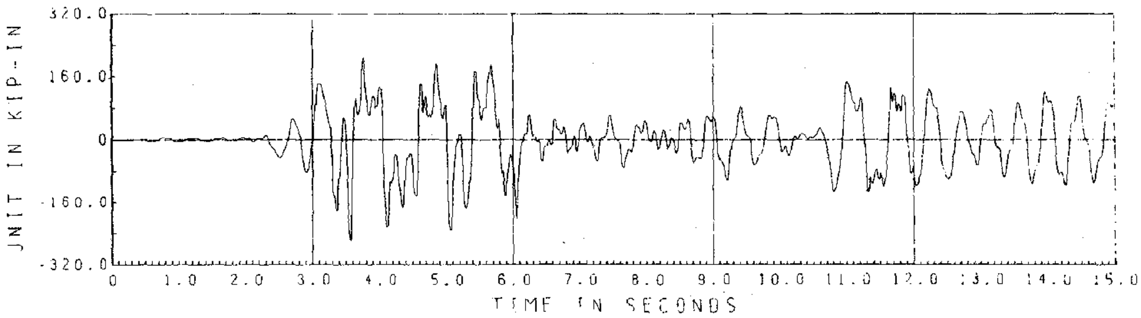

South Column Moment

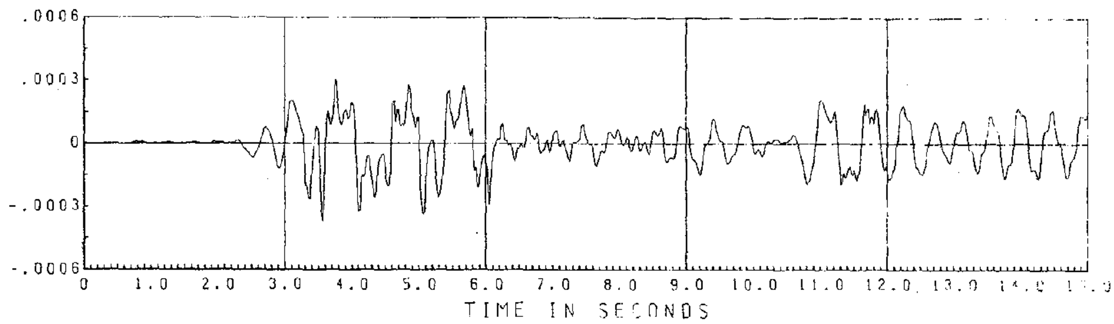

South Column Average Curavture (6" gage)

Fig. 2.5d.7 EC 1000 I Column Moments and Curvatures

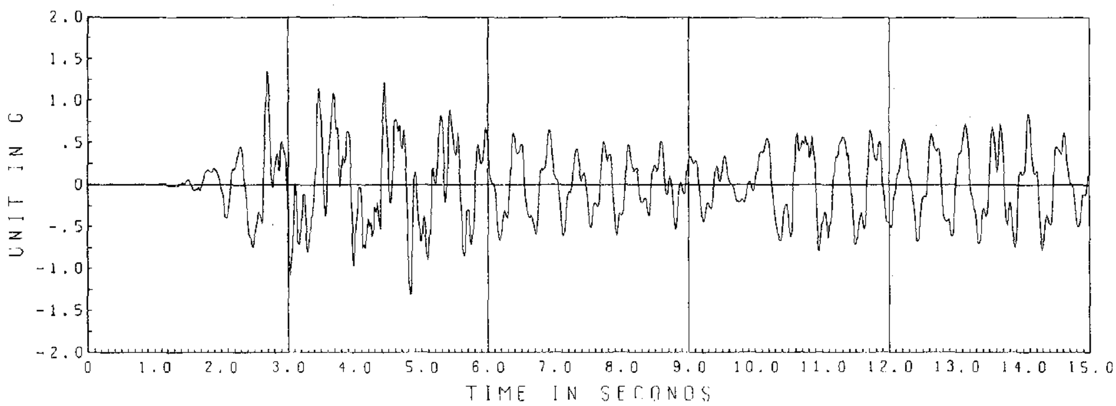

3rd Floor Acceleration

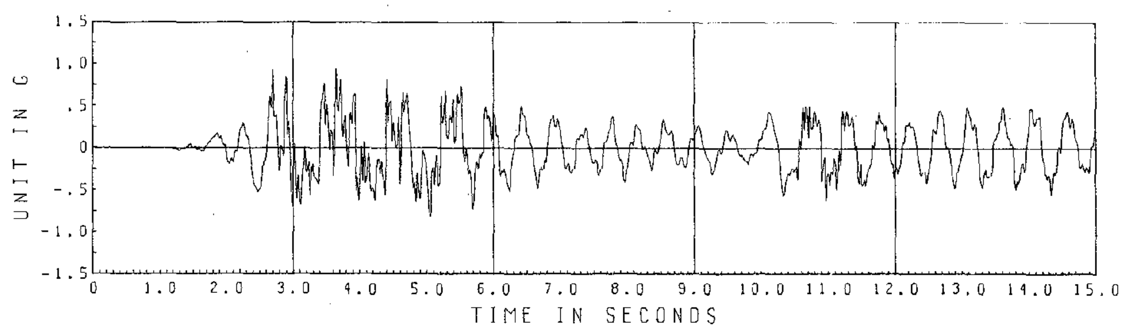

2nd Floor Acceleration

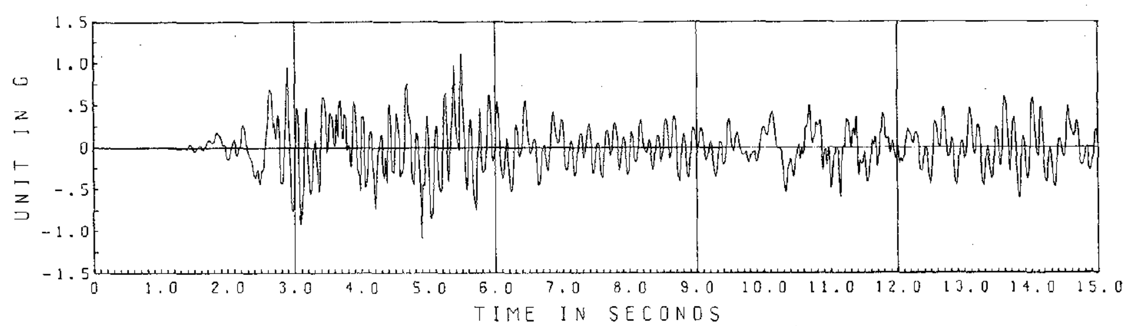

1st Floor Acceleration

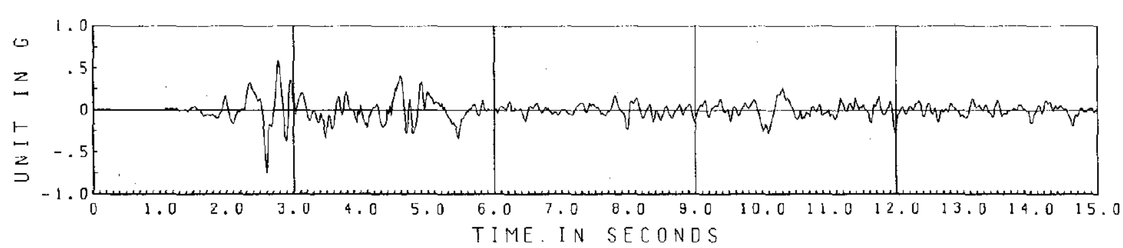

Table Acceleration

Fig. 2.5e.2 EC 1000/850 I Accelerations

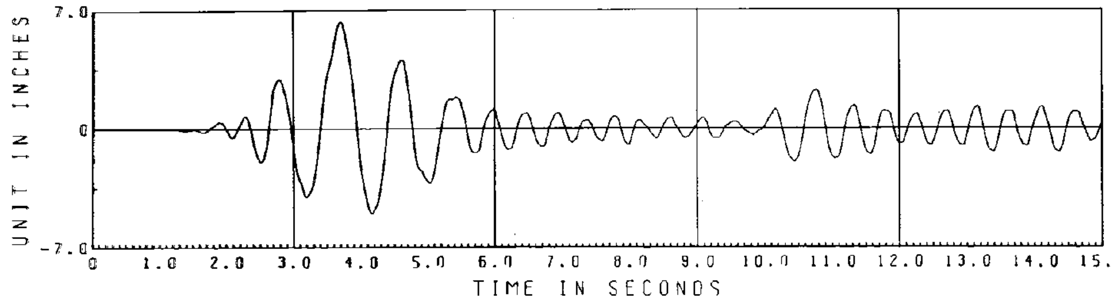

3rd Floor Relative Displacement

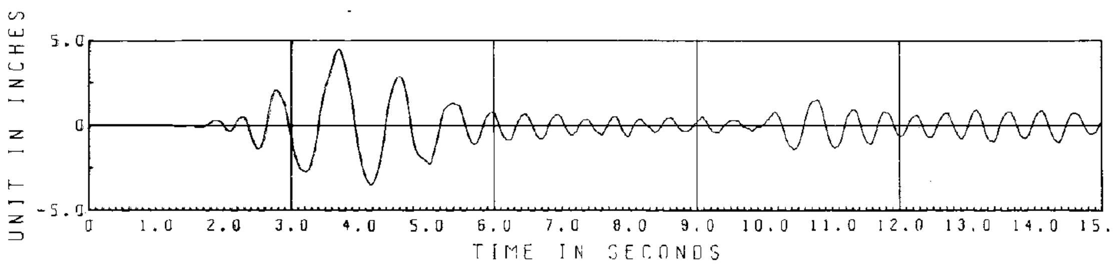

2nd Floor Relative Displacement

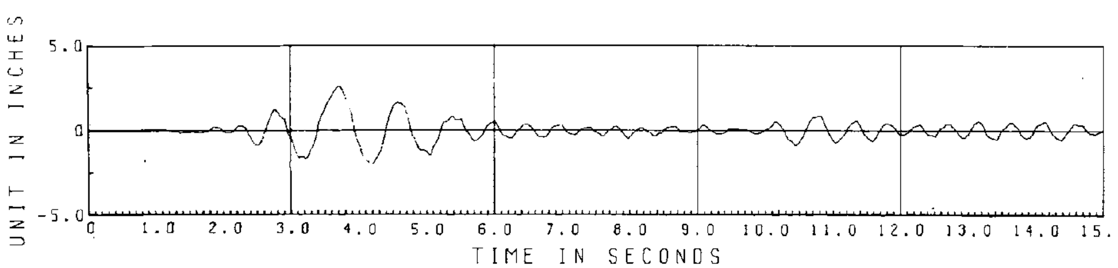

1st Floor Relative Displacement

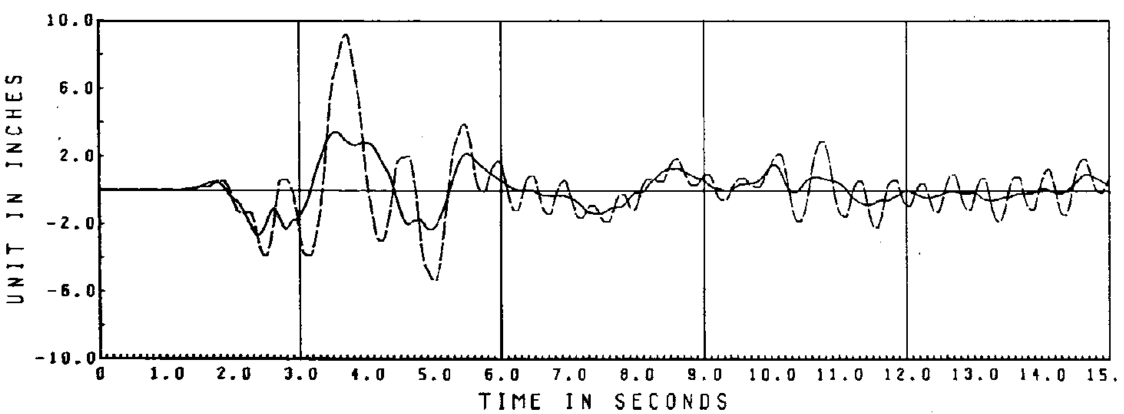

– Table Displacement -- 3rd Floor Displacement

Fig. 2.5e.3 EC 1000/850 I Displacements

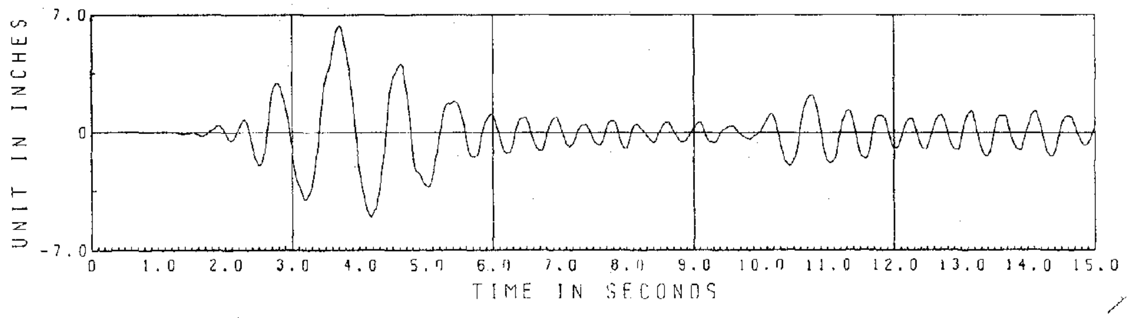

3rd Floor Relative Displacement

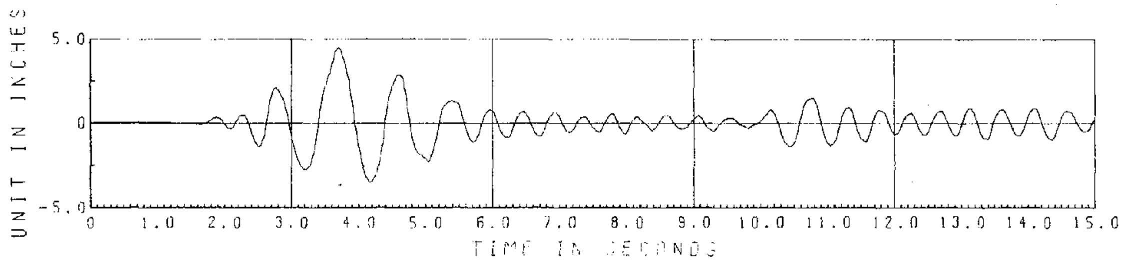

2nd Floor Relative Displacement

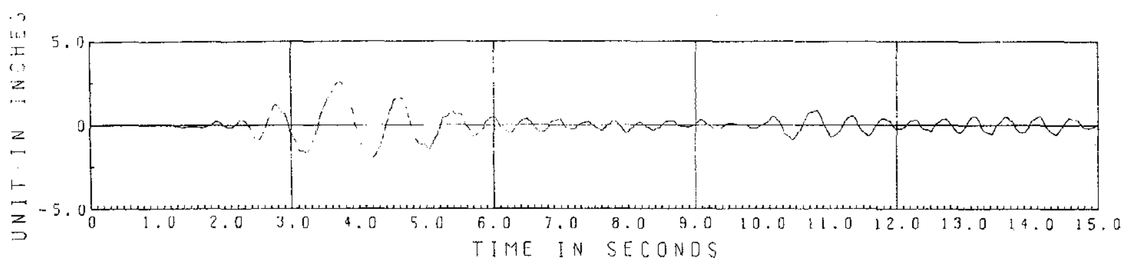

1st Floor Relative Displacement

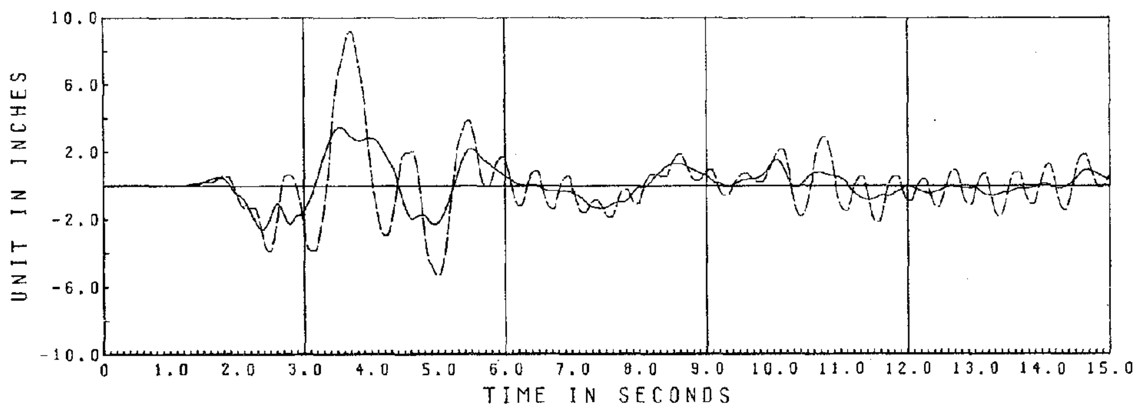

- Table Displacement -- 3rd Floor Displacement

Fig. 2.5e.3 EC 1000/850 I Displacements

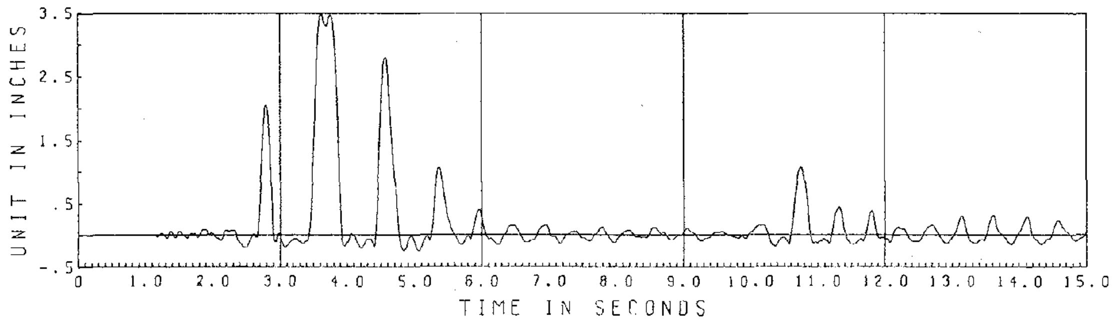

North Column West Frame

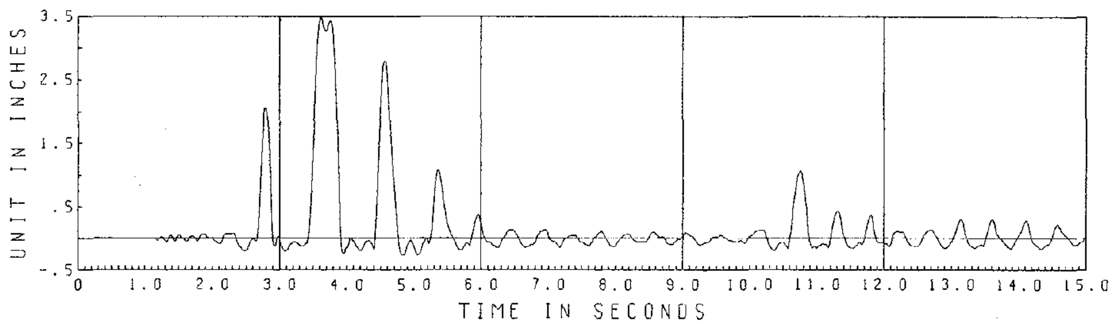

North Column East Frame

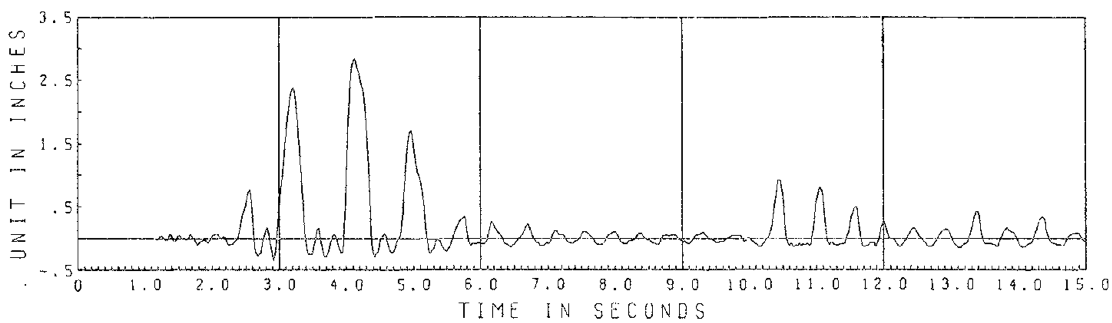

South Column West Frame

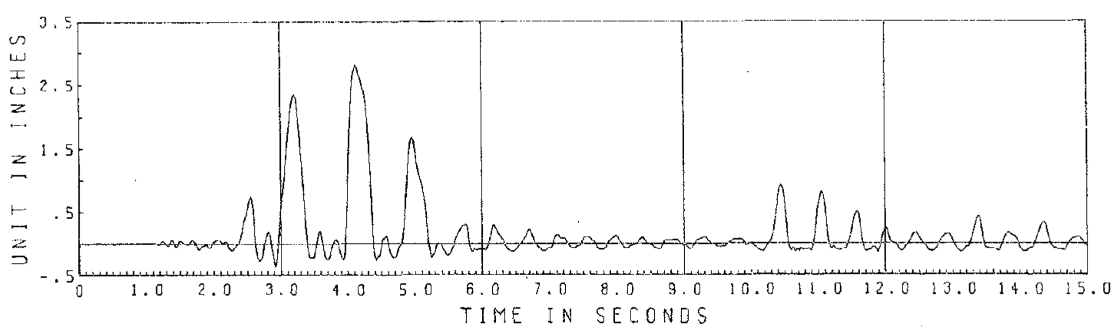

South Column East Frame

Fig. 2.5e.4 EC 1000/850 I Relative Column Vertical Displacements

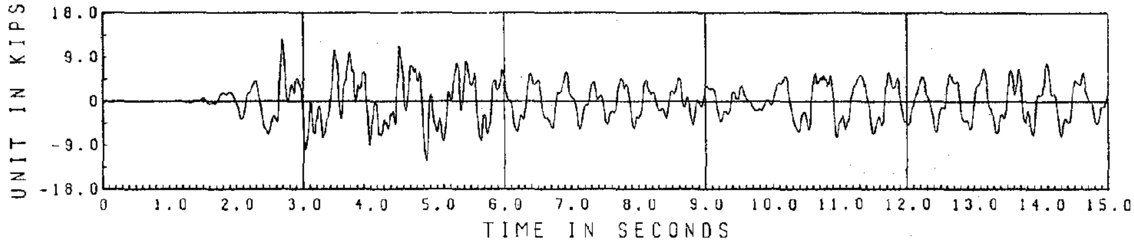

3rd Floor Shear

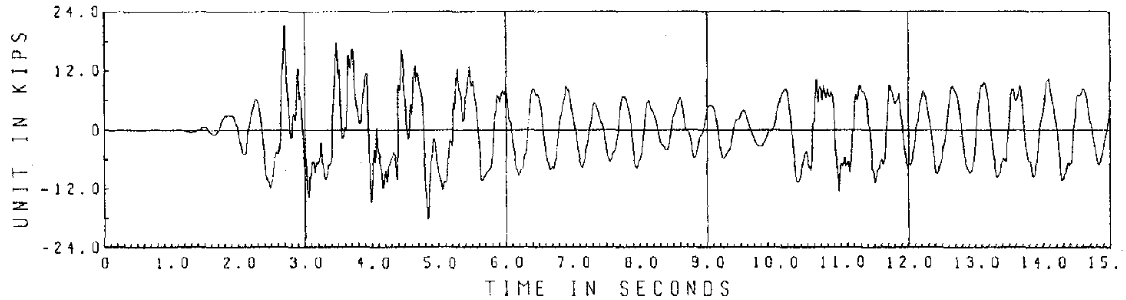

2nd Floor Shear

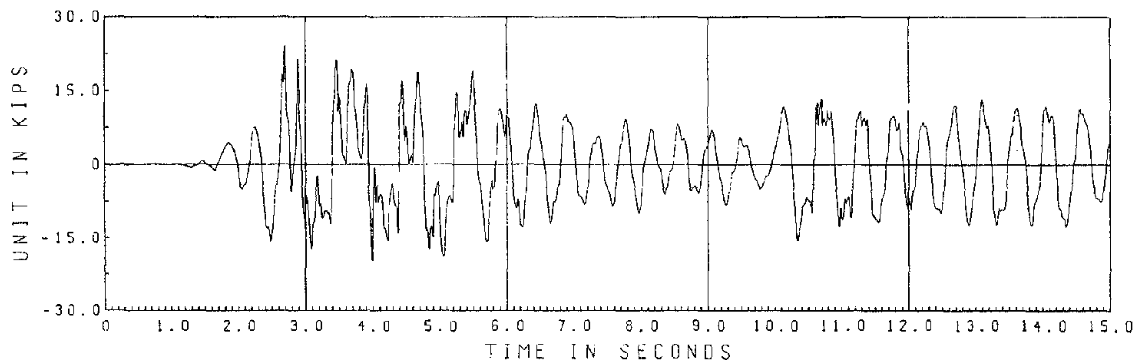

Base Shear

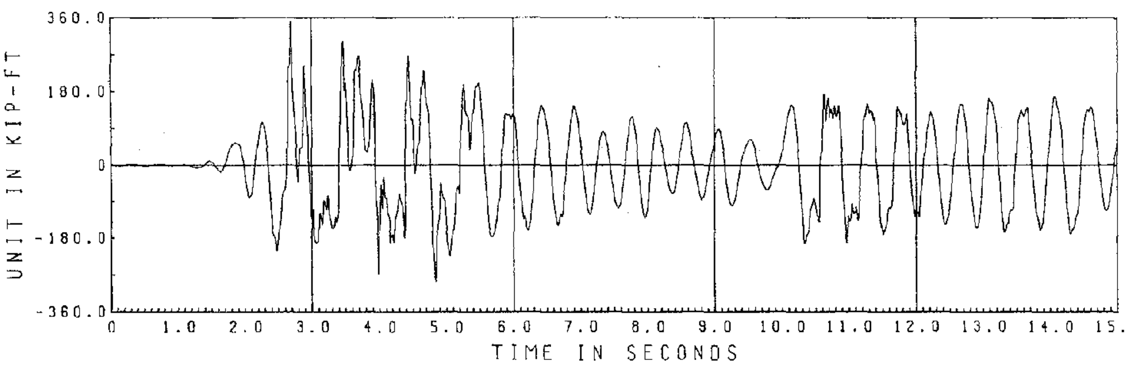

Base Overturning Moment

Fig. 2.5e.5 EC 1000/850 I Story Forces

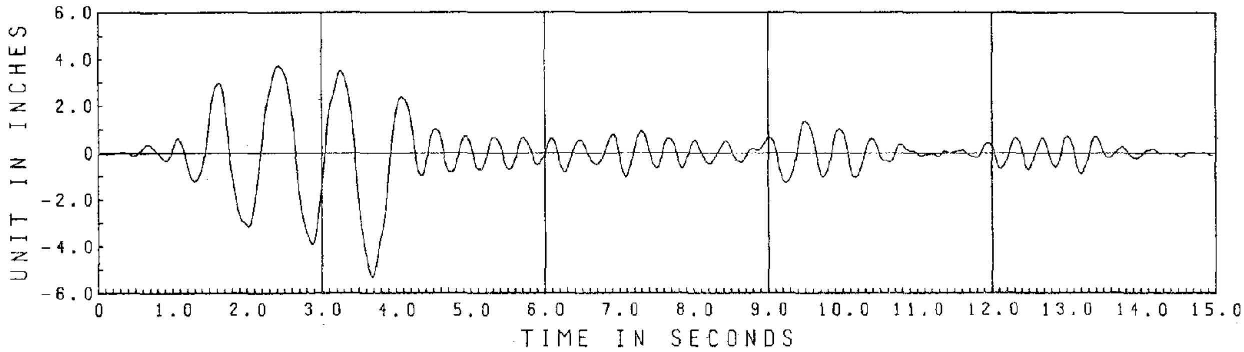

3rd Floor Relative Displacement

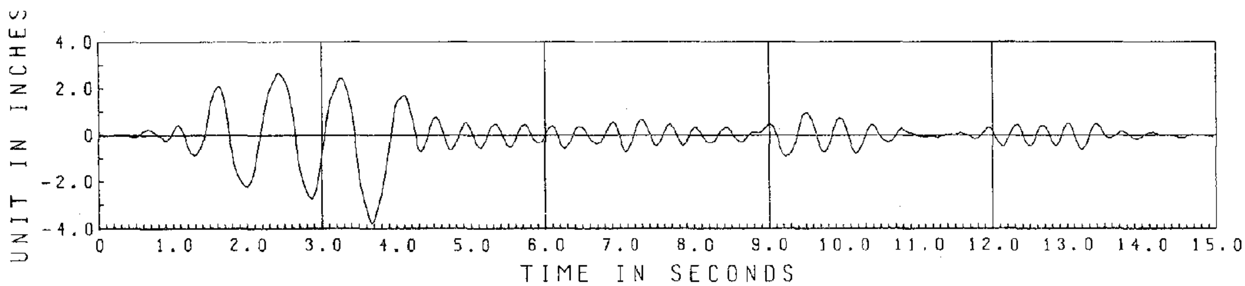

2nd Floor Relative Displacement

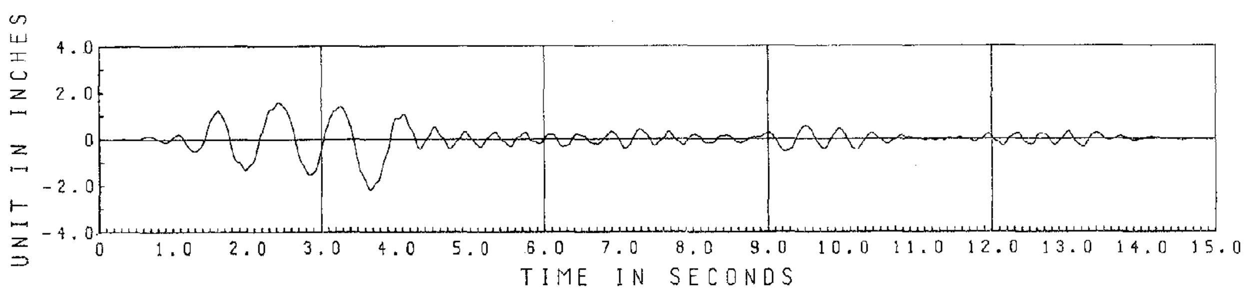

1st Floor Relative Displacement

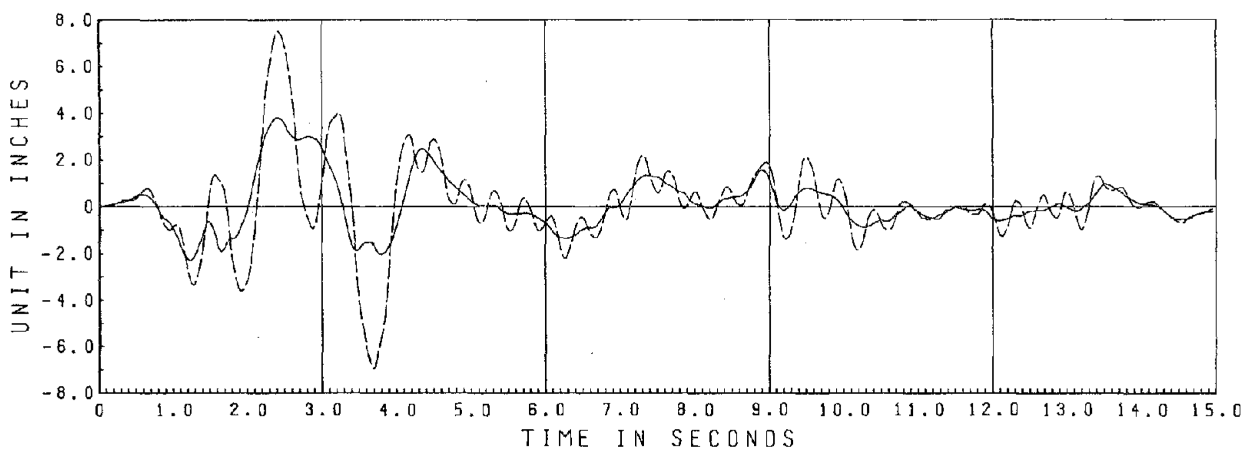

- Table Displacement -- 3rd Floor Absolute Displacement

Fig. 2.5f.3 EC 300 II Displacements

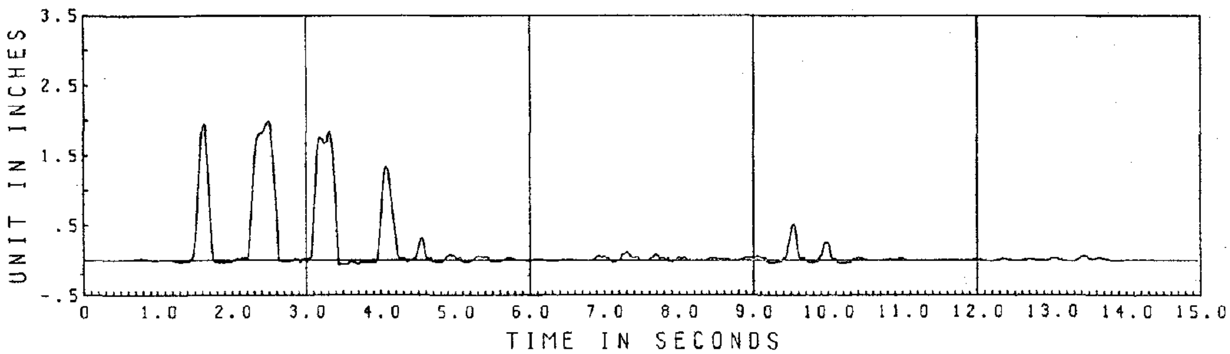

North Column West Frame

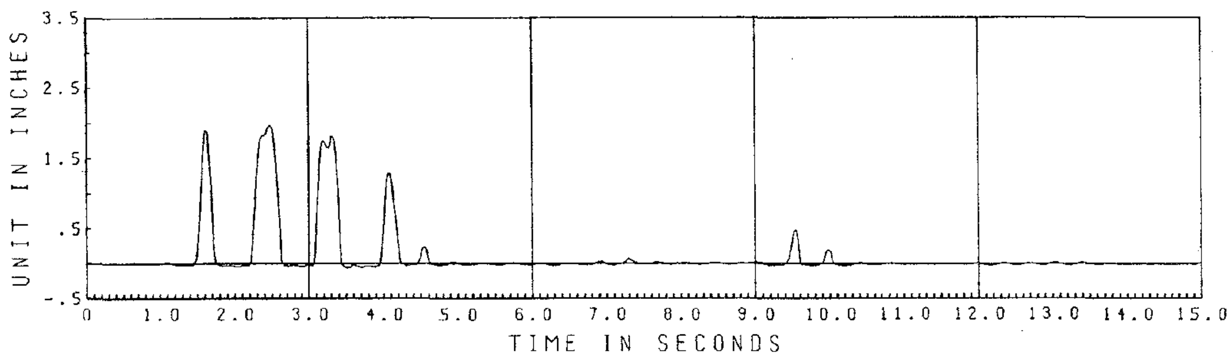

North Column East Frame

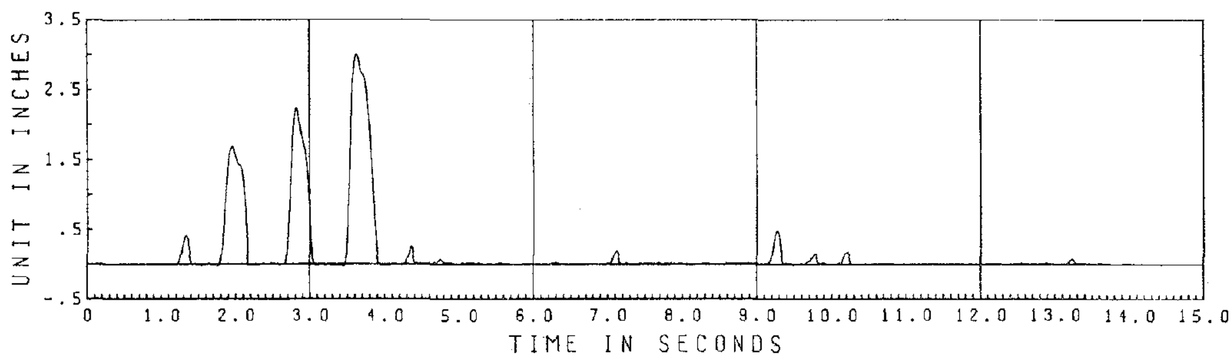

South Column West Frame

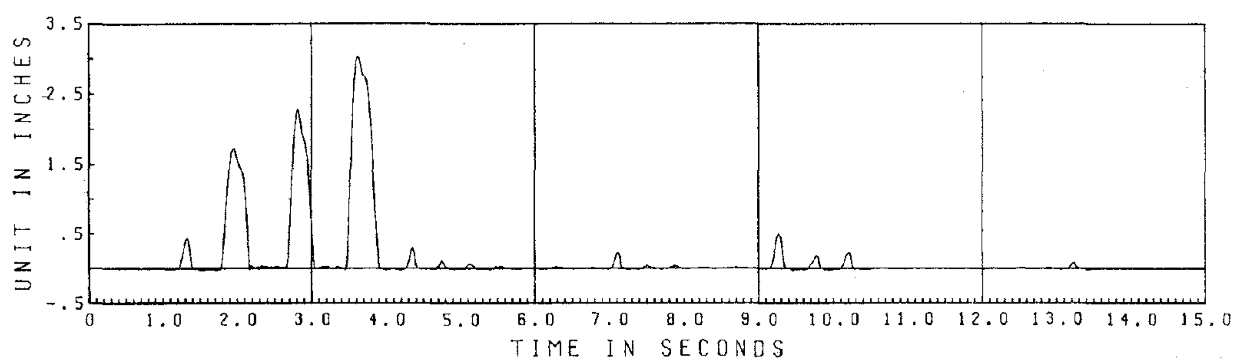

South Column East Frame

Fig. 2.5f.4 EC 300 II Relative Vertical Displacements

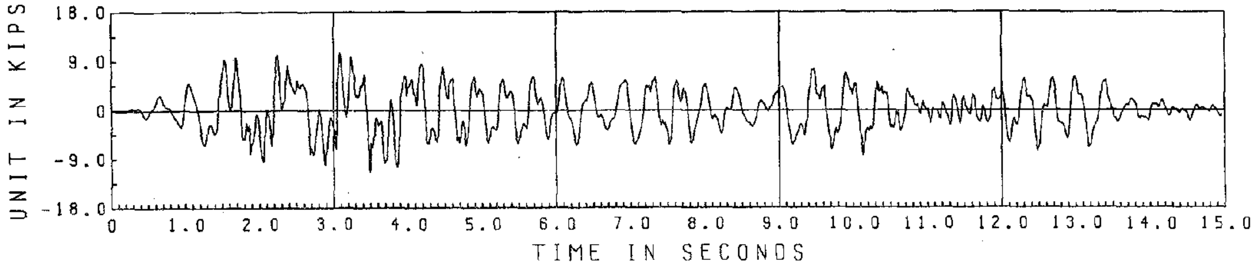

3rd Floor Shear

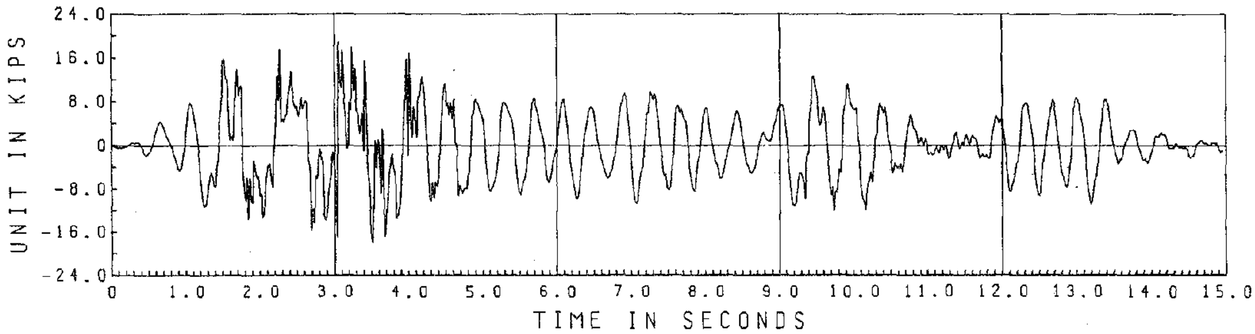

2nd Floor Shear

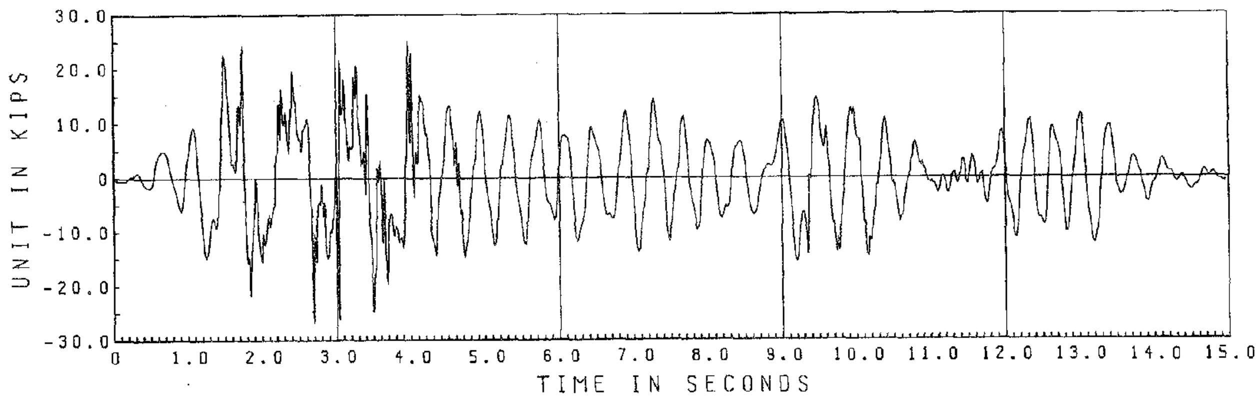

Base Shear

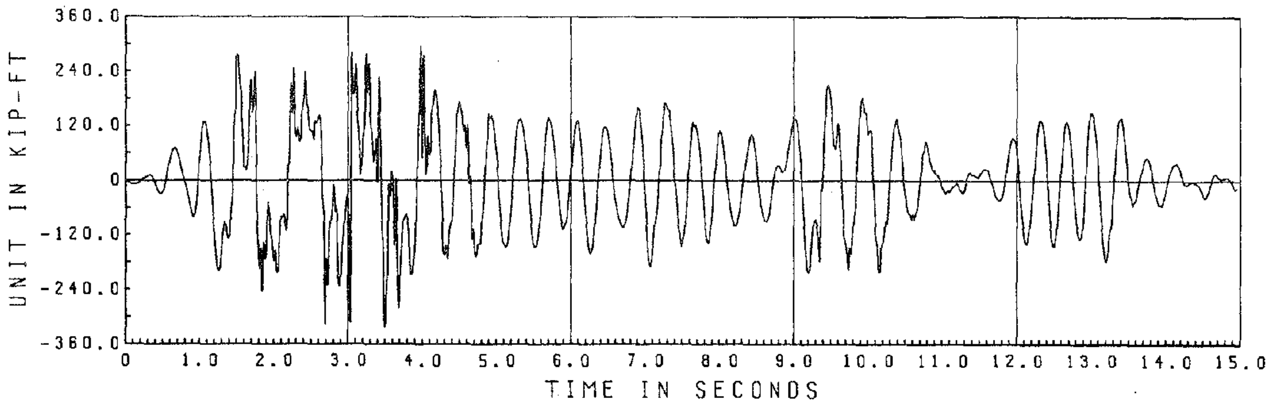

Base Overturning Moment

Fig. 2.5f.5 EC 300 II Story Forces

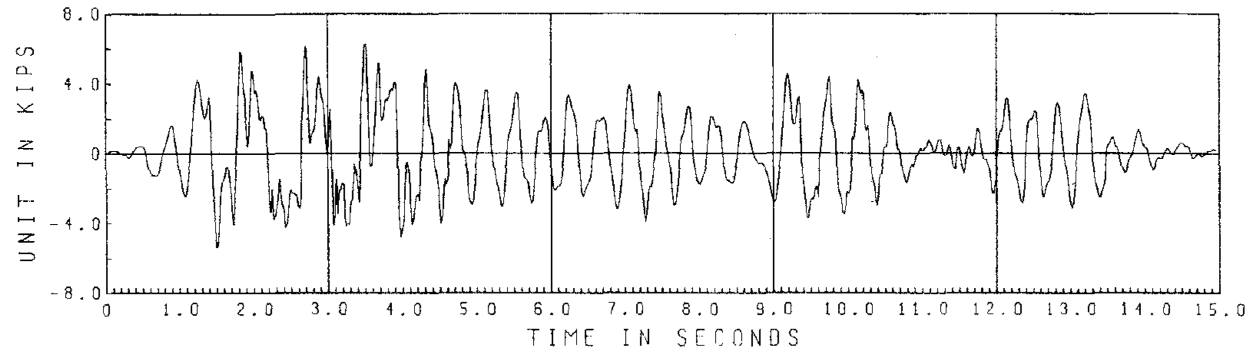

North Column Shear

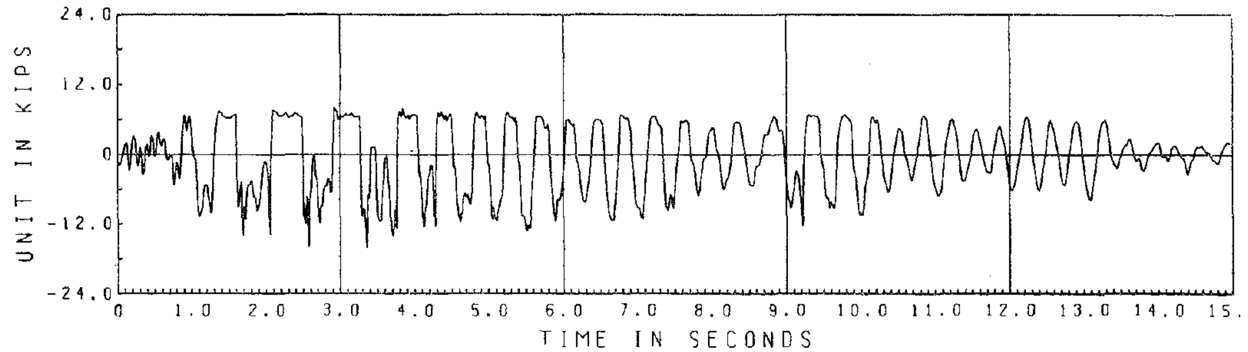

North Column Axial Force

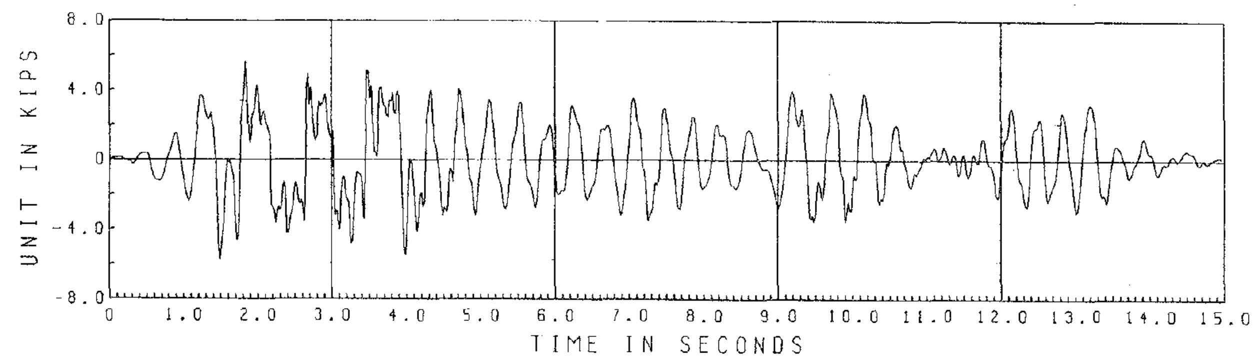

South Column Shear

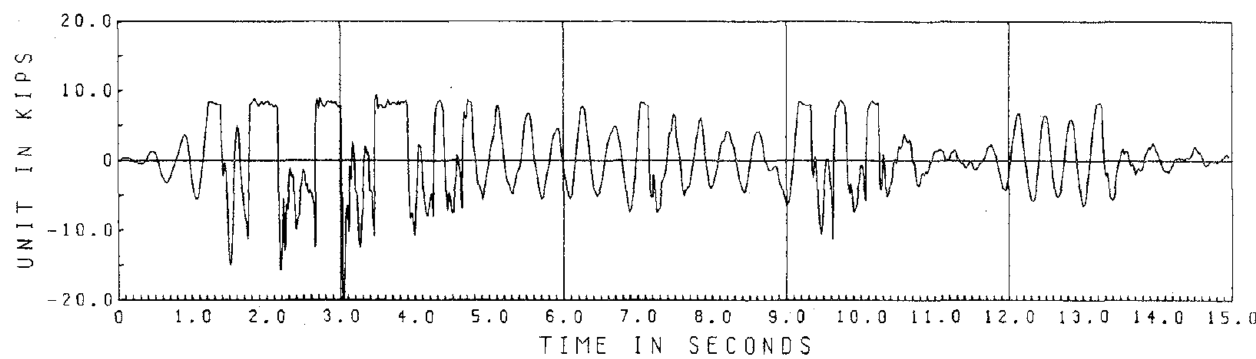

South Column Axial Force

Fig. 2.5f.6 EC 300 II Member Forces

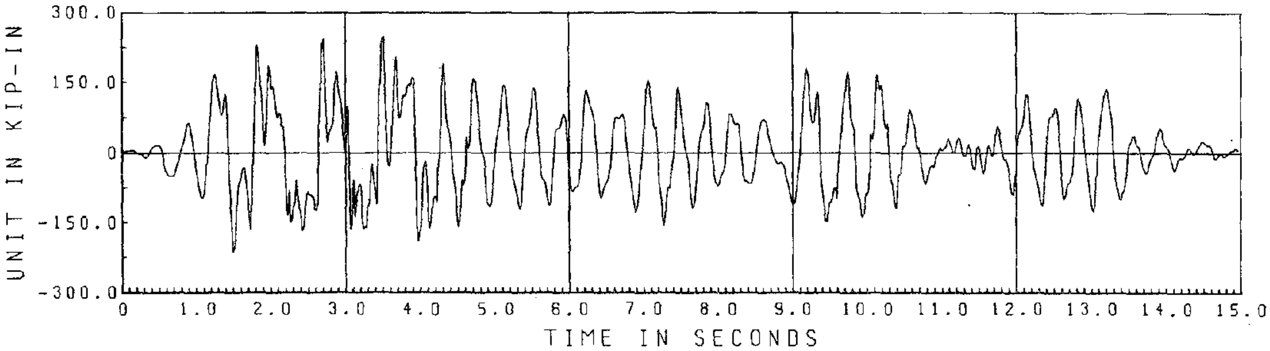

North Column Moment

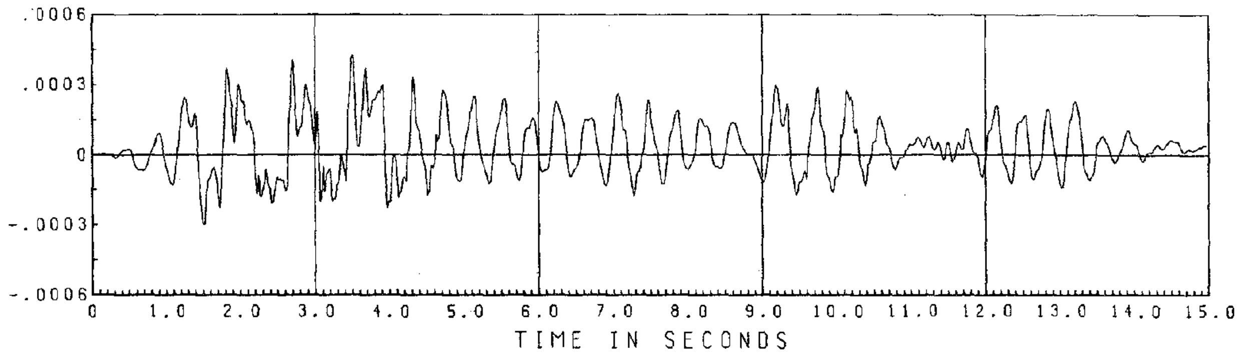

North Column Average Curvature (6" gage)

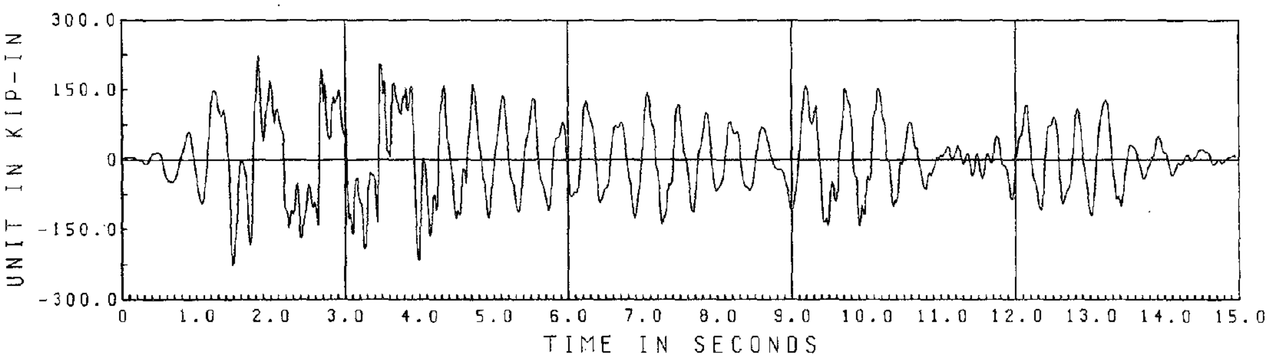

South Column Moment

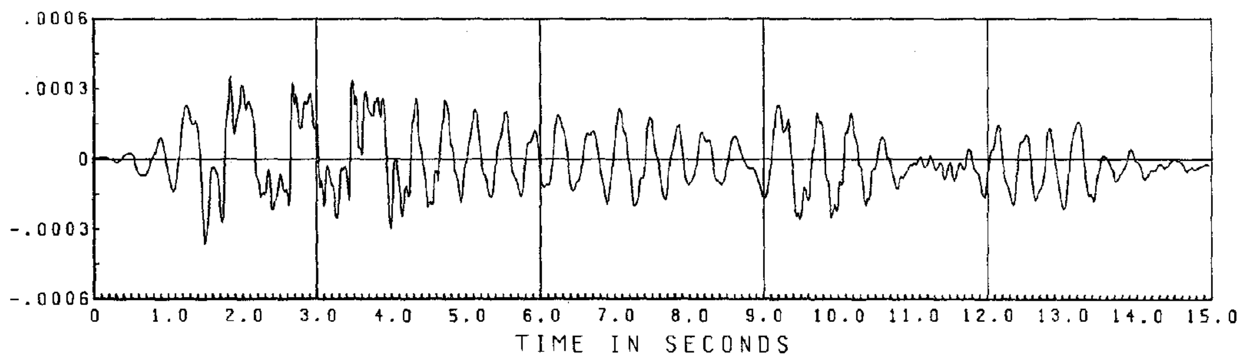

South Column Average Curvature (6" gage)

Fig. 2.5f.7 EC 300 II Column Moments and Curvatures

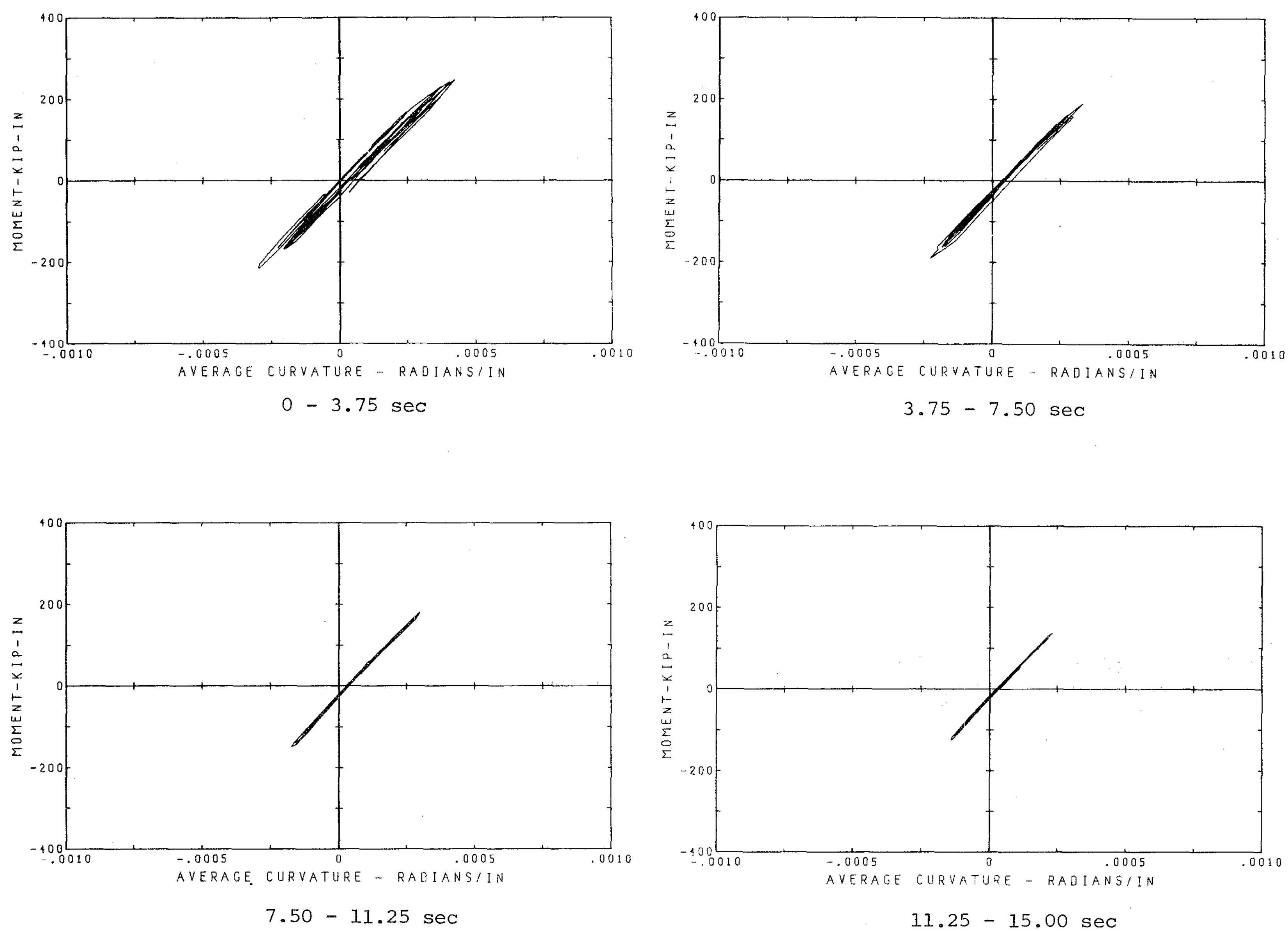

0 - 3.75 sec

3.75 - 7.50 sec

7.50 - 11.25 sec

11.25 - 15.00 sec

Fig. 2.5f.8 EC 300 II North Column Moment vs Average Curvature

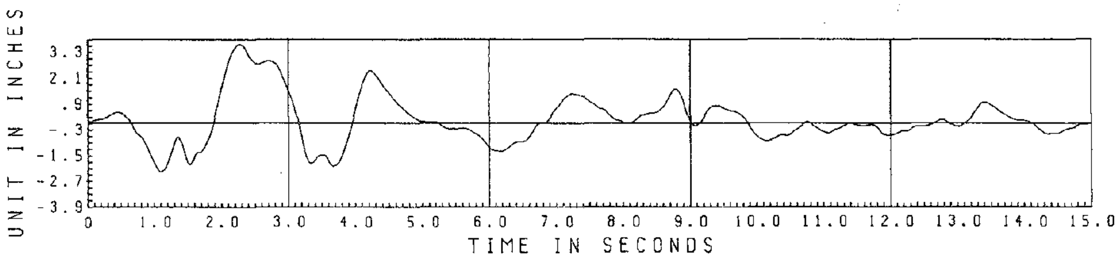

Table Displacement

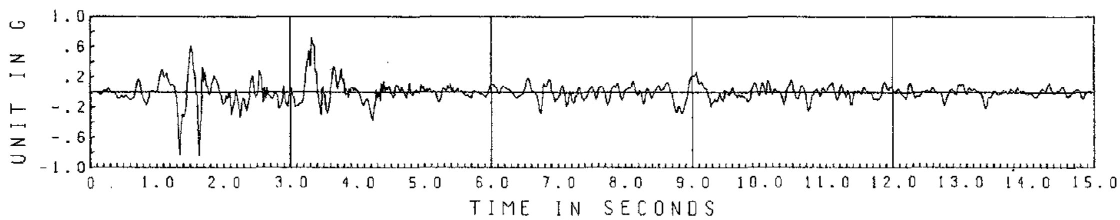

Table Acceleration

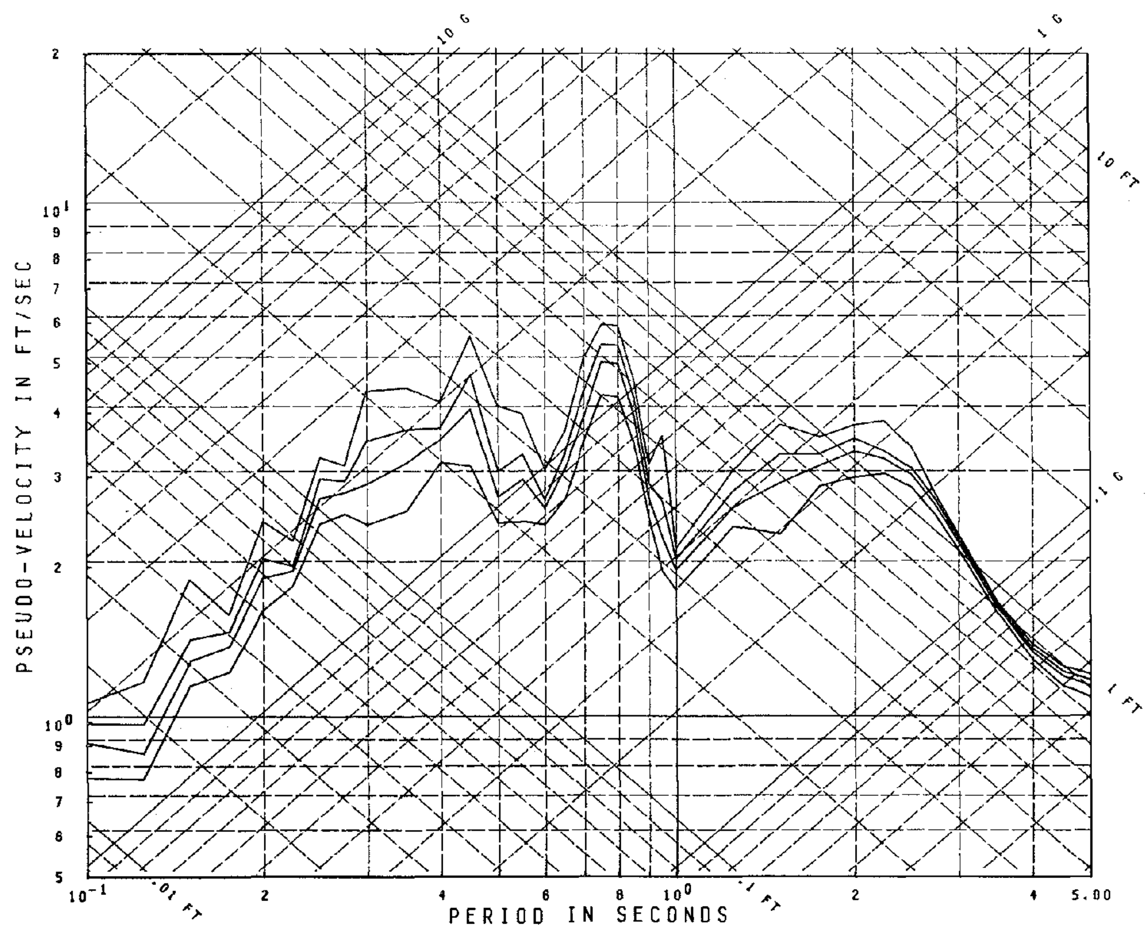

EC 300/675 II

Fig. 2.5g.1 Response Spectra; Damping Ratios = .01, .02, .03, .05

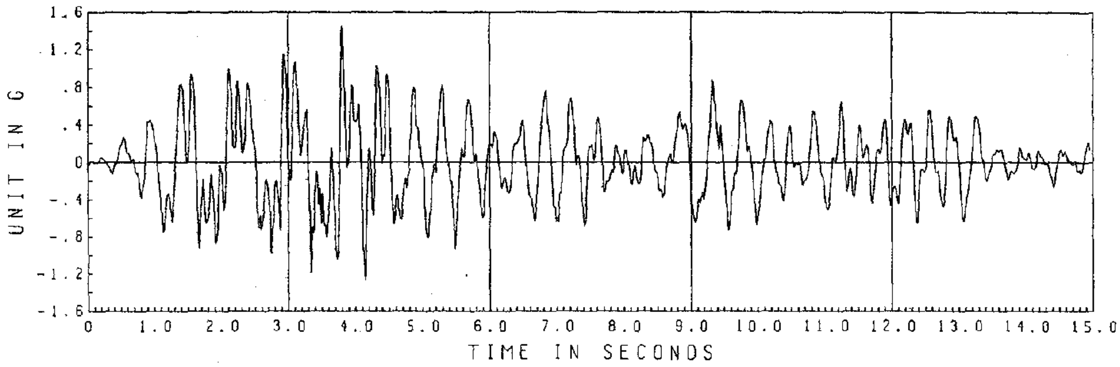

3rd Floor Acceleration

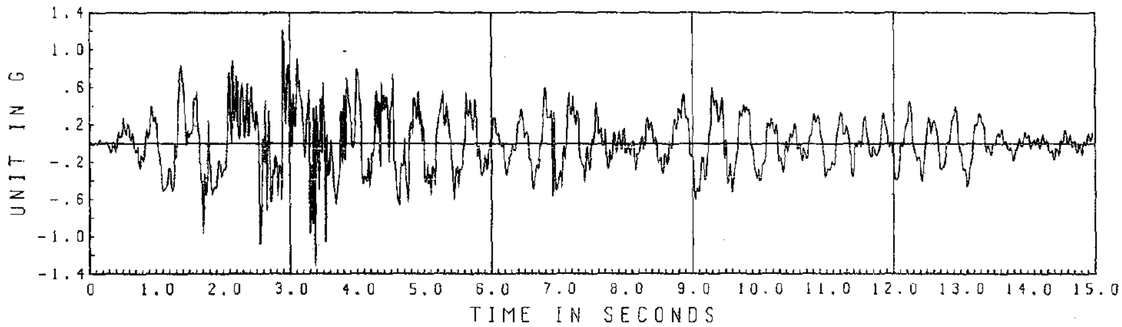

2nd Floor Acceleration

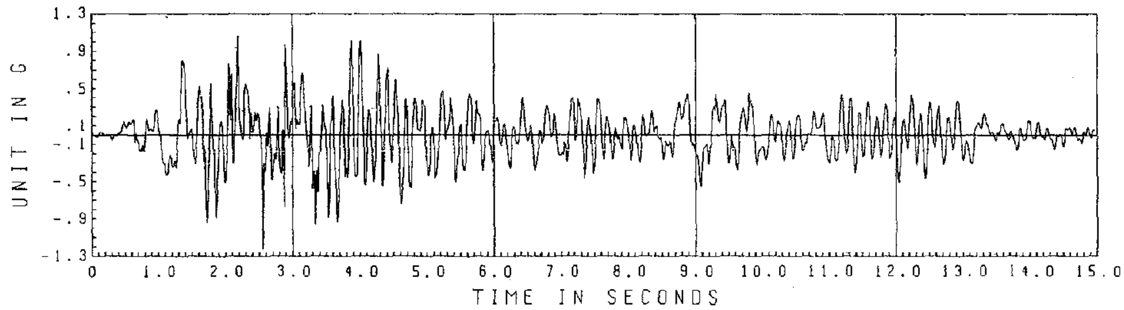

1st Floor Acceleration

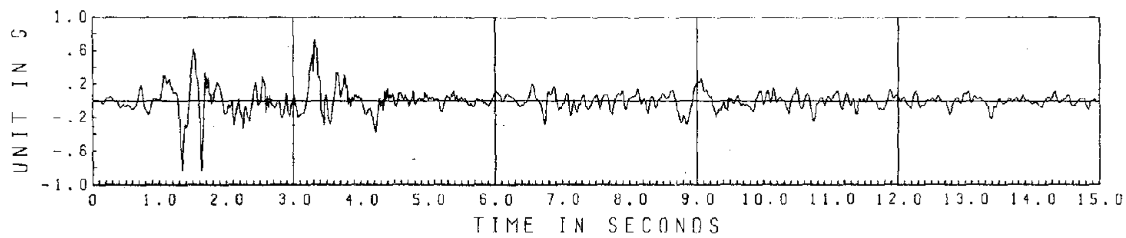

Table Acceleartion

Fig. 2.5g.2 EC 300/675 II Accelerations

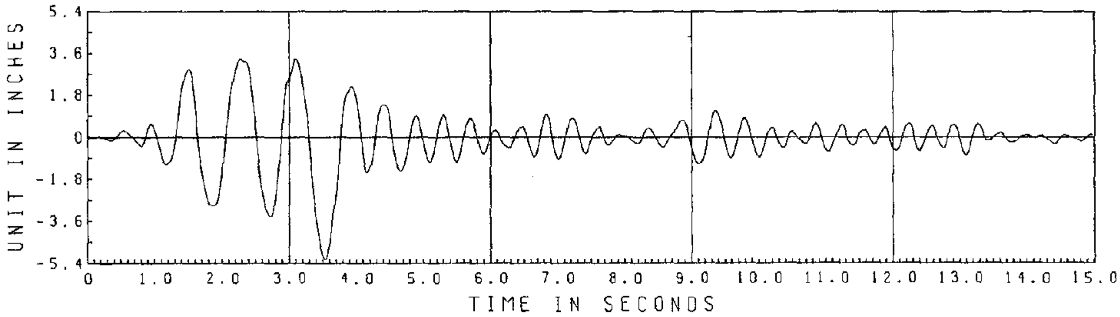

3rd Floor Relative Displacement

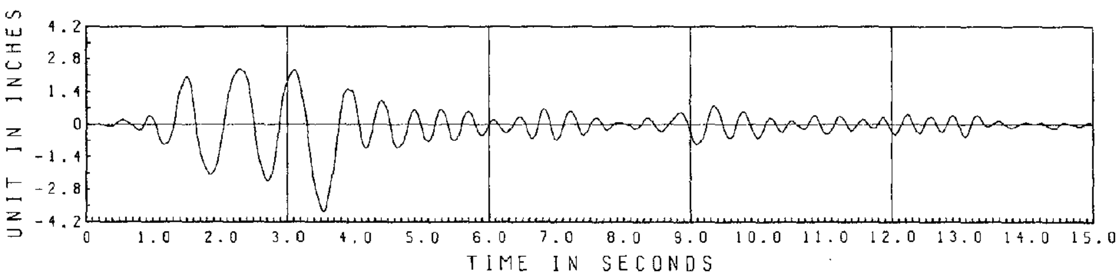

2nd Floor Relative Displacement

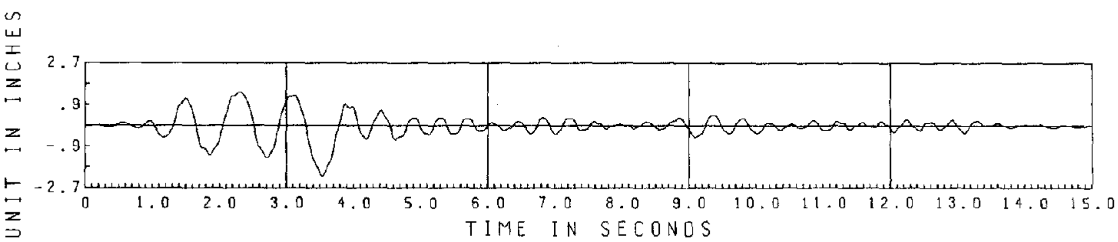

1st Floor Relative Displacement

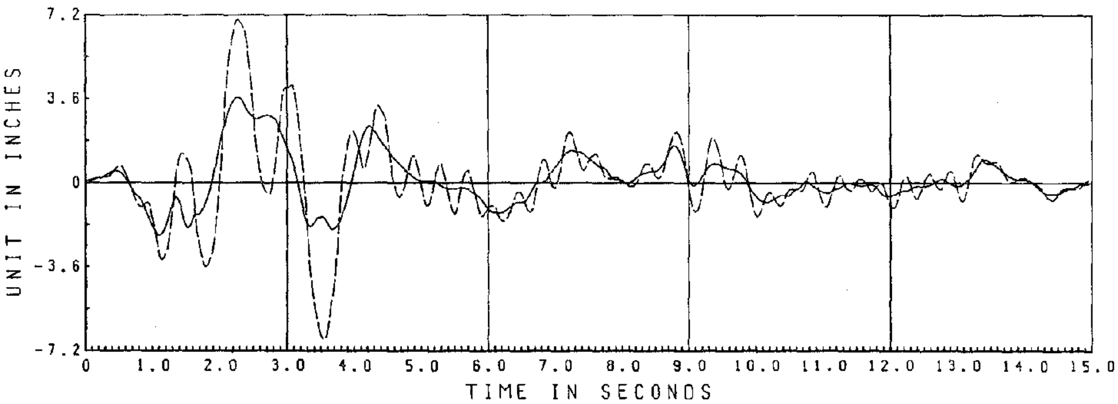

- Table Displacement -- 3rd Floor Absolute Displacement

Fig. 2.5g.3 EC 300/675 II Displacements

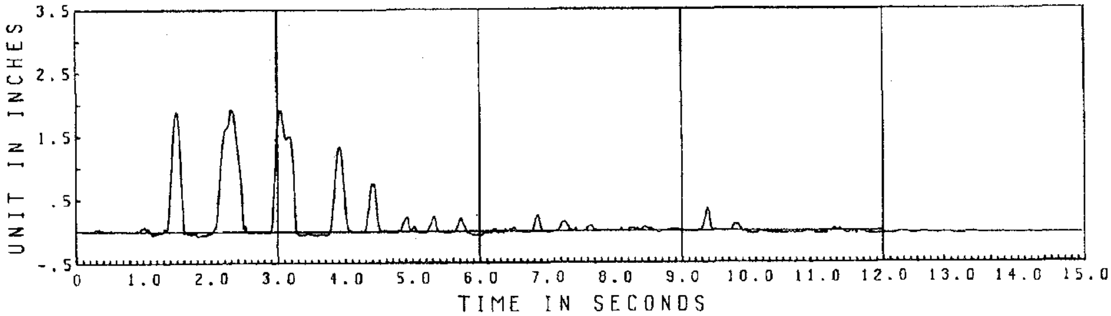

North Column West Frame

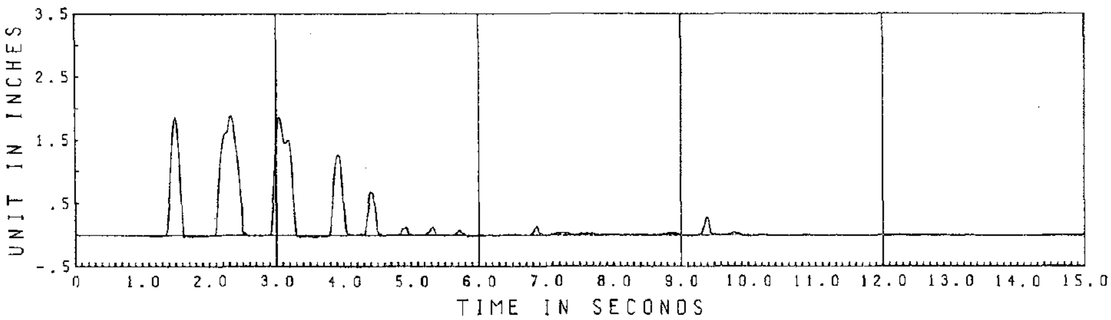

North Column East Frame

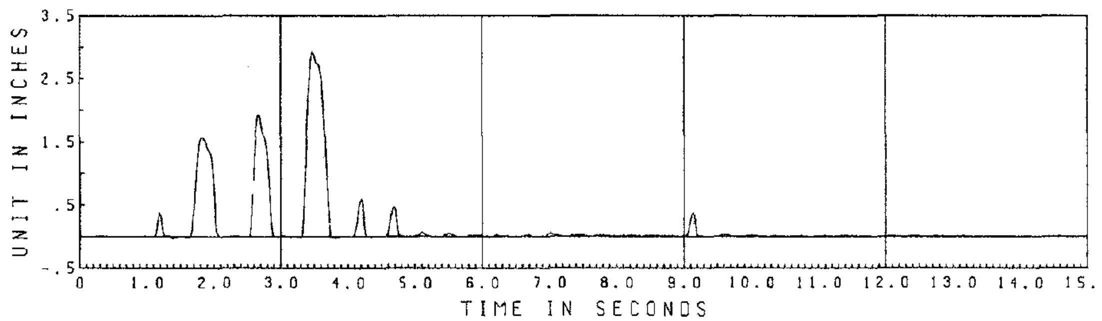

South Column West Frame

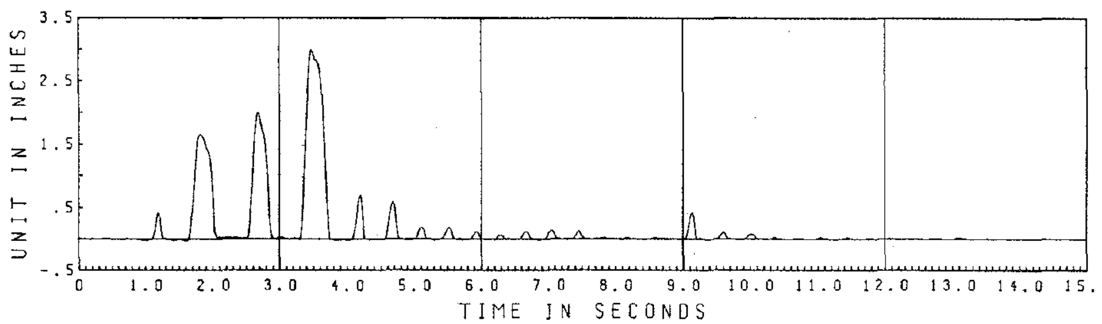

South Column East Frame

Fig. 2.5g.4 EC 300/675 II Relative Column Vertical Displacements

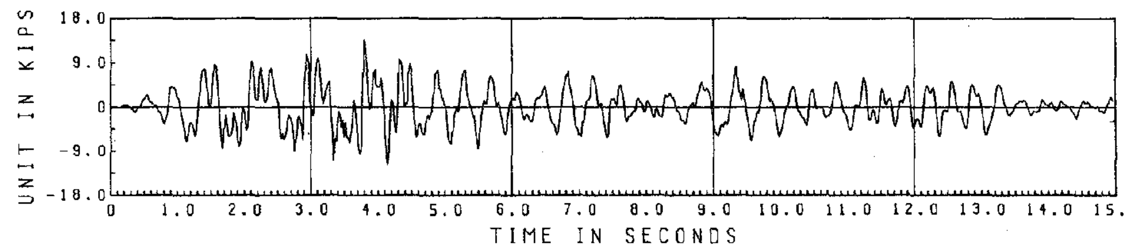

3rd Floor Shear

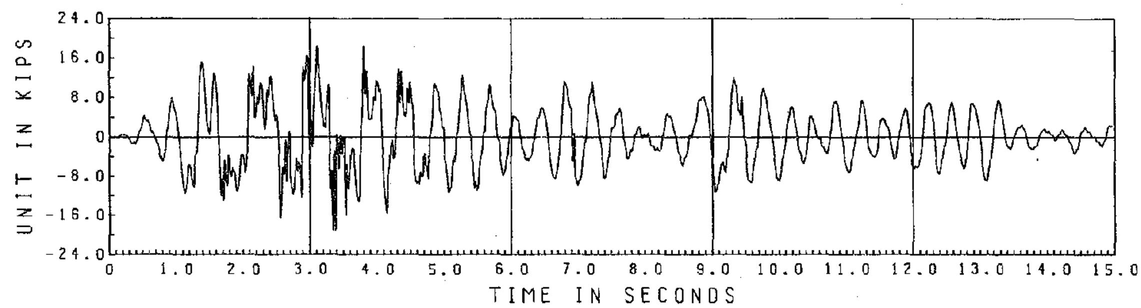

2nd Floor Shear

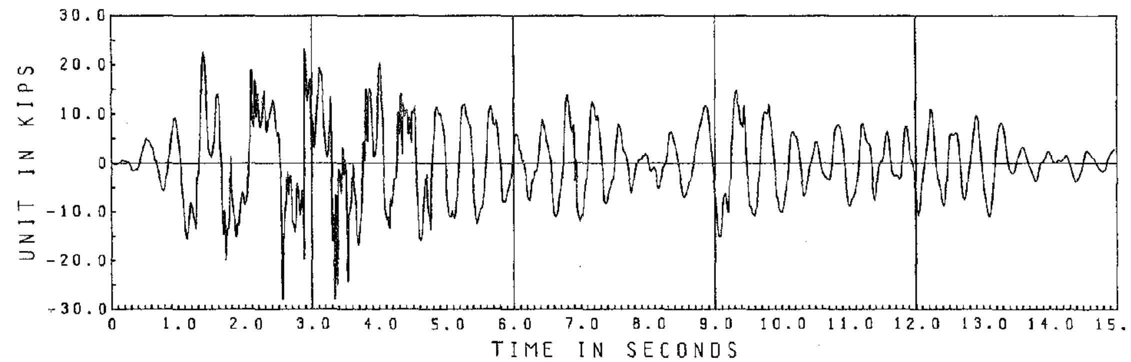

Base Shear

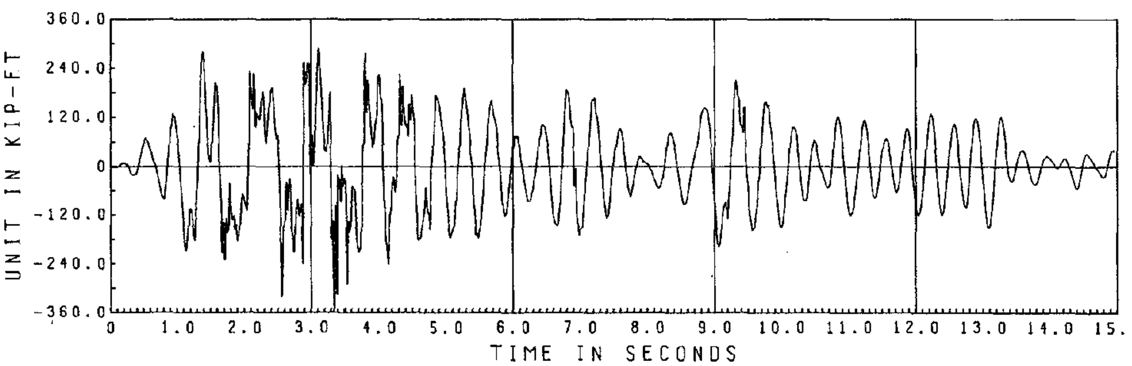

Base Overturning Moment

Fig. 2.5g.5 EC 300/675 II Story Forces

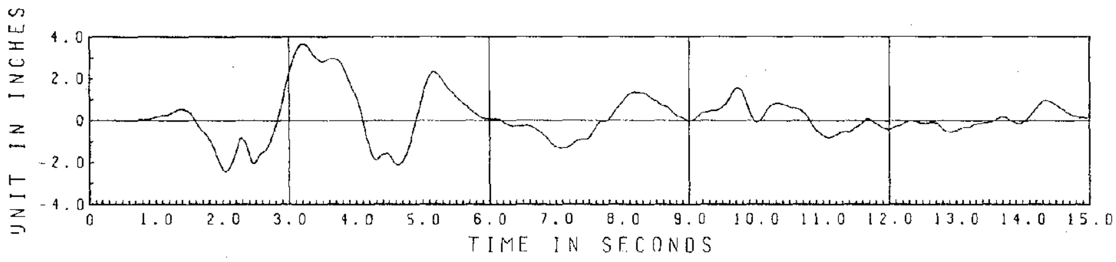

Table Displacement

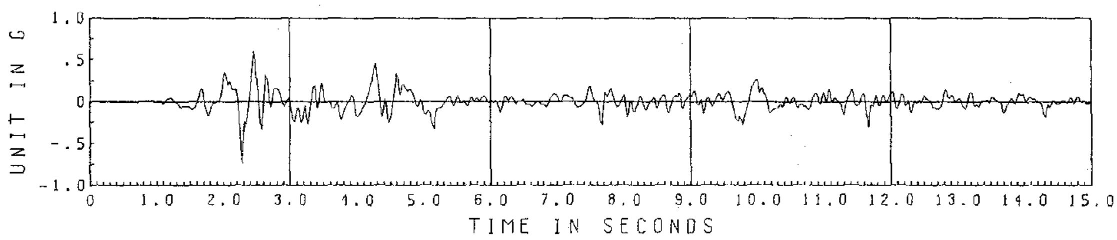

Table Acceleration

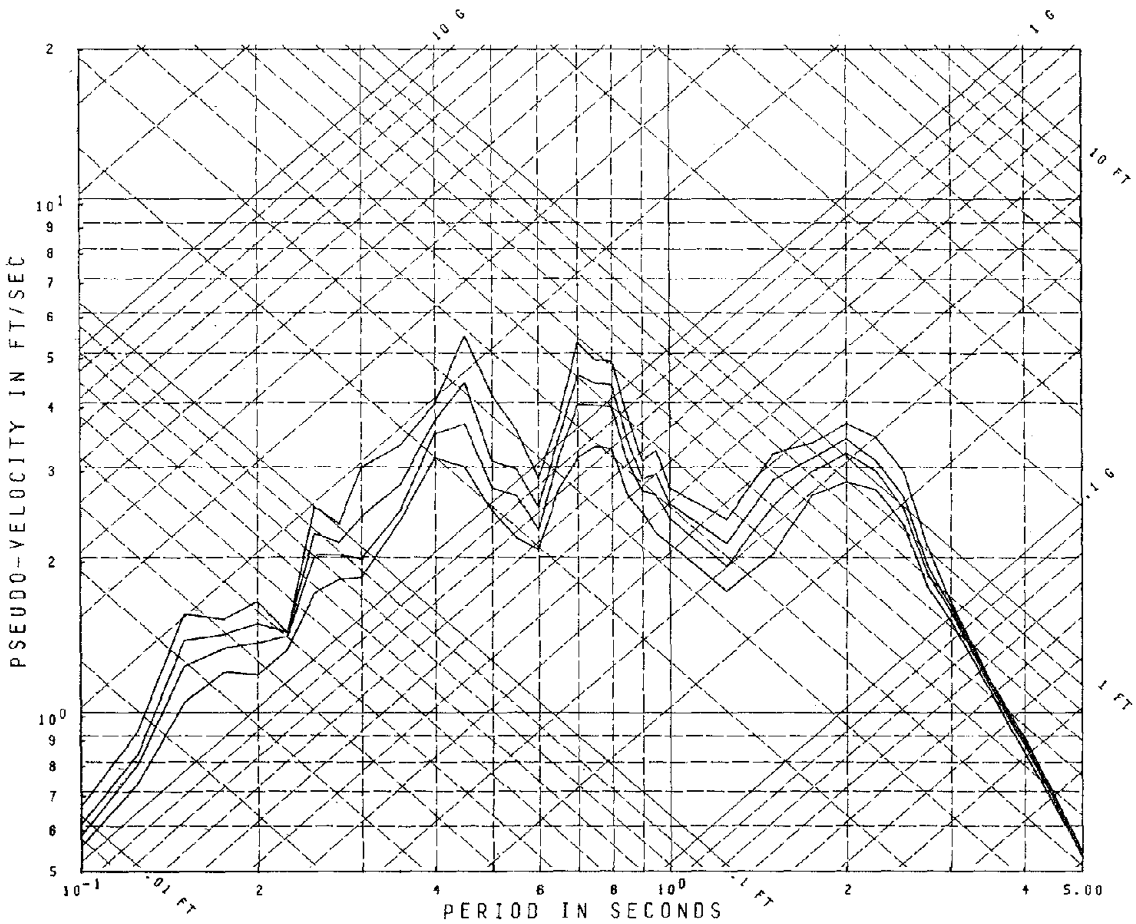

EC 1000

Fig. 2.5h.1 Response Spectra; Damping Ratios = .01, .02, .03, .05

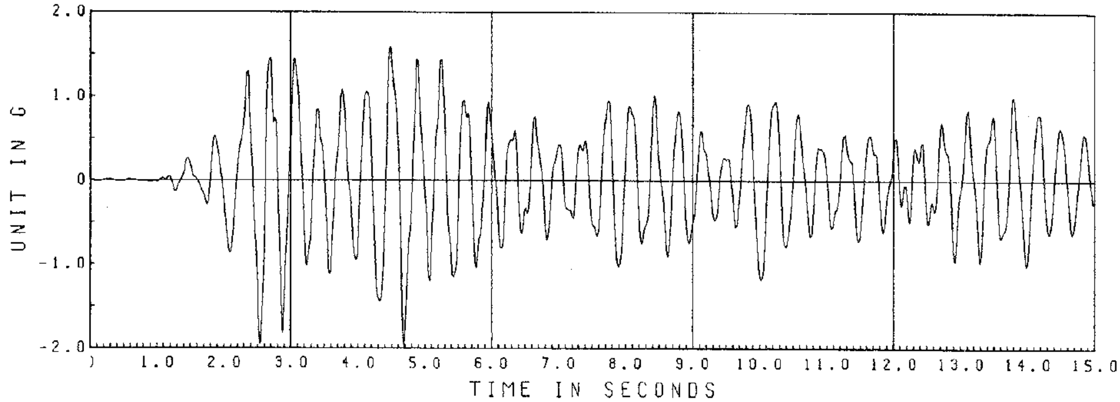

3rd Floor Acceleration

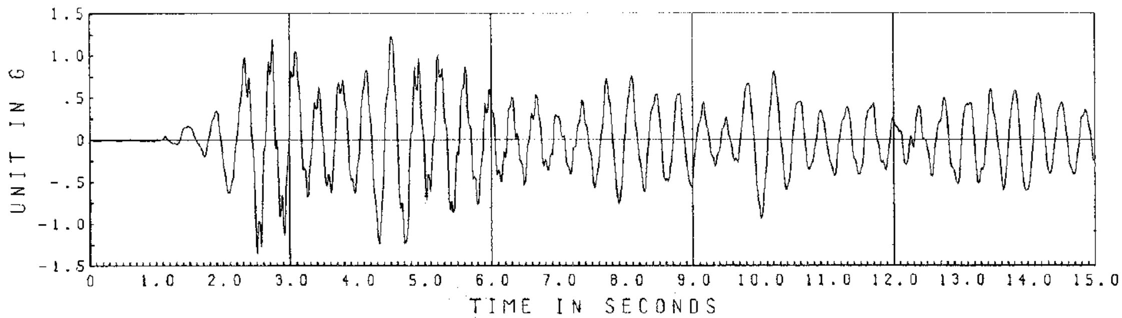

2nd Floor Acceleration

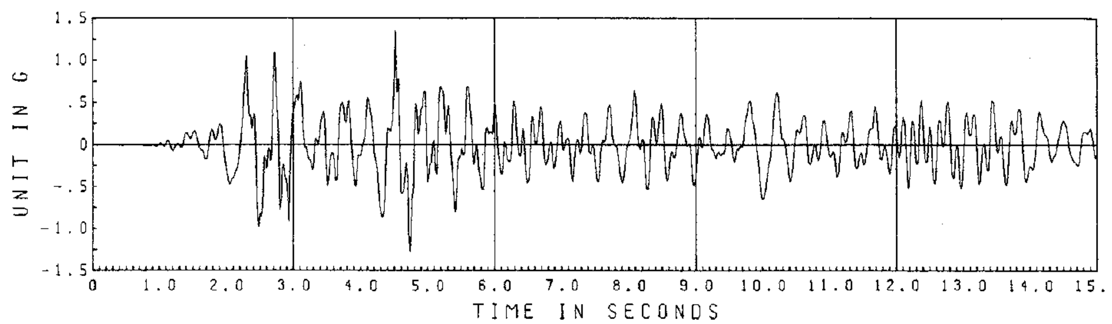

1st Floor Acceleration

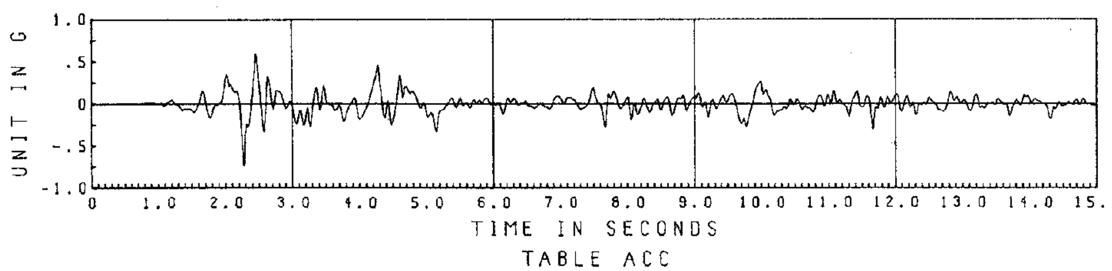

Fig. 2.5h.2 EC 1000 Accelerations

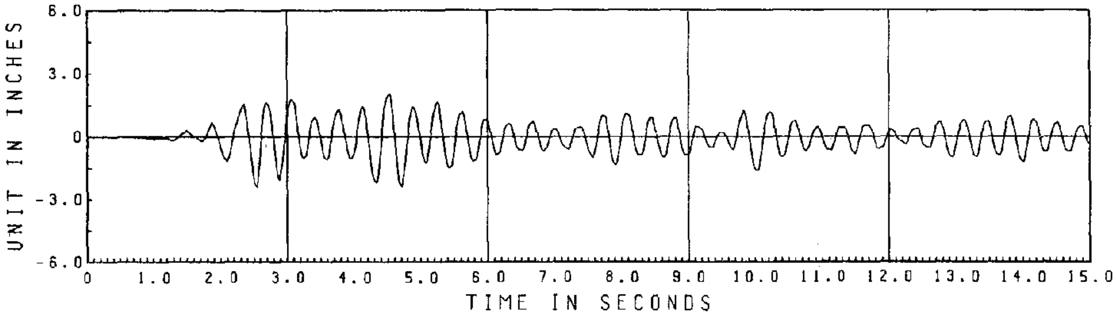

3rd Floor Relative Displacement

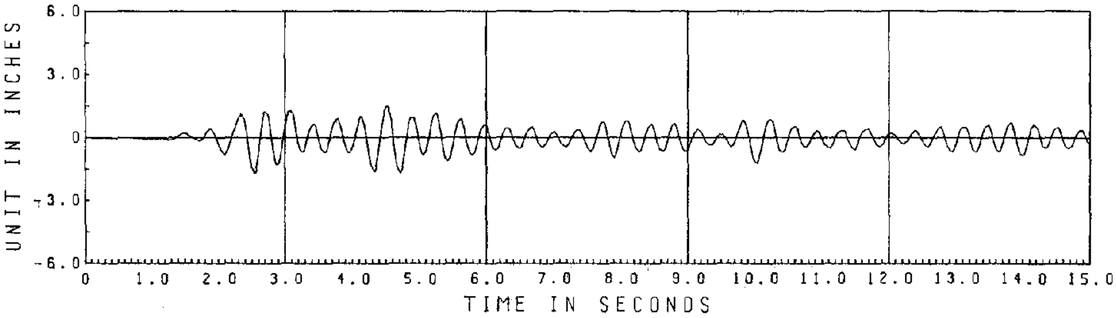

2nd Floor Relative Displacement

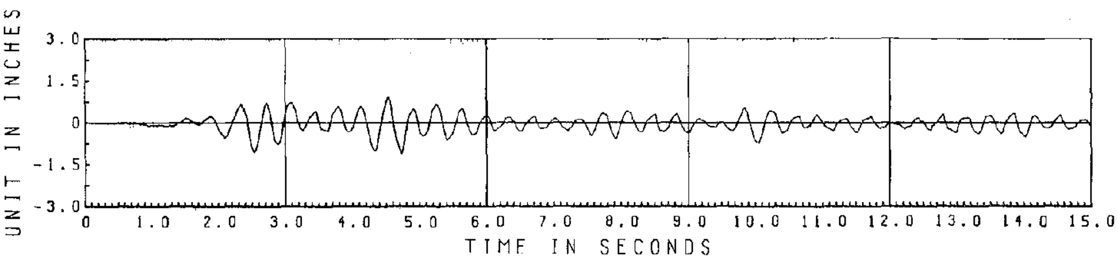

1st Floor Relative Displacement

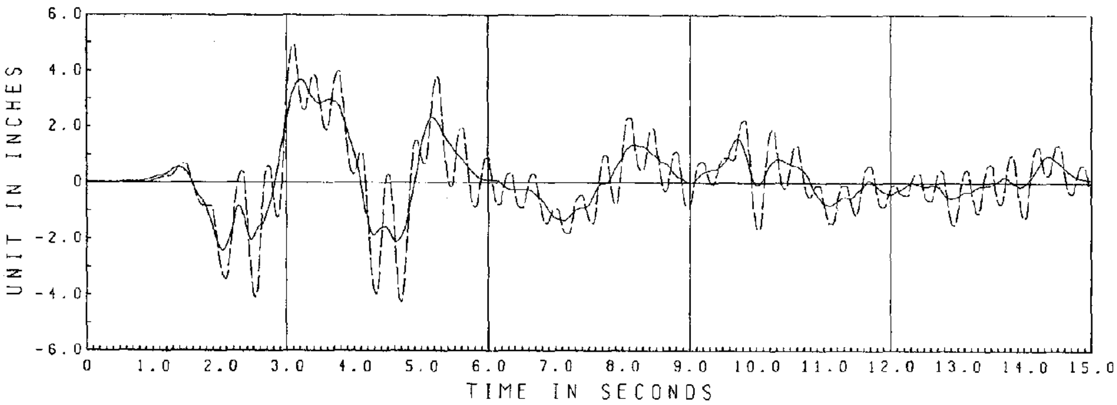

- Table Displacement — -- 3rd Floor Absolute Displacement

Fig. 2.5h.3 EC 1000 Displacements

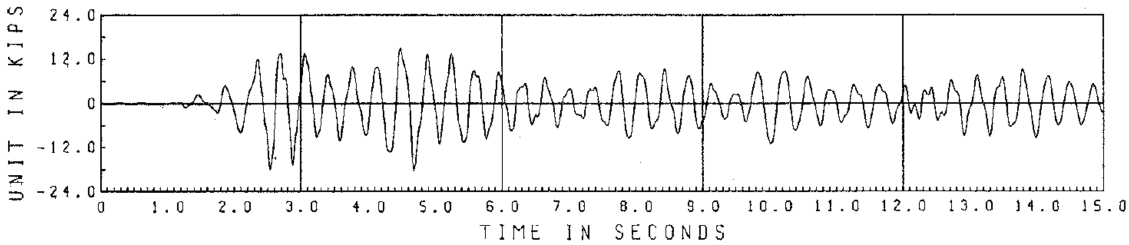

3rd Floor Shear

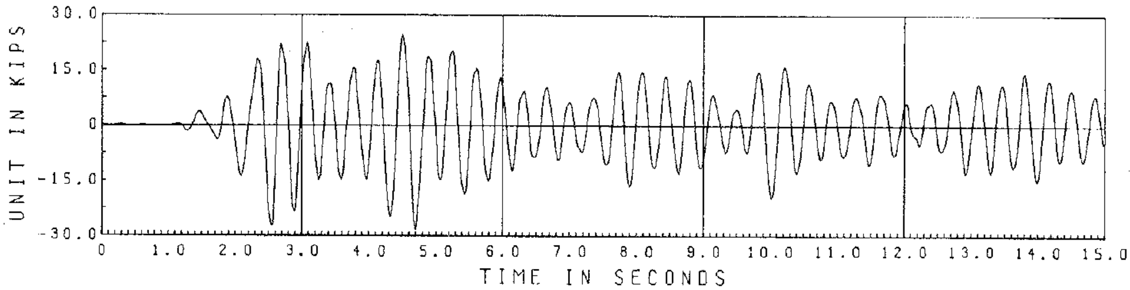

2nd Floor Shear

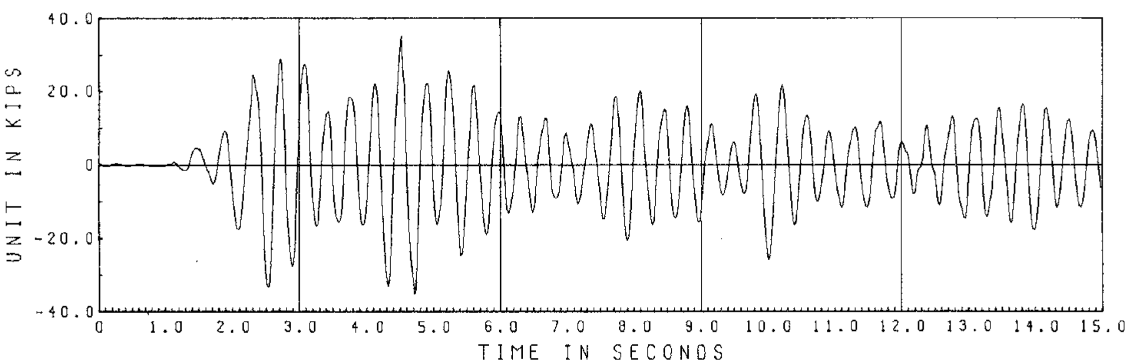

Base Shear

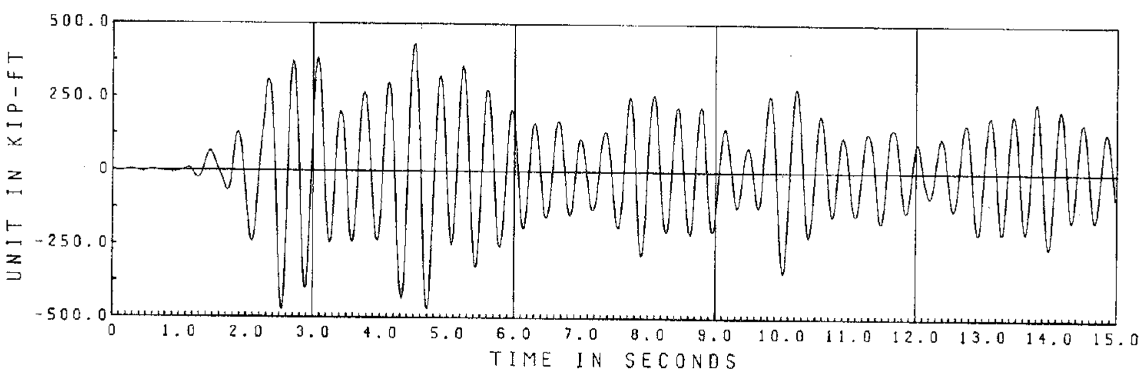

Base Overturning Moment

Fig. 2.5h.4 EC 1000 Story Forces

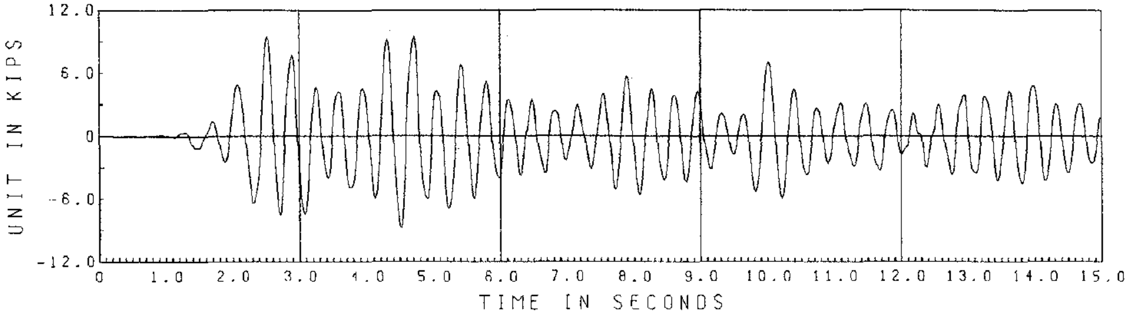

North Column Shear

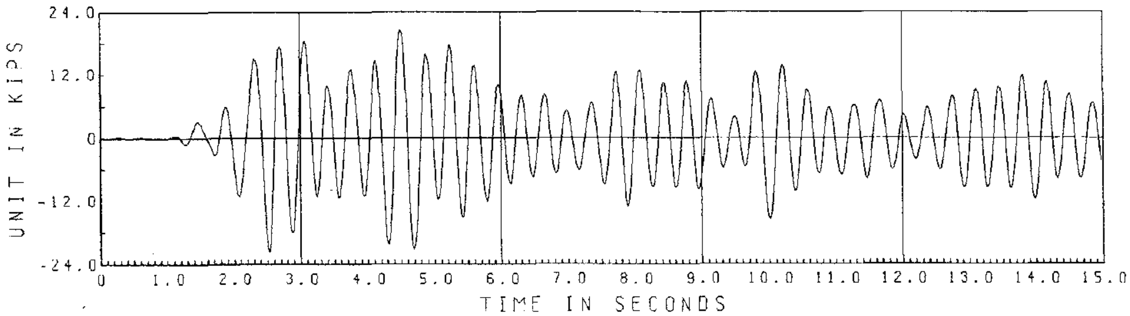

North Column Axial Force

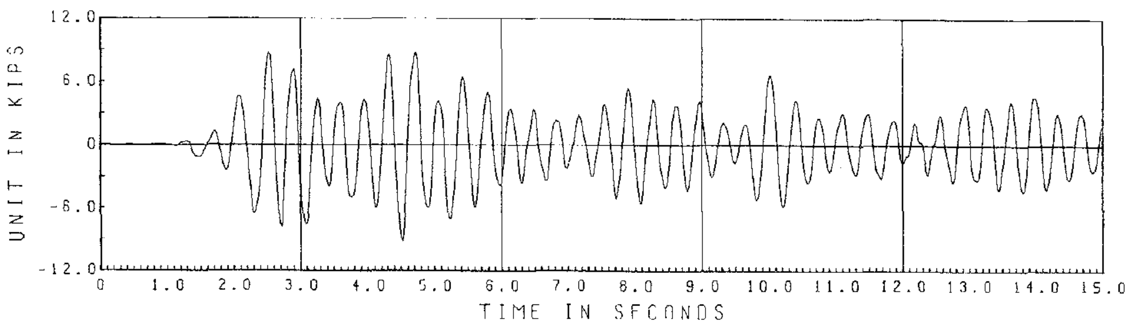

South Column Shear

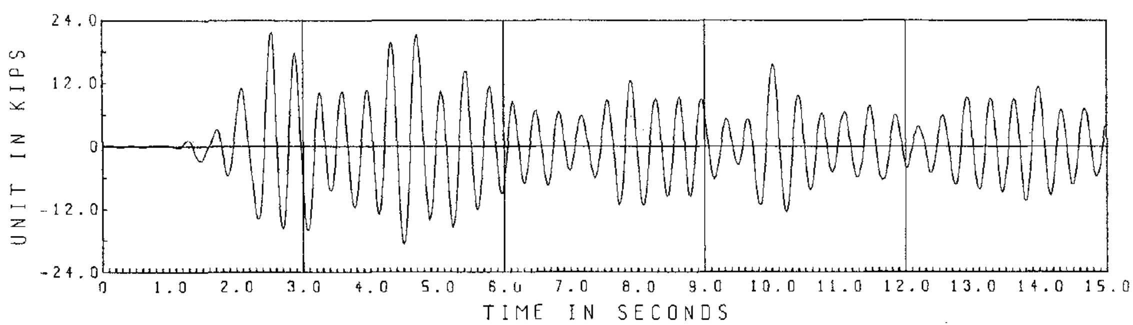

South Column Axial Force

Fig. 2.5h.5 EC 1000 Member Forces

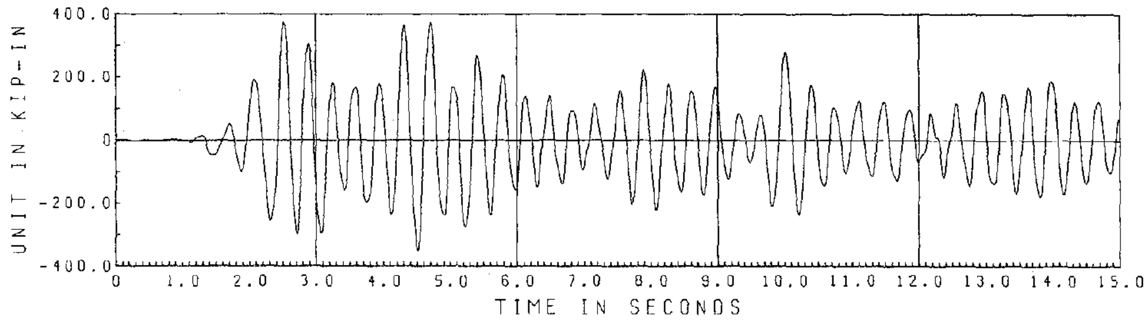

North Column Moment

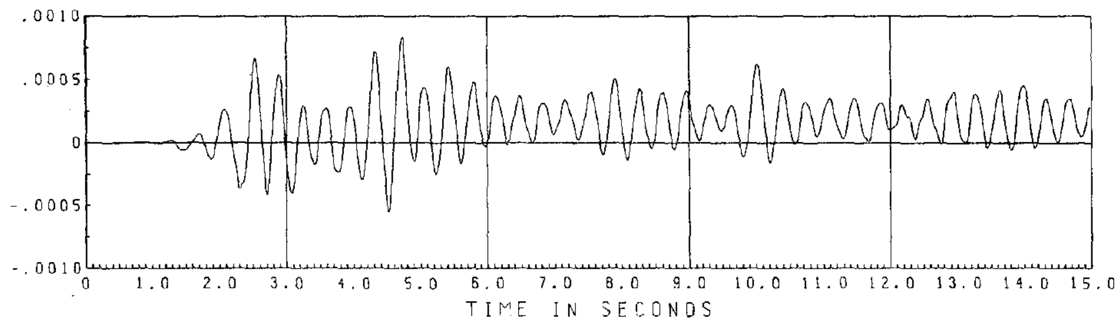

North Column Average Curvature (6" gage)

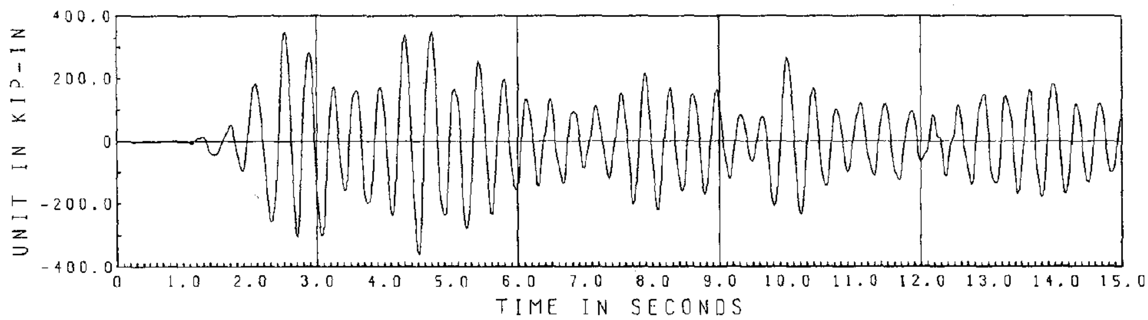

South Column Moment

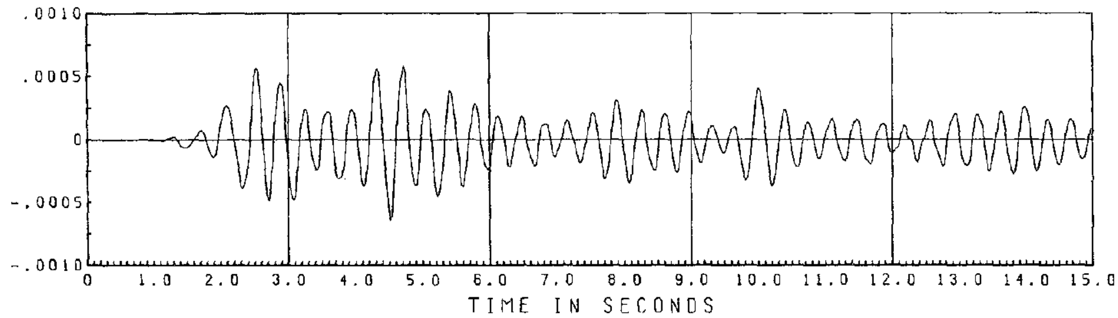

South Column Average Curvature (6" gage)

Fig. 2.5h.6 EC 1000 Column Moments and Curvatures

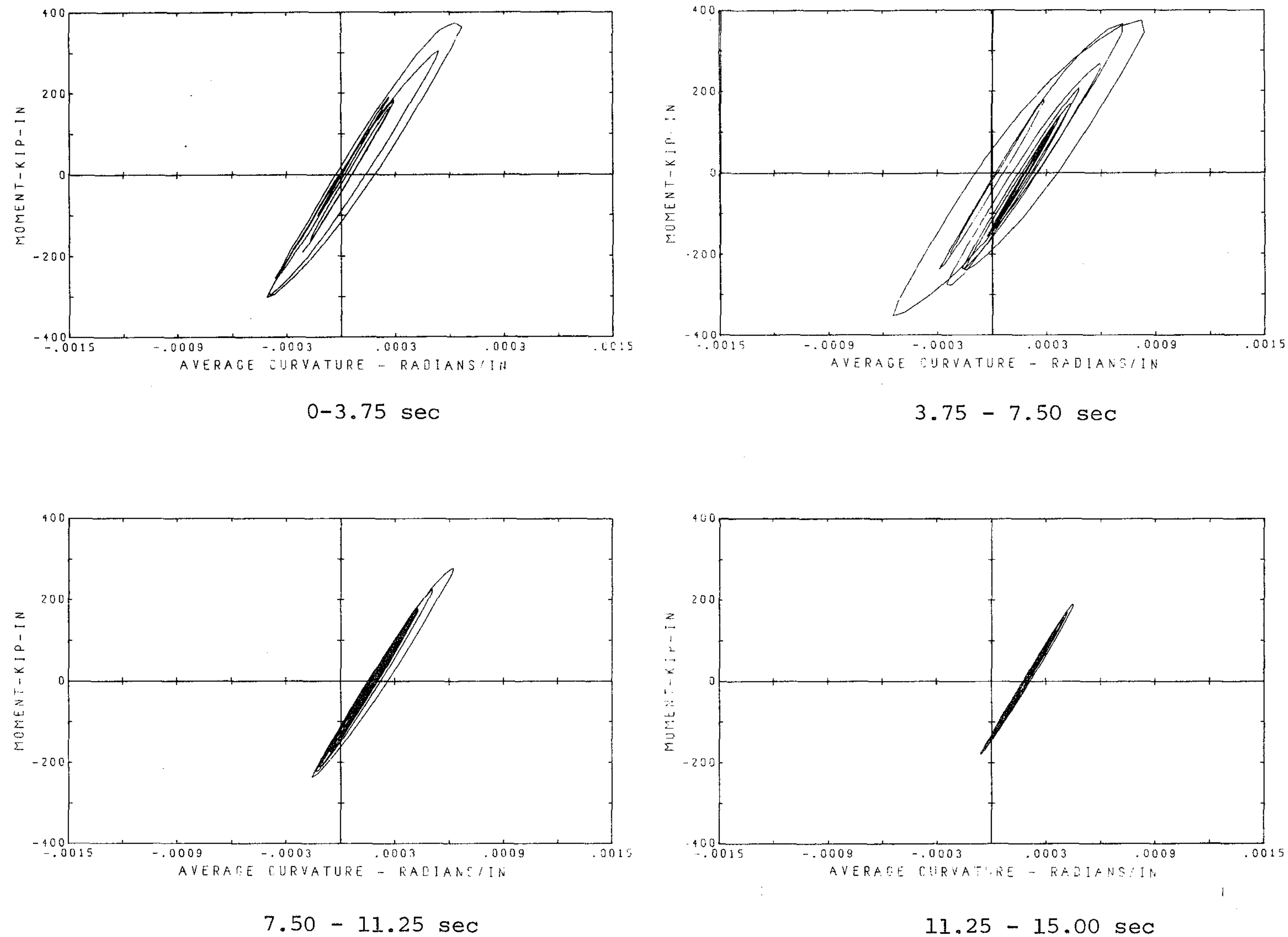

Fig. 2.5h.7 EC 1000 North Column Moment vs Average Curvature

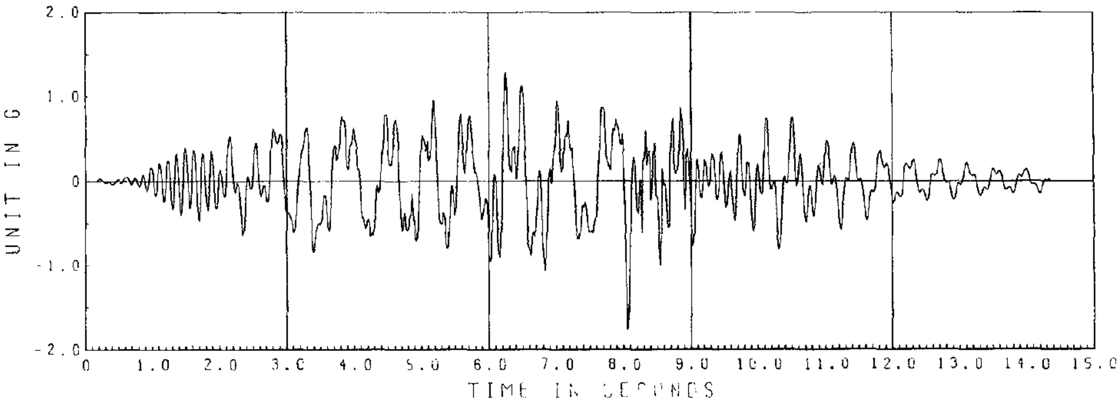

3rd Floor Acceleration

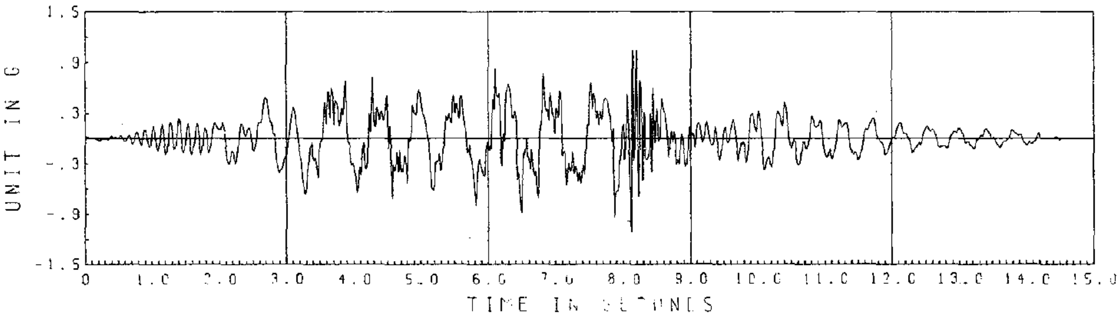

2nd Floor Acceleration

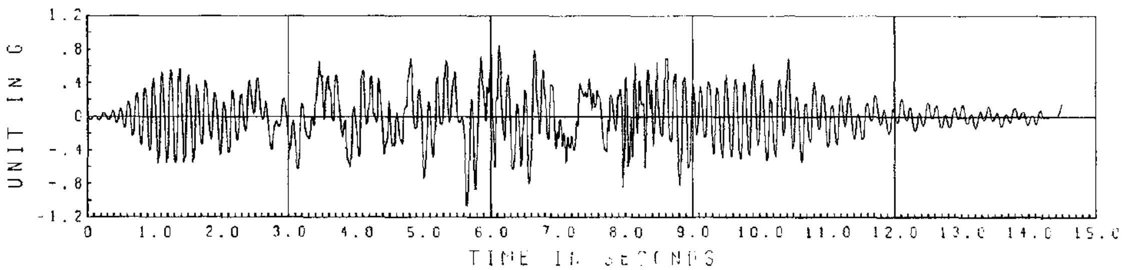

1st Floor Acceleration

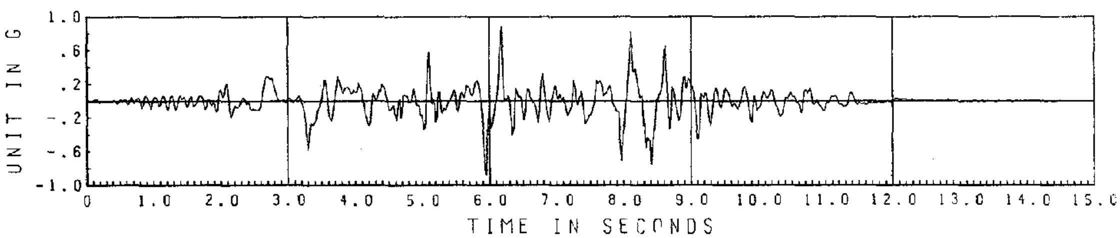

Table Acceleration

Fig. 2.5i.2 PAC 400 I Accelerations

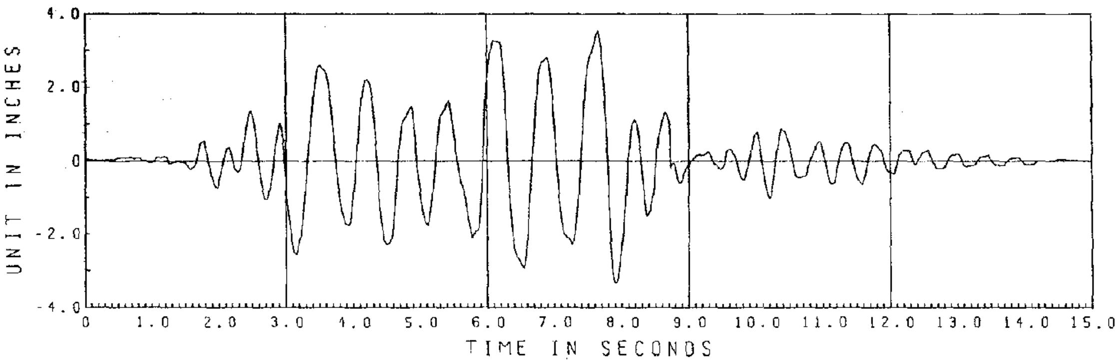

3rd Floor Relative Displacement

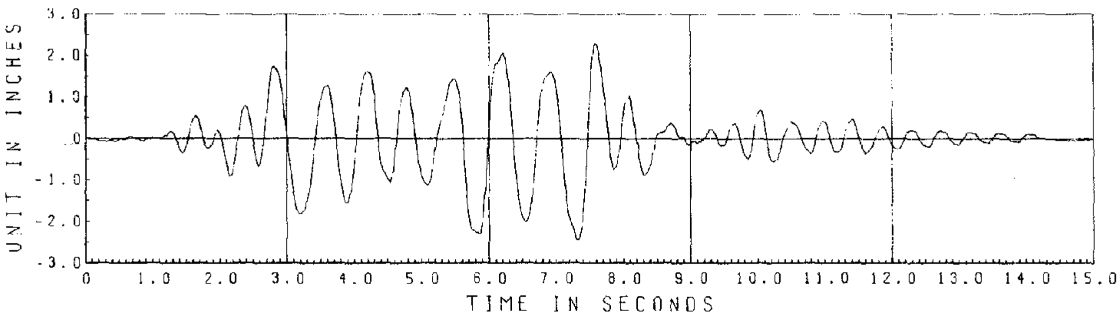

2nd Floor Relative Displacement

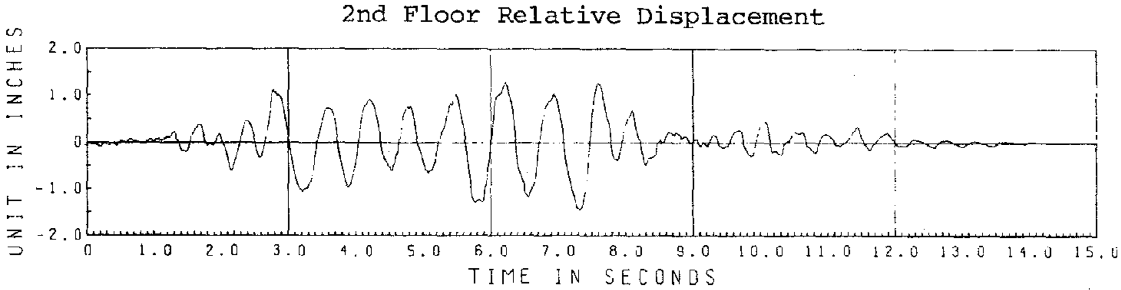

1st Floor Relative Displacement

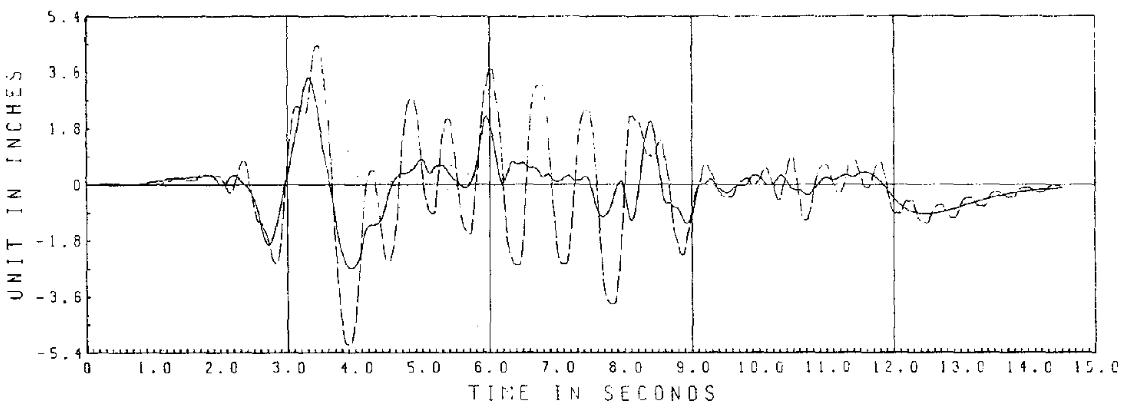

- Table Displacement -- 3rd Floor Absolute Displacement

Fig. 2.5i.3 PAC 400 I Displacements

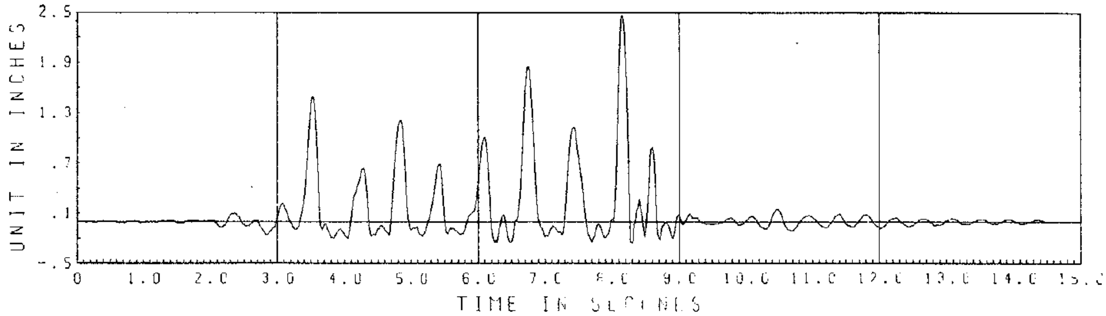

North Column West Frame

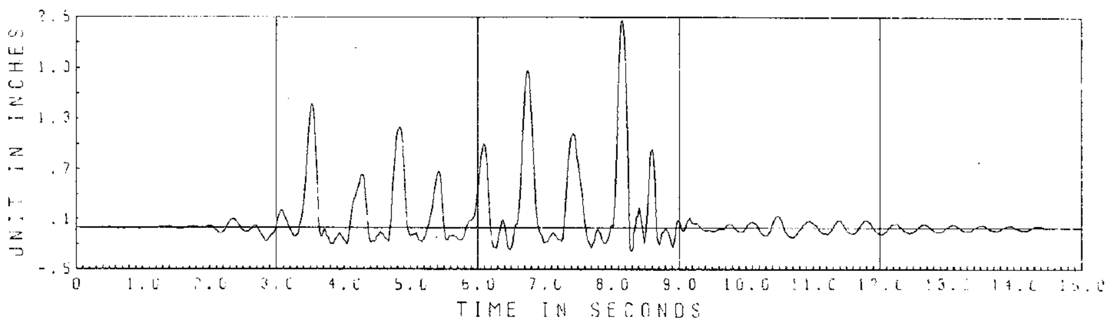

North Column East Frame

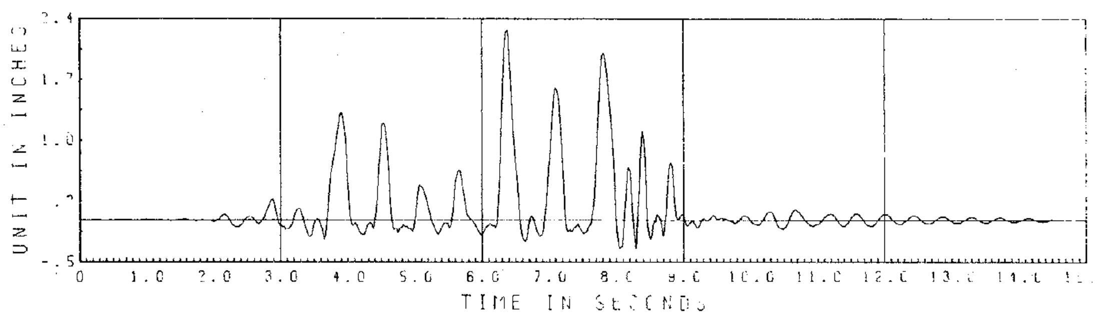

South Column West Frame

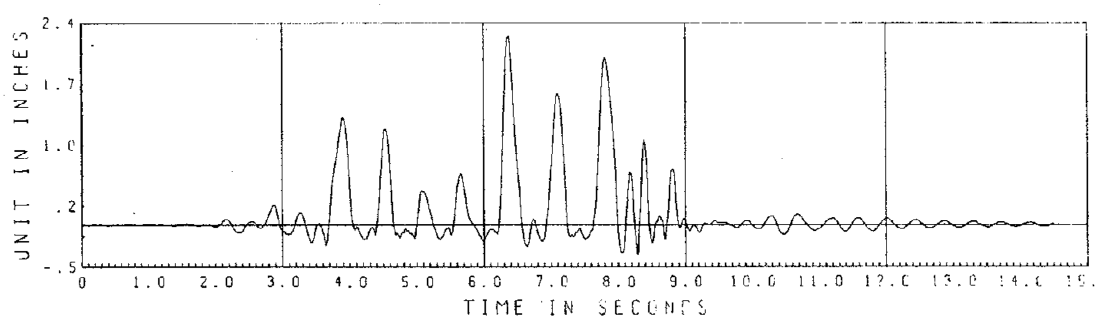

South Column East Frame

Fig. 2.5i.4 PAC 400 I Relative Column Vertical Displacements

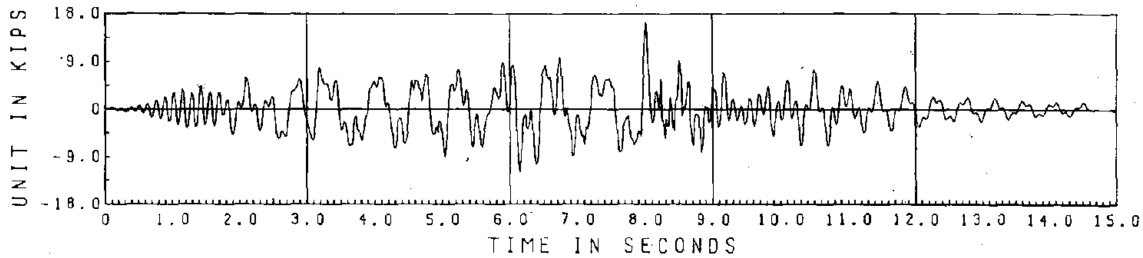

3rd Floor Shear

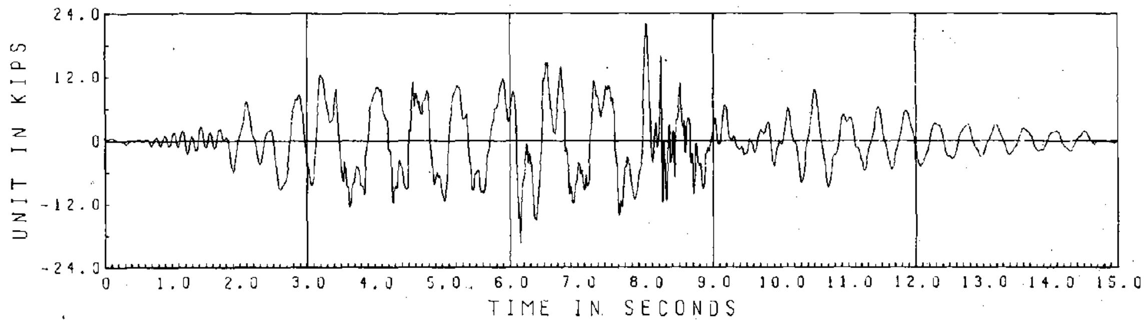

2nd Floor Shear

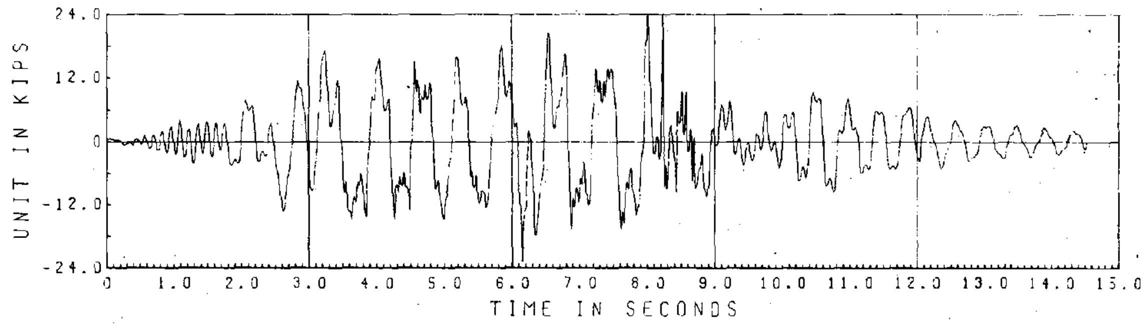

Base Shear

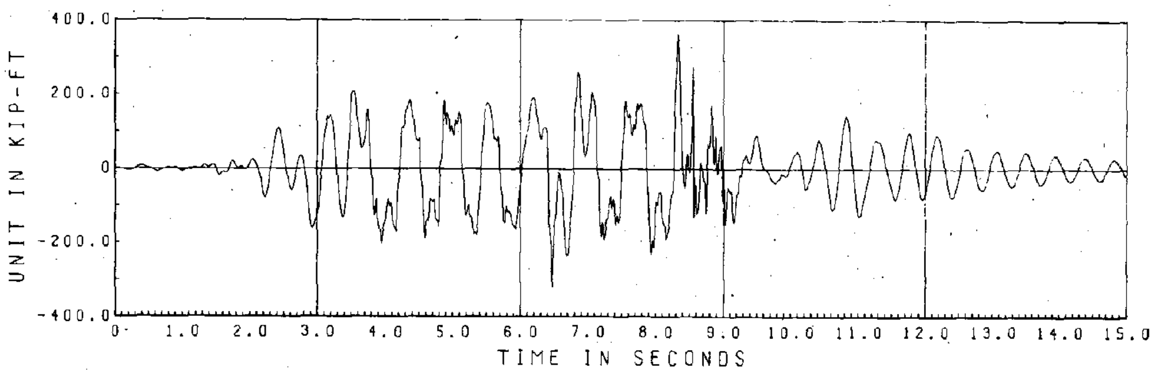

Base Overturning Moment

Fig. 2.5i.5 PAC 400 I Story Forces

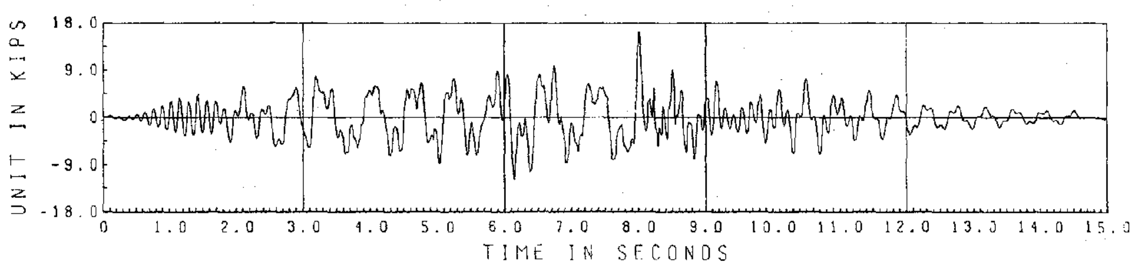

3rd Floor Shear

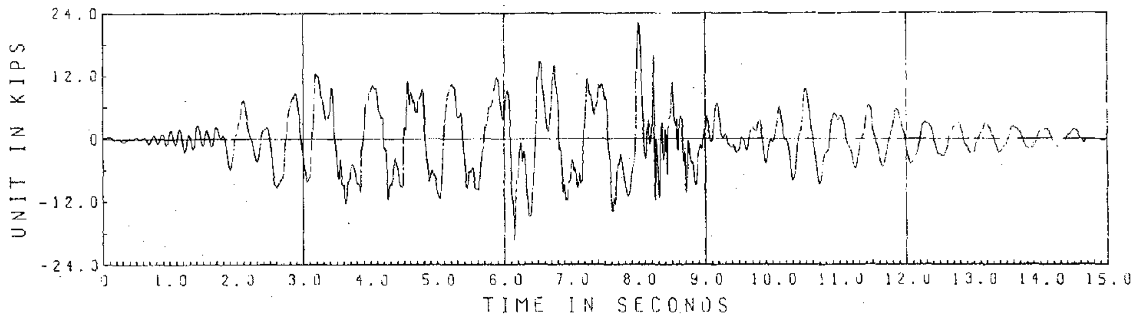

2nd Floor Shear

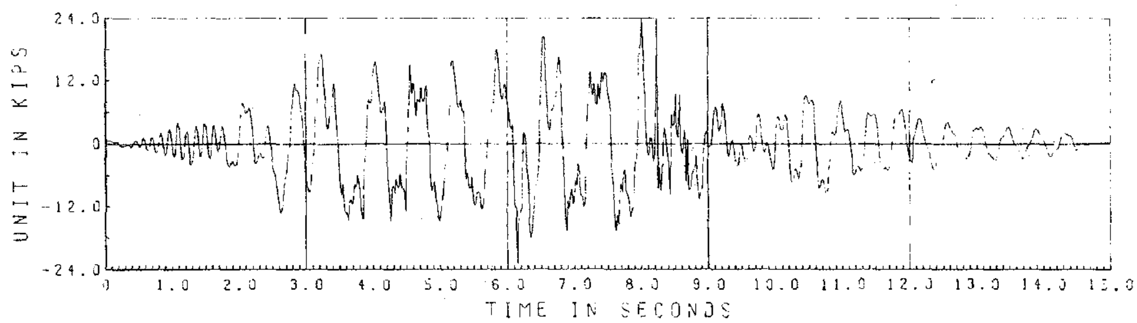

Base Shear

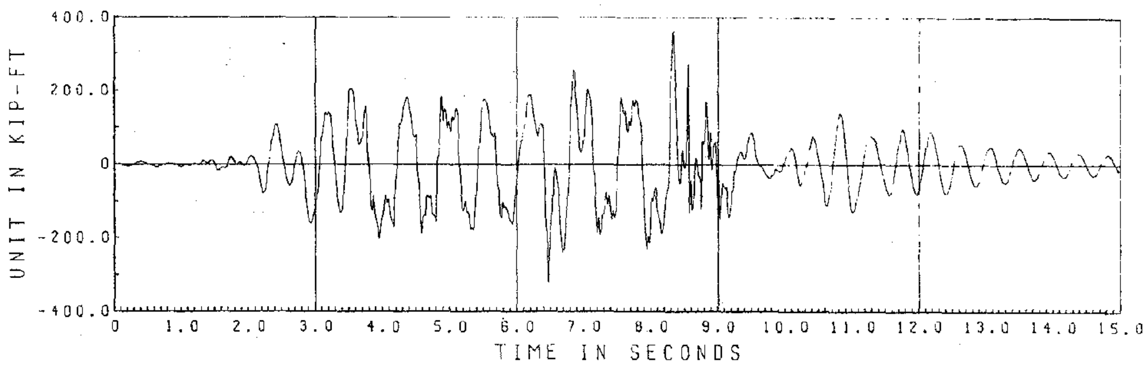

Base Overturning Moment

Fig. 2.5i.5 PAC 400 I Story Forces

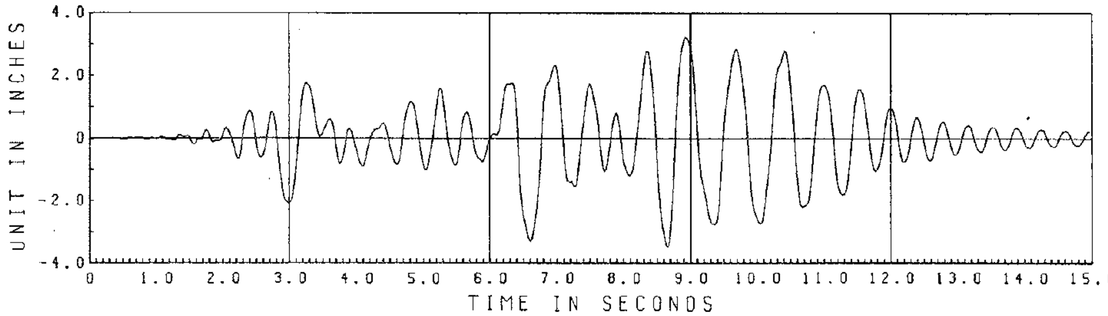

3rd Floor Relative Displacement

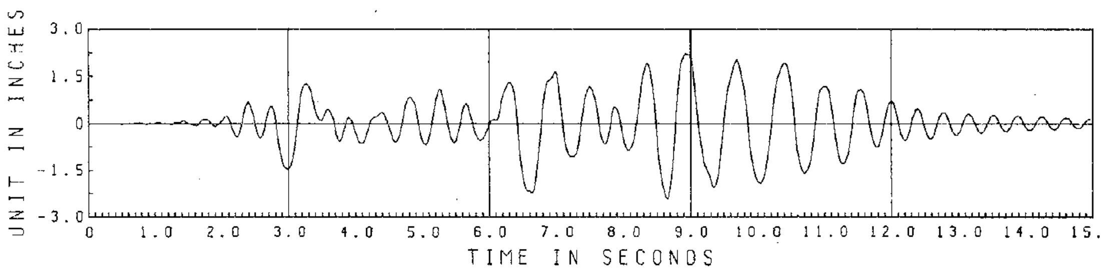

2nd Floor Relative Displacement

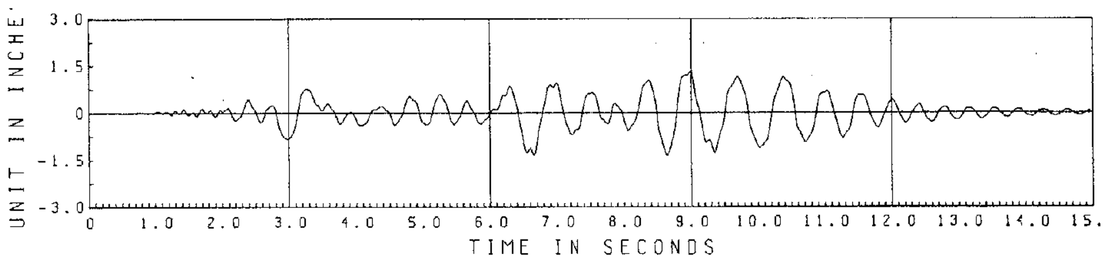

1st Floor Relative Displacement

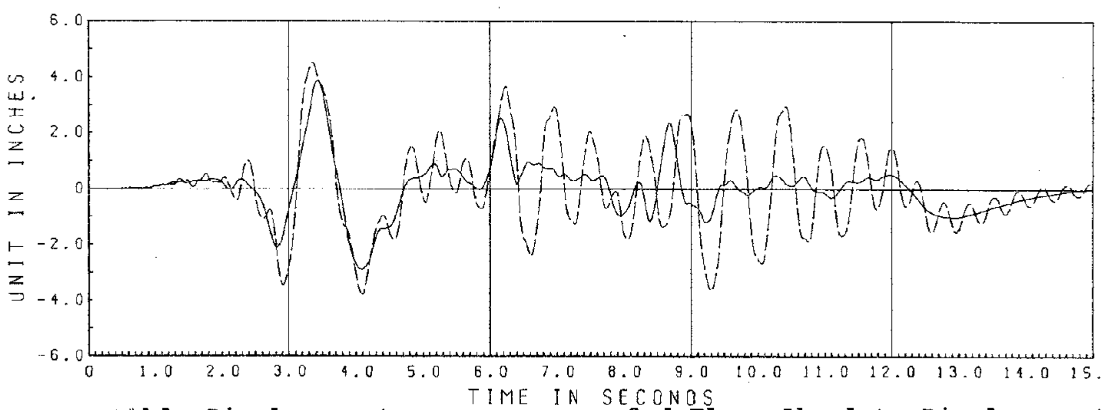

- Table Displacement -- 3rd Floor Absolute Displacement

Fig. 2.5j.3 PAC 700 II Displacements

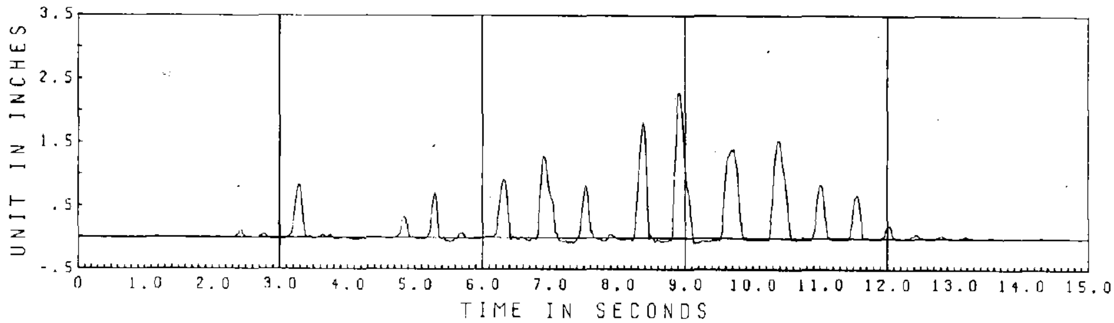

North Column West Frame

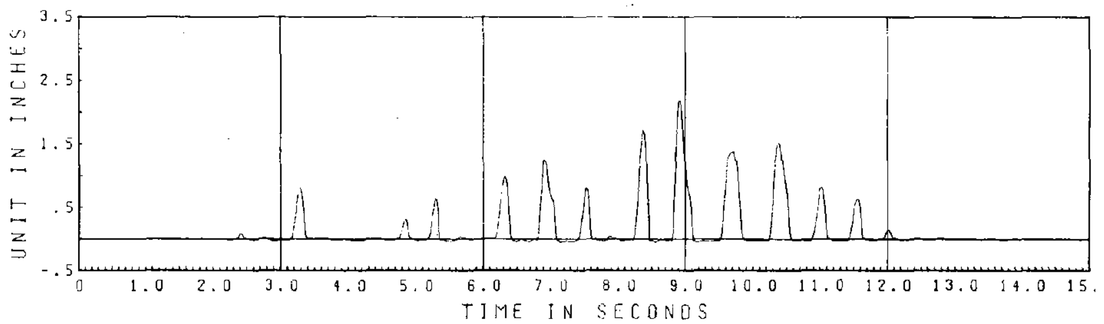

North Column East Frame

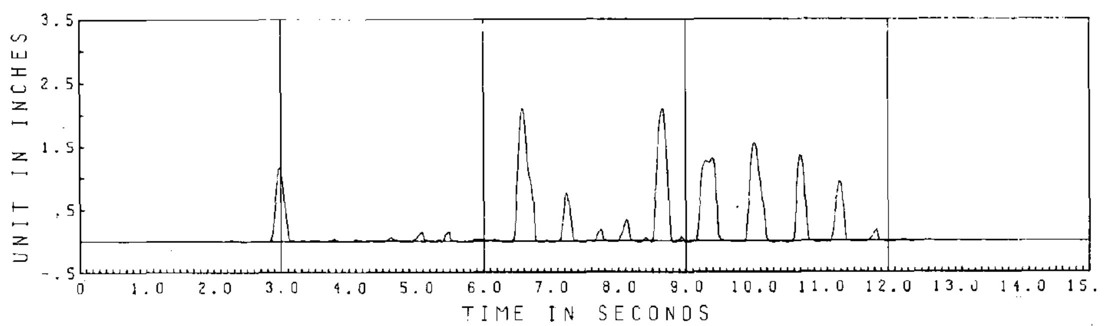

South Column West Frame

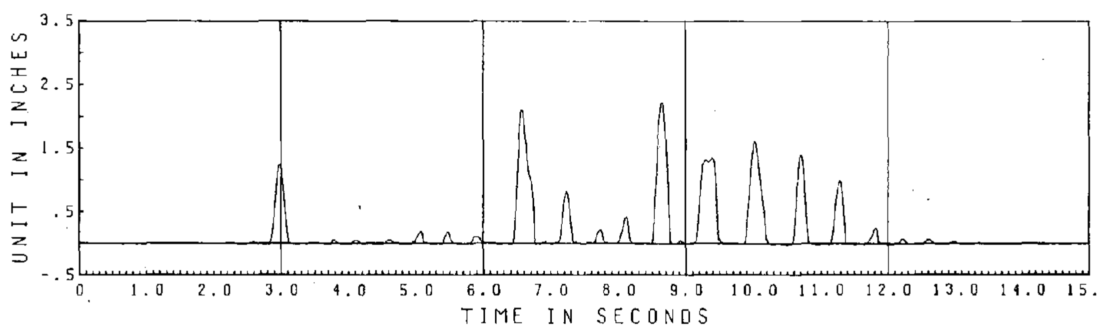

South Column East Frame

Fig. 2.5j.4 PAC 700 II Relative Column Vertical Displacements

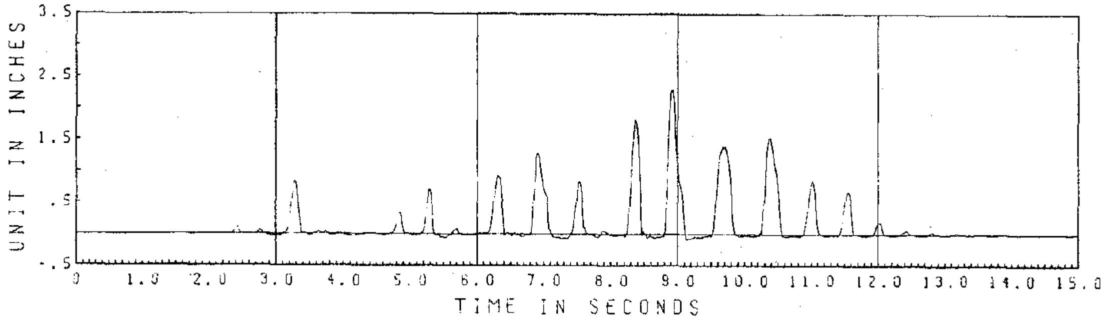

North Column West Frame

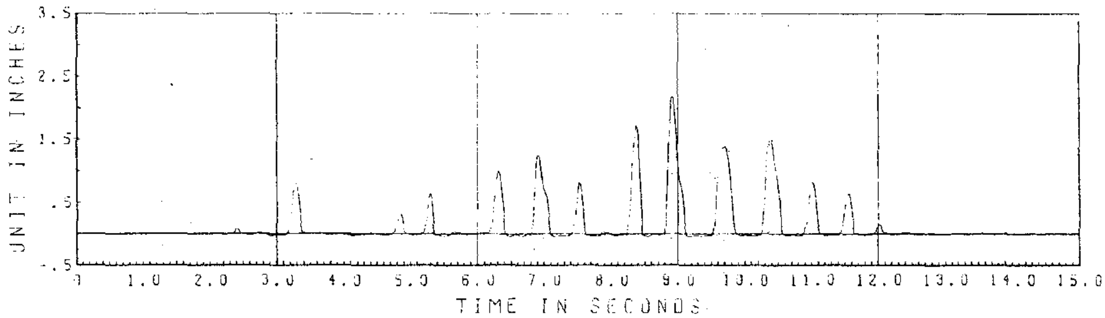

North Column East Frame

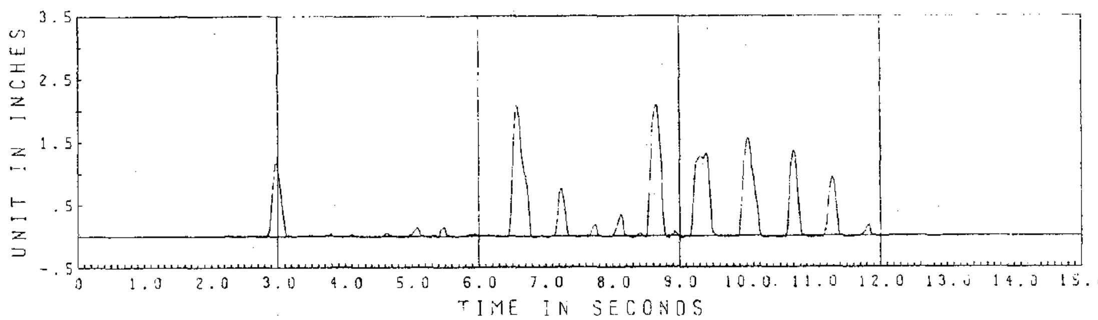

South Column West Frame

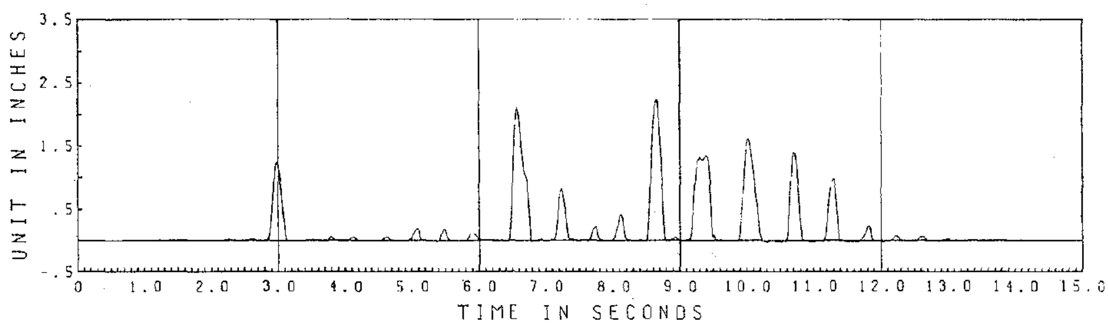

South Column East Frame

Fig. 2.5j.4 PAC 700 II Relative Column Vertical Displacements

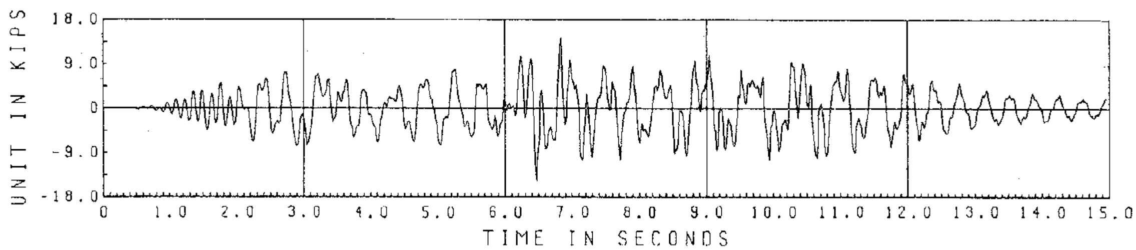

3rd Floor Shear

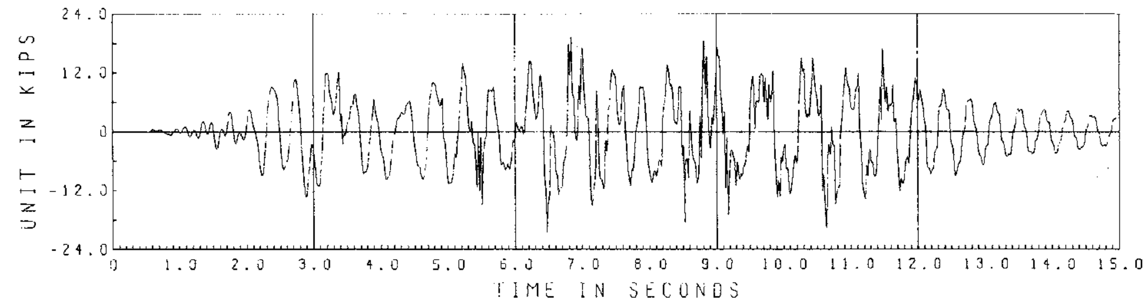

2nd Floor Shear

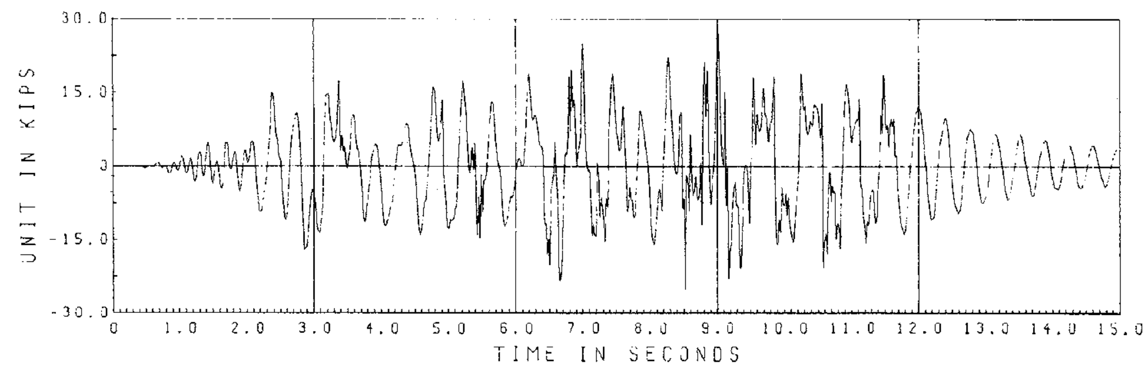

Base Shear

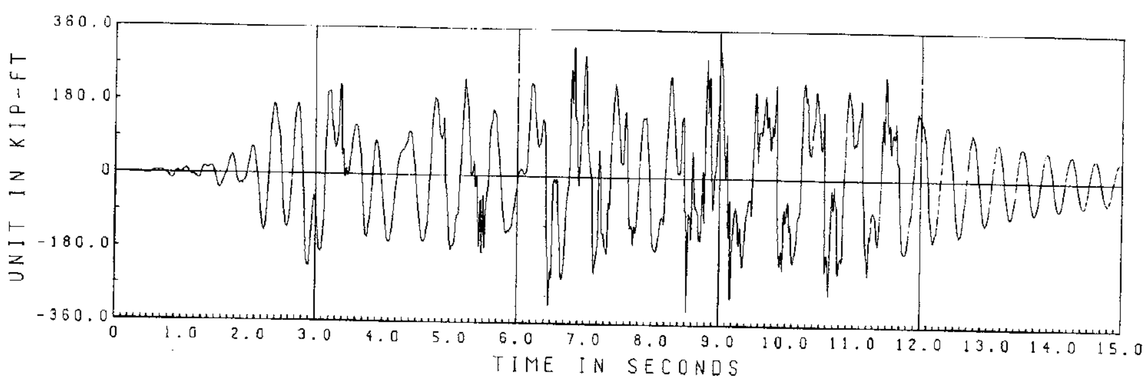

Base Overturning Moment

Fig. 2.5j.5 PAC 700 II Story Forces

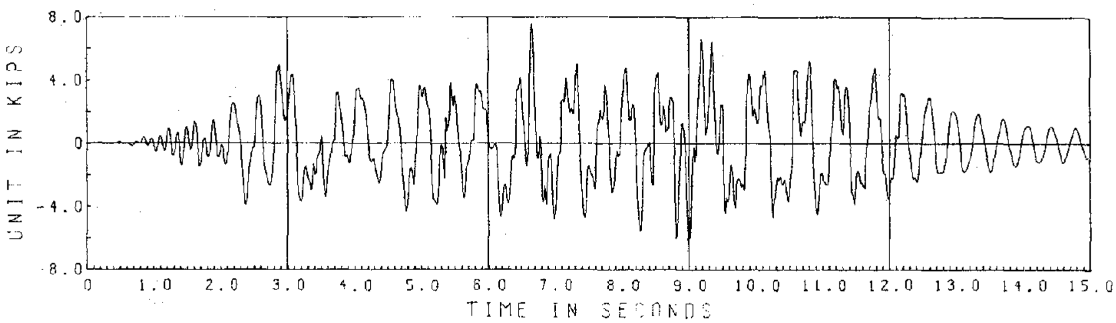

North Column Shear

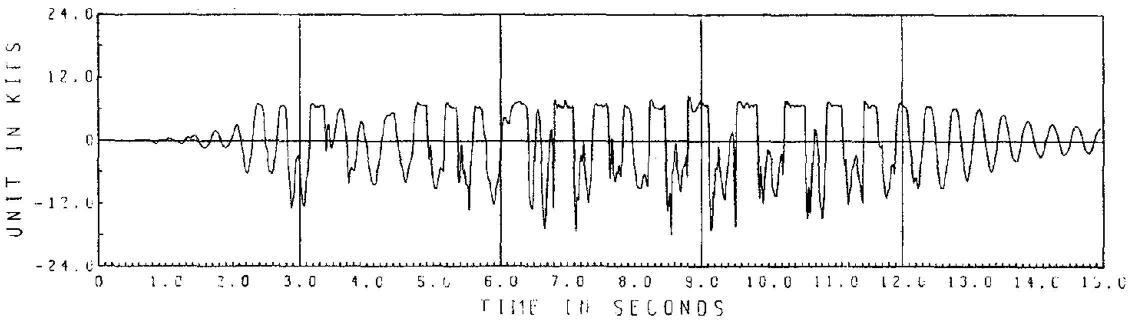

North Column Axial Force

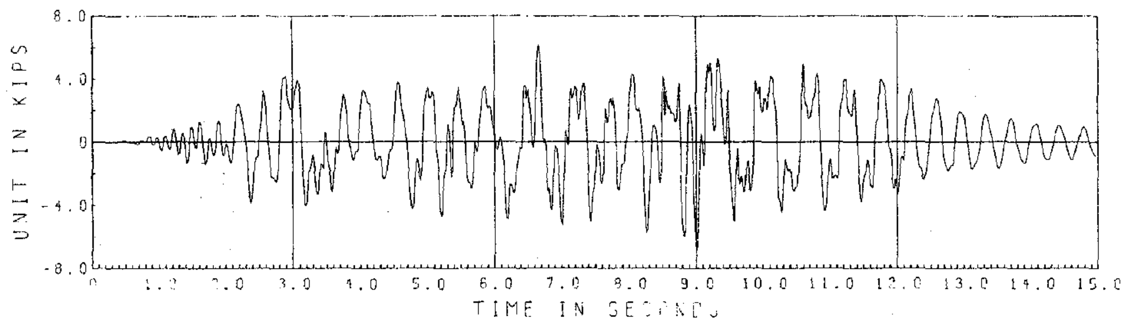

South Column Shear

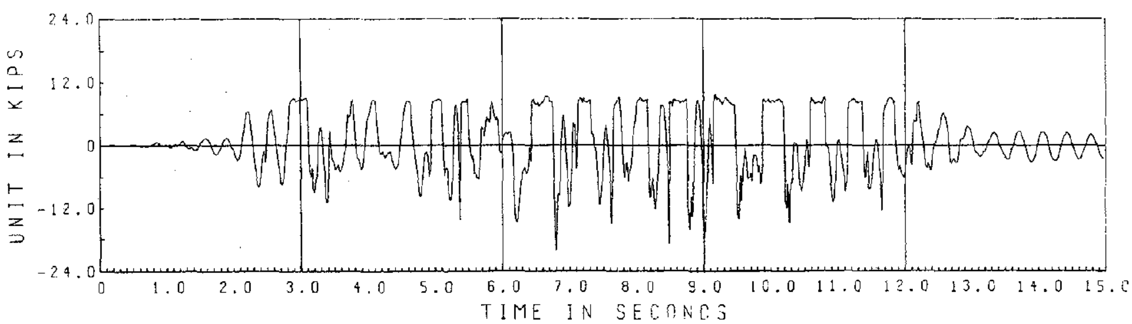

South Column Axial Force

Fig. 2.5j.6 PAC 700 II Member Forces

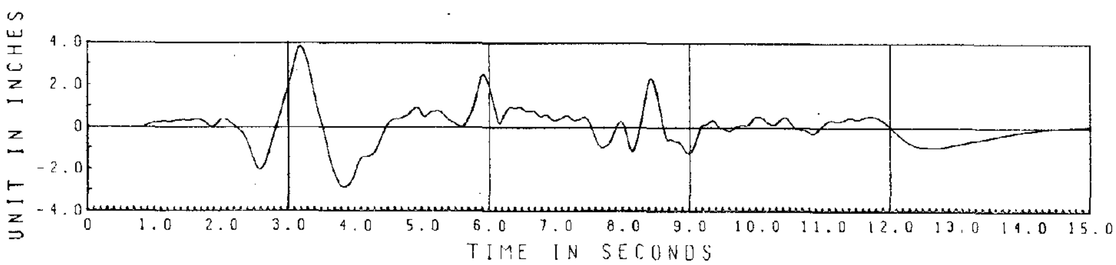

Table Displacement

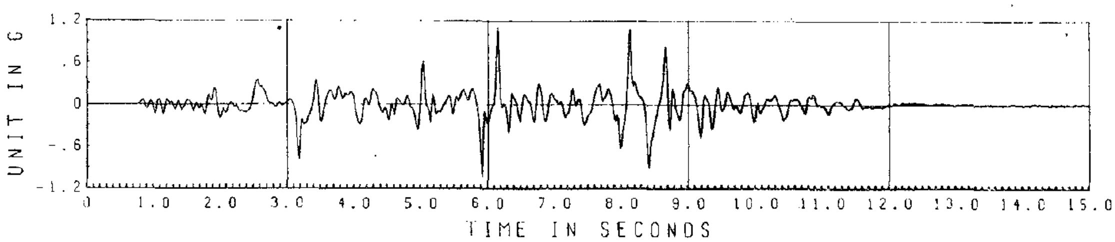

Table Acceleration

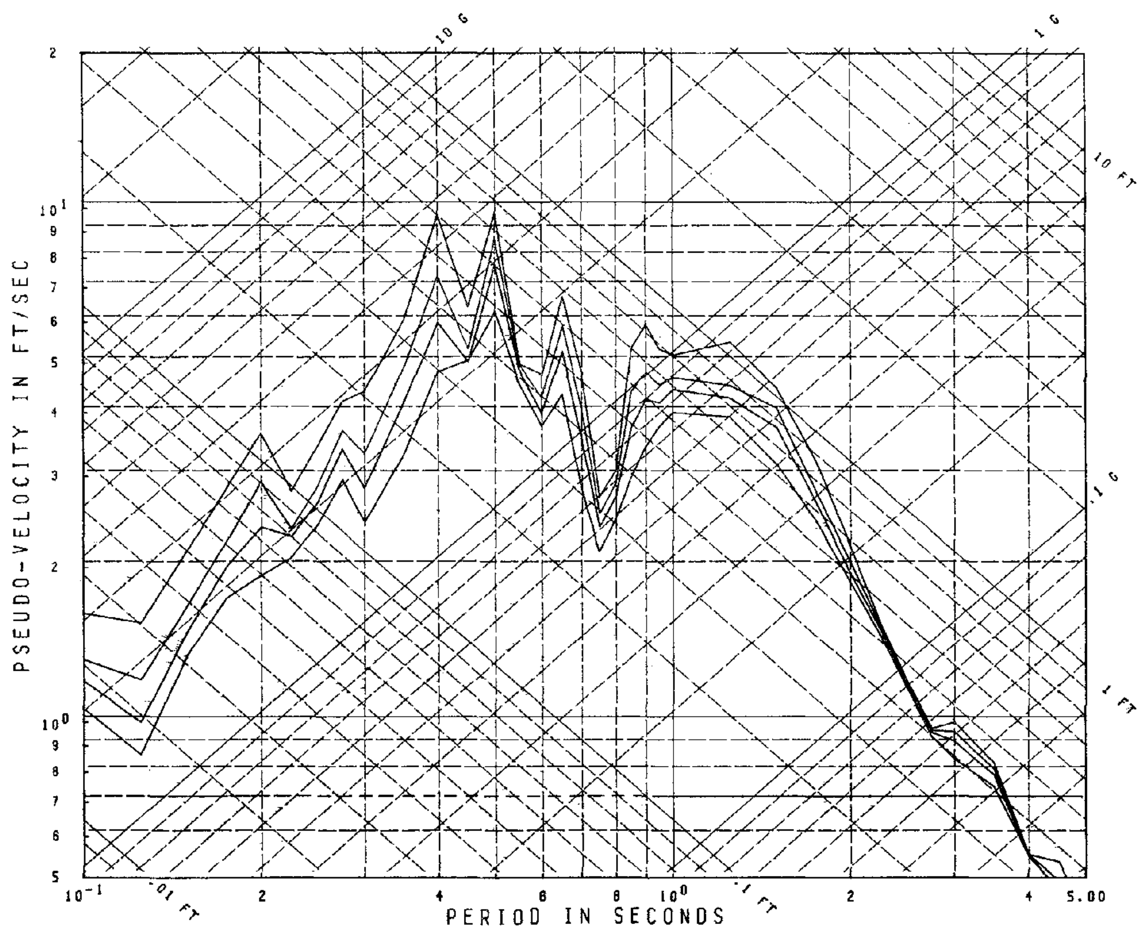

PAC 700

Fig. 2.5k.1 Response Spectra; Damping Ratios = .01, .02, .03, .05

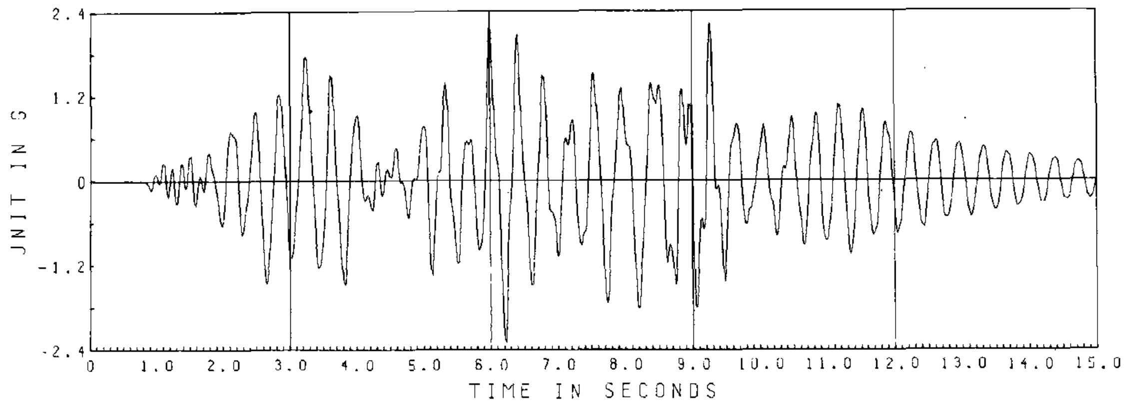

3rd Floor Acceleration

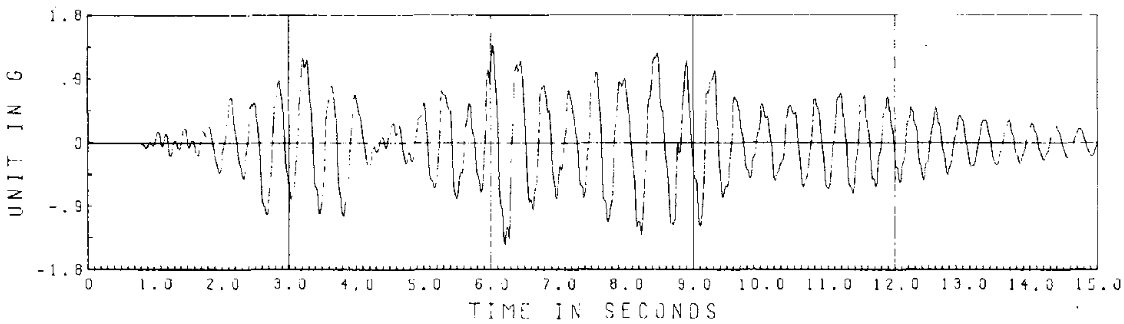

2nd Floor Acceleration

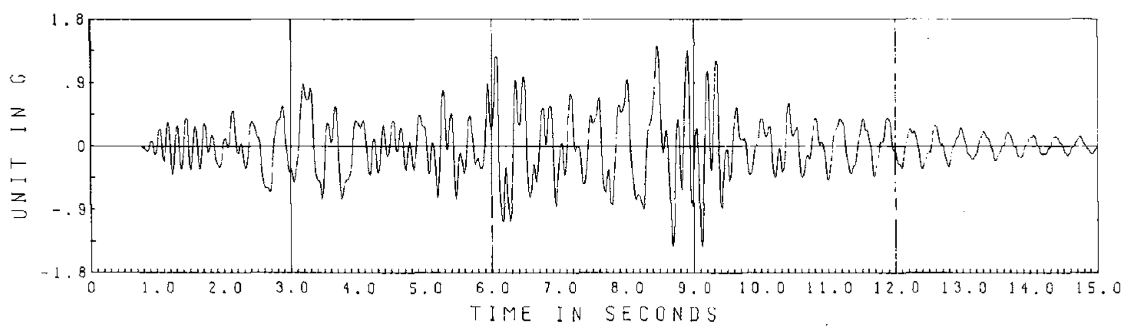

1st Floor Acceleration

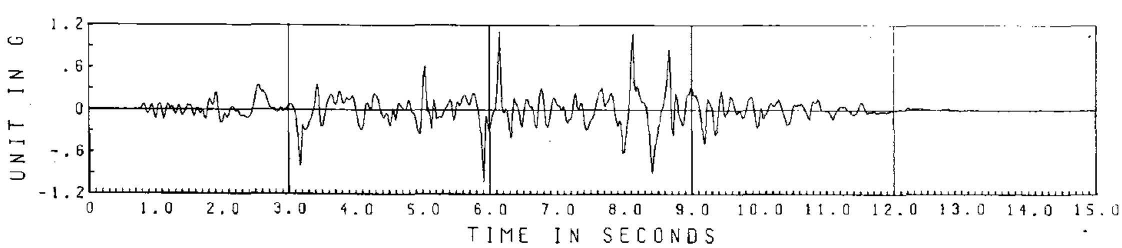

Table Acceleration

Fig. 2.5k.2 PAC 700 Accelerations

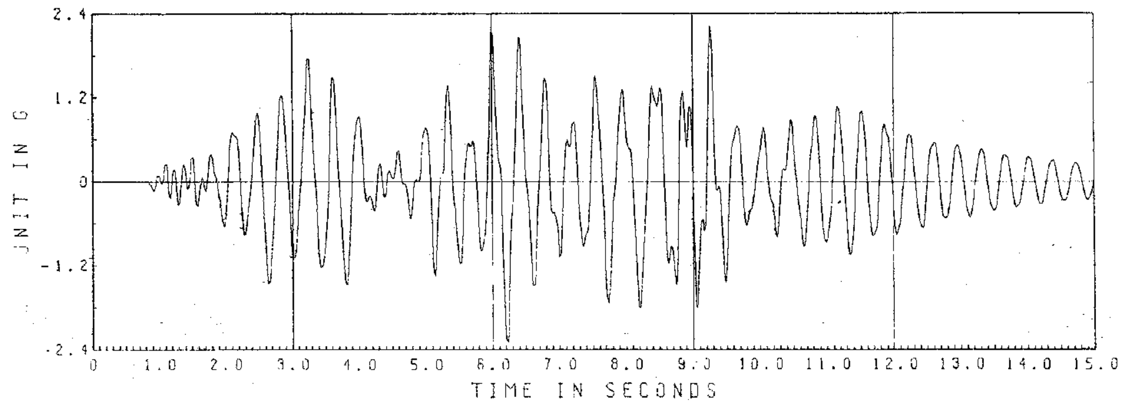

3rd Floor Acceleration

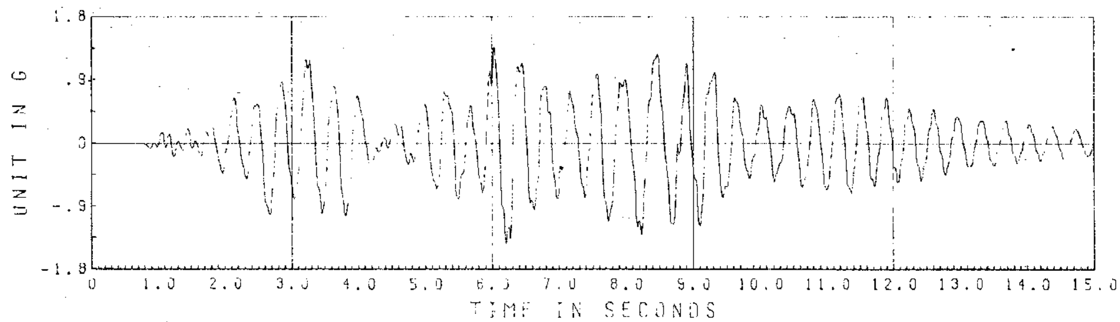

2nd Floor Acceleration

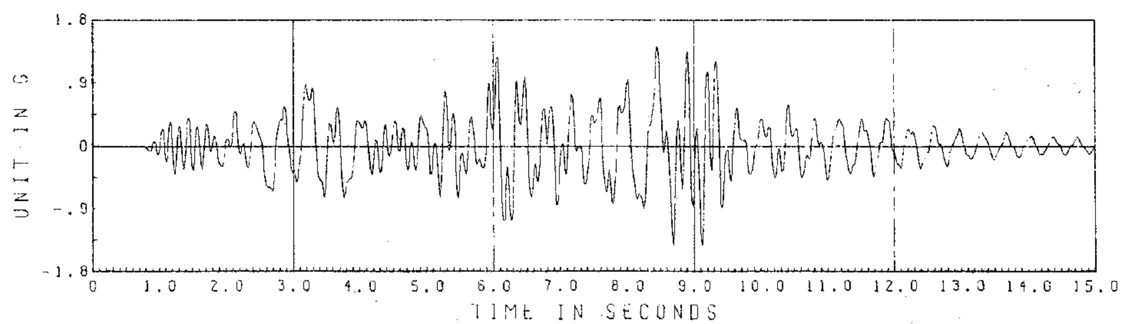

1st Floor Acceleration

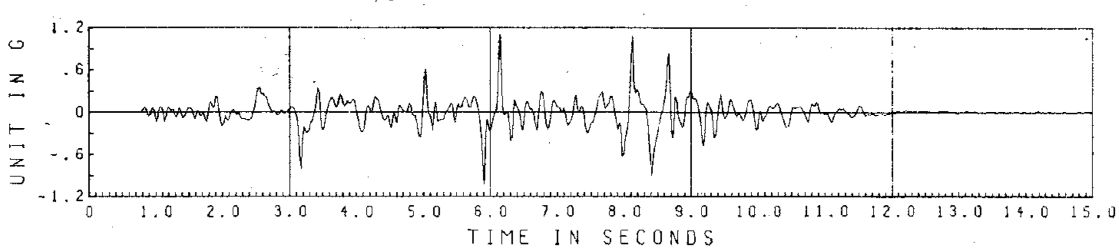

Table Acceleration

Fig. 2.5k.2 PAC 700 Accelerations

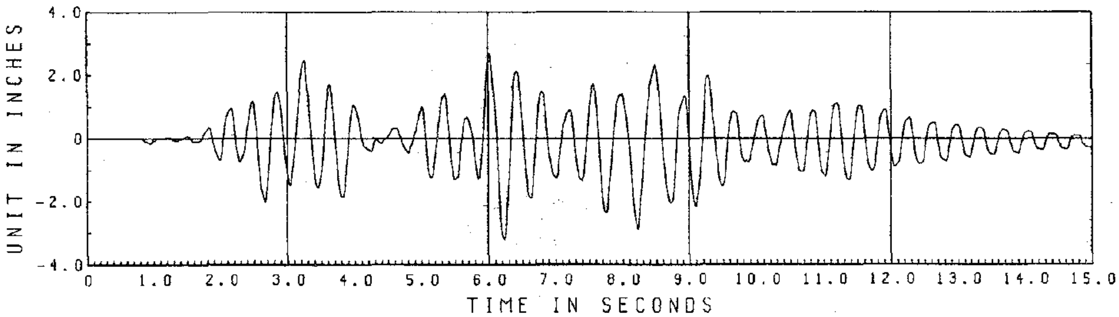

3rd Floor Relative Displacement

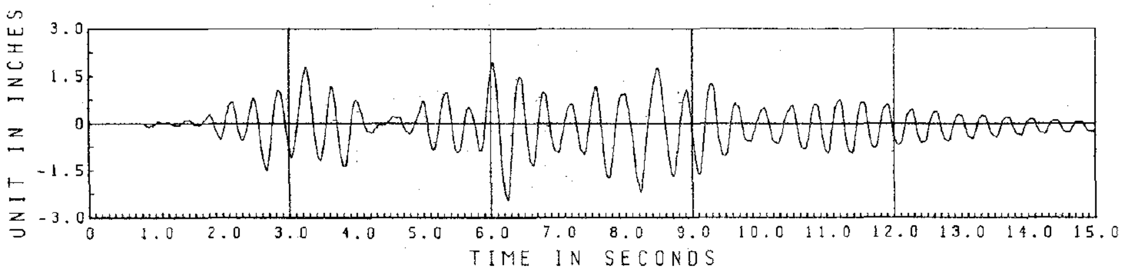

2nd Floor Relative Displacement

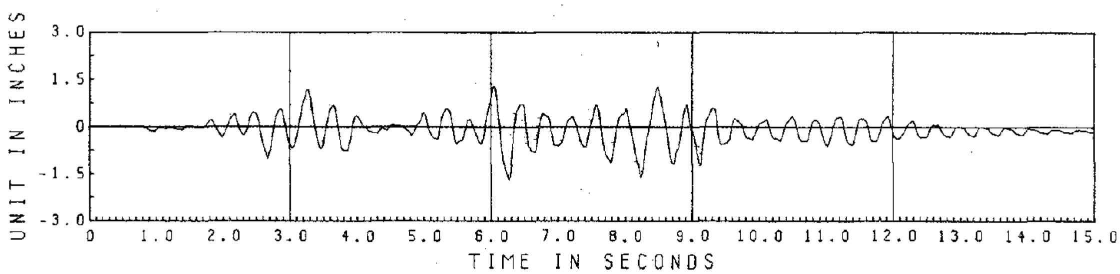

1st Floor Relative Displacement

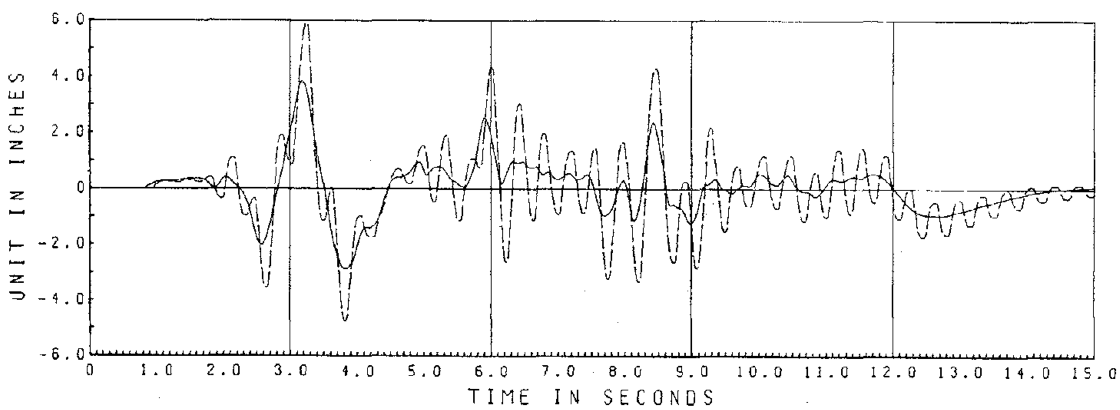

- Table Displacement -- 3rd Floor Absolute Displacement

Fig. 2.5k.3 PAC 700 Displacements

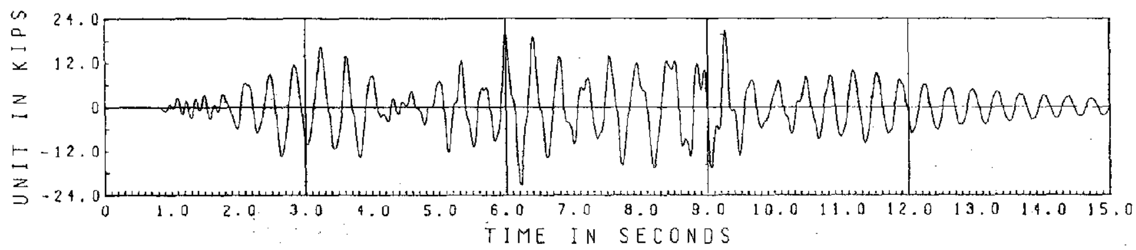

3rd Floor Shear

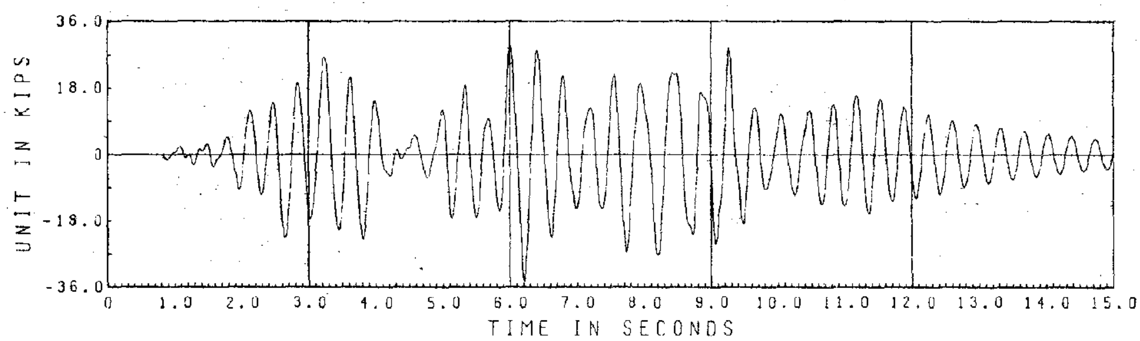

2nd Floor Shear

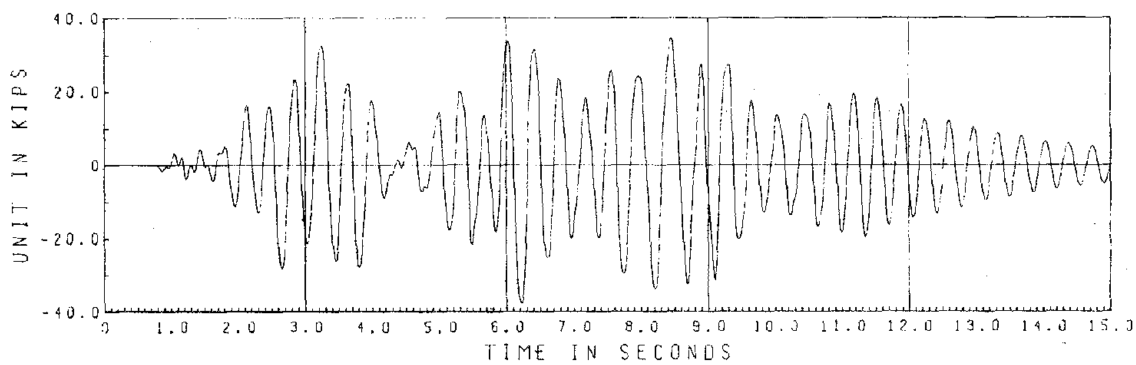

Base Shear

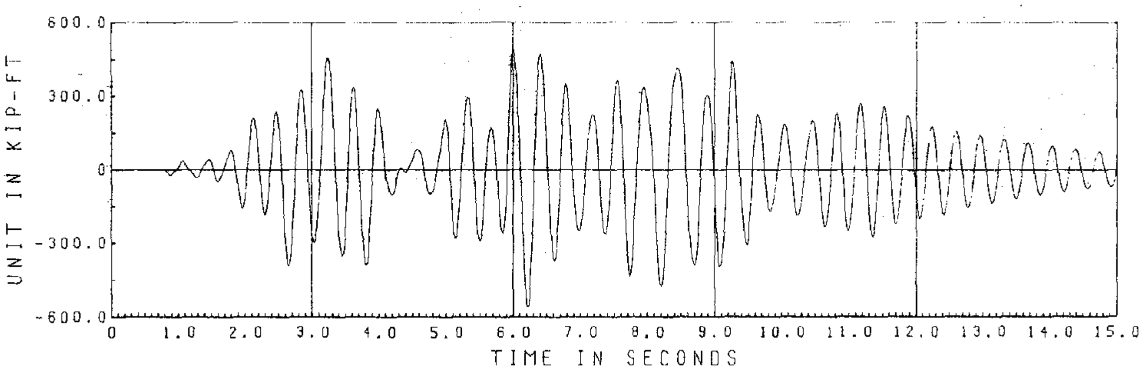

Base Overturning Moment

Fig. 2.5k.4 PAC 700 Story Forces

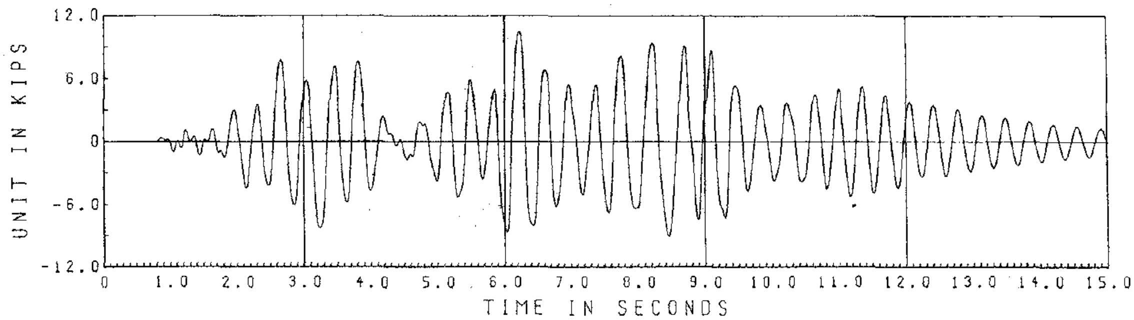

North Column Shear

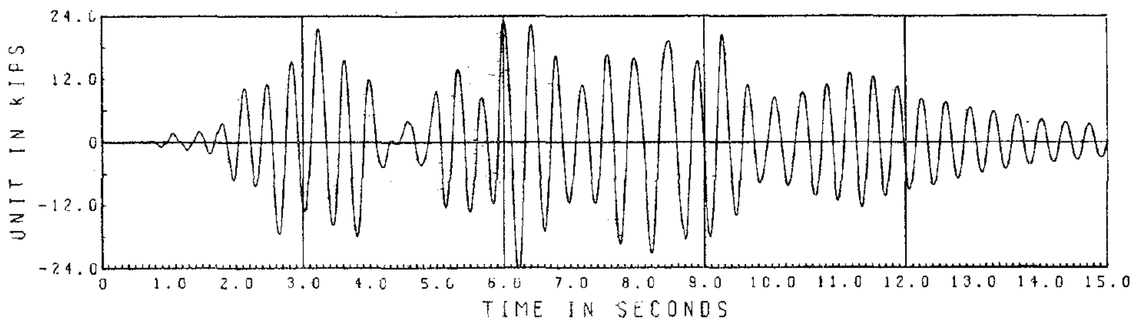

North Column Axial Force

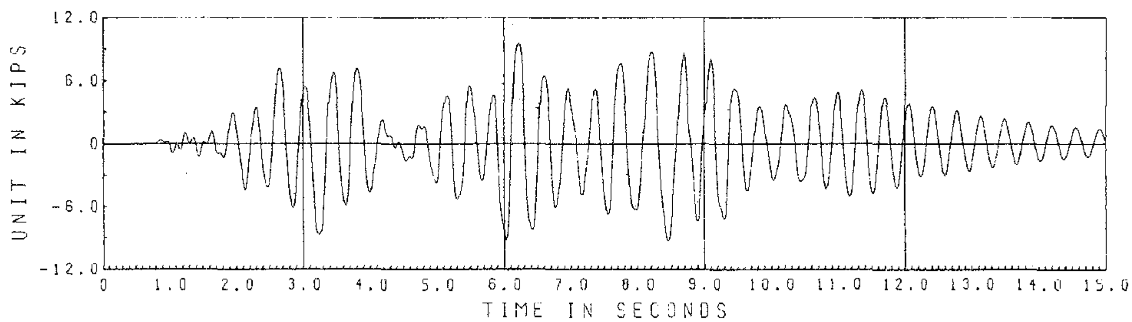

South Column Shear

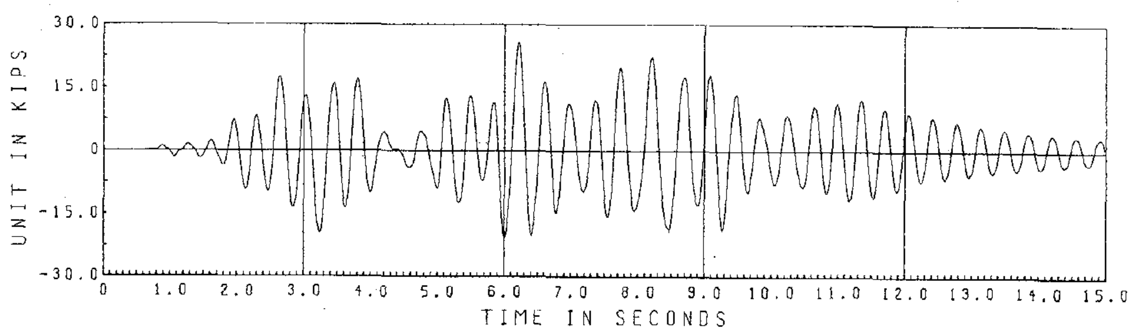

South Column Axial Force

Fig. 2.5k.5 PAC 700 Member Forces

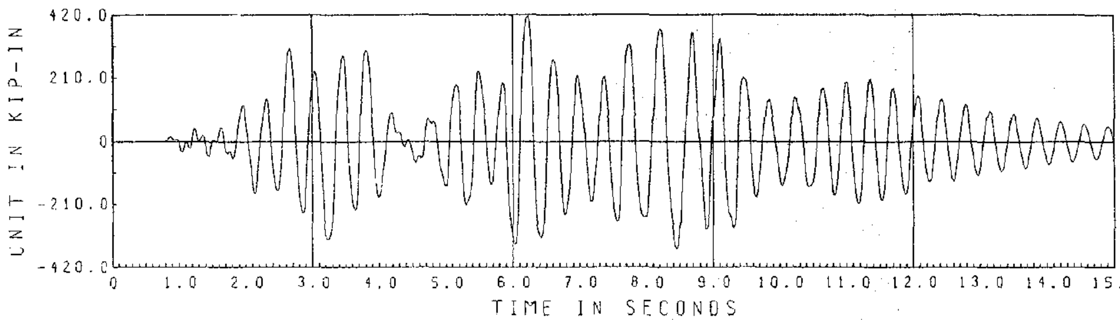

North Column Moment

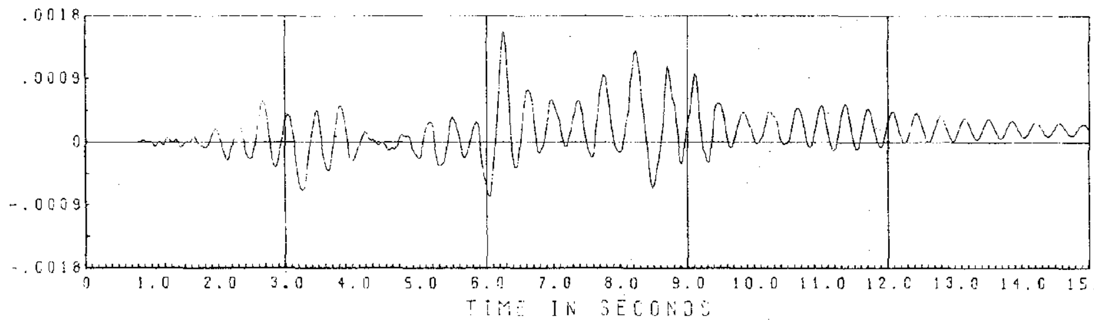

North Column Average Curvature (6" gage)

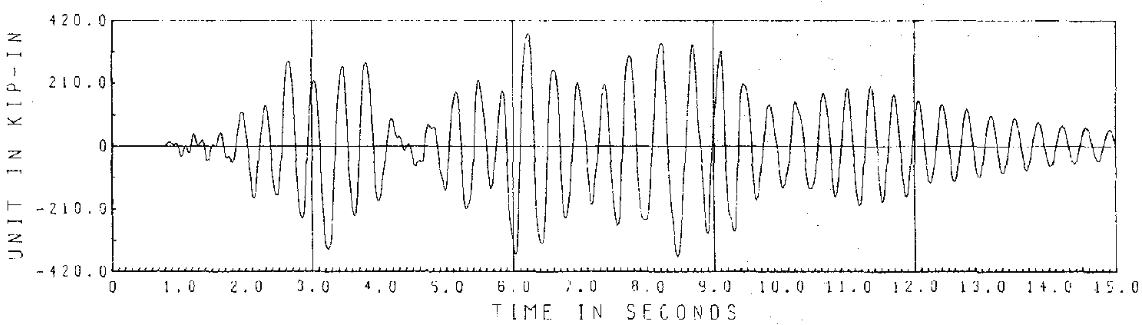

South Column Moment

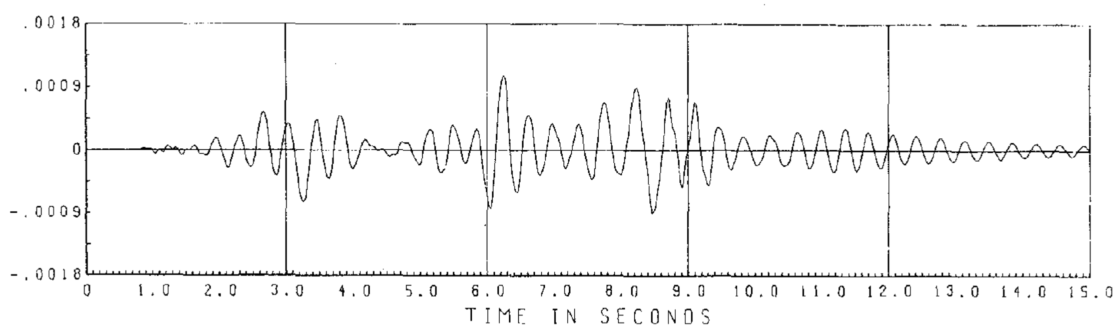

South Column Average Curvature (6" gage)

Fig. 2.5k.6 PAC 700 Column Moments and Curvatures

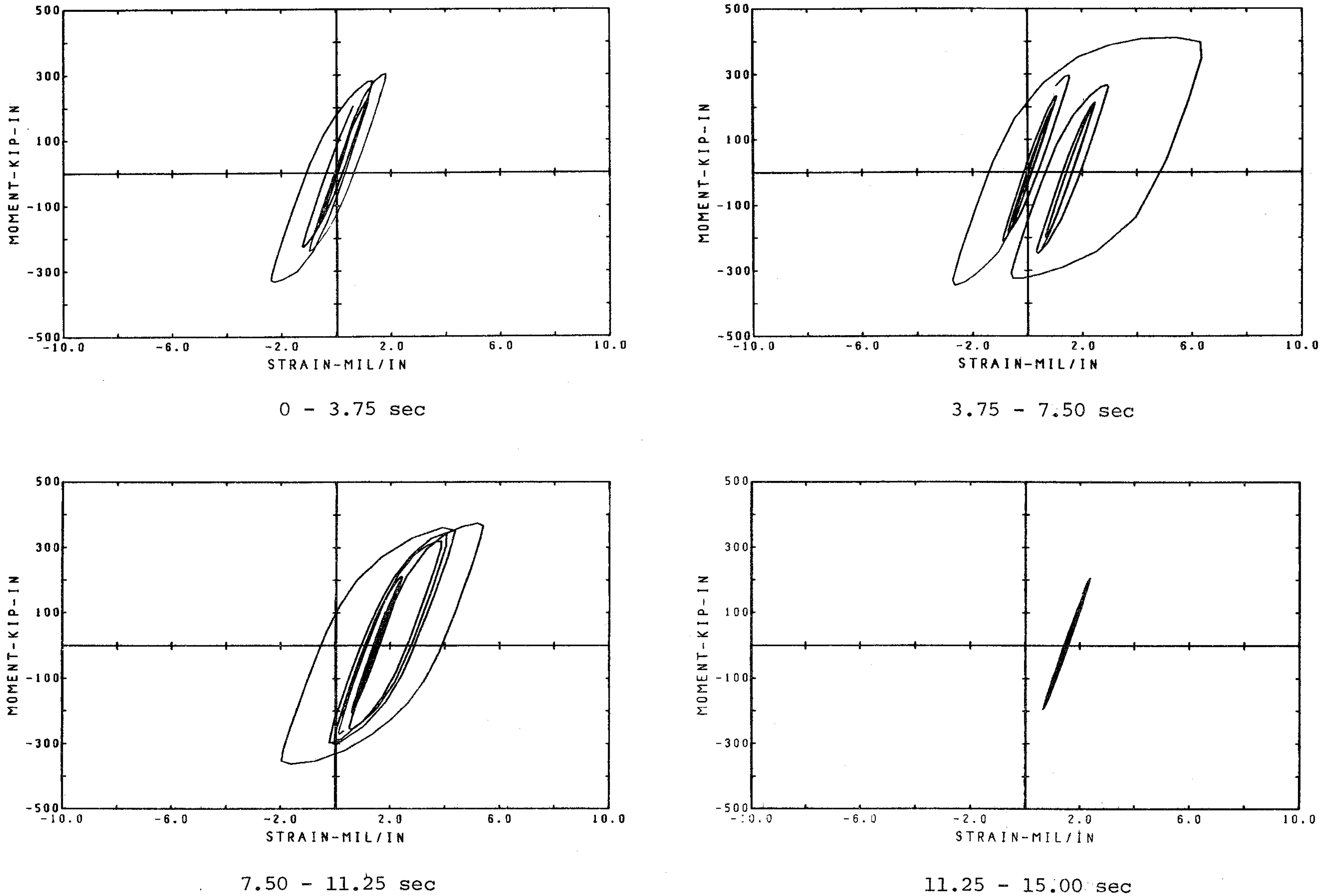

Fig. 2.5k.7 PAC 700 Column Moment vs Flexural Strain

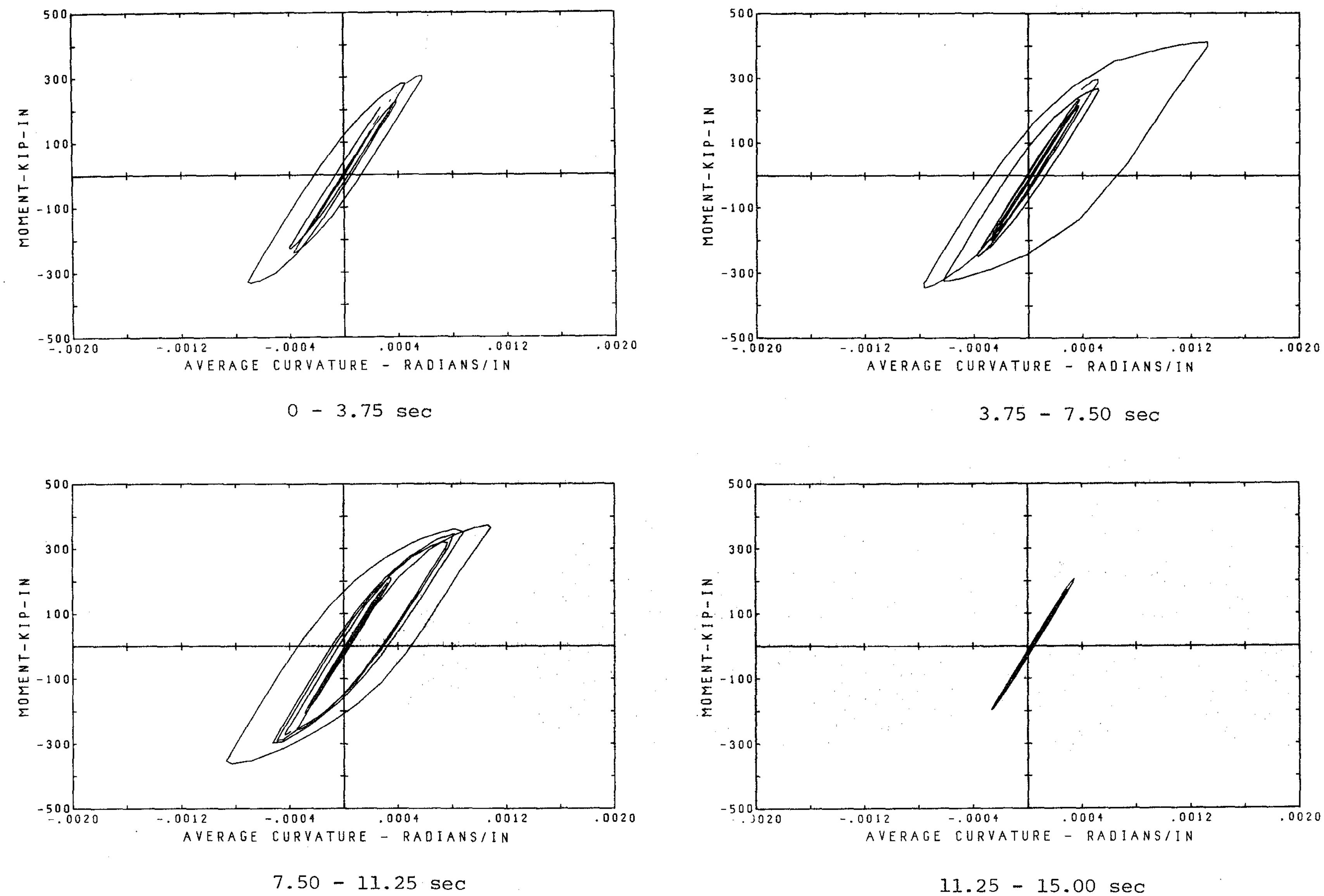

Fig. 2.5k.8 PAC 700 North Column Moment vs Average Curvature

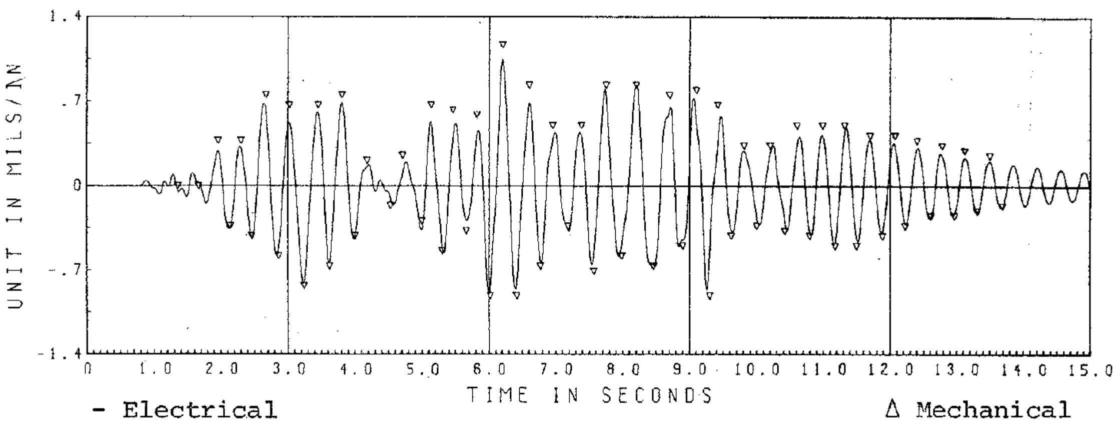

2nd Floor Girder

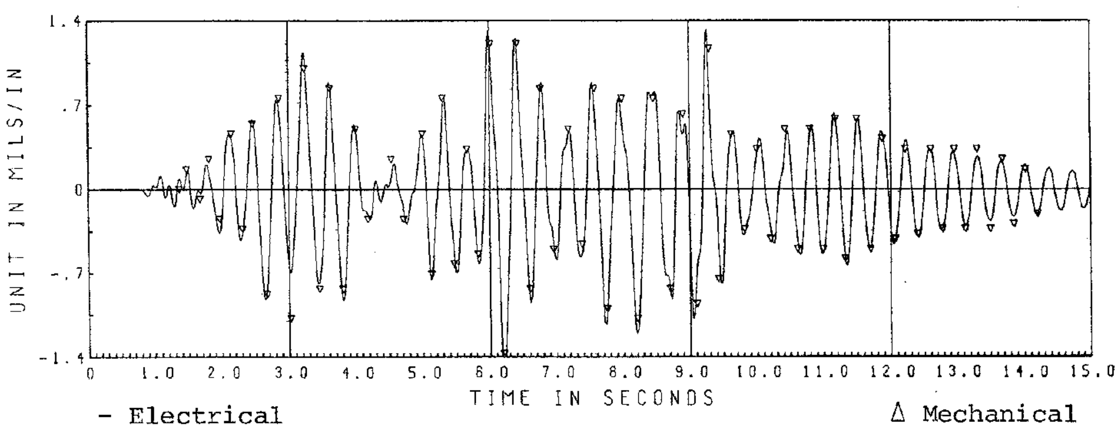

2nd Floor Column

Fig. 2.5k.9 PAC 700 Mechanical Strain Gage Comparisons

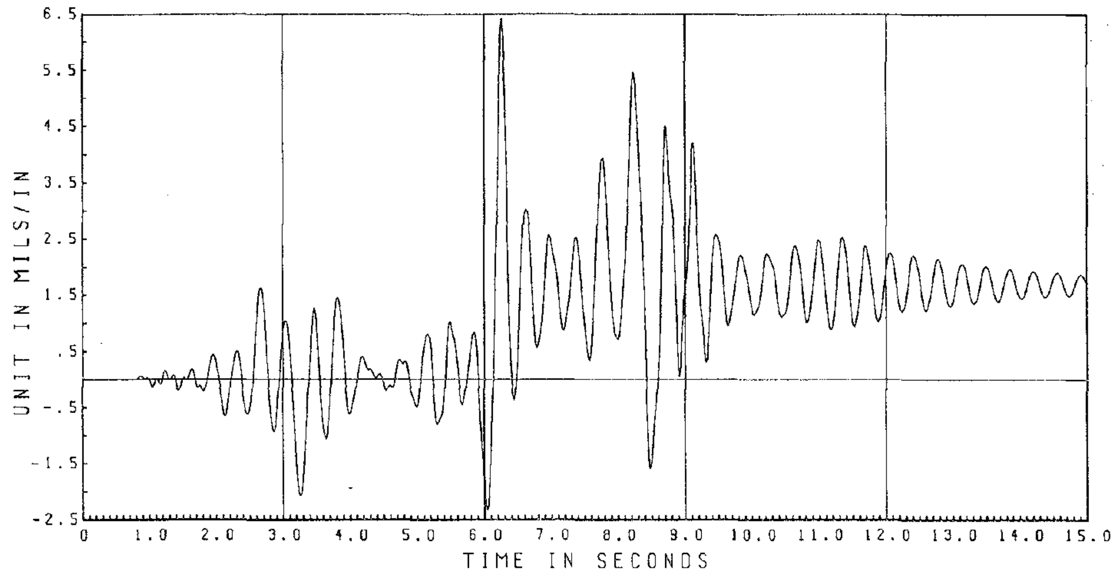

Strain at Top of 6" Gage Length

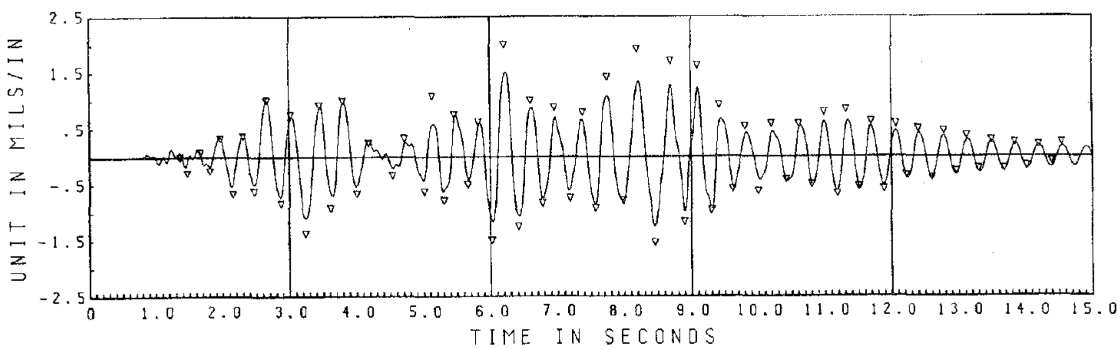

Strain at Center of 6" Gage Length

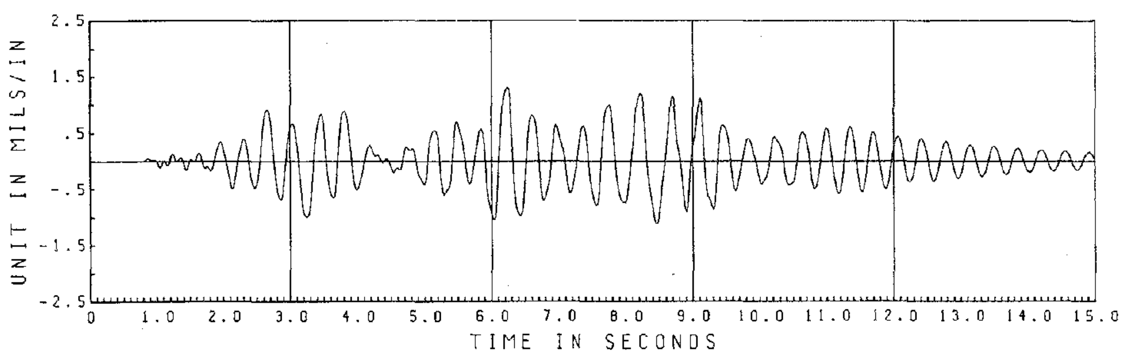

Strain at Bottom of 6" Gage Length

- Electrical Δ Mechanical

Fig. 2.5k.10 PAC 700 Column NB Mechanical Strain Gage Comparisons

3. ANALYTICAL CORRELATION OF TEST DATA

As was mentioned in the introduction, a primary impetus for this initial experimental program was to provide a basis for the evaluation of currently available nonlinear analytical techniques in predicting uplift behavior. In addition to this initial study of the uplift phenomenon, the data obtained in the nonlinear fixed-base tests were also to be used to evaluate nonlinear frame analysis procedures employing concentrated plastic hinges at the member ends. To carry out these evaluations, selected test accelerograms were used as the input records for the nonlinear analysis of the appropriate mathematical models. The analytical responses obtained were then compared directly with the corresponding experimental data.

The computer program utilized for the analytical work was DRAIN-2D, described fully by Kanaan and Powell (3). DRAIN-2D is a general two-dimensional structure program for nonlinear earthquake response analysis. It is applicable to cases having identical seismic excitation of all support points. The full set of incremental equations of motion are numerically integrated using the assumption of constant average nodal accelerations within each integration time step. Unbalanced loads resulting from stiffness changes are corrected in the following time step, necessitating fairly small time steps to avoid large "overshoots" at instants of significant stiffness change. Damping capabilities presently available in the program include arbitrary combinations of mass proportional, original stiffness proportional, and tangent stiffness proportional viscous damping.

3.1 Uplift Response

The basic uplifting mathematical model is shown in Fig. 3.1.1. The uplift phenomenon was approximated by specifying the vertical foundation support elements to be bilinear elastic, with zero tensile force capacity and with zero stiffness in the upward direction. All structural members in the frame, except these support elements, were assumed to behave in a linear manner. Static loads were applied prior to all dynamic analyses so their influence was considered in the nonlinear support response.

Table interaction in the pitching mode was not considered directly in the uplift analysis, but could be accommodated partially by adjusting the structure support spring stiffnesses. This omission quite possibly could account for the greater difficulty encountered in achieving good correlation of data for the phase II tests, where the stiffer set of impact pads were employed. More will be said of this later.

The improvement of data correlation was accomplished by adjustment of the damping assumed for the basic mathematical model already described. This adjustment process was performed solely on the basis of physical insight into the model's behavior. The more systematic approaches of system identification have not yet been applied to the seismic response of systems with this degree of complexity.

The uplift tests for which analyses were performed were the EC 1000 I test and the EC 300 II test. It was felt that these tests were representative of phase I and phase II nonlinear tests. Integration time steps of .01 and .005 seconds were used for the phase I and phase II tests, respectively. The smaller time step for phase II analysis was utilized to avert potential analytical complications due to the more severe impact conditions in that case.

As was indicated by the experimental results, the stiffness of the impact pads beneath the column bases had a very pronounced effect on the fundamental frequency of vibration of the structure. This analytical relationship, assuming a rigid support beneath the impact pads, is shown in Fig. 3.1.2.

In Fig. 3.1.3 are shown the analytical mode shapes and frequencies of the mathematical models used for phase I and phase II calculations. From these mode shapes, it is apparent why a great deal of 2nd mode response was evident in the 1st floor accelerations, as was mentioned previously in Chapter 2. The very slight influence of the pad stiffness on the mode shapes is interesting to note, in view of its rather significant effect on the first mode frequency.

3.1a <u>Phase I Computations</u>

As was mentioned previously, the EC 1000 I test was selected as an appropriate signal for the phase I nonlinear analysis. An effective impact pad stiffness of 40 kip/in in the mathematical model matched very closely the observed fundamental frequency, although this is nearly 10% below the actual value. A damping estimate of 2% critical for the observed first mode frequency was selected as a reasonable preliminary estimate, based on observed decay curves for the structure.

The mass proportional, original stiffness proportional and tangent stiffness proportional viscous damping coefficients employed in the computer analysis are designated α, β_o, and β, respectively. Since a rigid body motion was possible for this structure, and it would not be expected to exhibit much damping in this type of response, mass proportional damping, which increases with decreasing frequency, was not deemed a reasonable type of damping to employ. For the first analysis, therefore, it was decided to try original stiffness porportional viscous damping, with β_o equal to .00293, corresponding to about 2% critical first mode damping. The results of this analysis are shown in Fig. 3.1a.1; the response quantities plotted are the top floor displacement relative to the table and the relative vertical displacements of the two column bases. As can be seen in the time history plots, the rigid body motion evidently was damped too heavily in this analysis.

Based on the results of this first analysis it was decided to reduce the effective damping of the rigid body motion. For this reason, the type of damping was changed to tangent stiffness proportional, with β equal to the same value of .00293. Because the effective tangent stiffness of the rigid body motion is zero, this mechanism should have produced less damping in the uplifting portion of the response. The results of this second analysis are shown in Fig. 3.1a.2 and, indeed, the results are considerably improved.

From the results of this second analysis, however, it seemed that there still was too much damping in the system. Therefore, for the third analysis β was reduced from .00293 to .002196, corresponding to a reduction in the first mode critical damping ratio to about 1 1/2%. The results of this analysis are shown in Fig. 3.1a.3. Here the correlation between analysis and experiment is much improved, and was in fact deemed satisfactory from an engineering viewpoint. The shear and axial forces developed in the two 1st floor columns during this analysis are shown in Fig. 3.1a.4.

3.1b Phase II Computations

The phase II correlation was more complicated than the phase I case due largely, it was felt, to two separate problems. The stiffer impact pads, as fabricated did not exhibit a consistent behavior from one pad to another, nor for each individual pad throughout the test sequence. Most of this problem was associated with bond deterioration between the neoprene material and the steel plates used to attach the pads to the structure's foundation. Secondly, the stiffer impact pads resulted in a more obvious pitching mode interaction problem between the structure and the shaking table. This problem was treated by reducing the effective stiffness of the spring support elements in the basic mathematical uplift model to about 50 per cent of the actual value, so that the observed first mode frequency was reasonably well matched; this is not a completely satisfactory solution but it eventually gave acceptable results.

As was mentioned previously, the EC 300 II test was selected as the basis of analytical correlation for phase II tests. It seemed reasonable that the same type of damping, i.e. tangent stiffness proportional viscous damping, should be used for this analysis as was used successfully in the phase I computations. As a first attempt, the same damping coefficient, .002196, was used. The results of this analysis, which had an effective first mode damping coefficient of 1.8%, are shown in Fig. 3.1b.1. They indicate that the damping was too high, so the damping ratio was reduced to about 1 1/2% for the next analysis by lowering β to .001758. The results of this analysis are shown in Fig. 3.1b.2; there is some improvement in the correlation, but it was not yet deemed acceptable.

As the correlation seemed to be improving, it was decided to continue lowering the damping in the system. Fig. 3.1b.3 shows the results of an analysis with β equal to .001621, corresponding to an effective first mode damping ratio of 1.4%. Fig. 3.1b.4 shows the results of an analysis with β equal to .0015, corresponding to a first mode damping ratio of 1.26%. This analysis appeared to have reduced the damping too far. Fig. 3.1b.5 shows the results of the final analysis, performed with β equal to .00153, corresponding to an effective first mode damping ratio of 1.3%. It was felt that this was about the best results obtainable without modeling the table interaction, and due to the other complications mentioned earlier, it was decided to assume these results were within reasonable engineering accuracy. The local force comparisons shown in Fig. 3.1b.6 again depict the first floor column shears and axial forces.

3.2 Fixed-Base Response

The basic "fixed-base" mathematical model is shown in Fig. 3.2.1. As can be seen, the shaking table pitching mode was considered in this model. The spring elements supporting the table were taken to be linear in both tension and compression, within the force limits expected in the analysis. The table itself was assumed to rotate as a rigid body. One additional modification from the mathematical model used in the uplift analyses was the addition of a second beam-column element, parallel to the lower half of each first floor column. Since both beam-column elements used in the analysis were bilinear in nature, this parallel configuration allowed a more general trilinear or quadrilinear moment-curvature relationship.

The model parameters which were available for adjustment were the moment-curvature relationship for the first floor columns, the support spring stiffness for the shaking table and the viscous damping coefficients. In preliminary studies, it was found that a table support spring stiffness of 400 kip/in matched well the 1st mode frequency of vibration. The frequencies and mode shapes of the resulting mathematical model are shown in Fig. 3.2.2.

From experimental observation, it was concluded that a trilinear moment-curvature relationship would adequately model the first floor column members. The moment values used for the "corners", M_1 and M_2 in Figure 3.2.3, were taken initially to roughly fit the experimental curve of Figure 2.5k.8, for the hysteresis cycle of greatest amplitude. It was also decided rather arbitrarily to begin analysis using only original stiffness proportional viscous damping.

For the first attempt at analytical correlation, the EC 1000 test signal was used as the input. A value of .0014 was chosen as the initial value of β_o, and values of 100 kip-in and 350 kip-in were used as M_1 and M_2, respectively. The results of this analysis for the 3rd floor relative displacement are shown in Figure 3.2.4.

From the first analysis it appeared there was too much damping present in the system, so the value of β was lowered to .00125; this lowered the 1st mode damping ratio from 1.3% to approximately 1.2%. The results of this analysis are shown in Figure 3.2.5.

It still appeared that too much damping was present in the system, so analyses were carried out with values of β_o of .00108 and .0008. These results are shown in Figs. 3.2.6 and 3.2.7, respectively. There was no significant improvement in the correlation between analytical and experimental results. Even though the first mode damping ratio was down to .75% for the last analysis, apparently too much damping still was present.

At this point, it was decided that the excessive energy dissipation noted above might be due to the hysteretic characteristics of the moment-curvature relationship of the 1st floor columns rather than to the damping coefficient. Another analysis was carried out with the value of M_1 increased to 200 kip-in and β_o again set to .00108. This value of β_o produces a first mode damping ratio of 1%. The results of this analysis are shown in Figure 3.2.9; the three plots depict the 3rd floor relative displacement, the north column shear and the north column axial force, respectively. The correlation appears excellent, and no futher analyses were carried out for this input signal.

It was decided, however, to attempt another analysis using the PAC 700 input signal, during which the greatest amplitude plastic hinge rotation was observed. For this analysis, values of 100 kip-in and 300 kip-in were used for M_1 and M_2, respectively. A value of .00196 was specified for β_o. The results of this analysis are shown in Figure 3.2.9; the quantities plotted were the same as for Figure 3.2.8.

From the results of this last analysis, one deficiency of the analytical model is pointed out; the lack of any form of stiffness degradation mechanism. The large amplitude response was matched relatively well, but there was again too much hysteretic energy dissipation for the lower amplitude portion of the response. The moment-curvature relationship used in the analysis matched well the large amplitude response, where considerable Bauschinger effect was observed, but did not match well the low amplitude response. This fact can be seen by examination of the hysteretic behavior shown in Figure 2.5k.7 and Figure 2.5k.8.

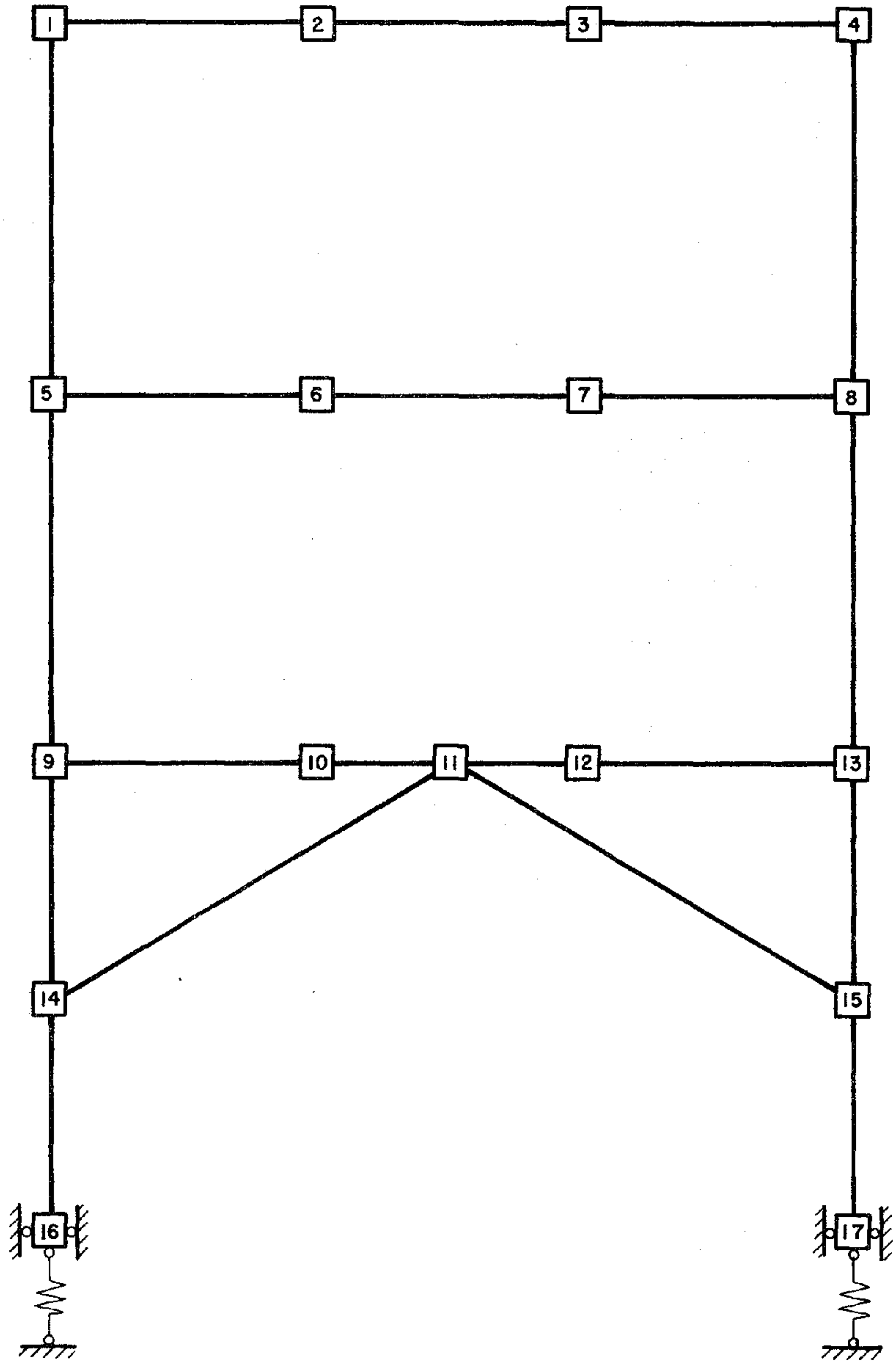

Fig. 3.1.1 Uplift Analytical Model

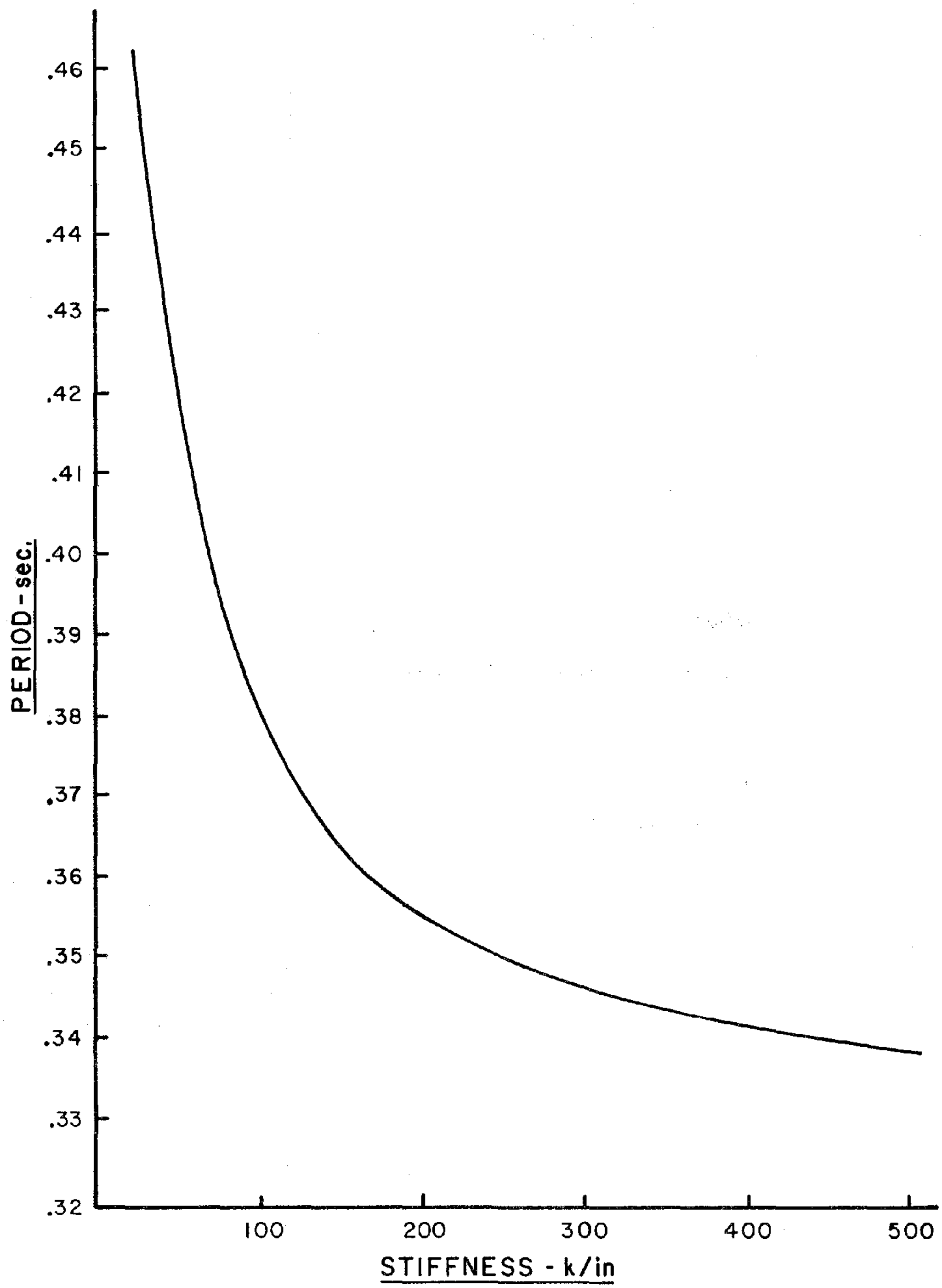

Fig. 3.1.2 Calculated 1st Mode Period
vs Impact Pad Stiffness.

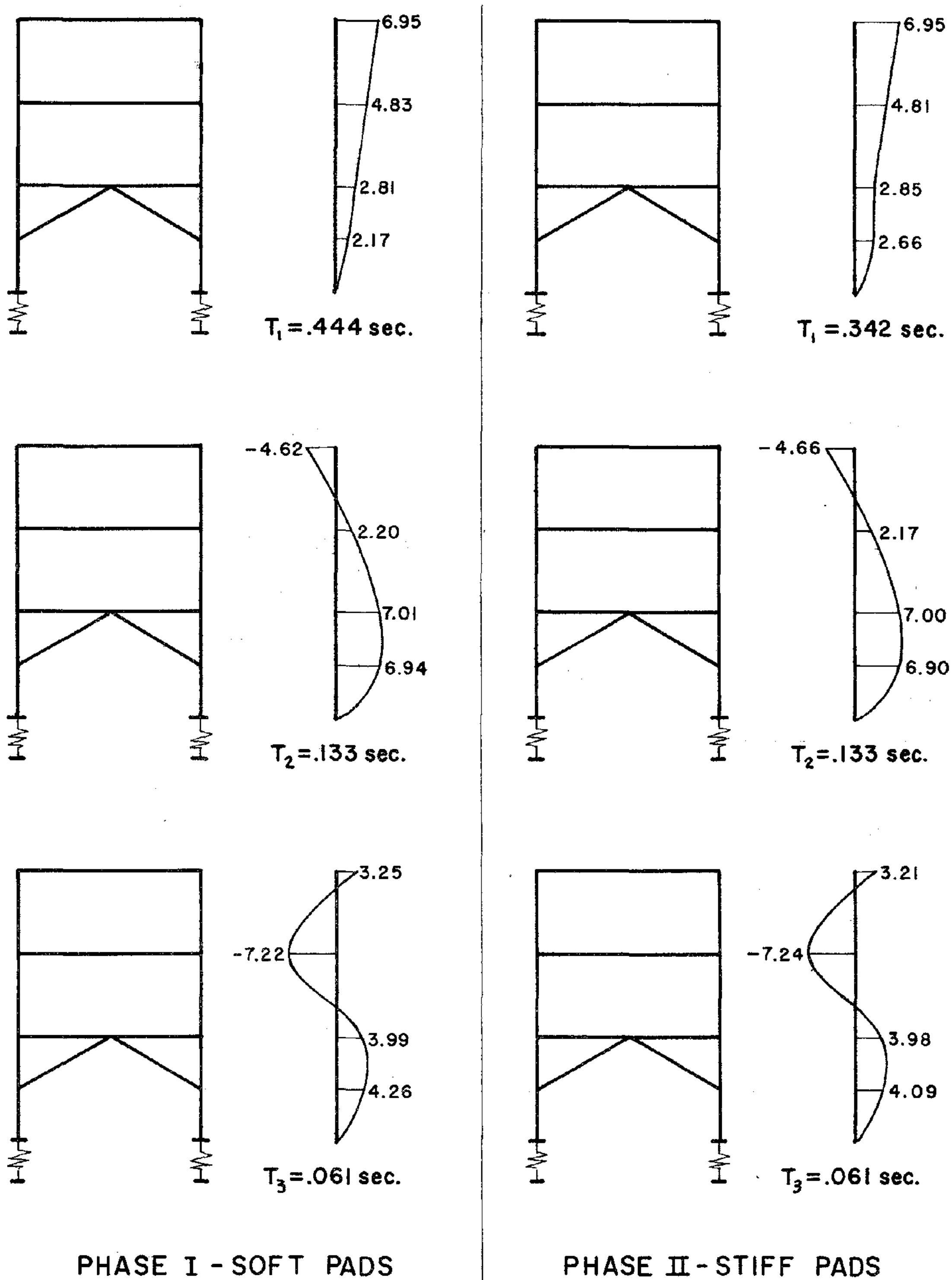

Fig. 3.1.3 Frequencies Calculated and Mode Shapes

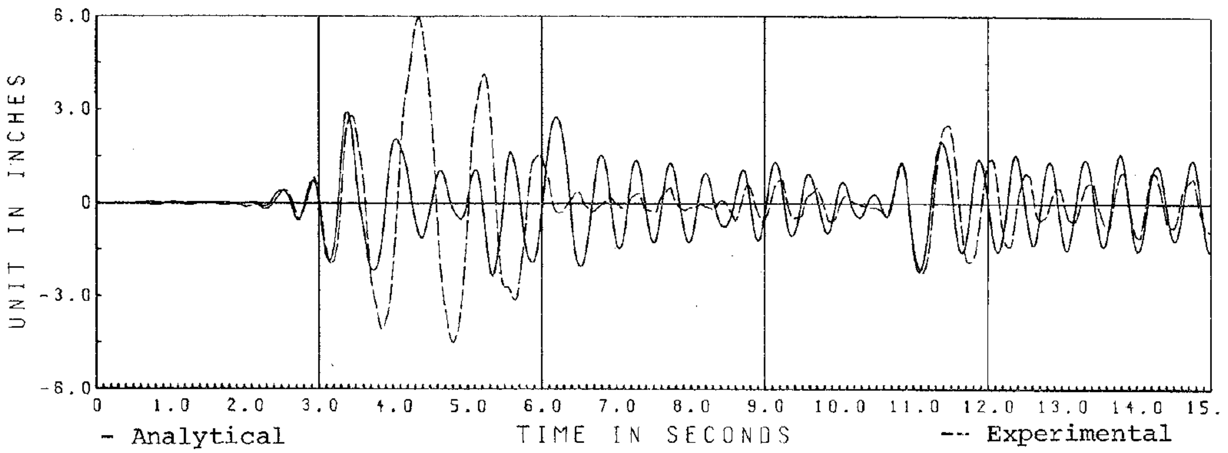

3rd Floor Relative Displacement

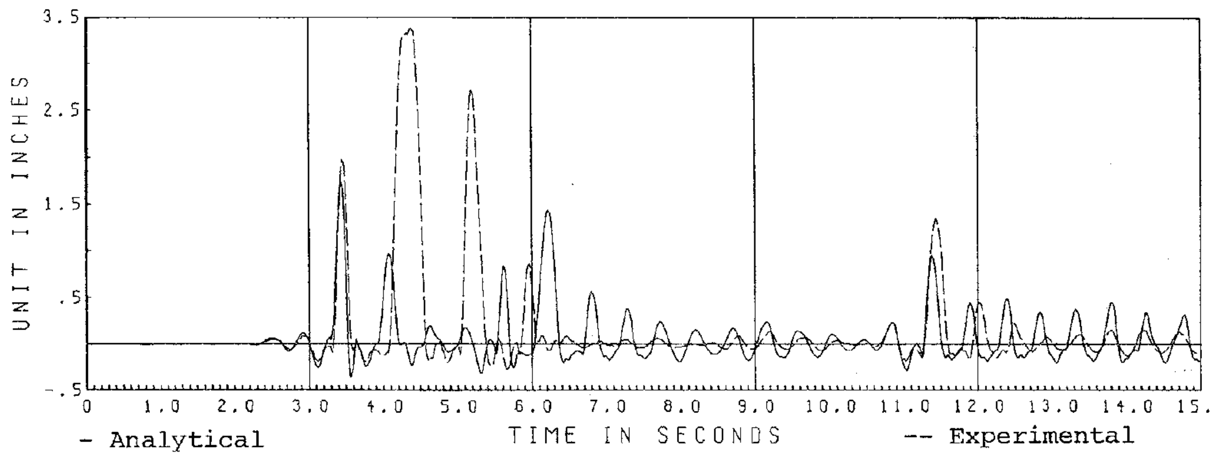

North Column Relative Vertical Displacement

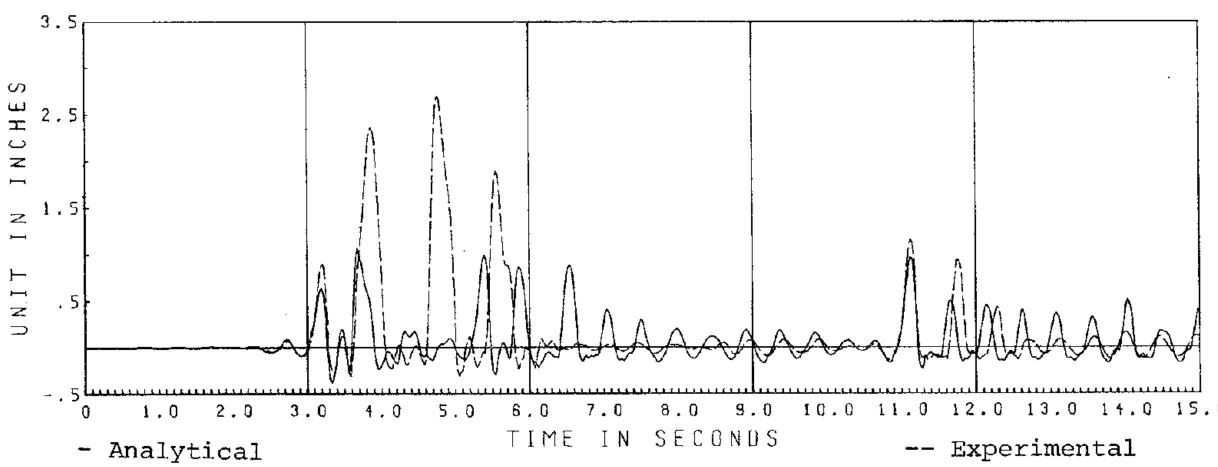

South Column Relative Vertical Displacement

Fig. 3.1a.1 EC 1000 I Analytical Comparisons, β_o = .00293

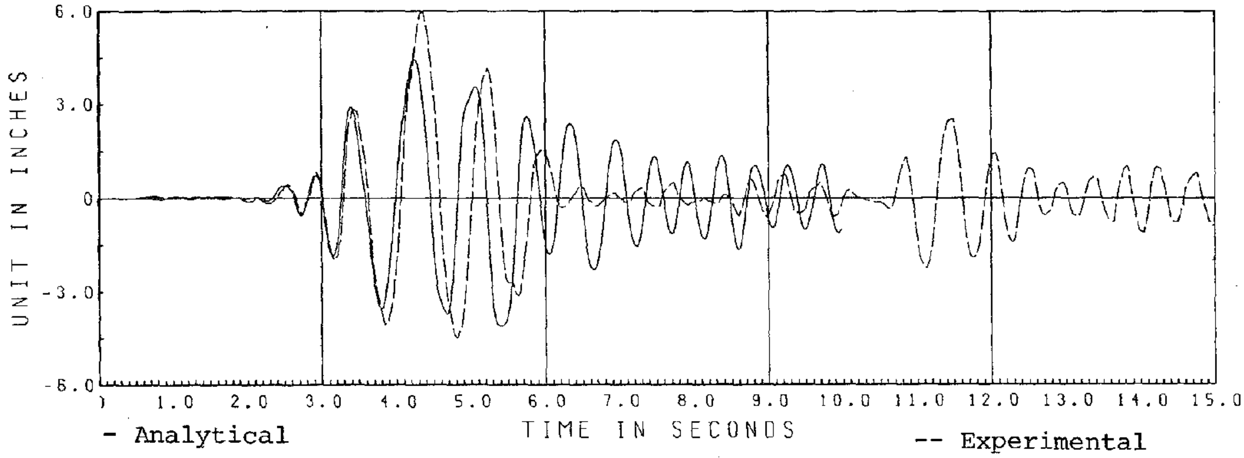

3rd Floor Relative Displacement

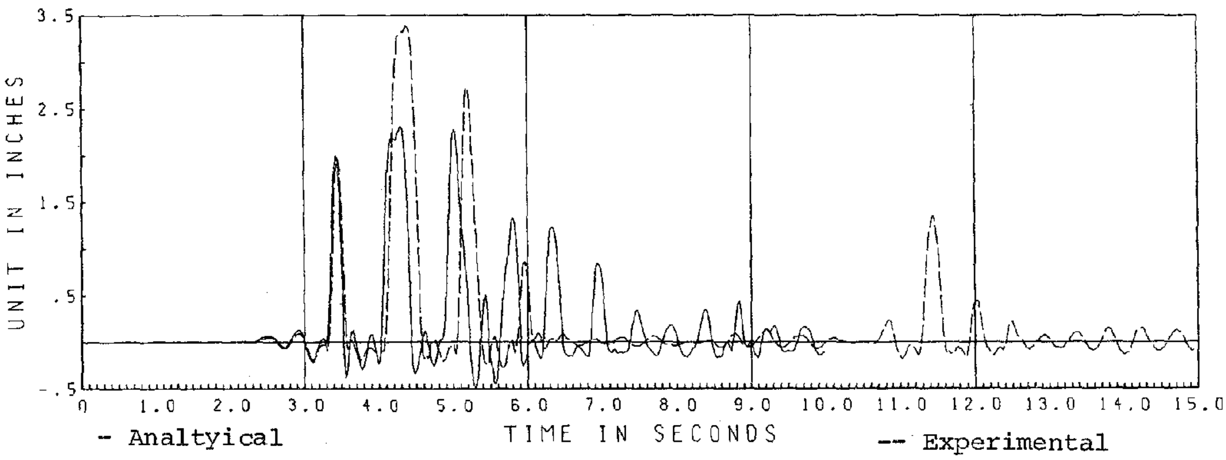

North Column Relative Vertical Displacement

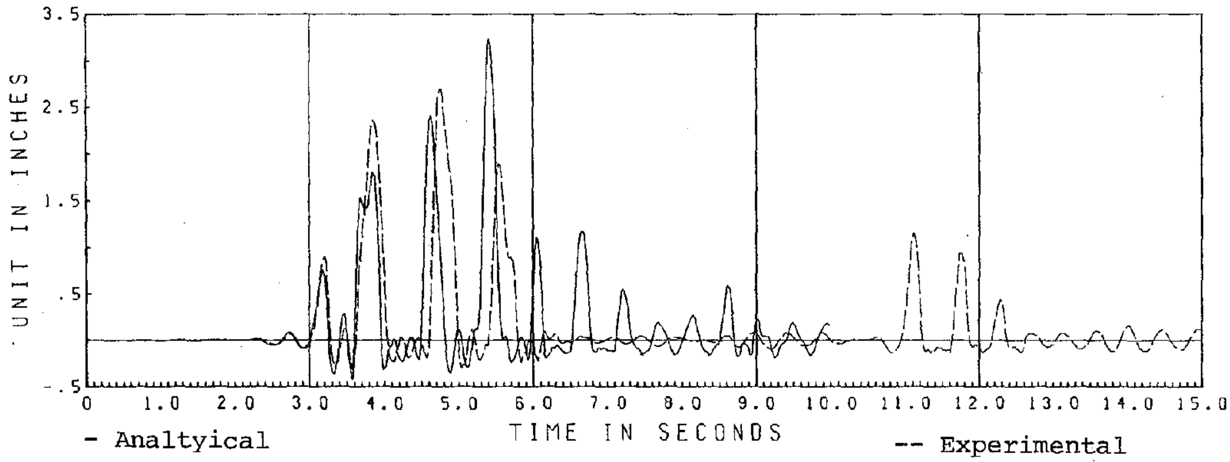

South Column Relative Vertical Displacement

Fig. 3.1a.2 EC 1000 I Analytical Comparisons, $\beta = .00293$

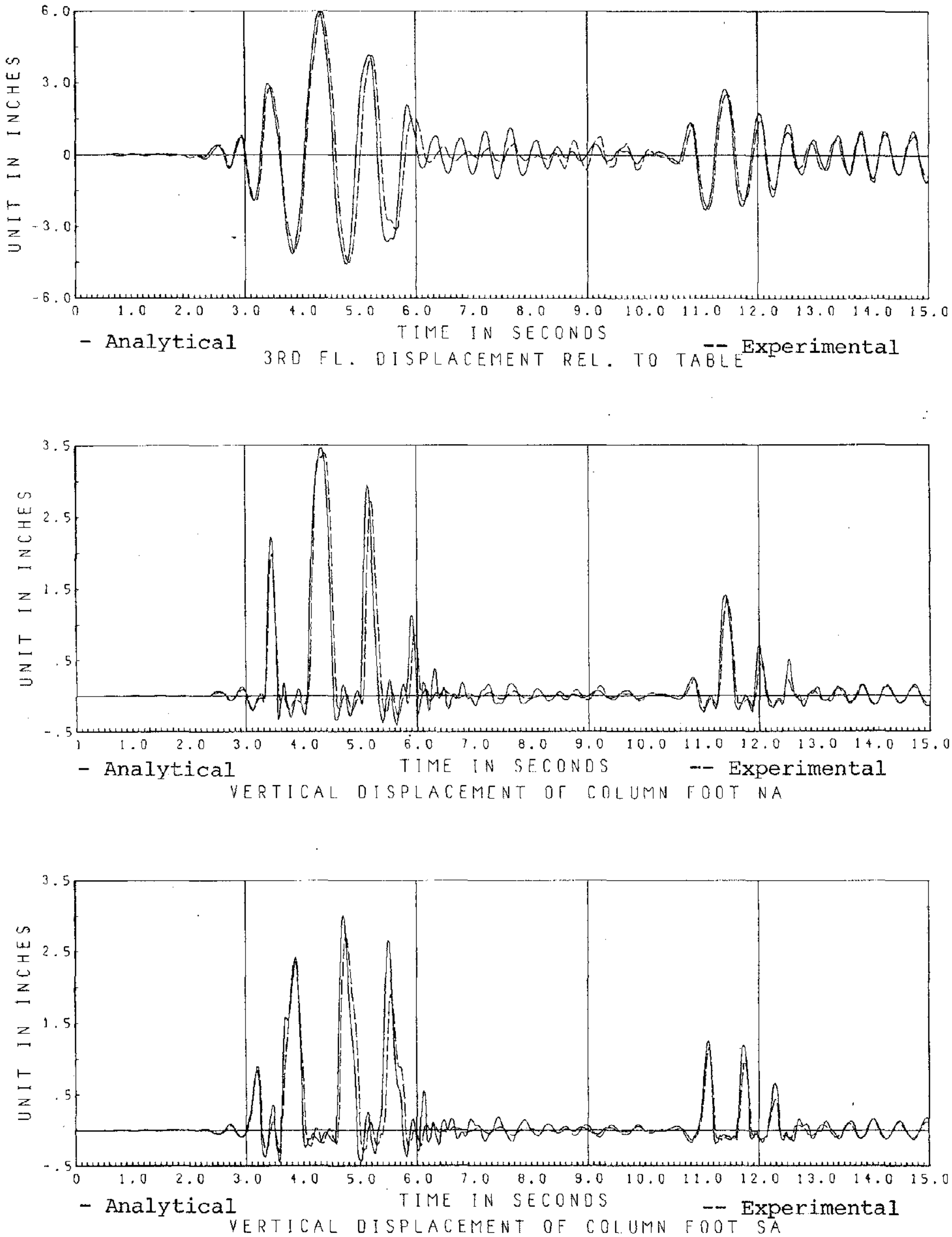

Fig. 3.1a.3 EC 1000 I Analytical Comparisons, β = .002196

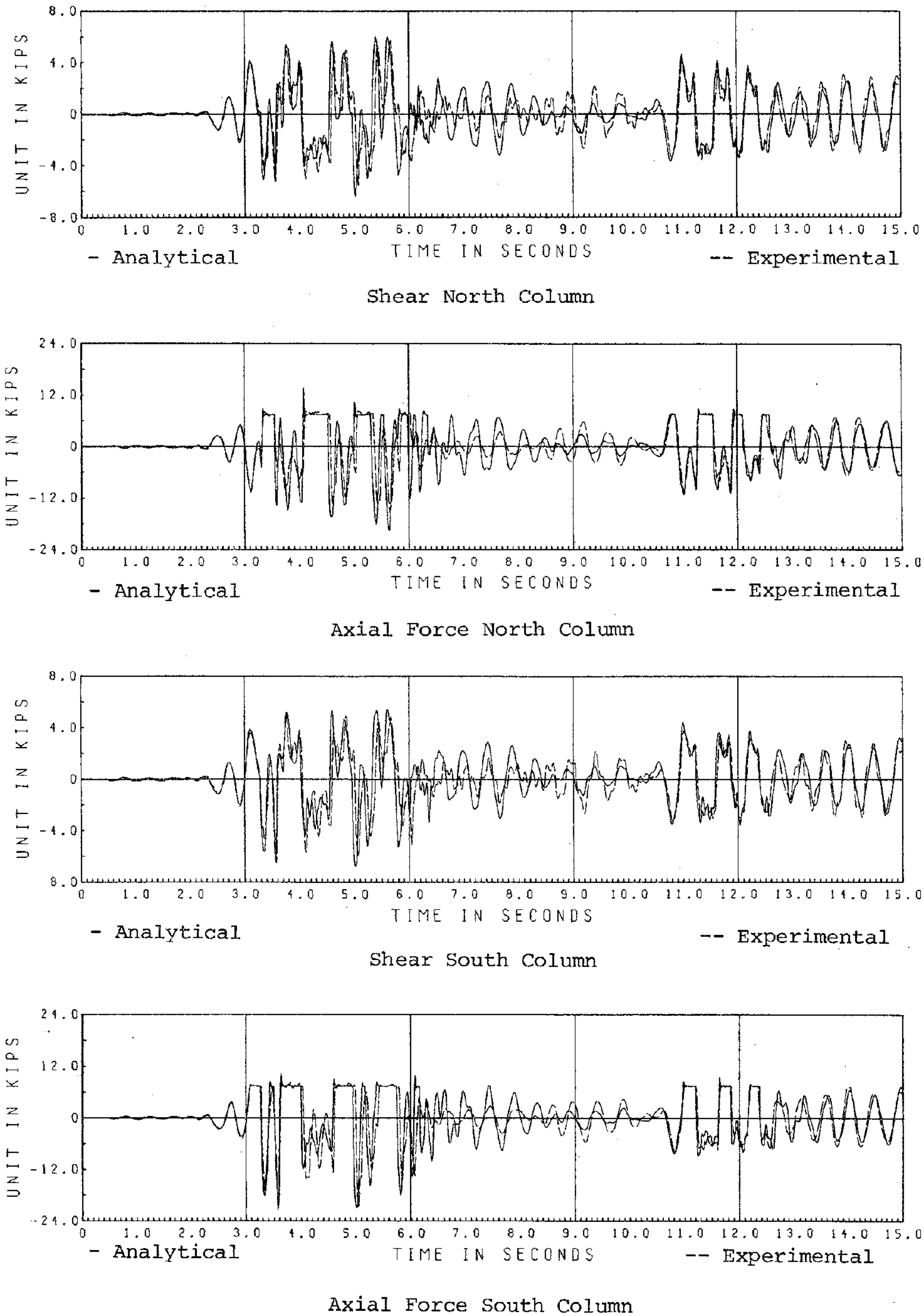

Fig. 3.1a.4 EC 1000 I Analytical Comparisons, $\beta = .002196$

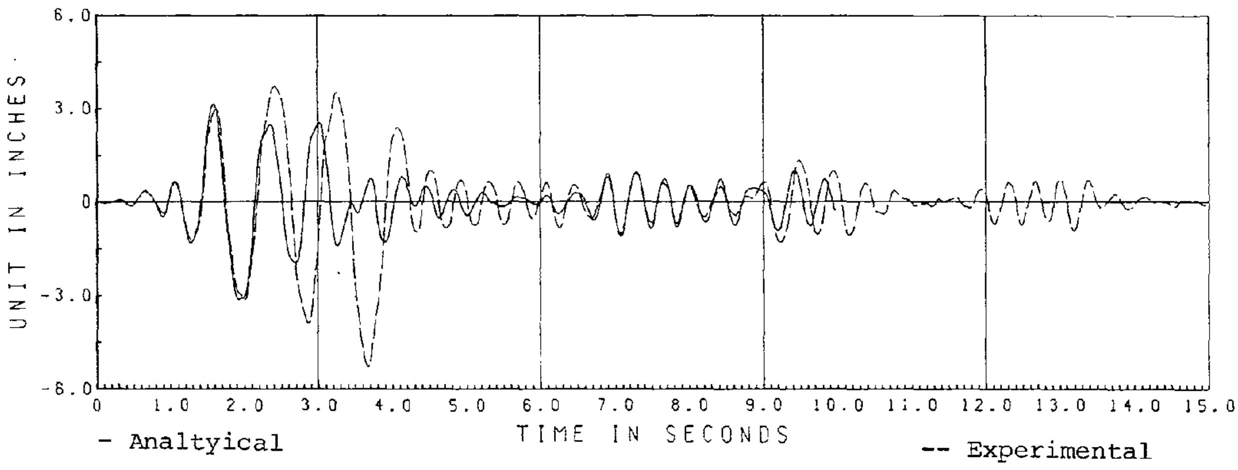

3rd Floor Relative Displacement

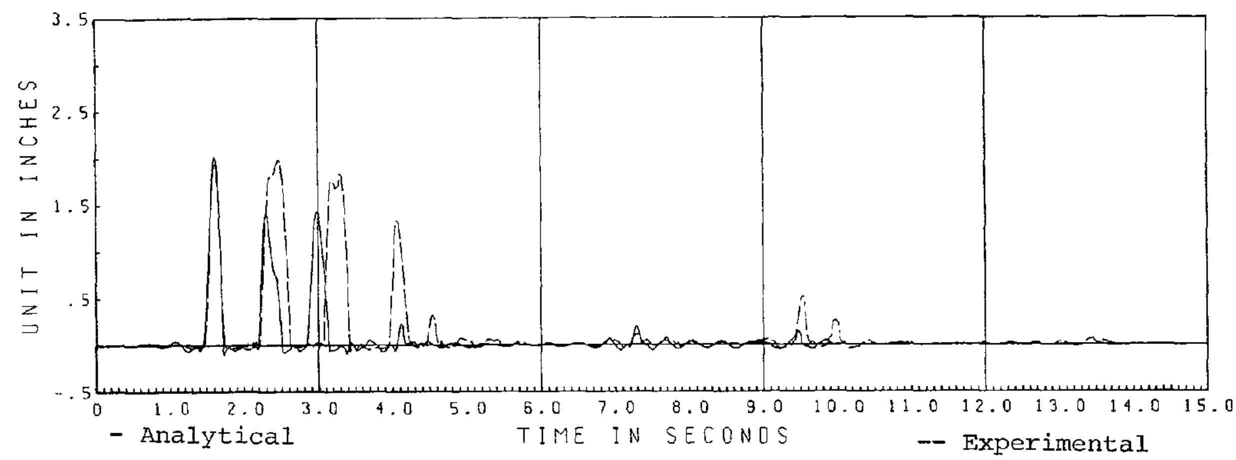

North Column Relative Vertical Displacement

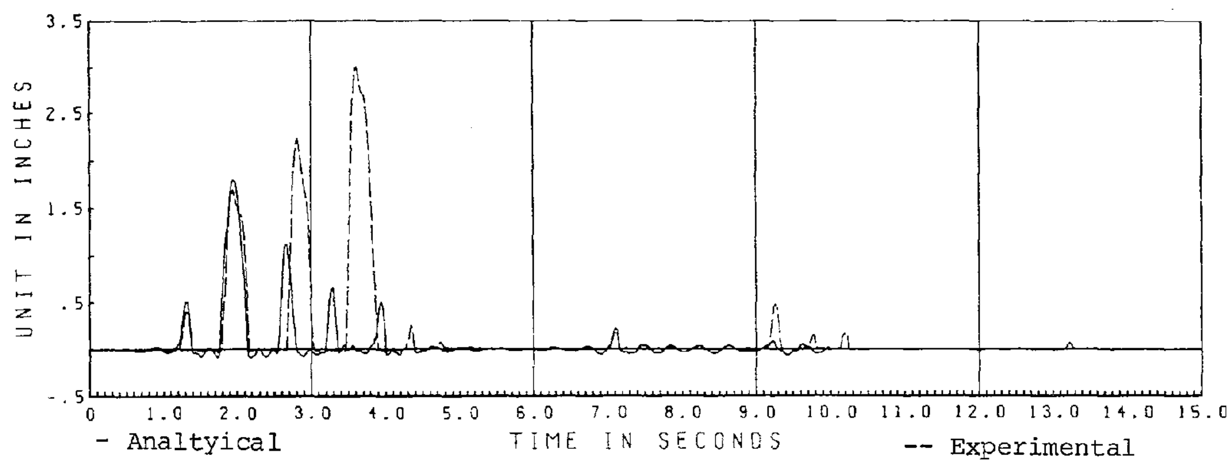

South Column Relative Vertical Displacement

Fig. 3.1b.1 EC 300 II Analytical Comparisons, β = .002196

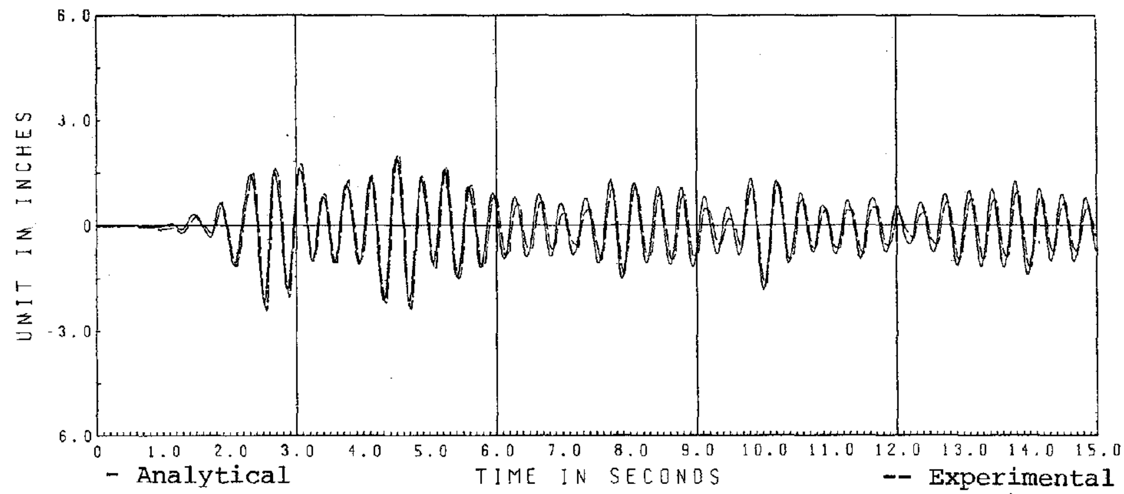

3rd Floor Relative Displacement

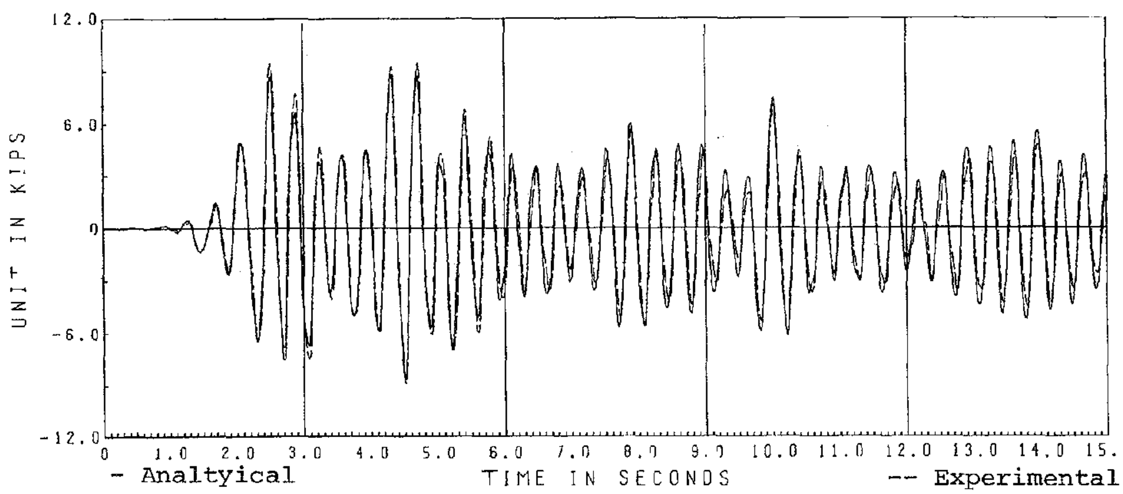

Shear North Column

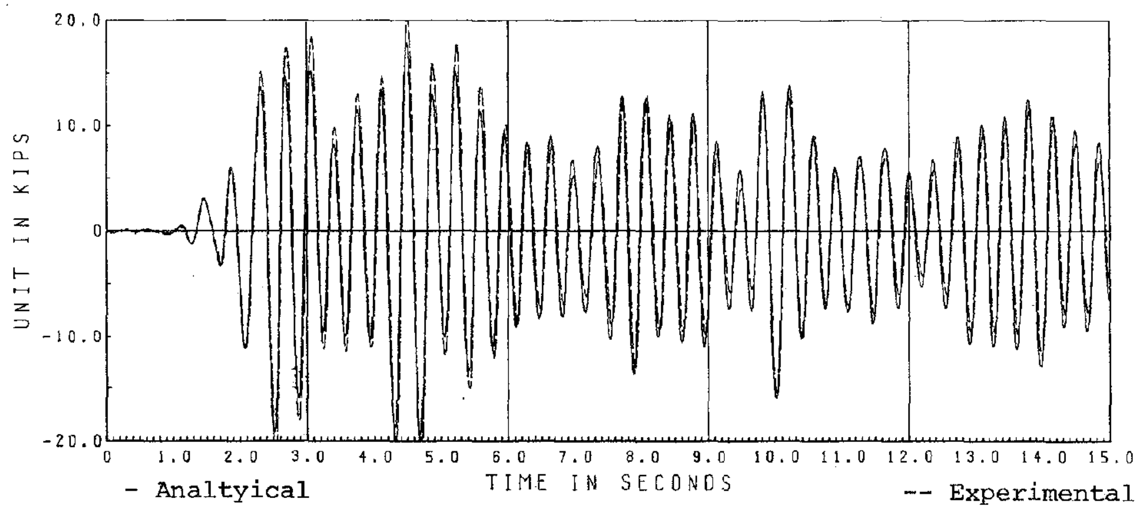

Axial Force North Column

Fig. 3.2.8 EC 1000 Analtyical Comparisons, β_o = .00108, M_1 = 200, M_2 = 350

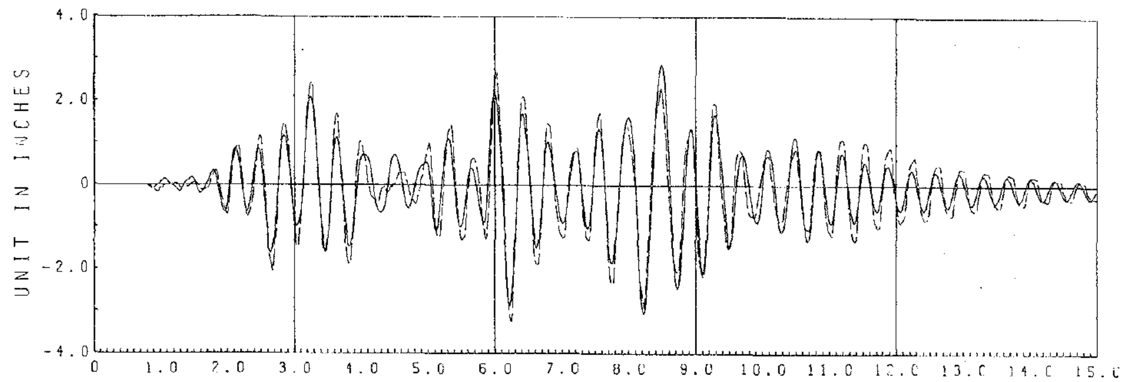

- Analytical -- Experimental

3rd Floor Relative Displacement

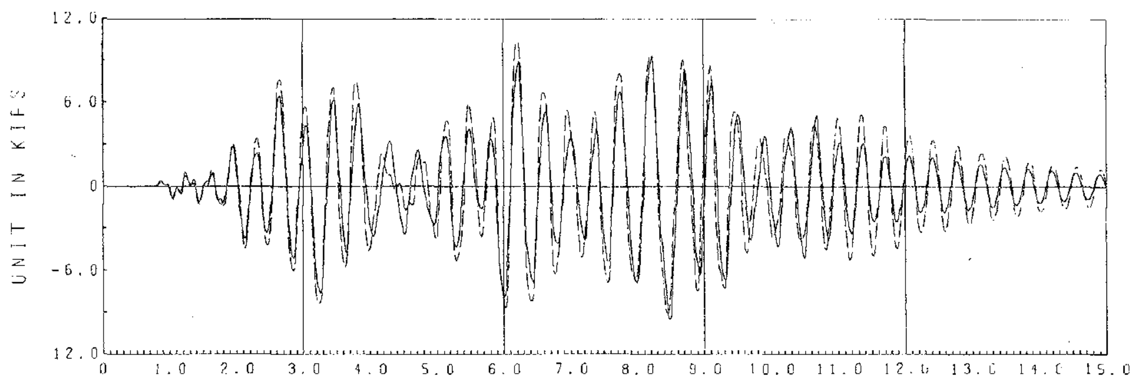

- Analytical -- Experimental

Shear North Column

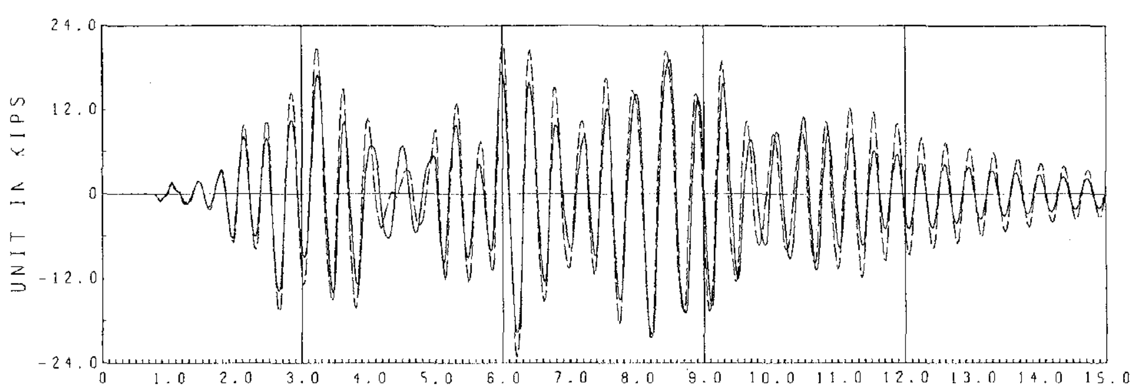

- Analytical -- Experimental

Axial Force North Column

Fig. 3.2.9 PAC 700 Analytical Comparisons, β_o = .00196, M_1 = 100, M_2 = 300

4. SUMMARY AND CONCLUSIONS

In this test program the uplifting response of a three story single-bay steel frame under simulated earthquake excitation was investigated, both experimentally and analytically. In addition, this uplift response was compared with the response to similar excitations during which the column bases were securely anchored to the foundation to prevent uplift.

It was demonstrated that the uplift phenomenon resulted in a definite reduction in the structural force response quantities, as compared to the cases for which uplift was prevented. The action of the uplift response mechanism as a structural "fuse" was clearly evident. For this frame, the internal forces were reduced by about one-third through allowing uplift, and local strain ductility demands on the structure were reduced from values of about 5 to less than unity. It was noted, however, that the rigid body motions possible for this single-bay frame with pinned column bases led to considerably larger relative story displacements when uplift was allowed.

It was also demonstrated that the uplift response for this frame was very accurately represented by means of an analytical procedure utilizing bilinear elastic support elements having zero tensile stiffness and force capacity in the upward direction. Good agreement with experimental results was achieved even when the column base separations approached four inches in amplitude, for this approximately one-half scale frame. The analtyical procedure predicted accurately the large rigid body rotations when a tangent stiffness proportional viscous damping matrix was employed.

Good agreement between experimental and analytical results also was achieved for the inelastic response tests with no uplift allowed. It was observed, however, that some problems occurred during the largest plastic hinge rotations due to the Bauschinger effect, which was not well simulated in the analytical model.

The results of this test program validate the hypothesis stated in the introduction that allowing column uplift in building frames can lead to more rational and economical designs. At least for the type of frame tested, analytical procedures are currently available to accurately predict the uplift behavior which is developed during very severe earthquake excitation.

As a consequence of the promising results reported in this preliminary study, it was decided to extend the research program to include a superstructure system more representative of a realistic prototype. The results of that combined experimental and analytical investigation are presented in a subsequent EERC report entitled "Earthquake Simulation Tests of a Nine-Story Steel Frame with Columns Allowed to Uplift."

REFERENCES

1. Beck, J. L. and Skinner, R. I., "The Seismic Response of a Reinforced Concrete Bridge Pier Designed to Step," Earthquake Engineering and Structural Dynamics, Vol. 2, No. 4, 1974, pp. 343-358.

2. Clough, R. W., and Tang, D. T., "Earthquake Simulator Study of a Steel Frame Structure, Vol. I: Experimental Results," Earthquake Engineering Research Center Report, EERC 75-6, University of California, Berkeley, April 1975.

3. Kanaan, A and Powell, G. H., "General Purpose Computer Program for Inelastic Dynamic Response of Plane Structures," Earthquake Engineering Research Center Report, EERC 73-5, University of California, Berkeley, April 1973.

4. Meek, J. W., "Effects of Foundation Tipping on Dynamic Response," ASCE Journal of the Structural Division, Vol. 101, no. ST1, July 1975.

5. Nigam, N. C. and Jennings, P. C., "Digital Calculation of Response Spectra from Strong-Motion Earthquake Records," Earthquake Engineering Research Laboratory, California Institute of Technology, Pasadena, 1968.

6. Rea, D. and Penzien, J., "Dynamic Response of a 20' x 20' Shaking Table," Proceedings of the 5th World Conference on Earthquake Engineering, Rome, 1973.

7. Tang, D., "Earthquake Simulator Study of a Steel Frame Structure, Vol. II: Analytical Results," Earthquake Engineering Research Center Report, EERC 75-36, University of California, Berkeley, 1975.

Appendix A

Data Channel Listings

Table A-1 Phase I Data Channel Schedule

CHANNEL	CHANNEL MNEMONIC	CHANNEL DESCRIPTION
0	Cmd H Acc	Command horizontal accl. signal
1	Cmd V Acc	Command vertical accl. signal
2	Cmd H Disp	Command horizontal displ. signal
3	Cmd V Disp	Command vertical displ. signal
4	Av H T Displ	Average horizontal table displ.
5	Av V T Displ	Average vertical table displ.
6	Av H T Acc	Average horitontal table accl.
7	Av V T Acc	Average vertical table accl.
8	Pitch	Angular accl. in pitching mode
9	Roll	Angular accl. in rolling mode
10	Twist	Angular accl. in twisting mode
11	Force H1	Force in horizontal actuator
12	Force H2	Force in horizontal actuator
13	Force H3	Force in horizontal actuator
14	Acc H1	Individual table accelerometer (hor)
15	Acc H2	Individual table accelerometer (hor)
16	Acc V1	Individual table accelerometer (vert)
17	Acc V2	Individual table accelerometer (vert)
18	Acc V3	Individual table accelerometer (vert)
19	Acc V4	Individual table accelerometer (vert)
20	Force V1	Force in vertical actuator
21	Force V2	Force in vertical actuator
22	Force V3	Force in vertical actuator
23	Force V4	Force in vertical actuator
24	Displ V1	Individual table vertical displ.
25	Displ V2	Individual table vertical displ.
26	Displ V3	Individual table vertical displ.
27	Displ V4	Individual table vertical displ.
28	Displ H1	Individual table horizontal displ.
29	Displ H2	Individual table horizontal displ.
30	Displ H3	Individual table horizontal displ.
31	blank	
32	PS Force-1	Force in passive stabilizer
33	PS Force-2	Force in passive stabilizer
34	PS Force-3	Force in passive stabilizer
35	PS Force-4	Force in passive stabilizer
36	Flr Acc 1	1st floor acceleration
37	Flr Acc 2	2nd floor acceleration
38	Flr Acc 3	3rd floor acceleration
39	blank	
40	Flr Disp 1	1st floor absolute displacement
41	Flr Disp 2	2nd floor absolute displacement
42	Flr Disp 3	3rd floor absolute displacement
43	Uplift NA	Vertical displacement of column base NA
44	Uplift NBO	Vertical displ. of outside column base NB
45	Uplift NBI	Vertical displ. of inside column base NB

46	Uplift SA	Vertical displ. of column base SA
47	Uplift SB	Vertical displ. of column base SB
48	Contact Na	Contact switch under column NA
49	Contact NB	Contact switch under column NB
50	Contact SA	Contact switch under column SA
51	Contact SB	Contact switch under column SB
52	Clstr-NAO-1	Col. NA strain outside face 1st floor
53	Clstr-NAI-1	Col. NA strain inside face 1st floor
54	Clstr-SAO-1	Col. SA strain outside face 1st floor
55	CLstr-SAI-1	Col. SA strain inside face 1st floor
56	Clrot-NAO-1	Col. NA DCDT outside face 1st floor
57	Clrot-NAI-1	Col. NA DCDT inside face 1st floor
58	Clrot-SAO-1	Col. SA DCDT outside face 1st floor
59	Clrot-SAI-1	Col SA DCDT inside face 1st floor
60	Clflx-NAM-1	Col. NA flex. strain @ midheight 1st floor
61	Clflx-SAM-1	Col. SA flex. strain @ midheight 1st floor
62	Clflx-NBM-1	Col. NB flex. strain @ midheight 1st floor
63	Clflx-SBM-;	Col. SB flex. strain @ midheight 1st floor
64	Clstr-NBO-1	Col. NB strain outside face 1st floor
65	Clstr-NBI-1	Col. NB strain inside face 1st floor
66	Clstr-SBO-1	Col. SB strain oustide face 1st floor
67	Clstr-SBI-1	Col. SB strain inside face 1st floor
68	Clrot-NBO-1	Col. NB DCDT outside face 1st floor
69	Clrot-NBI-1	Col. NB DCDT inside face 1st floor
70	Clrot-SBO-1	Col. SB DCDT outside face 1st floor
71	Clrot-SBI-1	Col. SB DCDT inside face 1st floor
72	Clflx-NAB-1	Col. NA flex. strain bottom station 1st flr.
73	Clflx-NAT-1	Col. NA flex strain top station 1st flr.
74	Slflx-SAB-1	Col. SA flex strain bottom station 1st flr.
75	Clflx-SAT-1	Col. SA flex. strain top station 1st flr.
76	Bmflx-NO-1	Beam flex. strain north end outside station
77	Bmflx-NI-1	Beam flex. strain north end inside station
78	Bmflx-SI-1	Beam flex. strain south end inside station
79	Bmflx-SO-1	Beam flex. strain south end outside station
80	Clrot-NBO-2	Col. NB DCDT outside face 2nd floor
81	Clrot-NBI-2	Col. NB DCDT inside face 2nd floor
82	Clrot-SBO-2	Col. SB DCDT outside face 2nd floor
83	Clrot-SBI-2	Col. SB DCDT inside face 2nd floor
84	Clflx-NBT-2	Col. NB flex. strain top station 2nd flr.
85	Clflx-NBB-2	Col. NB flex. strain bottom station 2nd flr.
86	Clflx-SBT-2	Col. SB flex. strain top station 2nd flr.
87	Clflx-SBB-2	Col. SB flex. strain bottom station 2nd flr.
88	Clflx-NAY-2	Col. NA post-yield strain 2nd floor
89	Clflx-NBY-2	Col. NB post-yield strain 2nd floor
90	Clflx-SAY-2	Col. SA post-yield strain 2nd floor
91	Clflx-SBY-2	Col. SB post-yield strain 2nd floor
92	Clflx-NAT-2	Col. NA flex. strain top station 2nd flr.
93	Clflx-NAB-2	Col. NA flex. strain bottom station 2nd flr.
94	Clflx-SAT-2	Col. SA flex. strain top station 2nd flr.
95	Clflx-SAB-2	Col. SA flex. strain bottom station 2nd flr.
96	Clrot-NAO-2	Col. NA DCDT outside face 2nd floor
97	Clrot-NAI-2	Col. NA DCDT inside face 2nd floor
98	Clrot-SAO-2	Col. SA DCDT outside face 2nd floor
99	Clrot-SAI-2	Col. SA DCDT inside face 2nd floor

100	Bmflx-NAY-2	Beam post-yield strain north end frame A
101	Bmflx-NBY-2	Beam post-yield strain north end frame B
102	Bmflx-SAY-2	Beam post-yield strain south end frame A
103	Bmflx-SMY-2	Beam post-yield strain south end frame B
104	Bmflx-NO-2	Beam flex. strain north end outside station
105	Bmflx-NI-2	Beam flex. strain north end inside station
106	Bmflx-SI-2	Beam flex. strain south end inside station
107	Bmflx-SO-2	Beam flex. strain south end outside station
108	Bmrot-NOT-2	Beam DCDT north outside station top face
109	Bmrot-NOB-2	Beam DCDT north outside station bottom face
110	Bmrot-SOT-2	Beam DCDT south outside station top face
111	Bmrot-SOB-2	Beam DCDT south soutside station bottom face
112	Jtrot-NT	Joint DCDT north end top side
113	Jtrot-NB	Joint DCDT north end bottom side
114	Jtrot-ST	Joint DCDT south end top side
115	Jtrot-SB	Joint DCDT south end bottom side
116	Bmrot-NIT	Beam DCDT north inside station top face
117	Bmrot-NIB	Beam DCDT north inside station bottom face
118	Bmrot-SIT	Beam DCDT south inside station top face
119	Bmrot-SIB	Beam DCDT south inside station bottom face
120	Clflx-NAT-3	Col. NA flex. strain top station 3rd flr.
121	Clflx-NAB-3	Col. NA flex. strain bottom station 3rd flr.
122	Clflx-SAT-3	Col. SA flex. strain top station 3rd flr.
123	Clflx-SAB-3	Col. SA flex. strain bottom station 3rd flr.

Table A-2 Phase II Data Channel Schedule

CHANNEL	CHANNEL MNEMONIC	CHANNEL DESCRIPTION
0	Cmd H Acc	Command horizontal accl. signal
1	Cmd V Acc	Command vertical accl. signal
2	Cmd H Disp	Command horizontal displ. signal
3	Cmd V Disp	Command vertical displ. signal
4	Av H T Displ	Average horizontal table displ.
5	Av V T Displ	Average vertical table displ.
6	Av H T Acc	Average horizontal table accl.
7	AV V T Acc	Average vertical table accl.
8	Pitch	Angular accl. in pitching mode
9	Roll	Angular accl. in rolling mode
10	Twist	Angular accl. in twisting mode
11	Force H1	Force in horizontal actuator
12	Force H2	Force in horizontal actuator
13	Force H3	Force in horizontal actuator
14	Acc H1	Individual table accelerometer (hor)
15	Acc H2	Individual table accelerometer (hor)
16	Acc V1	Individual table accelerometer (vert)
17	Acc V2	Individual table accelerometer (vert)
18	Acc V3	Individual table accelerometer (vert)
19	Acc V4	Individual table accelerometer (vert)
20	Force V1	Force in vertical actuator
21	Force V2	Force in vertical actuator
22	Force V3	Force in vertical actuator
23	Force V4	Force in vertical actuator
24	Displ V1	Individual table vertical displ.
25	Displ V2	Individual table vertical displ.
26	Displ V3	Individual table vertical displ.
27	Displ V4	Individual table vertical displ.
28	Displ H1	Individual table horizontal displ.
29	Displ H2	Individual table horizontal displ.
30	Displ H3	Individual table horizontal displ.
31	blank	
32	PS Force-1	Force in passive stabilizer
33	PS Force-2	Force in passive stabilizer
34	PS Force-3	Force in passive stabilizer
35	PS Force-4	Force in passive stabilizer
36	Flr Acc 1	1st floor acceleration
37	Flr Acc 2	2nd floor acceleration
38	Flr Acc 3	3rd floor acceleration
39	blank	
40	Flr Disp 1	1st floor absolute displacement
41	Flr Disp 2	2nd floor absolute displacement
42	Flr Disp 3	3rd floor absolute displacement
43	blank	
44	Uplift NA	Vertical displacement column base NA
45	Uplift NB	Vertical displacement column base NB

46	Uplift SA	Vertical displ. of column base SA
47	Uplift SB	Vertical displ. of column base SB
48	Clstr-NBO-L	Col NB midheight strain out face lower station
49	Clstr-NBO-M	Col NB midheight strain out face mid station
50	Clstr-NBO-U	Col Nb midheight strain out face upper station
51	Clstr-NBI-U	Col NB midheight strain in face upper station
52	Clstr-NAO-1	Col. NA strain outside face 1st floor
53	Clstr-NAI-1	Col. NA strain inside face 1st floor
54	Clstr-SAO-1	Col. SA strain outside face 1st floor
55	Clstr-SAI-1	Col. SA strain inside face 1st floor
56	Clrot-NAO-1	Col. NA DCDT outside face 1st floor
57	Clrot-NAI-1	Col. NA DCDT inside face 1st floor
58	Clrot-SAO-1	Col. SA DCDT outside face 1st floor
59	Clrot-SAI-1	Col. SA DCDT inside face 1st floor
60	Clflx-NAM-1	Col. NA flex. strain @ midheight 1st floor
61	Clflx-SAM-1	Col. SA flex. strain @ midheight 1st floor
62	Clstr-NBI-M	Col. NB midheight strain in face mid station
63	Clflx-SBM-1	Col. SB flex. strain @ midheight 1st floor
64	Clstr-NBO-1	Col. NB strain outside face 1st floor
65	Clstr-NBI-1	Col. NB strain inside face 1st floor
66	Clstr-SBO-1	Col. SB strain outside face 1st floor
67	Clstr-SBI-1	Col. SB strain inside face 1st floor
68	Clrot-NBO-1	Col. NB DCDT outside face 1st floor
69	Clrot-NBI-1	Col. NB DCDT inside face 1st floor
70	Clrot-SBO-1	Col. SB DCDT outside face 1st floor
71	Clrot-SBI-1	Col. SB DCDT inside face 1st floor
72	Clflx-NAB-1	Col. NA flex. strain bottom station 1st flr.
73	Clflx-NAT-1	Col. NA flex. strain top station 1st flr.
74	Clflx-SAB-1	Col. SA flex. strain bottom station 1st flr.
75	Clflx-SAT-1	Col. SA flex. strain top station 1st flr.
76	Bmflx-NO-1	Beam flex. strain north end outside station
77	Bmflx-NI-1	Beam flex. strain north end inside station
78	Bmflx-SI-1	Beam flex. strain south end inside station
79	Bmflx-SO-1	Beam flex. strain south end outside station
80	Clrot-NBO-2	Col. NB DCDT outside face 2nd floor
81	Clrot-NBI-2	Col. NB DCDT inside face 2nd floor
82	Clrot-SBO-2	Col. SB DCDT outside face 2nd floor
83	Clrot-SBI-2	Col. SB DCDT inside face 2nd floor
84	Clflx-NBT-2	Col. NB flex. Strain top station 2nd flr.
85	Clflx-NBB-2	Col. NB flex. strain bottom station 2nd flr.
86	Clflx-SBT-2	Col. SB flex. strain top station 2nd flr.
87	Clflx-SBB-2	Col. SB flex. strain bottom station 2nd flr.
88	Clflx-NAY-2	Col. NA post-yield strain 2nd floor
89	Clflx-NBY-2	Col. NB post-yield strain 2nd floor
90	Clflx-SAY-2	Col. SA post-yield strain 2nd floor
91	Clflx-SBY-2	Col. SB post-yield strain 2nd floor
92	Clflx-NAT-2	Col. NA flex. strain top station 2nd flr.
93	Clflx-NAB-2	Col. NA flex. strain bottom station 2nd flr.
94	Clflx-SAT-2	Col. SA flex. strain top station 2nd flr.
95	Clflx-SAB-2	Col. SA flex. strain bottom station 2nd flr.
96	Clrot-NAO-2	Col. NA DCDT outside face 2nd floor
97	Clrot-NAI-2	Col. NA DCDT inside face 2nd floor
98	Clrot-SAO-2	Col. SA DCDT outside face 2nd floor
99	Clrot-SAI-2	Col. SA DCDT inside face 2nd floor

100	Bmflx-NAY-2	Beam post-yield strain north end frame A
101	Bmflx-NBY-2	Beam post-yield strain north end frame B
102	Bmflx-SAY-2	Beam post-yield strain south end frame A
103	Bmflx-SMY-2	Beam post-yield strain south end frame B
104	Bmflx-NO-2	Beam flex. strain north end outside station
105	Bmflx-NI-2	Beam flex. strain north end inside station
106	Bmflx-SI-2	Beam flex. strain south end inside station
107	Bmflx-SO-2	Beam flex. strain south end outside station
108	Bmrot-NOT-2	Beam DCDT north outside station top face
109	Bmrot-NOB-2	Beam DCDT north outside station bottom face
110	Bmrot-SOT-2	Beam DCDT south outside station top face
111	Bmrot-SOB-2	Beam DCDT south outside station bottom face
112	Jtrot-NT	Joint DCDT north end top side
113	Jtrot-NB	Joint DCDT north end bottom side
114	Jtrot-ST	Joint DCDT south end top side
115	Jtrot-SB	Joint DCDT south end bottom side
116	Bmrot-NIT	Beam DCDT north inside station top face
117	Bmrot-NIB	Beam DCDT north inside station bottom face
118	Bmrot-SIT	Beam DCDT south inside station top face
119	Bmrot-SIB	Beam DCDT south inside station bottom face
120	Clflx-NAT-3	Col. NA flex. strain top station 3rd flr.
121	Clflx-NAB-3	Col. NA flex. strain bottom station 3rd flr.
122	Clflx-SAT-3	Col. SA flex. strain top station 3rd flr.
123	Clflx-SAB-3	Col. SA flex. strain bottom station 3rd flr.
124	Contact NA	Contact switch under column base NA
125	Contact NB	Contact switch under column base NB
126	Contact SA	Contact switch under column base SA
127	Contact SB	Contact switch under column base SB

Table A-3 Data Channel Schedule for EC 200 and EC 1000

CHANNEL	CHANNEL MNEMONIC	CHANNEL DESCRIPTION
0	Cmd H Acc	Command horizontal accl. signal
1	Cmd V Acc	Command vertical accl. signal
2	Cmd H Disp	Command horizontal displ. signal
3	Cmd V Disp	Command vertical displ. signal
4	Av H T Displ	Average horizontal table displ.
5	Av V T Displ	Average vertical table displ.
6	Av H T Acc	Average horizontal table accl.
7	Av V T Acc	Average vertical table accl.
8	Pitch	Angular accl. in putching mode
9	Roll	Angular accl. in rolling mode
10	Twist	Angular accl. in twisting mode
11	Force H1	Force in horizontal actuator
12	Force H2	Force in horizontal actuator
13	Force H3	Force in horizontal actuator
14	Acc H1	Individual table accelerometer (hor)
15	Acc H2	Individual table accelerometer (hor)
16	Acc V1	Individual table accelerometer (vert)
17	Acc V2	Individual table accelerometer (vert)
18	Acc V3	Individual table accelerometer (vert)
19	Acc V4	Individual table accelerometer (vert)
20	Force V1	Force in vertical actuator
21	Force V2	Force in vertical actuator
22	Force V3	Force in vertical actuator
23	Force V4	Force in vertical actuator
24	Displ V1	Individual table vertical displ.
25	Displ V2	Individual table vertical displ.
26	Displ V3	Individual table vertical displ.
27	Displ V4	Individual table vertical displ.
28	Displ H1	Individual table horizontal displ.
29	Displ H2	Individual table horizontal displ.
30	Displ H3	Individual table horizontal displ.
31	blank	
32	PS Force-1	Force in passive stabilizer
33	PS Force-2	Force in passive stabilizer
34	PS Force-3	Force in passive stabilizer
35	PS Force-4	Force in passive stabilizer
36	Flr Acc 1	1st floor acceleration
37	Flr Acc 2	2nd floor acceleration
38	Flr Acc 3	3rd floor acceleration
39	blank	
40	Flr Disp 1	1st floor absolute displacement
41	Flr Disp 2	2nd floor absolute displacement
42	Flr Disp 3	3rd floor absolute displacement
43	Uplift NA	Vertical displacement of column base NA
44	Uplift NBO	Vertical displ. of outside column base NB
45	Uplift NBI	Vertical displ. of inside column base NB

46	Uplift SA	Vertical displ. of column base SA
47	Uplift SB	Vertical displ. of column base SB
48	blank	
49	blank	
50	blank	
51	blank	
52	Clstr-NAO-1	Col. NA strain outside face 1st floor
53	Clstr-NAI-1	Col. NA strain inside face 1st floor
54	Clstr-SAO-1	Col. SA strain outside face 1st floor
55	Clstr-SAI-1	Col. SA strain inside face 1st floor
56	Clrot-NAO-1	Col. NA DCDT outside face 1st floor
57	Clrot-NAI-1	Col. NA DCDT inside face 1st floor
58	Clrot-SAO-1	Col. SA DCDT outside face 1st floor
59	Clrot-SAI-1	Col. SA DCDT inside face 1st floor
60	Clflx-NAM-1	Col. NA flex. strain @ midheight 1st floor
61	Clflx-SAM-1	Col. SA flex. strain @ midheight 1st floor
62	Clflx-NBM-1	Col. NB flex. strain @ midheight 1st floor
63	Clflx-SBM-1	Col. SB flex. strain @ midheight 1st floor
64	Clstr-NBO-1	Col. NB strain outside face 1st floor
65	Clstr-NBI-1	Col. NB strain inside face 1st floor
66	Clstr-SBO-1	Col. SB strain outside face 1st floor
67	Clstr-SBI-1	Col. SB strain inside face 1st floor
68	Clrot-NBO-1	Col. NB DCDT outside face 1st floor
69	Clrot-NBI-1	Col. NB DCDT inside face 1st floor
70	Clrot-SBO-1	Col. SB DCDT outside face 1st floor
71	Clrot-SBI-1	Col. SB DCDT inside face 1st floor
72	Clflx-NAB-1	Col. NA flex. strain bottom station 1st flr.
73	Clflx-NAT-1	Col. NA flex. strain top station 1st flr.
74	Clflx-SAB-1	Col. SA flex. strain bottom station 1st flr.
75	Clflx-SAT-1	Col. SA flex. strain top station 1st flr.
76	Bmflx-NO-1	Beam flex. strain north end outside station
77	Bmflx-NI-1	Beam flex. strain north end inside station
78	Bmflx-SI-1	Beam flex. strain south end inside station
79	Bmflx-SO-1	Beam flex. strain south end outside station
80	Clrot-NBO-2	Col. NB DCDT outside face 2nd floor
81	Clrot-NBI-2	Col. NB DCDT inside face 2nd floor
82	Clrot-SBO-2	Col. SB DCDT outside face 2nd floor
83	Clrot-SBI-2	Col. SB DCDT inside face 2nd floor
84	Clflx-NBT-2	Col. NB flex. strain top station 2nd flr.
85	Clflx-NBB-2	Col. NB flex. strain bottom station 2nd flr.
86	Clflx-SBT-2	Col. SB flex. strain top station 2nd flr.
87	Clflx-SBB-2	Col. SB flex. strain bottom station 2nd flr.
88	Clflx-NAY-2	Col. NA post-yield strain 2nd floor
89	Clflx-NBY-2	Col. NB post-yield strain 2nd floor
90	Clflx-SAY-2	Col. SA post-yield strain 2nd floor
91	Clflx-SBY-2	Col. SB post-yield strain 2nd floor
92	Clflx-NAT-2	Col. NA flex. strain top station 2nd flr.
93	Clflx-NAB-2	Col. NA flex. strain bottom station 2nd flr.
94	Clflx-SAT-2	Col. SA flex. strain top station 2nd flr.
95	Clflx-SAB-2	Col. SA flex. strain bottom station 2nd flr.
96	Clrot-NAO-2	Col. NA DCDT outside face 2nd floor
97	Clrot-NAI-2	Col. NA DCDT inside face 2nd floor
98	Clrot-SAO-2	Col. SA DCDT outside face 2nd floor
99	Clrot-SAI-2	Col. SA DCDT inside face 2nd floor

100	Bmflx-NAY-2	Beam post-yield strain north end frame A
101	Bmflx-NBY-2	Beam post-yield strain north end frame B
102	Bmflx-SAY-2	Beam post-yield strain south end frame A
103	Bmflx-SMY-2	Beam post-yield strain south end frame B
104	Bmflx-NO-2	Beam flex. strain north end outside station
105	Bmflx-NI-2	Beam flex. strain north end inside station
106	Bmflx-SI-2	Beam flex. strain south end inside station
107	Bmflx-SO-2	Beam flex. strain south end outside station
108	Bmrot-NOT-2	Beam DCDT north outside station top face
109	Bmrot-NOB-2	Beam DCDT north outside station bottom face
110	Bmrot-SOT-2	Beam DCDT south outside station top face
111	Bmrot-SOB-2	Beam DCDT south outside station bottom face
112	Jtrot-NT	Joint DCDT north end top side
113	Jtrot-NB	Joint DCDT north end bottom side
114	Jtrot-ST	Joint DCDT south end top side
115	Jtrot-SB	Joint DCDT south end bottom side
116	Bmrot-NIT	Beam DCDT north inside station top face
117	Bmrot-NIB	Beam DCDT north inside station bottom face
118	Bmrot-SIT	Beam DCDT south inside station top face
119	Bmrot-SIB	Beam DCDT south inside station bottom face
120	Clflx-NAT-3	Col. NA flex. strain top station 3rd flr.
121	Clflx-NAB-3	Col. NA flex. strain bottom station 3rd flr.
122	Clflx-SAT-3	Col. SA flex. strain top station 3rd flr.
123	Clflx-SAB-3	Col. SA flex. strain bottom station 3rd flr.

Table A-4 Data Channel Schedule for PAC 700

CHANNEL	CHANNEL MNEMONIC	CHANNEL DESCRIPTION
0	Cmd H Acc	Command horizontal accl. signal
1	Cmd V Acc	Command vertical accl. signal
2	Cmd H Disp	Command horizontal displ. signal
3	Cmd V Disp	Command vertical displ. signal
4	Av H T Displ	Average horizontal table displ.
5	Av V T Displ	Average vertical table displ.
6	Av H T Acc	Average horizontal table accl.
7	Av V T Acc	Average vertical table accl.
8	Pitch	Angular accl. in pitching mode
9	Roll	Angular accl. in rolling mode
10	Twist	Angular accl. in twisting mode
11	Force H1	Force in horizontal actuator
12	Force H2	Force in horizontal actuator
13	Force H3	Force in horizontal actuator
14	Acc H1	Individual table accelerometer (hor)
15	Acc H2	Individual table accelerometer (hor)
16	Acc V1	Individual table accelerometer (vert)
17	Acc V2	Individual table accelerometer (vert)
18	Acc V3	Individual table accelerometer (vert)
19	Acc V4	Individual table accelerometer (vert)
20	Force V1	Force in vertical actuator
21	Force V2	Force in vertical actuator
22	Force V3	Force in vertical actuator
23	Force V4	Force in vertical actuator
24	Displ V1	Individual table vertical displ.
25	Displ V2	Individual table vertical displ.
26	Displ V3	Individual table vertical displ.
27	Displ V4	Individual table vertical displ.
28	Displ H1	Individual table horizontal displ.
29	Displ H2	Individual table horizontal displ.
30	Displ H3	Individual table horizontal displ.
31	blank	
32	PS Force-1	Force in passive stabilizer
33	PS Force-2	Force in passive stabilizer
34	PS Force-3	Force in passive stabilizer
35	PS Force-4	Force in passive stabilizer
36	Flr Acc 1	1st floor acceleration
37	Flr Acc 2	2nd floor acceleration
38	Flr Acc 3	3rd floor acceleration
39	blank	
40	Flr Disp 1	1st floor absolute displacement
41	Flr Disp 2	2nd floor absolute displacement
42	Flr Disp 3	3rd floor absolute displacement
43	blank	
44	Uplift NA	Vertical displacement column base NA
45	Uplift NB	Vertical displacement column base NB

46	Uplift SA	Vertical displ. of column base SA
47	Uplift SB	Vertical displ. of column base SB
48	Clstr-NBO-L	Col. NB midheight strain out face lower station
49	Clstr-NBO-M	Col. NB midheight strain out face mid station
50	Clstr-NBO-U	Col. NB midheight strain out face upper station
51	Clstr-NBI-U	Col. NB midheight strain in face upper station
52	Clstr-NAO-1	Col. NA strain outside face 1st floor
53	Clstr-NAI-1	Col. NA strain inside face 1st floor
54	Clstr-SAO-1	Col. SA strain outside face 1st floor
55	Clstr-SAI-1	Col. SA strain inside face 1st floor
56	Clrot-NAO-1	Col. NA DCDT outside face 1st floor
57	Clrot-NAI-1	Col. NA DCDT inside face 1st floor
58	Clrot-SAO-1	Col. SA DCDT outside face 1st floor
59	Clrot-SAI-1	Col. SA DCDT inside face 1st floor
60	Clflx-NAM-1	Col. NA flex. strain @ midheight 1st floor
61	Clflx-SAM-1	Col. SA Flex. strain @ midheight 1st floor
62	Clstr-NBI-M	Col. NB midheight strain in face mid station
63	Clflx-SBM-1	Col. SB flex. strain @ midheight 1st floor
64	Clstr-NBO-1	Col. NB strain outside face 1st floor
65	Clstr-NBI-1	Col. NB strain inside face 1st floor
66	Clstr-SBO-1	Col. SB strain outside face 1st floor
67	Clstr-SBI-1	Col. SB strain inside face 1st floor
68	Clrot-NBO-1	Col. NB DCDT outside face 1st floor
69	Clrot-NBI-1	Col. NB DCDT inside face 1st floor
70	Clrot-SBO-1	Col. SB DCDT outside face 1st floor
71	CLrot-SBI-1	Col. SB DCDT inside face 1st floor
72	Clflx-NAB-1	Col. NA flex. strain bottom station 1st flr.
73	Clflx-NAT-1	Col. NA flex. strain top station 1st flr.
74	Clflx-SAB-1	Col. SA flex. strain bottom station 1st flr.
75	Clflx-SAT-1	Col. SA flex. strain top station 1st flr.
76	Bmflx-NO-1	Beam flex. strain north end outside station
77	Bmflx-NI-1	Beam flex. strain north end inside station
78	Bmflx-SI-1	Beam flex. strain south end inside station
79	Bmflx-SO-1	Beam flex. strain south end outside station
80	Clrot-NBO-2	Col. NB DCDT outside face 2nd floor
81	Clrot-NBI-2	Col. NB DCDT inside face 2nd floor
82	Clrot-SBO-2	Col. SB DCDT outside face 2nd floor
83	Clrot-SBI-2	Col. SB DCDT inside face 2nd floor
84	Clflx-NBT-2	Col. NB flex. strain top station 2nd flr.
85	Clflx-NBB-2	Col. NB flex. strain bottom station 2nd flr.
86	Clflx-SBT-2	Col. SB flex. strain top station 2nd flr.
87	Clflx-SBB-2	Col. SB flex. strain bottom station 2nd flr.
88	Clflx-NAY-2	Col. NA post-yield strain 2nd floor
89	Clflx-NBY-2	Col. NB post-yeild strain 2nd floor
90	Clflx-SAY-2	Col. SA post-yield strain 2nd floor
91	Clflx-SBY-2	Col. SB post-yield strain 2nd floor
92	Slflx-NAT-2	Col. NA flex. strain top station 2nd flr.
93	Clflx-NAB-2	Col. NA flex. strain bottom station 2nd flr.
94	CLflx-SAT-2	Col. SA flex. strain top station 2nd flr.
95	Clflx-SAB-2	Col. SA flex. strain bottom station 2nd flr.
96	Clrot-NAO-2	Col. NA DCDT outside face 2nd floor
97	Clrot-NAI-2	Col. NA DCDT inside face 2nd floor
98	Clrot-NAO-2	Col. SA DCDT outside face 2nd floor
99	Clrot-SAI-2	Col. SA DCDT inside face 2nd floor

100	Bmflx-NAY-2	Beam post-yield strain north end frame A
101	Bmflx-NBY-2	Beam post-yield strain north end frame B
102	Bmflx-SAY-2	Beam post-yield strain south end frame A
103	Bmflx-SMY-2	Beam post-yield strain south end frame B
104	Bmflx-NO-2	Beam flex. strain north end outside station
105	Bmflx-NI-2	Beam flex. strain north end inside station
106	Bmflx-SI-2	Beam flex. strain south end inside station
107	Bmflx-SO-2	Beam flex. strain south end outside station
108	Bmrot-NOT-2	Beam DCDT north outside station top face
109	Bmrot-NOB-2	Beam DCDT north outside station bottom face
110	Bmrot-SOT-2	Beam DCDT south outside station top face
111	Bmrot-SOB-2	Beam DCDT south outside station bottom face
112	Jtrot-NT	Joint DCDT north end top side
113	Jtrot-NB	Joint DCDT north end bottom side
114	Jtrot-ST	Joint DCDT south end top side
115	Jtrot-SB	Joint DCDT south end bottom side
116	Bmrot-NIT	Beam DCDT north inside station top face
117	Bmrot-NIB	Beam DCDT north inside station bottom face
118	Bmrot-SIT	Beam DCDT south inside station top face
119	Bmrot-SIB	Beam DCDT south inside station bottom face
120	Clflx-NAT-3	Col. NA flex. strain top station 3rd flr.
121	Clflx-NAB-3	Col. NA flex. strain bottom station 3rd flr.
122	Clflx-SAT-3	Col. SA flex. strain top station 3rd flr.
123	Clflx-SAB-3	Col. SA flex. strain bottom station 3rd flr.

Appendix B

List of Dynamic Tests Performed

SEQUENCE	FILE NAME	SIGNAL	SPANS	COMMENTS
1	200875.2	EC	100/000	Phase I
2	200875.3	EC	300/000	"
3	220875.2	EC	400/000	"
4	220875.2	EC	500/000	"
5	220875.6	EC	600/000	"
6	220875.8	EC	700/000	"
7	220875.10	EC	800/000	"
8	220875.12	EC	900/000	"
9	250875.2	EC	200/000	EC 200 I in this report
10	250875.4	EC	1000/000	EC 1000 I in this report (filmed)
11	250875.6	EC	200/200	Phase I
12	250875.8	EC	200/400	"
13	250875.10	EC	200/200	" (V. Signal gain doubled)
14	250875.12	EC	500/330	"
15	250875.14	EC	600/500	"
16	270875.2	EC	700/595	"
17	270875.4	EC	800/680	"
18	270875.6	EC	900/765	"
19	270875.8	EC	1000/850	EC 1000/850 I in this report
20	270875.10	PAC	100/000	Phase I
21	270875.12	PAC	200/000	"
22	270875.14	PAC	300/000	"
23	270875.16	PAC	350/000	"
24	270875.18	PAC	400/000	PAC 400 I in this report
25	280875.2	EC	200/000	EC 200 in this report (Base Fixed)
26	280875.4	EC	400/000	Base Fixed
27	280875.6	EC	600/000	" "
28	280875.8	EC	800/000	" "
29	280875.10	EC	900/000	" "
30	280875.12	EC	1000/000	EC 1000 in this report
31	290875.2	EC	400/340	Base Fixed
32	290875.4	EC	800/680	" "
33	290875.6	EC	1000/850	" "
34	290875.8	PAC	100/000	" "
35	290875.10	PAC	200/000	" "
36	290875.12	PAC	300/000	" "
37	020975.2	PAC	400/000	" " (filmed)
38	160175.1	PAC	400/000	" "
39	160175.2	PAC	600/000	" "
40	160175.3	PAC	700/000	PAC 700 in this report (Base Fixed)
41	200176.3	PAC	150/000	Phase II
42	200176.4	PAC	400/000	" "
43	200176.5	PAC	500/000	" "
44	200176.6	PAC	600/000	" "
45	200176.7	PAC	700/000	PAC 700 II in this report
46	210176.1	EC	100/000	EC 100 II in this report
47	210176.2	EC	200/000	Phase II
48	210176.3	EC	250/000	" "
49	210176.4	EC	300/000	EC 300 II in this report
50	220176.1	EC	100/300	Phase II
51	220176.2	EC	200/500	" "
52	220176.3	EC	300/675	EC 300/675 in this report

EARTHQUAKE ENGINEERING RESEARCH CENTER REPORTS

EARTHQUAKE ENGINEERING RESEARCH CENTER REPORTS

NOTE: Numbers in parentheses are Accession Numbers assigned by the National Technical Information Service; these are followed by a price code. Copies of the reports may be ordered from the National Technical Information Service, 5285 Port Royal Road, Springfield, Virginia, 22161. Accession Numbers should be quoted on orders for reports (PB--- ---) and remittance must accompany each order. Reports without this information were not available at time of printing. Upon request, EERC will mail inquirers this information when it becomes available.

EERC 67-1 "Feasibility Study of Large-Scale Earthquake Simulator Facility," by J. Penzien, J. G. Bouwkamp, R. W. Clough, and D. Rea - 1967 (PB 187 905)A07

EERC 68-1 Unassigned

EERC 68-2 "Inelastic Behavior of Beam-to-Column Subassemblages under Repeated Loading," by V. V. Bertero - 1968 (PB 184 888)A05

EERC 68-3 "A Graphical Method for Solving the Wave Reflection-Refraction Problem," by H. D. McNiven and Y. Mengi - 1968 (PB 187 943)A03

EERC 68-4 "Dynamic Properties of McKinley School Buildings," by D. Rea, J. G. Bouwkamp, and R. W. Clough - 1968 (PB 187 902)A07

EERC 68-5 "Characteristics of Rock Motions during Earthquakes," by H. B. Seed, I. M. Idriss, and F. W. Kiefer - 1968 (PB 188 338)A03

EERC 69-1 "Earthquake Engineering Research at Berkeley," - 1969 (PB 187 906)A11

EERC 69-2 "Nonlinear Seismic Response of Earth Structures," by M. Dibaj and J. Penzien - 1969 (PB 187 904)A08

EERC 69-3 "Probabilistic Study of the Behavior of Structures during Earthquakes," by R. Ruiz and J. Penzien - 1969 (PB 187 886)A06

EERC 69-4 "Numerical Solution of Boundary Value Problems in Structural Mechanics by Reduction to an Initial Value Formulation," by N. Distefano and J. Schujman - 1969 (PB 187 942)A02

EERC 69-5 "Dynamic Programming and the Solution of the Biharmonic Equation," by N. Distefano - 1969 (PB 187 941)A03

EERC 69-6 "Stochastic Analysis of Offshore Tower Structures," by A. K. Malhotra and J. Penzien - 1969 (PB 187 903)A09

EERC 69-7 "Rock Motion Accelerograms for High Magnitude Earthquakes," by H. B. Seed and I. M. Idriss - 1969 (PB 187 940)A02

EERC 69-8 "Structural Dynamics Testing Facilities at the University of California, Berkeley," by R. M. Stephen, J. G. Bouwkamp, R. W. Clough and J. Penzien - 1969 (PB 189 111)A04

EERC 69-9 "Seismic Response of Soil Deposits Underlain by Sloping Rock Boundaries," by H. Dezfulian and H. B. Seed - 1969 (PB 189 114)A03

EERC 69-10 "Dynamic Stress Analysis of Axisymmetric Structures under Arbitrary Loading," by S. Ghosh and E. L. Wilson - 1969 (PB 189 026)A10

EERC 69-11 "Seismic Behavior of Multistory Frames Designed by Different Philosophies," by J. C. Anderson and V. V. Bertero - 1969 (PB 190 662)A10

EERC 69-12 "Stiffness Degradation of Reinforcing Concrete Members Subjected to Cyclic Flexural Moments," by V. V. Bertero, B. Bresler, and H. Ming Liao - 1969 (PB 202 942)A07

EERC 69-13 "Response of Non-Uniform Soil Deposits to Travelling Seismic Waves," by H. Dezfulian and H. B. Seed - 1969 (PB 191 023)A03

EERC 69-14 "Damping Capacity of a Model Steel Structure," by D. Rea, R. W. Clough, and J. G. Bouwkamp - 1969 (PB 190 663)A06

EERC 69-15 "Influence of Local Soil Conditions on Building Damage Potential during Earthquakes," by H. B. Seed and I. M. Idriss - 1969 (PB 191 036)A03

EERC 69-16 "The Behavior of Sands under Seismic Loading Conditions," by M. L. Silver and H. B. Seed - 1969 (AD 714 982)A07

EERC 70-1 "Earthquake Response of Gravity Dams," by A. K. Chopra - 1970 (AD 709 640)A03

EERC 70-2 "Relationships between Soil Conditions and Building Damage in the Caracas Earthquake of July 29, 1967," by H. B. Seed, I. M. Idriss, and H. Dezfulian - 1970 (PB 195 762)A05

EERC 70-3 "Cyclic Loading of Full Size Steel Connections," by E. P. Popov and R. M. Stephen - 1970 (PB 213 545)A04

EERC 70-4 "Seismic Analysis of the Charaima Building, Caraballeda, Venezuela," by Subcommittee of the SEAONC Research Committee: V. V. Bertero, P. F. Fratessa, S. A. Mahin, J. H. Sexton, A. C. Scordelis, E. L. Wilson, L. A. Wyllie, H. B. Seed, and J. Penzien, Chairman - 1970 (PB 201 455)A06

EERC 70-5 "A Computer Program for Earthquake Analysis of Dams," by A. K. Chopra and P. Chakrabarti - 1970 (AD 723 994)A05

EERC 70-6 "The Propagation of Love Waves Across Non-Horizontally Layered Structures," by J. Lysmer and L. A. Drake - 1970 (PB 197 896)A03

EERC 70-7 "Influence of Base Rock Characteristics on Ground Response," by J. Lysmer, H. B. Seed, and P. B. Schnabel - 1970 (PB 197 897)A03

EERC 70-8 "Applicability of Laboratory Test Procedures for Measuring Soil Liquefaction Characteristics under Cyclic Loading," by H. B. Seed and W. H. Peacock - 1970 (PB 198 016)A03

EERC 70-9 "A Simplified Procedure for Evaluating Soil Liquefaction Potential," by H. B. Seed and I. M. Idriss - 1970 (PB 198 009)A03

EERC 70-10 "Soil Moduli and Damping Factors for Dynamic Response Analysis," by H. B. Seed and I. M. Idriss - 1970 (PB 197 869)A03

EERC 71-1 "Koyna Earthquake of December 11, 1967 and the Performance of Koyna Dam," by A. K. Chopra and P. Chakrabarti - 1971 (AD 731 496)A06

EERC 71-2 "Preliminary In-Situ Measurements of Anelastic Absorption in Soils using a Prototype Earthquake Simulator," by R. D. Borcherdt and P. W. Rodgers - 1971 (PB 201 454)A03

EERC 71-3 "Static and Dynamic Analysis of Inelastic Frame Structures," by F. L. Porter and G. H. Powell - 1971 (PB 210 135)A06

EERC 71-4 "Research Needs in Limit Design of Reinforced Concrete Structures," by V. V. Bertero - 1971 (PB 202 943)A04

EERC 71-5 "Dynamic Behavior of a High-Rise Diagonally Braced Steel Building," by D. Rea, A. A. Shah, and J. G. Bouwkamp - 1971 (PB 203 584)A06

EERC 71-6 "Dynamic Stress Analysis of Porous Elastic Solids Saturated with Compressible Fluids," by J. Ghaboussi and E. L. Wilson - 1971 (PB 211 396)A06

EERC 71-7 "Inelastic Behavior of Steel Beam-to-Column Subassemblages," by H. Krawinkler, V. V. Bertero, and E. P. Popov - 1971 (PB 211 355)A14

EERC 71-8 "Modification of Seismograph Records for Effects of Local Soil Conditions," by P. Schnabel, H. B. Seed, and J. Lysmer - 1971 (PB 214 450)A03

EERC 72-1 "Static and Earthquake Analysis of Three Dimensional Frame and Shear Wall Buildings," by E. L. Wilson and H. H. Dovey - 1972 (PB 212 904)A05

EERC 72-2 "Accelerations in Rock for Earthquakes in the Western United States," by P. B. Schnabel and H. B. Seed - 1972 (PB 213 100)A03

EERC 72-3 "Elastic-Plastic Earthquake Response of Soil-Building Systems," by T. Minami - 1972 (PB 214 868)A08

EERC 72-4 " Stochastic Inelastic Response of Offshore Towers to Strong Motion Earthquakes," by M. K. Kaul - 1972 (PB 215 713)A05

EERC 72-5 "Cyclic Behavior of Three Reinforced Concrete Flexural Members with High Shear," by E. P. Popov, V. V. Bertero, and H. Krawinkler - 1972 (PB 214 555)A05

EERC 72-6 "Earthquake Response of Gravity Dams Including Reservoir Interaction Effects," by P. Chakrabarti and A. K. Chopra - 1972 (AD 762 330)A08

EERC 72-7 "Dynamic Properties of Pine Flat Dam," by D. Rea, C. Y. Liaw, and A. K. Chopra - 1972 (AD 763 928)A05

EERC 72-8 "Three Dimensional Analysis of Building Systems," by E. L. Wilson and H. H. Dovey - 1972 (PB 222 438)A06

EERC 72-9 "Rate of Loading Effects on Uncracked and Repaired Reinforced Concrete Members," by S. Mahin, V. V. Bertero, D. Rea and M. Atalay - 1972 (PB 224 520)A08

EERC 72-10 "Computer Program for Static and Dynamic Analysis of Linear Structural Systems," by E. L. Wilson, K.-J. Bathe, J. E. Peterson and H. H. Dovey - 1972 (PB 220 437)A04

EERC 72-11 "Literature Survey - Seismic Effects on Highway Bridges," by T. Iwasaki, J. Penzien, and R. W. Clough - 1972 (PB 215 613)A19

EERC 72-12 "SHAKE - A Computer Program for Earthquake Response Analysis of Horizontally Layered Sites," by P. B. Schnabel and J. Lysmer - 1972 (PB 220 207)A06

EERC 73-1 "Optimal Seismic Design of Multistory Frames," by V. V. Bertero and H. Kamil - 1973

EERC 73-2 "Analysis of the Slides in the San Fernando Dams during the Earthquake of February 9, 1971," by H. B. Seed, K. L. Lee, I. M. Idriss, and F. Makdisi - 1973 (PB 223 402)A14

EERC 73-3 "Computer Aided Ultimate Load Design of Unbraced Multistory Steel Frames," by M. B. El-Hafez and G. H. Powell - 1973 (PB 248 315)A09

EERC 73-4 "Experimental Investigation into the Seismic Behavior of Critical Regions of Reinforced Concrete Components as Influenced by Moment and Shear," by M. Celebi and J. Penzien - 1973 (PB 215 884)A09

EERC 73-5 "Hysteretic Behavior of Epoxy-Repaired Reinforced Concrete Beams," by M. Celebi and J. Penzien - 1973 (PB 239 568)A03

EERC 73-6 "General Purpose Computer Program for Inelastic Dynamic Response of Plane Structures," by A. Kanaan and G. H. Powell - 1973 (PB 221 260)A08

EERC 73-7 "A Computer Program for Earthquake Analysis of Gravity Dams Including Reservoir Interaction," by P. Chakrabarti and A. K. Chopra - 1973 (AD 766 271)A04

EERC 73-8 "Behavior of Reinforced Concrete Deep Beam-Column Subassemblages under Cyclic Loads," by O. Küstü and J. G. Bouwkamp - 1973 (PB 246 117)A12

EERC 73-9 "Earthquake Analysis of Structure-Founation Systems," by A. K. Vaish and A. K. Chopra - 1973 (AD 766 272)A07

EERC 73-10 "Deconvolution of Seismic Response for Linear Systems," by R. B. Reimer - 1973 (PB 227 179)A08

EERC 73-11 "SAP IV: A Structural Analysis Program for Static and Dynamic Response of Linear Systems," by K.-J. Bathe, E. L. Wilson, and F. E. Peterson - 1973 (PB 221 967)A09

EERC 73-12 "Analytical Investigations of the Seismic Response of Long, Multiple Span Highway Bridges," by W. S. Tseng and J. Penzien - 1973 (PB 227 816)A10

EERC 73-13 "Earthquake Analysis of Multi-Story Buildings Including Foundation Interaction," by A. K. Chopra and J. A. Gutierrez - 1973 (PB 222 970)A03

EERC 73-14 "ADAP: A Computer Program for Static and Dynamic Analysis of Arch Dams," by R. W. Clough, J. M. Raphael, and S. Mojtahedi - 1973 (PB 223 763)A09

EERC 73-15 "Cyclic Plastic Analysis of Structural Steel Joints," by R. B. Pinkney and R. W. Clough - 1973 (PB 226 843)A08

EERC 73-16 "QUAD-4: A Computer Program for Evaluating the Seismic Response of Soil Structures by Variable Damping Finite Element Procedures," by I. M. Idriss, J. Lysmer, R. Hwang, and H. B. Seed - 1973 (PB 229 424)A05

EERC 73-17 "Dynamic Behavior of a Multi-Story Pyramid Shaped Building," by R. M. Stephen, J. P. Hollings, and J. G. Bouwkamp - 1973 (PB 240 718)A06

EERC 73-18 "Effect of Different Types of Reinforcing on Seismic Behavior of Short Concrete Columns," by V. V. Bertero, J. Hollings, O. Küstü, R. M. Stephen, and J. G. Bouwkamp - 1973

EERC 73-19 "Olive View Medical Center Materials Studies, Phase I," by B. Bresler and V. V. Bertero - 1973 (PB 235 986)A06

EERC 73-20 "Linear and Nonlinear Sesismic Analysis Computer Programs for Long Multiple-Span Highway Bridges," by W. S. Tseng and J. Penzien - 1973

EERC 73-21 "Constitutive Models for Cyclic Plastic Deformation of Engineering Materials," by J. M. Kelly and P. P. Gillis - 1973 (PB 226 024)A03

EERC 73-22 "DRAIN-2D User's Guide," by G. H. Powell - 1973 (PB 227 016)A05

EERC 73-23 "Earthquake Engineering at Berkeley - 1973 " 1973 (PB 226 033)A11

EERC 73-24 Unassigned

EERC 73-25 "Earthquake Response of Axisymmetric Tower Structures Surrounded by Water," by C. Y. Liaw and A. K. Chopra - 1973 (AD 773 052)A09

EERC 73-26 "Investigation of the Failures of the Olive View Stairtowers during the San Fernando Earthquake and Their Implications on Seismic Design," by V. V. Bertero and R. G. Collins - 1973 (PB 235 106)A13

EERC 73-27 "Further Studies on Seismis Behavior of Steel Beam-Column Subassemblages," by V. V. Bertero, H. Krawinkler, and E. P. Popov - 1973 (PB 234 172)A06

EERC 74-1 "Seismic Risk Analysis," by C. S. Oliveira - 1974 (PB 235 920)A06

EERC 74-2 "Settlement and Liquefaction of Sands under Multi-Directional Shaking," by R. Pyke, C. K. Chan, and H. B. Seed - 1974

EERC 74-3 "Optimum Design of Earthquake Resistant Shear Buildings," by D. Ray, K. S. Pister, and A. K. Chopra - 1974 (PB 231 172)A06

EERC 74-4 "LUSH - A Computer Program for Complex Response Analysis of Soil-Structure Systems," by J. Lysmer, T. Udaka, H. B. Seed, and R. Hwang - 1974 (PB 236 796)A05

EERC 74-5 "Sensitivity Analysis for Hysteretic Dynamic Systems: Applications to Earthquake Engineering," by D. Ray - 1974 (PB 233 213)A06

EERC 74-6 "Soil Structure Interaction Analyses for Evaluating Seismic Response," by H. B. Seed, J. Lysmer, and R. Hwang - 1974 (PB 236 519)A04

EERC 74-7 Unassigned

EERC 74-8 "Shaking Table Tests of a Steel Frame - A Progress Report," by R. W. Clough and D. Tang - 1974 (PB 240 869)A03

EERC 74-9 "Hysteretic Behavior of Reinforced Concrete Flexural Members with Special Web Reinforcement," by V. V. Bertero, E. P. Popov, and T. Y. Wang - 1974 (PB 236 797)A07

EERC 74-10 "Applications of Realiability-Based, Global Cost Optimization to Design of Earthquake Resistant Structures," by E. Vitiello and K. S. Pister - 1974 (PB 237 231)A06

EERC 74-11 "Liquefaction of Gravelly Soils under Cyclic Loading Conditions," by R. T. Wong, H. B. Seed, and C. K. Chan - 1974 (PB 242 042)A03

EERC 74-12 "Site-Dependent Spectra for Earthquake-Resistant Design," by H. B. Seed, C. Ugas, and J. Lysmer - 1974 (PB 240 953)A03

EERC 74-13 "Earthquake Simulator Study of a Reinforced Concrete Frame," by P. Hidalgo and R. W. Clough - 1974 (PB 241 944)A13

EERC 74-14 "Nonlinear Earthquake Response of Concrete Gravity Dams," by N. Pal - 1974 (AD/A 006 583)A06

EERC 74-15 "Modeling and Identification in Nonlinear Structural Dynamics - I. One Degree of Freedom Models," by N. Distefano and A. Rath - 1974 (PB 241 548)A06

EERC 75-1 "Determination of Seismic Design Criteria for the Dumbarton Bridge Replacement Structure, Vol. I: Description, Theory and Analytical Modeling of Bridge and Parameters," by F. Baron and S.-H. Pang - 1975 (PB 259 407)A15

EERC 75-2 "Determination of Seismic Design Criteria for the Dumbarton Bridge Replacement Structure, Vol. II: Numerical Studies and Establishment of Seismic Design Criteria," by F. Baron and S.-H. Pang - 1975 (PB 259 408)A11 [For set of EERC 75-1 and 75-2 (PB 241 454)A09]

EERC 75-3 "Seismic Risk Analysis for a Site and a Metropolitan Area," by C. S. Oliveira - 1975 (PB 248 134)A09

EERC 75-4 "Analytical Investigations of Seismic Response of Short, Single or Multiple-Span Highway Bridges," by M.-C. Chen and J. Penzien - 1975 (PB 241 454)A09

EERC 75-5 "An Evaluation of Some Methods for Predicting Seismic Behavior of Reinforced Concrete Buildings," by S. A. Mahin and V. V. Bertero - 1975 (PB 246 306)A16

EERC 75-6 "Earthquake Simulator Story of a Steel Frame Structure, Vol. I: Experimental Results," by R. W. Clough and D. T. Tang - 1975 (PB 243 981)A13

EERC 75-7 "Dynamic Properties of San Bernardino Intake Tower," by D. Rea, C.-Y Liaw and A. K. Chopra - 1975 (AD/A 008 406)A05

EERC 75-8 "Seismic Studies of the Articulation for the Dumbarton Bridge Replacement Structure, Vol. 1: Description, Theory and Analytical Modeling of Bridge Components," by F. Baron and R. E. Hamati - 1975 (PB 251 539)A07

EERC 75-9 "Seismic Studies of the Articulation for the Dumbarton Bridge Replacement Structure, Vol. 2: Numerical Studies of Steel and Concrete Girder Alternates," by F. Baron and R. E. Hamati - 1975 (PB 251 540)A10

EERC 75-10 "Static and Dynamic Analysis of Nonlinear Structures," by D. P. Mondkar and G. H. Powell - 1975 (PB 242 434)A08

EERC 75-11 "Hysteretic Behavior of Steel Columns," by E. P. Popov, V. V. Bertero, and S. Chandramouli - 1975 (PB 252 365)A11

EERC 75-12 "Earthquake Engineering Research Center Library Printed Catalog " - 1975 (PB 243 711)A26

EERC 75-13 "Three Dimensional Analysis of Building Systems (Extended Version)," by E. L. Wilson, J. P. Hollings, and H. H. Dovey - 1975 (PB 243 989)A07

EERC 75-14 "Determination of Soil Liquefaction Characteristics by Large-Scale Laboratory Tests," by P. De Alba, C. K. Chan, and H. B. Seed - 1975 (NUREG 0027)A08

EERC 75-15 "A Literature Survey - Compressive, Tensile, Bond and Shear Strength of Masonry," by R. L. Mayes and R. W. Clough - 1975 (PB 246 292)A10

EERC 75-16 "Hysteretic Behavior of Ductile Moment-Resisting Reinforced Concrete Frame Components," by V. V. Bertero and E. P. Popov - 1975 (PB 246 388)A05

EERC 75-17 "Relationships Between Maximum Acceleration, Maximum Velocity, Distance from Source, Local Site Conditions for Moderately Strong Earthquakes," by H. B. Seed, R. Murarka, J. Lysmer, and I. M. Idriss - 1975 (PB 248 172)A03

EERC 75-18 "The Effects of Method of Sample Preparation on the Cyclic Stress-Strain Behavior of Sands," by J. Mulilis, C. K. Chan, and H. B. Seed - 1975 (Summarized in EERC 75-28)

EERC 75-19 "The Seismic Behavior of Critical Regions of Reinforced Concrete Components as Influenced by Moment, Shear and Axial Force," by M. B. Atalay and J. Penzien - 1975 (PB 258 842)A11

EERC 75-20 "Dynamic Properties of an Eleven Story Masonry Building," by R. M. Stephen, J. P. Hollings, J. G. Bouwkamp, and D. Jurukovski - 1975 (PB 246 945)A04

EERC 75-21 "State-of-the-Art in Seismic Strength of Masonry - An Evaluation and Review," by R. L. Mayes and R. W. Clough - 1975 (PB 249 040)A07

EERC 75-22 "Frequency Dependent Stiffness Matrices for Viscoelastic Half-Plane Foundations," by A. K. Chopra, P. Chakrabarti, and G. Dasgupta - 1975 (PB 248 121)A07

EERC 75-23 "Hysteretic Behavior of Reinforced Concrete Framed Walls," by T. Y. Wang, V. V. Bertero, and E. P. Popov - 1975

EERC 75-24 "Testing Facility for Subassemblages of Frame-Wall Structural Systems," by V. V. Bertero, E. P. Popov, and T. Endo - 1975

EERC 75-25 "Influence of Seismic History on the Liquefaction Characteristics of Sands," by H. B. Seed, K. Mori, and C. K. Chan - 1975 (Summarized in EERC 75-28)

EERC 75-26 "The Generation and Dissipation of Pore Water Pressures during Soil Liquefaction," by H. B. Seed, P. P. Martin, and J. Lysmer - 1975 (PB 252 648)A03

EERC 75-27 "Identification of Research Needs for Improving Aseismic Design of Building Structures," by V. V. Bertero - 1975 (PB 248 136)A05

EERC 75-28 "Evaluation of Soil Liquefaction Potential during Earthquakes," by H. B. Seed, I. Arango, and C. K. Chan - 1975 (NUREG 0026)A13

EERC 75-29 "Representation of Irregular Stress Time Histories by Equivalent Uniform Stress Series in Liquefaction Analyses," by H. B. Seed, I. M. Idriss, F. Makdisi, and N. Banerjee - 1975 (PB 252 635)A03

EERC 75-30 "FLUSH - A Computer Program for Approximate 3-D Analysis of Soil-Structure Interaction Problems," by J. Lysmer, T. Udaka, C.-F. Tsai, and H. B. Seed - 1975 (PB 259 332)A07

EERC 75-31 "ALUSH - A Computer Program for Seismic Response Analysis of Axisymmetric Soil-Structure Systems," by E. Berger, J. Lysmer, and H. B. Seed - 1975

EERC 75-32 "TRIP and TRAVEL - Computer Programs for Soil-Structure Interaction Analysis with Horizontally Travelling Waves," by T. Udaka, J. Lysmer, and H. B. Seed - 1975

EERC 75-33 "Predicting the Performance of Structures in Regions of High Seismicity," by J. Penzien - 1975 (PB 248 130)A03

EERC 75-34 "Efficient Finite Element Analysis of Seismic Structure-Soil-Direction," by J. Lysmer, H. B. Seed, T. Udaka, R. N. Hwang, and C.-F. Tsai - 1975 (PB 253 570)A03

EERC 75-35 "The Dynamic Behavior of a First Story Girder of a Three-Story Steel Frame Subjected to Earthquake Loading," by R. W. Clough and L.-Y. Li - 1975 (PB 248 841)A05

EERC 75-36 "Earthquake Simulator Story of a Steel Frame Structure, Volume II - Analytical Results," by D. T. Tang - 1975 (PB 252 926)A10

EERC 75-37 "ANSR-I General Purpose Computer Program for Analysis of Non-Linear Structural Response," by D. P. Mondkar and G. H. Powell - 1975 (PB 252 386)A08

EERC 75-38 "Nonlinear Response Spectra for Probabilistic Seismic Design and Damage Assessment of Reinforced Concrete Structures," by M. Murakami and J. Penzien - 1975 (PB 259 530)A05

EERC 75-39 "Study of a Method of Feasible Directions for Optimal Elastic Design of Frame Structures Subjected to Earthquake Loading," by N. D. Walker and K. S. Pister - 1975 (PB 247 781)A06

EERC 75-40 "An Alternative Representation of the Elastic-Viscoelastic Analogy," by G. Dasgupta and J. L. Sackman - 1975 (PB 252 173)A03

EERC 75-41 "Effect of Multi-Directional Shaking on Liquefaction of Sands," by H. B. Seed, R. Pyke, and G. R. Martin - 1975 (PB 258 781)A03

EERC 76-1 "Strength and Ductility Evaluation of Existing Low-Rise Reinforced Concrete Buildings - Screening Method," by T. Okada and B. Bresler - 1976 (PB 257 906)A11

EERC 76-2 "Experimental and Analytical Studies on the Hysteretic Behavior of Reinforced Concrete Rectangular and T-Beams," by S.-Y. M. Ma, E. P. Popov, and V. V. Bertero - 1976 (PB 260 843)A12

EERC 76-3 "Dynamic Behavior of a Multistory Triangular-Shaped Building," by J. Petrovski, R. M. Stephen, E. Gartenbaum, and J. G. Bouwkamp - 1976

EERC 76-4 "Earthquake Induced Deformations of Earth Dams," by N. Serff and H. B. Seed - 1976

EERC 76-5 "Analysis and Design of Tube-Type Tall Building Structures," by H. de Clercq and G. H. Powell - 1976 (PB 252 220)A10

EERC 76-6 "Time and Frequency Domain Analysis of Three-Dimensional Ground Motions,San Fernando Earthquake," by T. Kubo and J. Penzien - 1976 (PB 260 556)A11

EERC 76-7 "Expected Performance of Uniform Building Code Design Masonry Structures," by R. L. Mayes, Y. Omote, S. W. Chen, and R. W. Clough - 1976

EERC 76-8 "Cyclic Shear Tests on Concrete Masonry Piers, Part I - Test Results," by R. L. Mayes, Y. Omote, and R. W. Clough - 1976 (PB 264 424)A06

EERC 76-9 "A Substructure Method for Earthquake Analysis of Structure-Soil Interaction," by J. A. Gutierrez and A. K. Chopra - 1976 (PB 247 783)A08

EERC 76-10 "Stabilization of Potentially Liquefiable San Deposits using Gravel Drain Systems," by H. B. Seed and J. R. Booker - 1976 (PB 248 820)A04

EERC 76-11 "Influence of Design and Analysis Assumptions on Computed Inelastic Response of Moderately Tall Frames," by G. H. Powell and D. G. Row - 1976

EERC 76-12 "Sensitivity Analysis for Hysteretic Dynamic Systems: Theory and Applications," by D. Ray, K. S. Pister, and E. Polak - 1976 (PB 262 859)A04

EERC 76-13 "Coupled Lateral Torsional Response of Buildings to Ground Shaking," by C. L. Kan and A. K. Chopra - 1976 (PB 257 907)A09

EERC 76-14 "Seismic Analyses of the Banco de America," by V. V. Bertero, S. A. Mahin, and J. A. Hollings - 1976

EERC 76-15 "Reinforced Concrete Frame 2: Seismic Testing and Analytical Correlation," by R. W. Clough and J. Gidwani - 1976 (PB 261 323)A08

EERC 76-16 "Cyclic Shear Tests on Masonry Piers, Part II - Analysis of Test Results," by R. L. Mayes, Y. Omote, and R. W. Clough - 1976

EERC 76-17 "Structural Steel Bracing Systems: Behavior under Cyclic Loading," by E. P. Popov, K. Takanashi, and C. W. Roeder - 1976 (PB 260 715)A05

EERC 76-18 "Experimental Model Studies on Seismic Response of High Curved Overcrossings," by D. Williams and W. G. Godden - 1976

EERC 76-19 "Effects of Non-Uniform Seismic Disturbances on the Dumbarton Bridge Replacement Structure," by F. Baron and R. E. Hamati - 1976

EERC 76-20 "Investigation of the Inelastic Characteristics of a Single Story Steel Structure using System Identification and Shaking Table Experiments," by V. C. Matzen and H. D. McNiven - 1976 (PB 258 453)A07

EERC 76-21 "Capacity of Columns with Splice Imperfections," by E. P. Popov, R. M. Stephen and R. Philbrick - 1976 (PB 260 378)A04

EERC 76-22 "Response of the Olive View Hospital Main Building during the San Fernando Earthquake," by S. A. Mahin, V. V. Bertero, A. K. Chopra, and R. Collins," - 1976

EERC 76-23 "A Study on the Major Factors Influencing the Strength of Masonry Prisms," by N. M. Mostaghel, R. L. Mayes, R. W. Clough, and S. W. Chen - 1976

EERC 76-24 "GADFLEA - A Computer Program for the Analysis of Pore Pressure Generation and Dissipation during Cyclic or Earthquake Loading," by J. R. Booker, M. S. Rahman, and H. B. Seed - 1976 (PB 263 947)A04

EERC 76-25 "Rehabilitation of an Existing Building: A Case Study," by B. Bresler and J. Axley - 1976

EERC 76-26 "Correlative Investigations on Theoretical and Experimental Dynamic Behavior of a Model Bridge Structure," by K. Kawashima and J. Penzien - 1976 (PB 263 388)A11

EERC 76-27 "Earthquake Response of Coupled Shear Wall Buildings," by T. Srichatrapimuk - 1976 (PB 265 157)A07

EERC 76-28 "Tensile Capacity of Partial Penetration Welds," by E. P. Popov and R. M. Stephen - 1976 (PB 262 899)A03

EERC 76-29 "Analysis and Design of Numerical Integration Methods in Structural Dynamics," by H. M. Hilber - 1976 (PB 264 410)A06

EERC 76-30 "Contribution of a Floor System to the Dynamic Characteristics of Reinforced Concrete Buildings," by L. E. Malik and V. V. Bertero - 1976

EERC 76-31 "The Effects of Seismic Disturbances on the Golden Gate Bridge," by F. Baron, M. Arikan, R. E. Hamati - 1976

EERC 76-32 "Infilled Frames in Earthquake-Resistant Construction," by R. E. Klingner and V. V. Bertero - 1976 (PB 265 892)A13

UCB/EERC-77/01 "PLUSH - A Computer Program for Probabilistic Finite Element Analysis of Seismic Soil-Structure Interaction," by M. P. Romo Organista, J. Lysmer, and H. B. Seed - 1977

UCB/EERC-77/02 "Soil-Structure Interaction Effects at the Humboldt Bay Power Plant in the Ferndale Earthquake of June 7, 1975," by J. E. Valera, H. B. Seed, C.-F. Tsai, and J. Lysmer - 1977 (B 265 795)A04

UCB/EERC-77/03 "Influence of Sample Disturbance on Sand Response to Cyclic Loading," by K. Mori, H. B. Seed, and C. K. Chan - 1977 (PB 267 352)A04

UCB/EERC-77/04 "Seismological Studies of Strong Motion Records," by J. Shoja-Taheri - 1977 (PB 269 655)A10

UCB/EERC-77/05 "Testing Facility for Coupled Shear Walls," by L.-H. Lee, V. V. Bertero, and E. P. Popov - 1977

UCB/EERC-77/06 "Developing Methodologies for Evaluating the Earthquake Safety of Existing Buildings," No. 1 - B. Bresler; No. 2 - B. Bresler, T. Okada, and D. Zisling; No. 3 - T. Okada and B. Bresler; No. 4 - V. V. Bertero and B. Bresler - 1977 (PB 267 354)A08

UCB/EERC-77/07 "A Literature Survey - Transverse Strength of Masonry Walls," by Y. Omote, R. L. Mayes, S. W. Chen, and R. W. Clough - 1977

UCB/EERC-77/08 "DRAIN-TABS: A Computer Program for Inelastic Earthquake Response of Three Dimensional Buildings," by R. Guendelman-Israel and G. H. Powell - 1977

UCB/EERC-77/09 "SUBWALL: A Special Purpose Finite Element Computer Program for Practical Elastic Analysis and Design of Structural Walls with Substructure Option," by D. Q. Le, H. Petersson, and E. P. Popov - 1977

UCB/EERC-77/10 "Experimental Evaluation of Seismic Design Methods for Broad Cylindrical Tanks," by D. P. Clough - 1977

UCB/EERC-77/11 "Earthquake Engineering Research at Berkeley - 1976," - 1977

UCB/EERC-77/12 "Automated Design of Earthquake Resistant Multistory Steel Building Frames," by N. D. Walker, Jr. - 1977

UCB/EERC-77/13 "Concrete Confined by Rectangular Hoops and Subjected to Axial Loads," by J. Vallenas, V. V. Bertero, and E. P. Popov - 1977

UCB/EERC-77/14 "Seismic Strain Induced in the Ground during Earthquakes," by Y. Sugimura - 1977

UCB/EERC-77/15 "Bond Deterioration under Generalized Loading," by V. V. Bertero, E. P. Popov, and S. Viwathanatepa - 1977

UCB/EERC-77/16 "Computer-Aided Optimum Design of Ductile Reinforced Concrete Moment-Resisting Frames," by S. W. Zagajeski and V. V. Bertero - 1977

UCB/EERC-77/17 "Earthquake Simulation Testing of a Stepping Frame with Energy-Absorbing Devices," by J. M. Kelly and D. F. Tsztoo - 1977

UCB/EERC-77/18 "Inelastic Behavior of Eccentrically Braced Steel Frames under Cyclic Loadings," by C. W. Roeder and E. P. Popov - 1977

UCB/EERC-77/19 "A Simplified Procedure for Estimating Earthquake-Induced Deformation in Dams and Embankments," by F. I. Makdisi and H. B. Seed - 1977

UCB/EERC-77/20 "The Performance of Earth Dams during Earthquakes," by H. B. Seed, F. I. Makdisi, and P. de Alba - 1977

UCB/EERC-77/21 "Dynamic Plastic Analysis Using Stress Resultant Finite Element Formulation by P. Lukkunapvasit and J. M. Kelly 1977

UCB/EERC-77/22 "Preliminary Experimental Study of Seismic Uplift of a Steel Frame," by R. W. Clough and A. A. Huckelbridge 1977